Functional interactions of the adenovirus serotype 5 E4orf3 protein

John Dimmock, BSc.

Thesis submitted for the qualification of PhD

University of Warwick

Department of Biological Sciences

September 2002

Table of Contents

Table of figures

Acknowledgements

I would like to thank my supervisor, Dr Keith Leppard, for his invaluable guidance and advice (and patience beyond the call of duty), my friends in the department (past and present), for keeping me laughing (albeit hysterically), and everyone at home for keeping me sane(-ish). That's you, Mum, Dad, imogen, kate and the two grannies. This thesis could not have been completed without all of you. Give yourselves a pat on the back.

Declaration

All work in this thesis was performed by the author unless otherwise stated. None of the material preseted herein has at any time been presented for examination for any other degree.

Dedication

For those who thought I could do it

and helped me along the way, thankyou. You know who you are.

Summary

In recent years, interest in the cellular structures known as PML Oncogenic Domains (PODs) has been growing, as it has become increasingly clear that these structures may be implicated in several cellular functions, such as the regulation of the levels of active proteins in the nucleus, transcriptional regulation, suppression of growth and transformation, antiviral response, cell-cycle regulation and apoptosis. The PODs constitute large, multi-protein complexes associated with the nuclear matrix, and are visualised under immunofluorescence analysis as discrete dots numbering 10 to 20 per nucleus. A major protein component of the PODs, the promyelocytic leukaemia protein (PML), appears to be central to the function of these nuclear bodies. Notably, disruption of the PODs is observed in several malignant tissues, at the beginning of mitosis, and during infection with several viruses. During the course of a wild-type adenovirus infection, the PML protein is redistributed from the normal punctate, nuclear bodies, into "track-like" structures, which colocalise with the viral protein, E4orf3. By identifying a mutant adenovirus defective in track formation, it was possible to assign responsibility for POD reorganisation to this single viral gene product. Western blotting analysis of PML has demonstrated the existence of a characteristic pattern of PML isoforms, some apparently modified by the ubiquitin-like protein, SUMO-1. Analysis of the PML species present in adenovirus infected cells has shown that this characteristic pattern is altered, with the loss of SUMO-1-modified isoforms, and the appearance of a novel, infection specific band.

This thesis describes attempts to further investigate the nature and functional significance of the interaction between the viral E4orf3 protein and the cellular protein, PML, as occurs during adenovirus infection, by expressing Orf3 and mutants of Orf3 in eukaryotic cells through the use of plasmid based gene expression systems. By these methods, Orf3 was confirmed as necessary and sufficient for the redistribution of PML from the PODs to the "track-like" structures associated with adenovirus infection, and regions of the Orf3 protein implicated in the nuclear retention of the protein or protein stability were identified. Further, a potential link between POD redistribution and the adenovirus infection-specific PML isoform was investigated using Western blotting analysis on cell lysates derived from eukaryotic cells expressing Orf3 or mutants of Orf3 in isolation from other viral compnents. To facilitate these investigations, attempts were made to develop cell lines capable of permanent expression of Orf3 protein. These experiments led to the identification of a potentially cytopathic effect associated with the long-term expression of Orf3 in eukaryotic cells. Attempts were also made to construct whole, infectious virus, expressing mutant Orf3 proteins.

Abbreviations

Ad: Adenovirus

Ad2: Adenovirus serotype 2

Ad5: Adenovirus serotype 5

APL: Acute promyelocytic leukaemia

ASK1: Apoptosis signal-regulating kinase 1

ATRA: All-trans retinoic acid

BH3: Bcl-2 homologous region 3

BLMs: Bloom's syndrome protein

BRK: Primary baby rat kidney cells

BSA: Bovine serum albumin

CBP: CREB-binding protein

cdk: Cyclin-dependent kinase subunit

CIAP: Calf intestinal alkaline phosphate

CMV: Cytomegalovirus

CTL: Cytotoxic T lymphocyte

CVB: Coxsackievirus group B

DBP: DNA binding protein

DMEM: Dulbecco's modified Eagles medium

DMSO: Dimethyl sulphoxide

DNA: Deoxyribonucleic acid

DTT: Diothiothreitol

E2F: E2 binding protein

EBV: Epstein-Barr virus

E.coli: *Escherichia coli*

EDC: Epidermal differentiation complex

EDTA: Ethylenediaminetetra-acetic acid

eIF3-p48: Eukaryotic translation initiation factor-3

eIF-4E: Eukaryotic translation initiation factor 4E

ESI: Electron microscopic imaging

FCS: Foetal calf serum

FITC: Fluorescein isothiocyanate

FU: Fluorine-substituted uridine

GAPDH: Glyceraldehyde 3 phosphate deydrogenase

GAS: IFN-g activation site

Hepes: N-2-hydroxyethylpiperazine-N'-2-ethanesulphonic acid

HIP-I: Huntingtin interacting protein I

HMG1: High mobility group 1 protein sequence

hPML: Human PML

hr: Hour

HSV: Herpes Simplex Virus

HTLV: Human T-cell leukaemia virus

IE: Immediate-early protein

Ig: Immunoglobulin

IF: Immunofluorescence

IFN: Interferon

Immuno-FISH: Immunofluorescence in situ hybridisation

ISRE: IFN-stimulated response element

JNK: Jun NH2-terminal kinase

Kr: Kremer bodies

LANDS: Lymphocyte associated nuclear domains

LBamp: LB containing (100microgram/ml) ampicillin

MARs: Matrix associated regions

MHC: Major Histocompatibility Complex

MKP: MAP kinase phosphatase

MMTV: Murine mammary tumour virus

mRNA: Messenger RNA

NB: Nuclear Body

NCS: Newborn calf serum

ND: Nuclear dots

NF-1: Nuclear factor-1

NLS: Nuclear localisation signal

Nonidet P40: NP40

ORF: Open reading frame

Orf3: Adenovirus E4orf3 protein

Orf6: Adenovirus E4orf6 protein

PARP: Poly(ADP-ribose)polymerase

PBS: Phosphate buffered saline

PBC: Primary biliary cirrhosis

PCD: Programmed Cell Death

PEG: Polyethylene glycol

p.i: Post-infection

PIG3: p53 induced gene 3

PML: Promyelocytic leukaemia protein

POD: Promyelocytic oncogenic domain

Pol: DNA polymerase

p.t: Post-transfection

PT: Virion proteinase

PTP: Terminal protein precursor

RARα: Retinoic acid receptor alpha gene

Rfp: Ret finger protein

RGD: Arg-gly-asp sequence

RNA: Ribonucleic acid

SDS: Sodium Dodecyl Sulphate

SDS-PAGE: SDS polyacrylamide gel electrophoresis

SMN: Survival of motor neurons protein

TBP: TATA-binding protein

TNF: Tumour Necrosis Factor

UbH domain: Ubiquitin-like domain

VSV: Vesicular stomatitis virus

55K: Adenovirus E1b-55kDa protein

1. Introduction

1.1. The Adenoviridae

The adenoviruses comprise a group of related pathogens, first isolated and characterised by investigators searching for the etiological agents of acute respiratory infections. The prototype viral strain was isolated from adenoid tissues and in 1956 the agents were named *adenoviruses*. Epidemiological studies confirmed that adenoviruses were the cause of a large number of acute febrile respiratory symptoms among military recruits (Commission on Acute Respiratory Disease, 1947; Dingle *et al.*, 1968; Ginsberg *et al.*, 1955). They are not however, the etiological agent of the common cold, accounting for only a small proportion of acute respiratory morbidity, and only 5% to 10% of respiratory illness in children. Adenoviruses can also cause epidemic conjunctivitis (Jawetz, 1959), and have been linked with a variety of clinical syndromes including infantile gastroenteritis (Morris *et al.*, 1975; Yolken, 1982).

1.1.1. Classification

The Adenoviruses constitute the *Adenoviridae* family of viruses, which is divided into two genera, the *Mastadenovirus* and the *Aviadenovirus* (Norrby, 1969). The *Aviadenovirus* genus contains viruses of birds, while the *Mastadenovirus* genus includes human, simian, porcine, bovine, equine, canine and opossum viruses. There is antigenic cross-reactivity among members within each genus, but no known antigen common to all adenoviruses.

To date, 51 human serotypes have been identified (De Jong *et al.*, 1999) on the basis of resistance to neutralisation by antisera to other known adenovirus serotypes. This type-specific neutralisation is due primarily to antibody binding to epitopes on the virion hexon protein and the terminal knob portion of the fiber protein (Norrby, 1966; Toogood *et al.*, 1992). These serotypes are classified into six sub-groups based on their ability to agglutinate red blood cells (Hierholzer, 1973; Hierholzer *et al.*, 1988; Rosen, 1960). A variety of additional classification schemes have been fielded, but all produce similar groupings, suggesting that the scheme based on haemagglutination is a reasonable standard.

1.1.2. Virion structure

Adenoviruses are icosahedral particles that are 70-100nm in diameter (Horne *et al.*, 1959), containing DNA (13% of mass), protein (87% of mass), no membrane or lipid, and trace amounts of carbohydrate. The virions consist of a protein shell around the DNA-containing core. The protein shell (capsid) is made up of 252 capsomere subunits of which 240 are hexons and 12 are pentons (Ginsberg *et al.*, 1966). Electrophoretic analyses of purified virions disrupted with sodium dodecylsulphate (Ishibashi and Maizel, 1974; Maizel *et al.*, 1968; van Oostrum and Burnett, 1985) and comparison of results thus obtained with genomic open reading frames (ORFs), suggests 11 virion proteins.

The hexon protein is made up of three tightly associated molecules of polypeptide II. This trimer is often referred to as the hexon capsomere, and is surrounded by six neighbours on the virion. Five copies of polypeptide III associate to form the penton base protein (van Oostrum and Burnett, 1985) which is found at each vertex of the virion, surrounded by five neighbours. Polypeptide IV forms the trimeric fiber protein (van Oostrum and Burnett, 1985) which projects from each penton base at each vertex of the icosahedron. The combination of penton base and fiber protein is called the penton capsomere. Polypeptides VI, VIII and IX likely stabilise the hexon capsomere lattice, and VI and VIII probably bridge the gap between capsid and core. Polypeptide IIIa is associated with hexon units that surround the penton after pyridine dissociation of virions and probably links adjacent facets of the capsid and serves a bridging function between hexons and polypeptide VII of the core (see fig.1.1).

The core of the virion contains polypeptides V, VII, X and the genome terminal protein. Polypeptide VII is the major core component and probably serves as a histone-like centre around which the viral DNA is wrapped (Chatterjee *et al.*, 1986; Mirza and Weber, 1982). Polypeptide V can bind to a penton base (Everitt *et al.*, 1975) and might bridge between the core and capsid. The function of the pX protein is unknown. The terminal protein is covalently attached to the 5' ends of viral DNA (see fig.1.1) and is able to mediate circularization of the viral DNA through the formation of a protease-sensitive, phosphodiester bond between the β-hydroxyl group of a serine residue of the terminal protein, and the 5' hydroxyl of the terminal deoxycytosine residue (Desiderio and Kelly, 1981; Smart and Stillman, 1982). It is present in only two copies per virion, having served as a primer for DNA replication

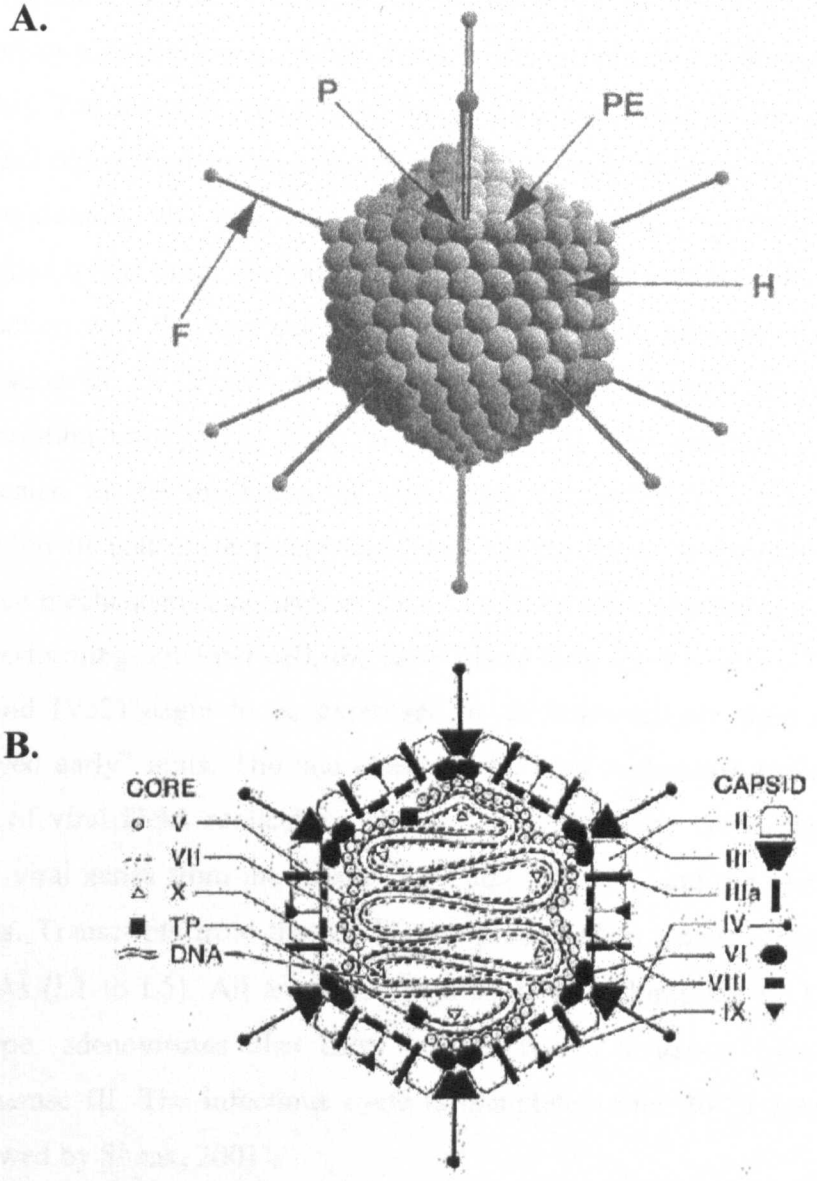

Figure 1.1. Diagrammatic representation of the adenovirus particle. A: A three-dimensional representation of the virion. Indicated are hexons (H), peripentonal hexons (PE), pentons (P) and fibre (F) (S.Riley, unpublished). **B:** A stylised cross-section of the virus particle based on current understanding of polypeptide components. Virion constituents are designated by their polypeptide number except for the terminal protein (TP). From Stewart *et al.,* 1991.

(Arrand and Roberts, 1979; Challberg *et al.,* 1982; Lichy *et al.,* 1981; Tamanoi and Stillman, 1982) and as a mediator of attachment of the viral genome to the nuclear matrix (Bodnar *et al.,* 1989; Fredman and Engler, 1993; Schaack *et al.,* 1990).

1.1.3. Genome Organisation

All adenoviruses examined to date have the same general genome organisation, which is to say that specific genes are at the same relative positions on the genome, with the exception of the VA RNA gene which is positioned differently on the avian CELO virus genome than in its mammalian counterpart (Larsson *et al.*, 1986). The genome comprises a single, linear double-stranded DNA molecule, with short terminal repeats (STRs). The inverted structure of the STRs plays a role in DNA replication. Each terminal repeat contains an origin of replication, each identical to the other.

Conventionally, the viral replication cycle is divided into *early* and *late* phases, separated by the onset of viral DNA replication. Early events begin immediately upon interaction with the host cell, and include adsorption, penetration, transcription and translation of an "early" set of genes. The viral chromosome carries five early transcription units (E1A, E1B, E2, E3, and E4). The products of these genes are implicated in the mediation of viral gene expression and DNA replication, the induction of cell cycle progression, and the blocking of apoptosis and other cell-defence mechanisms (see section 1.1.5). In HeLa cells infected at a multiplicity of 10 plaque-forming units per cell, the early phase lasts for 5-6 hours. Two viral proteins (IX and IVa2) begin to be expressed at an indeterminate time and so constitute "delayed early" units. The late phase of the viral replication cycle begins with the onset of viral DNA replication, and is characterised by the expression of a set of "late" viral genes from the "major late" unit (MLTU), and the assembly of progeny virions. Transcripts from the MLTU are processed to generate five families of late mRNAs (L1 to L5). All are transcribed by RNA polymerase II. Depending on the serotype, adenoviruses also carry one or two VA genes, transcribed by RNA polymerase III. The infectious cycle is completed after 20-24 hours in HeLa cells (reviewed by Shenk, 2001).

Both strands of the DNA are transcribed. The rightward reading strand yields E1A, E1B, IX, major late, VA RNA and E3. The leftward reading strand encodes the E4, E2 and IVa2 units.

The genes transcribed by RNA polymerase II give rise to multiple RNAs that are differentiated by the use of alternative splicing and in some cases, by the use of different poly(A) sites. The alternative products of the same transcription unit may be related in their sequence, or have no sequence in common at all. Often, the individual transcription units encode polypeptides of related function. Among the early genes,

for example, the E1A unit encodes two proteins that activate transcription and induce host cells to enter S phase. E1B encodes two proteins that cooperate with E1A products to induce cell growth. E2 encodes three proteins that function in DNA replication, and E3 encodes products that modulate the response of the host to infection. However, the E4 unit encodes what appears to be a disparate set of functions, as will be discussed in detail below.

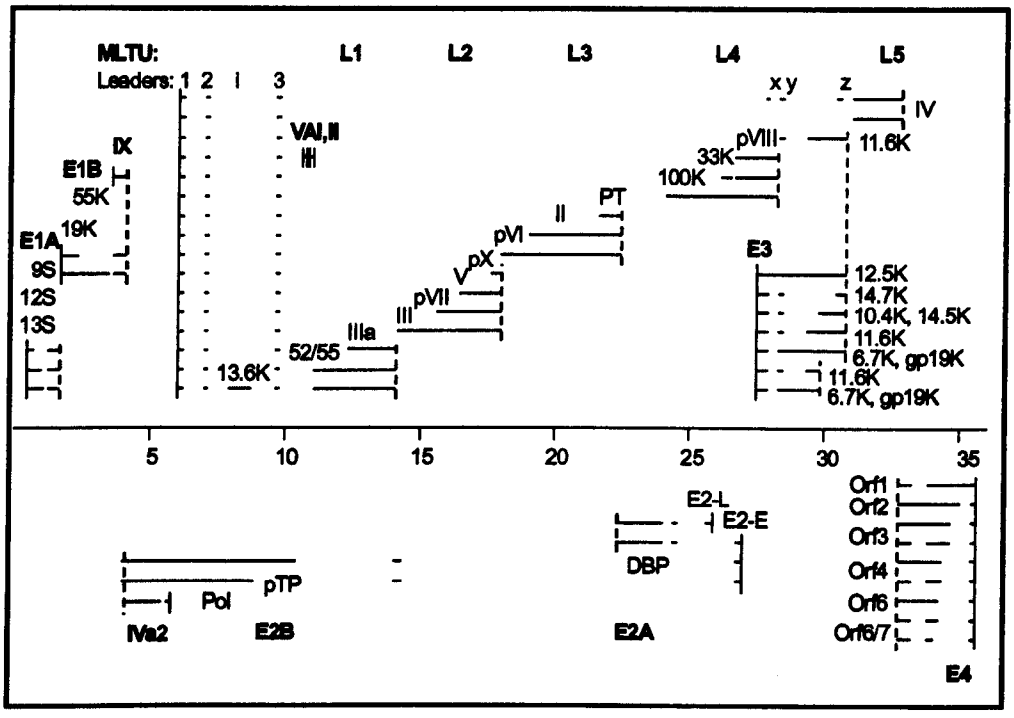

Fig 1.2. Human adenovirus type 5 transcription map. Adapted from Leppard (1998). The virus genome is represented in the centre by a line numbered to show the distance from the conventional left end in kb. Genes or gene regions are indicated in bold. mRNAs are shown as solid lines, the gaps indicating introns. Solid vertical lines indicate RNA polymerase II promoters, and broken vertical lines indicate polyadenylation sites. RNA polymerase III transcripts are shown as paired vertical lines. mRNAs transcribed from the r-strand are shown above the genome, those from the l-strand below. Proteins translated from the mRNAs are indicated adjacent to the mRNA.
Abbreviations: PT, virion proteinase; DBP, DNA binding protein; pTP, terminal protein precursor; Pol, DNA polymerase.

1.1.4. Replicative cycle

Studies of the replicative cycle have primarily focused on the closely related human serotypes, Ad2 and Ad5, as these viruses have proven easy to cultivate, and a host of mutants have been generated. Insights gained using these viruses have shown to be applicable to the other adenoviruses. The replicative cycle is divided into two broad stages, the early and late stages of infection. The early phase is characterised by

adsorption of the virus to the host cell, penetration, transcription and translation of early genes. The early viral gene products are responsible for regulation of viral gene expression and DNA replication, induce cell cycle progression, block apoptosis and antagonise host antiviral measures. In HeLa cells, the early phase lasts for five to six hours, after which replication of viral DNA is first detected. At this point, the infection is entering late phase, characterised by the expression of "late" genes and the assembly of progeny virus (approximately 10^4 progeny virus particles per cell, plus unassembled excess protein and DNA). The infectious cycle is completed after 20 to 24 hours in HeLa cells.

Adsorption is mediated by the fiber protein at the distal, carboxy-terminal portion of the protein. Specificity of attachment may be due to sequence heterogeneity between serotypes at this "knob" region. Ad infection is initiated by the formation of a high affinity complex between the fibre protein and a host cell protein that for most Ad serotypes is the 46kDa coxsackievirus group B (CVB) and adenovirus (Ad) receptor (HCVADR, formerly HCAR), a cell surface protein with two immunoglobulin-like regions (IG1 and IG2) (Bergelson *et al.*, 1997; Tomko *et al.*, 1997; Tomko *et al.*, 2000). A second molecule, the MHC class I, may also be involved in Ad type 2 and Ad type 5 uptake (Hong *et al.*, 1997).

Entry of the particle into the host cell requires penton base binding to cellular integrins, primarily $\alpha_v\beta_3$ and $\alpha_v\beta_5$ vitronectin-binding integrins, through an arg-gly-asp (RGD) sequence present in the polypeptide III molecules of the penton base (reviewed by Shenk, 2001; Wickham *et al.*, 1993). This interaction results in diffusion of the particle into clathrin-coated pits, followed by internalisation by receptor-mediated endocytosis.

Upon internalisation, the early endosome is disrupted, probably after a drop in pH (reviewed by Shenk, 2001) which the virus may harness somehow to escape to the cytosol, from where it moves to the nucleus by a process probably involving microtubules (Suomalainen *et al.*, 1999). The virion is disassembled in an ordered manner following internalisation, culminating in the release of the DNA at the nuclear pore (Dales and Chardonnet, 1973; Greber *et al.*, 1997).

1.1.5. The early viral genes

Early adenovirus gene expression has three main effects. These are to induce the host cell to enter into the S phase of the cell cycle thus creating the optimal environment for viral replication, to protect the cell from the various antiviral defences of the host organism including the cell's own responses to viral attack, and to synthesise viral gene products needed for viral DNA replication.

1.1.5.1. The E1A transcription unit

The viral E1A region unit (Jones and Shenk, 1979) is the first transcription unit to be activated after entry into the nucleus, producing two distinct early mRNAs with sedimentation coefficients of 13S and 12S, in turn generating two polypeptides of 280 and 243 amino acids respectively. The E1A proteins are able to activate expression of adenovirus transcription units by binding to a number of different cellular transcription factors and regulatory proteins. The 13S E1A protein is believed to bind directly to the TATA-binding protein (TBP), possibly relieving p53 suppression and ultimately resulting in upregulation of the basal transcription machinery. In addition to this interaction, the E1A proteins also act to activate transcription of viral genes through the E2F transcription factor. This protein is found to bind to the adenovirus E2 promoter at sites within the enhancer domain of the E1A gene. In complex with the cellular retinoblastoma tumour suppressor protein, pRB, E2F is inactive, but both E1A proteins are believed to bind to pRB, dissociating the E2F-pRB complex and liberating the transcriptional activation ability of the transcription factor. This activation of E2F by E1A influences the expression of viral genes, and in addition, affects the cell-cycle progression of the host cell.

Free E2F can activate transcription, and ectopic expression of E2F induces cells to enter S phase. E2F likely activates a series of genes that are important for cell growth and S phase that contain E2F binding sites in their promoters, including dihydrofolate reductase, thymidine kinase, thymidylate synthetase, cdc2, c-myc and others. It is likely that pRB is one of several proteins that regulate cell cycle progression through interactions with E2F. Indeed, two cellular pRB family members p107 and p130, have also been found to complex with E2F. Interestingly, these proteins can also be bound by E1A, dissociating E2F. The E1A proteins also complex with CBP, the cellular transcriptional activator p300 (Rikitake and Moran, 1992; Barbeau *et al.*, 1994; Shenk, 1996), and the p400 protein (likely a chromatin-modulating factor) (McMahon

et al., 1998; Fuchs *et al.*, 2001) resulting in deregulation of the cell cycle and entry into S-phase.

Other roles of the E1A unit include a role in inhibition of the antiviral effect of interferon by blocking the activation of interferon response genes. The transcription factor ISGF3 transduces interferon (IFN)-alpha signals and activates the transcription of cellular antiviral defence genes. E1A blocks ISGF3 DNA-binding in response to interferon activation (Kalvakolanu *et al.*, 1991). Bhattacharya *et al.* (1996) showed that p300 and/or CBP (CREB-binding protein), interact specifically with Stat2, one of the components of ISGF3, and that by inhibiting p300/CBP function, E1A represses ISGF3 function.

1.1.5.2. The E1B Transcription unit

The E1B transcription unit encodes two main proteins of 55kDa and 19kDa. When transiently expressed in cells, E1B-55kDa is detected throughout the cell in a diffuse, speckled pattern. During wild-type infection, the protein shows diffuse nuclear staining overlaid with a variable number of discrete foci (Leppard and Everett, 1999). It was thought to form a specific and predominantly nuclear complex with the E4orf6 (Sarnow *et al.*, 1984) that shuttles between the nucleus and cytoplasm mediated predominantly by the Orf6 protein (Dobbelstein *et al.*, 1997; Goodrum *et al.*, 1996). However, recent work has shown that E1B-55kDa is capable of independent nucleocytoplasmic shuttling, and that the 55kDa protein may in fact be the "driving force" for adenoviral late mRNA transport (Kratzer *et al.*, 2000; Dosch *et al.*, 2001). Orf6 is necessary for localisation of 55K to the periphery of the viral replication centres (Ornelles *et al.*, 1991), and the 55K/Orf6 complex has been shown to perform at least two functions in infection.

The deregulation of cell cycle control by E1A results in the accumulation of high levels of p53 in the nucleus, which can then induce apoptosis. The E1B-55kDa protein allows adenovirus to replicate successfully by blocking E1A-induced apoptosis (reviewed by White, 1995; Chinnadurai, 1998). This is achieved by targeting the cellular p53 tumour suppressor protein. This tumour suppressor is a sequence-specific DNA-binding protein that can activate transcription when it binds to p53 response elements, and in addition, can repress a variety of genes that lack a binding site for p53. It normally functions as a component of the G_1 checkpoint that is induced by DNA damage, acting as a sequence-specific transcriptional activator, and

can transactivate target genes such as that encoding the pro-apoptotic factor Bax, which is involved in the mitochondrial checkpoint of apoptosis. It also neutralises the anti-apoptotic functions of BCL-X_L and BCL-2 (Ko and Prives, 1996; Chao *et al.*, 1998). Under various stress conditions p53 undergoes post-translational modification that affects its conformation and binding to several proteins, resulting in its stabilisation and increased DNA-binding potential (Giaccia and Kastan, 1998; Levine, 1997), and high level expression can result in apoptosis. The *p53* gene is mutated in the majority of human cancers, indicating that loss of p53 function may have an important role in tumourigenesis (Jornvall *et al.*, 1982; Hollstein *et al.*, 1994). *p53-/-* mice are developmentally normal but are highly prone to developing spontaneous tumours (Donehower *et al.*, 1992), and *p53-/-* cells such as primary thymocytes are protected from DNA-induced apoptosis (Clarke *et al.*, 1993; Lowe *et al.*, 1993). The E1b-55kDa protein binds to, and blocks transcriptional activation by p53. The 55kDa protein colocalizes with p53 in cytoplasmic clusters in the absence of E4 proteins (Blair *et al.*, 1988; Zantema *et al.*, 1985), but upon E4orf6 coexpression, p53 is strongly destabilised and steady-state amounts of the protein are greatly reduced (Querido *et al.*, 1997; Steegenga *et al.*, 1998). Consequently, it appears that E1B-55kDa and E4orf6 work in complex to reduce p53 abundance.

The second major function of the complex is as a modulator of mRNA transport. When both proteins are expressed during infection, viral mRNAs are efficiently carried to the cytoplasm while most cellular mRNAs are retained in the nucleus (Babiss *et al.*, 1985; Beltz *et al.*, 1979; Pilder *et al.*, 1986). 55K-deficient mutants show failure of late mRNA export correlating with impaired release of RNA from its tight association with the nuclear matrix.

The smaller, 19kDa E1B protein is more effective at blocking apoptosis, acting on Bax in a similar manner to the cellular Bcl-2 protein (Han *et al.*, 1998; Ohi *et al.*, 1999). The cellular protein Bax, was found to act pro-apoptotically, disrupting the mitochondrial membrane potential. This could be rescued by E1B 19K, which was found to interact specifically with the protein through its Bcl-2 homologous region 3 (BH3) (Han *et al.*, 1998). BH3 regions are sufficient for the interaction of pro-apoptotic and anti-apoptotic Bcl-2 family members, and binding specificity at these regions was found to regulate mitochondrial membrane potential and apoptosis. E1B 19K may act to antagonise pro-apoptotic proteins rather than as an effector of survival. Current studies suggest that amongst other activities, certain of the

adenovirus E4 proteins may also be directed against apoptosis by a different mechanism, as will be discussed in detail below. The E1B-19kDa protein also protects against the effects of TNF-α, a cytokine secreted by activated macrophages and lymphocytes that can induce apoptosis resulting in cytolysis (Gooding *et al.*, 1991; Wold, 1993).

1.1.5.3. The E2 transcription unit

The E2 region encodes three proteins essential for viral DNA replication. These are the 80-kDa precursor terminal protein (Challberg *et al.*, 1980; Stillman *et al.*, 1981), the 72kDa ss DNA binding protein (DBP) (van der Vliet and Levine, 1973) and a 140-kDa polymerase, with both 5' to 3' polymerase activity and 3' to 5' exonuclease activity that probably serves a proofreading function (Field *et al.*, 1984). The E2 promoter can be activated by E1A directly, the E2 binding protein (E2F), or the 17kDa E4orf6/7 protein via interaction with E2F (Neill *et al.*, 1990; Raychaudhuri *et al.*, 1990).

1.1.5.4. The E3 transcription unit

The E3 encoded proteins appear to be important antagonists of the cytotoxic T lymphocyte (CTL) response, and TNF-α. The E3-gp19 kDa protein is a transmembrane protein that is held in the membrane of the endoplasmic reticulum, where it binds to the peptide-binding domain of MHC class I antigens, preventing these from leaving the ER and marking out infected cells to CTLs. In addition, either the E3-14.7kDa protein or an E3-14.5kDa/E3-10.4 kDa protein complex protects against some of the effects of TNF-α (reviewed by Burgert and Blusch, 2000).

1.1.5.5. The E4 transcription unit

To date, all sequenced human adenovirus genomes contain a gene that is closely related to the E4 gene, first identified in human Ad2. This locus of the viral genome has a primary transcript approximately 3kb in length, which contains at least seven ORFs (Open Reading Frames – see fig 1.3.). The transcript can produce more than eighteen distinct mRNAs through alternate splicing, giving rise to six different known peptides (Orf1,2,3,4,6,6/7), which have been demonstrated to exist in infected cells. Adenovirus mutants lacking the E4 region display a complex mix of aberrant

phenotypes including defects in viral gene expression, viral DNA replication, accumulation of late mRNAs, synthesis of viral proteins and virus-induced host cell shutoff (reviewed by Leppard, 1997). Most of these phenotypes can be assigned to lack of the E4orf6 and/or E4orf3 proteins.

The E4orf6 and E4orf3 proteins can both independently improve the stability of late RNA in the nucleus and play an as yet unidentified role in regulation of Ad DNA replication. In the absence of both proteins, DNA replication is seriously impaired and heterogeneous populations of large, concatemeric viral DNAs produced (Bridge *et al.*, 1989; Halbert *et al.*, 1985; Huang and Hearing, 1989a; Weiden and Ginsberg, 1994). Either one of these two proteins is sufficient for efficient virus production, their activities apparently being largely redundant, although Orf6 deficient virus does have some residual phenotypic similarities to the double mutant.

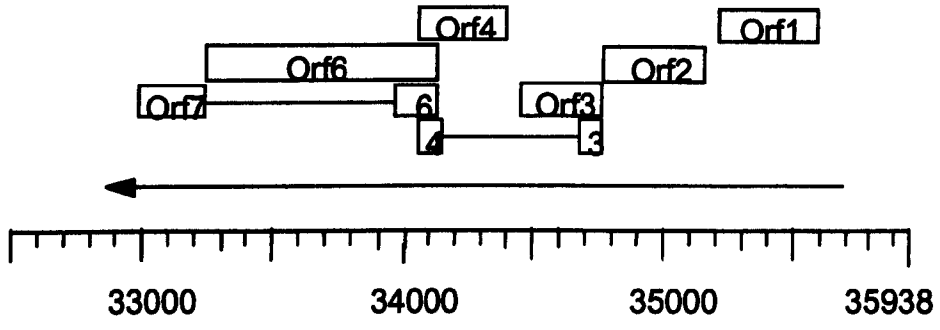

Fig 1.3. The E4 gene. The lengths are represented in bp from the conventional left end. The arrow represents the primary transcript travelling in a 5' to 3' direction, and the open boxes represent each of the potential encoded proteins. Proteins whose coding regions are disrupted by an intron are shown as boxes linked by a line. Overlapping regions have different polypeptide sequences unless they share the same number.
Adapted from Leppard (1997).

In accordance with their partially redundant roles in infection, both Orf3 and Orf6 have been reported to have transforming potential. E4orf6 has been demonstrated to cooperate with E1A and E1A plus E1B-55kDa, to transform primary baby rat kidney (BRK) cells in tissue culture (Moore *et al.*, 1996; Nevels *et al.*, 1997). It is likely that this is effected through modulation of p53 function. The E4orf6 protein works in complex with the E1B-55K protein to facilitate the export of viral mRNAs from the

nucleus, and to inhibit the export of most cellular mRNAs (see 1.1.5.2.). It also binds to p53, abrogating p53-induced apoptosis, independently of 55K. Nevels *et al.* (1999) reported that E4orf3 could also cooperate with the E1A and E1B proteins to transform BRK cells, acting synergistically with E4orf6 in the presence of E1B-55kDa. Using G418 selection, transformed cell lines were generated expressing E1A and E1B, E1A/B plus E4orf6 or E4orf3, and E1A/B plus E4orf6 and E4orf3. Those lines expressing E4orf6 had considerably lower p53 levels than other cell lines. Those expressing E4orf3 did not affect p53 levels, thus unlike E4orf6, the E4orf3 protein did not modulate the function or stability of p53. Using the same cell lines in combined immunoprecipitation-immunoblotting assays, it was demonstrated that E4orf3 could not be detected in interaction with p53 or the cellular protein, PML (see 1.2.3.), but did bind to E1B-55kDa. It has now been shown that the E4orf3-11kDa protein does interact with E1B-55kDa to relieve p53 inhibition indirectly (König *et al.*, 1999). E1B-55kDa transiently expressed in cells has a diffuse, cytoplasmic stain with characteristic clusters (Sarnow *et al.*, 1984 and this thesis). In a wild-type infection, this diffuse stain is overlaid with punctate nuclear 55K staining regions. When cells are infected with a virus mutant lacking a functional E4orf6 coding region, these punctate regions are increased in number and prominence. These nuclear foci have been found to colocalize both 55K and the virus E4orf3 protein, Orf3 being necessary for association of 55K with the nuclear matrix (Leppard and Everett, 1999).

König *et al.* (1999) showed that when transiently expressed in HeLa cells, E4orf3 redirects E1B-55kDa from the cytoplasm to nuclear tracks and went on to argue that the E4orf3 protein has a role in liberating p53 from 55K-induced inhibition of transcriptional activity. E4orf3, E1B-55kDa and p53 were transfected into HeLa cells in different combinations, and detected by immunofluorescence. In the absence of viral proteins, p53 was found in a nuclear distribution. In the presence of E1B-55kDa, it was relocated to cytoplasmic clusters. The addition of E4orf3 to the system relocated E1B-55kDa to nuclear tracks, while p53 was distributed over the nucleus in a similar pattern to that found in the absence of viral proteins. E4orf3 alone did not appear to have any effect on p53 distribution.

These same authors used a reporter plasmid with a p53-dependent promoter driving a luciferase reporter gene to measure p53 activity in human osteosarcoma-derived cell-lines (Saos-2 cells) either singly or doubly transfected with E1B-55kDa and/or E4orf3. A p53 expression plasmid was added as Saos-2 is a p53-null cell-line. The

results showed that E1B-55kDa alone reduced activity from the p53-dependent promoter while E4orf3 alone slightly increased p53 activity. More striking, was the result that coexpression of the two proteins led to an abolishment of E1B-55kDa inhibition of p53 activity. Cotransfection of 55K and E4orf6 had the effect of down-regulating p53 activity to an even greater extent than 55K alone. This effect was not reversed by the addition of E4orf3. The same group concluded that E4orf3 does not influence p53 stability.

To test whether the above observations were relevant to infection, König *et al.* (1999) used a variety of adenovirus mutants to infect A549 cells. During wild-type infection, E1B-55kDa moves from cytoplasmic clusters early in infection, to concentrate at replication centres within the nucleus. This localisation has been shown to depend on E4orf6. During infection with a mutant virus lacking the entire E4 region, the E1B-55kDa protein did not leave the cytoplasmic clusters. When cells were infected with mutant 366*+Orf3, which lacks the E4 region but expresses E4orf3, E1B-55kDa moved from cytoplasmic clusters to the nuclear tracks typical of E4orf3 localisation. Later in infection, E1B-55kDa did move to the replication centres suggesting E4orf3 is another mediator of the nuclear localisation of the protein in infected cells. In contrast with the gradual p53 degradation seen during wild type infection, this process was accompanied by a nuclear accumulation of p53. Under these circumstances, a large proportion of the p53 moved to within the virus replication centres, colocalising with viral DNA, while E1B-55kDa accumulated in the peripheries of these centres. These results support the suggestion that E4orf3 can dissociate p53 from association with E1B-55kDa not only when transiently expressed, but also during infection. E4orf3 expression precedes that of E4orf6 during infection, but ultimately 55K preferentially complexes with E4orf6 away from the tracks, and in concert these two proteins eliminate p53 activity. However, it is thought that certain viruses (CMV, HSV) might make use of upregulated p53 in their infectious process, and it may be the case that prior to E1B-55kDa/E4orf6 inactivation and degradation of p53, E4orf3 facilitates temporary p53 activity in adenovirus infected cells.

As well as these functions, the E4orf3 product is necessary and sufficient for the reorganisation of cellular, nuclear structures known as promyelocytic oncogenic domains (PODs). This phenomenon forms the major focus of the work discussed in this thesis, and the PODs and their viral interactions will be shortly be discussed in detail.

Of the remaining proteins, Orf6/7 regulates the Ad E2 promoter through its ability to bind to and stabilise E2F dimers (Huang and Hearing, 1989b). The Orf4 protein can induce caspase-independent cell death, and is important in down-regulating the expression of E1A and E4 genes which is effected through interaction with protein phosphatase 2A (Bondesson *et al.*, 1996). Orf1 has been shown to have oncogenic and transforming potential, promoting focus formation of CREF cells *in vitro* (Weiss *et al.*, 1996), and driving the formation of mammary tumours in female rats (Javier, 1994; Javier *et al.*, 1992). Orf2 is a soluble cytoplasmic protein with no known function (Dix and Leppard, 1995).

1.2. Nuclear Substructure

The deeper our understanding of the nucleus becomes, the less it appears to resemble the loosely organised "bag" of proteins and DNA originally envisaged by some. Indeed, it is becoming evident that the nucleus contains a variety of domains that are morphologically and functionally distinct as part of a defined, if dynamic, substructure. Stresses of various types including viral infection, oncogene expression and inherited human disorders, can cause profound and specific changes in nuclear organisation.

1.2.1. The Matrix

The nuclear substructure known as the matrix is a highly organised 3D framework consisting of proteins and ribonucleoproteins, as revealed by electron microscopy (Fey *et al.*, 1986). This structure remains after removal of the soluble proteins and chromatin. It consists of a nuclear lamina, completely enclosing the nucleus and lining the inside of the double membrane (Gerace and Burke, 1988), and an internal fibro-granular framework (Capco *et al.*, 1982; Verheijen *et al.*, 1988; He *et al.*, 1990). Many nucleus-specific processes such as RNA synthesis (Jackson and Cook, 1985), transport (Schroder *et al.*, 1987; Xing and Lawrence, 1991) and processing (Smith *et al.*, 1989; Zeitlin *et al.*, 1989) and DNA replication (Jackson and Cook, 1986; Nakayasu and Berezney, 1989) are matrix associated and linked to specific nuclear domains. Indeed, chromatin has specific sequences known as matrix associated regions or MARs (Mirkovitch *et al.*, 1984; Gasser *et al.*, 1989) via which it interacts with the nuclear matrix, resulting in the organisation of the chromatin into loops with an average size of 80-90 kbp (Jackson *et al.*, 1990). It is thought that the matrix may

function to order and regulate active regions within the nucleus by controlling spatial distribution. Individual chromosomes occupy discrete patches called chromosome territories, which are separated by interchromasomal domains resembling channels (Schardin *et al.*, 1985). Active genes are preferentially localised to the peripheries of the chromosome territories, where RNA transcripts are formed and shed into the interchromasomal domains for further processing and transport (Kurz *et al.*, 1996; Wansink *et al.*, 1996). Relative to less active chromosomes, transcriptionally active chromosomes have more surface area in contact with the channels. The arms of chromosomes have been shown to move within the nucleus during interphase and in a cell-cycle dependent manner (Li *et al.*, 1998; Robinett *et al.*, 1996). These observations would support the idea that to be replicated, DNA must be brought to the postulated "replication factories", presumably at the outskirts of chromosome territories. These sites would be large, multienzyme complexes, fixed within the nucleus, where movement of the chromosomes to the factories would be necessary for initiation of replication, and provide a point of regulation.

1.2.2. Nuclear Bodies

Several nuclear substructures have been observed by indirect immunofluorescence, that seem to comprise distinct "bodies" or regions, apart from the nucleolus (the factory in which 28S, 18S and 5.8S rRNAs are transcribed, processed and assembled. Among these are the snRNPs, coiled bodies and gems, and the PODs.

The U1, U2, U4/U6 and U5 small nuclear ribonucleoproteins (snRNPs) are nucleoplasmic RNA-protein complexes that function as subunits of the spliceosome. These structures yield speckled staining under immunofluorescence, upon a diffuse staining background, probably representing collections of splicing components.

Coiled bodies appear as bundles of tangled threads, under microscopic analysis. They contain high concentrations of coilin (Chan *et al.*, 1994), fibrillarin (Raska *et al.*, 1990; JimenezGarcia *et al.*, 1994) and certain splicing components (Huang and Spector, 1991; Carmo-Fonseca *et al.*, 1992). They are highly dynamic structures that disassemble during mitosis and reform during G_1 phase, and may have a role in snRNP transport, maturation or both. These structures are modified during Ad5 and HSV-1 infection (Bridge *et al.*, 1993; Phelan *et al.*, 1993), and proteins associated with them may have a role in Ad5 late splicing. Gems are often found paired to coiled bodies, and contain the SMN (survival of motor neurons) protein, encoded by the

gene responsible for a severe inherited form of human spinal muscular atrophy (Liu and Dreyfuss, 1996; Lefebvre *et al.*, 1995). Of growing interest is the role of the PODs also known as NDs (nuclear dots), Kremer bodies (Kr) and ND10s. These structures appear to be important to many cellular functions as will be discussed below.

1.2.3. PML Oncogenic Domains (PODs)

PODs were originally described as the autoantigenic target in patients with primary biliary cirrhosis (PBC) (Bernstein *et al.*, 1984; Powell *et al.*, 1984), but are components of most cell types, where they are visualised under immunofluorescence analysis as discrete dots numbering 10 to 20 per nucleus. The POD constitutes a large, multi-protein complex associated with the nuclear matrix. Under high magnification light microscopy and electron microscopy, larger PODs have been shown to have a "doughnut-like" shape, consisting of a dense fibrillar ring around a less-dense central core, with many pores and channels throughout (Boisvert *et al.*, 2000). The exact protein composition and number of PODs varies between cell-types and with the cell cycle, containing a heterogeneous mix of functionally important proteins such as ISG20 (Gongora *et al.*, 1997), PIC1/SUMO-1 (Boddy *et al.*, 1996), LYSP100 (Dent *et al.*, 1996), PLZF (Ruthardt *et al.*, 1998), INT6 (Desbois *et al.*, 1996), CBP/P300 (LaMorte *et al.*, 1998), RFP (Cao *et al.*, 1998), Daxx (Li *et al.*, 2000), BLM (Ishov *et al.*, 1999) and ribosomal protein P (Borden *et al.*, 1998). The promyelocytic leukaemia protein (PML) and Sp100 are generally considered consistent and therefore diagnostic components of PODs. Both these proteins were found to be autoantigens in PBC, antibodies against Sp100 and PML often co-occurring in the sera of patients.

While normally found attached to the insoluble nuclear matrix, PODs are dynamic structures sensitive to numerous external and internal stimuli such as heat shock, heavy metals, PML-RARα expression (a fusion protein associated with acute promyelocytic leukaemia, see below), interferon, transformation and amino acid starvation. The PODs are also strongly modified by infection with many viruses, including herpes simplex virus (Maul *et al.*, 1993), cytomegalovirus (Kelly *et al.*, 1995), Epstein-Barr virus (Szekely *et al.*, 1996), influenza (Guldner *et al.*, 1992), human T-cell leukaemia virus (Desbois *et al.*, 1996), and adenovirus (Carvalho *et al.*, 1995), through the action of viral regulatory proteins (reviewed by Sternsdorf *et al.*,

1997). In addition, a number of cellular POD proteins, including PML and Sp100, are highly interferon-inducible, suggesting a possible role for these structures in the early or late antiviral response.

Disruption of the PODs is also observed in patients with acute promyelocytic leukaemia (APL). This malignancy manifests as a block in the differentiation of promyelocytes, precursors of the granulocyte/neutrophil pathway. This leads to an accumulation of promyelocytes that infiltrate the bone marrow. This event is the result of a reciprocal translocation event, t(15;17) between *PML* on chromosome 15 and the retinoic receptor alpha gene (*RARα*) on chromosome 17 (de Thé *et al.*, 1990; Goddard *et al.*, 1991). The resultant PML-RARα fusion protein does not localise to the PODs and, what is more, interferes with wild-type PML, disrupting the PODs and resulting in a "microspeckled" appearance of PML under immunofluorescence (Dyck *et al.*, 1994; Koken *et al.*, 1994). Evidence suggests that the PML domain of *PMLRAR* plays a specific and critical role in the pathogenesis of APL (Kogan *et al.*, 2000). Disruption of the PODs is also observed in malignant tissues other than those of APL. In the case of hepatocarcinoma, both the PML and Sp100 proteins are altered (Terris *et al.*, 1995). Interestingly, both retinoic acid and arsenic trioxide, that have been shown to induce clinical remission through differentiation and apoptosis, respectively, induce the restoration of normal PODs (Dyck *et al.*, 1994; Koken *et al.*, 1994; Zhu *et al.*, 1997; Müller *et al.*, 1998). These results suggest that disruption of the PODs is required for malignant cell proliferation at least in these instances and further, imply that these structures may have a role during cell cycle regulation.

The heterogeneity of proteins that accumulate at these nuclear domains makes it difficult to identify a single function for the PODs. It seems likely that at least partially they act as nuclear storage sites for active proteins, accumulating or releasing them as is appropriate to the correct functioning of the cell. For example, certain proteins, such as the tumour suppressor BRCA1, only localise to PODs when overexpressed (Maul *et al.*, 1998), and the pRB tumour suppressor protein accumulates at these sites, but only when in its inactive, phosphorylated form (Alcalay *et al.*, 1998). In this scenario, the PML protein would play a central role in accumulating the components of PODs, as proteins such as CREB binding protein (CBP), Daxx, Bloom's syndrome protein (BLMs) and Sp100 do not localise to PODs

in the absence of PML. Indeed, PML overexpression has been shown to recruit CBP to the PODs (La Morte *et al.*, 1998).

1.2.4. The Promyelocytic leukaemia (PML) protein

The PML protein has been implicated in numerous cellular processes, including transcriptional regulation (Boisvert *et al.*, 2000), suppression of growth and transformation (Ahn *et al.*, 1995; Le *et al.*, 1996), antiviral response (see 1.2.4.7), cell-cycle regulation (see 1.2.4.2. and 1.2.4.5) and apoptosis (see 1.2.4.3).

The N-terminus of the protein contains 3 cysteine-rich metal binding domains which probably complex zinc. These regions have been shown to be essential for localisation of the protein to PODs, and are thought to mediate protein:protein interactions. The first cysteine-rich region makes up a RING motif. This motif is shared by a family of proteins found in a wide range of organisms from plants to viruses, and includes proteins with many different functions, including many proto-oncogenes and components of signal transduction pathways (Lovering *et al.*, 1993; Freemont *et al.*, 1991). The other two cysteine-rich regions are known as the B1 and B2 boxes. These are followed by an α-helical coiled-coil domain, involved in dimerisation. This RING-B-Box-coiled-coil pattern is common to a subgroup of RING finger proteins. Like PML, two other members of this subgroup (TIF1 and Rfp) also become oncogenic as a result of chromosomal translocations (Le Douarin *et al.*, 1995; Hasegawa *et al.*, 1996). The coiled-coil region is followed by a serine-rich domain, which is absent from the PML-RARα fusion protein, and is speculated to have a regulatory role.

Western blotting of PML in interphase cells reveals a complex family of isoforms derived from alternatively spliced transcripts and post-translational modifications, with a major band at 140 kDa (reviewed by Sternsdorf *et al.*, 1997).

1.2.4.1. Control and modulation of PML gene expression

Analysis of the PML promoter has identified several potential transcription factor binding sites. There is no associated TATA or CCAAT-box, and transcription is initiated at multiple sites (Stadler *et al.*, 1995). The PML promoter contains a potential binding site for the huntingtin interacting protein I (HIP-I), a protein implicated in caspase-8 activation and the initiation of apoptosis during the

pathogenesis of Huntington's disease, which could indicate constitutive promoter activity (Wanker *et al.*, 1997; Wanker, 2002). In addition, the transcription factor Ets probably plays a role in PML gene transcription. Transcription factors of this family are thought to regulate gene expression in many diverse processes such as transformation, differentiation and growth control (reviewed by Wasylyk *et al.*, 1993), which may bear a functional relationship to the role of PODs within the cell.

In addition, treatment with type I (α,β) or type II (γ) interferons (IFNs) strongly enhances PML gene expression at the RNA and protein levels (Chelbi-Alix *et al.*, 1995; Grotzinger *et al.*, 1996; Lavau *et al.*, 1995). The PML promoter contains an IFN-stimulated response element (ISRE) and an IFN-γ activation site (GAS). The ISRE alone is sufficient to mediate type I/II IFN-enhanced gene expression (Stadler *et al.*, 1995). What is more, IFN treated cells have been reported to express PML isoforms not detected in untreated cells (Grotzinger *et al.*, 1996) which may suggest that IFN modulates alternative splicing of the mRNAs, generating PML proteins of different functionality in response to invasion by virus.

1.2.4.2. PML, PIC1/SUMO-1 and Cell-Cycle regulation

As previously mentioned, the average size and number of PODs varies during the cell cycle (Koken *et al.*, 1995; Terris *et al.*, 1995). During S phase, PML and Sp100 are colocalized to the PODs (though no direct interaction between the two proteins has been demonstrated), although both proteins also have a diffuse nuclear component. Later, in G2, many cells have an increased number of POD. At the beginning of mitosis, the PODs (stained with anti-PML antibody) become disrupted and as cells enter prophase, the diffuse portion of PML is excluded from condensing chromosomes. In fact, both PML and Sp100 become separated from the PODs during mitosis and at the breakdown of the nuclear envelope, PML forms irregular accumulations where no Sp100 is present (Everett *et al.*, 1999). Once mitosis is complete, cells enter G1 when the process is reversed and the PODs reform (reviewed by Sternsdorf *et al.*, 1997). A proportion of the PML remains in the cytoplasm in punctate bodies. This pattern is characteristic of cells in G1.

The mechanism by which localisation of PML is controlled is of interest as it has implications not only in cell cycle regulation, but also for those investigating the disruption of PODs during virus infection and tumourigenesis. The POD-associated

protein SUMO-1 (also known as PIC1) is now known to modify a number of proteins in a reversible manner, correlating with an alteration of the target protein's sub-cellular localisation (reviewed by Johnson and Hochstrasser, 1997; Hodges *et al.*, 1998; Rodriguez *et al.*, 2001). Amongst these proteins is PML, which SUMO-1 has been observed to modify in a cell cycle related manner (Everett *et al.*, 1999). For these reasons, SUMO-1 is an important candidate for regulating the activity of the PML protein.

SUMO-1 is a member of a ubiquitin homology protein family, a heterogeneous group that is characterised by an ubiquitin-like domain (UbH domain) (Boddy *et al.*, 1996; Mahajan *et al.*, 1997). UbH domains often show amino acid changes in residues as compared with ubiquitin required for the normal ubiquitination/degradation pathway, suggesting a different role for these proteins (Watkins *et al.*, 993). In SUMO-1, the lysine residues necessary for polyubiquitination are not present, suggesting it functions as a monomer. It has a calculated mass of 11.5kDa, and has been shown to have a strong and specific covalent linkage with the PML protein (Boddy *et al.*, 1996; Müller *et al.*, 1998). SUMO-1 has also been implicated in nuclear pore complex function in protein transport, apoptosis, DNA recombination and repair where no direct link to PODs has been observed (reviewed by Sternsdorf *et al.*, 1997).

Studies transiently expressing SUMO-1 in NIH3T3 cells showed a nuclear staining pattern coincident with that of the endogenous mouse PML. Cotransfection of SUMO-1 and human PML (hPML) generated completely overlapping patterns of distribution (Boddy *et al.*, 1996). Of interest is the observation that there was no significant colocalisation between SUMO-1 and the PML-RARA fusion in the APL-derived cell line NB4, unless the cells had previously been treated with *trans*-retinoic acid, known to result in the formation of normal PODs in APL-derived cell lines (Boddy *et al.*, 1996). In a related observation, PML and SUMO-1 colocalised at the PODs during interphase, but as the PODs broke down during mitosis, separation occurred. Any remaining PML foci during mitosis have been shown by immunofluorescence not to colocalize with SUMO-1 (Everett *et al.*, 1999). These results imply a link between SUMO-1/PML colocalisation and POD formation/breakdown.

Further investigation revealed that SUMO-1 is in fact, covalently linked to a subset of PML in a reversible and phosphorylation-dependent manner. The SUMO-1-polymodified forms of PML are compartmentalised into the PODs, in contrast with

unmodified PML which is found in the soluble nucleoplasmic fraction. Zhong *et al.* (2000) showed that SUMO-1 conjugation of PML was necessary for NB recruitment of PML.

Endogenous PML in interphase cells can be detected by Western Blot analysis (using mAb 5E10, Stuurman *et al.*, 1992), revealing a complex family of isoforms derived from both alternatively spliced transcripts and the effects of secondary modifications. Above the major isoform at about 140kDa, are a three further species that are generally held to represent conjugation by 1, 2 and 3 molecules of SUMO-1 at separate lysine residues.

At mitosis, these three SUMO-1 modified isoforms of PML are absent, and instead a novel modified form of PML appears, migrating just slower than the major 140kDa band. The lower molecular mass isoforms of PML do not appear to be affected. In synchronised cells, the novel mitotic form of PML was observed along with a corresponding decrease in the levels of the SUMO-1-modified isoforms, at 11 hours after release from an aphidicolin block. By 13 hours, the interphase pattern had re-established itself, but a little of the mitosis-specific isoform remained (Everett *et al.*, 1999). The quantitative deconjugation of SUMO-1 from PML and the novel PML modification appear to be rapid events confined to mitosis itself.

Conjugation of SUMO-1 to over-expressed PML in an engineered cell line was shown to be inhibited by the phosphatase inhibitor calyculin A (Müller *et al.*, 1998), and treatment of culture cells with the phosphatase inhibitor generated an electrophoretic profile of PML with considerable similarity to that for mitotic cells (Everett *et al.*, 1999). The drug rapidly induced the loss of the endogenous SUMO-1-conjugated forms of PML, and in addition caused the production of a PML band that migrated just slower than the major isoform, suggesting that it represented the same species as was seen in mitotic cells. This mitosis specific isoform is highly labile, but was stabilised by phosphatase inhibitors, supporting the hypothesis that a major factor in the gel mobility of this form of PML is the presence of phosphate groups, and that it is in fact, the same species as that derived by hyperphosphorylation of PML by calyculin treatment. Treatment of interphase cells with okadiac acid, another phosphatase inhibitor, gave similar results. Taken together, these results suggest that SUMO-1-conjugation is dependent on PML phosphorylation state.

The predicted model during the cell cycle has deconjugation of SUMO-1 from the PML protein, probably by the SUMO-1 de-conjugation enzyme HsUlp1 (Li and

Hochstrasser., 1999), with the appearance of a novel, hyper-phosphorylated PML isoform. This results in POD disruption (observed in cells treated with calyculin A). This process is reversed at G_1, with the reformation of PODs. A MAP kinase phosphatase (MKP-4) has been detected in the PODs of about 20% of interphase cells (Muda *et al.*, 1997), and the cdk inhibitor p27KIP1 (Quignon *et al.*, 1998) has been reported to localise to these structures, connecting PODs and cell cycle regulated phosphorylation.

1.2.4.3. PML and Programmed Cell Death (PCD)

Programmed cell death, also known as cell suicide, is a normal physiological process important in development, maintenance of tissue homeostasis, and in the elimination of cells that would otherwise constitute a danger to the organism, such as virus-infected or genetically altered cells. Disruption of this process is involved in several diseases. Programmed cell death is distinct from necrosis. The latter is characteristic of cells that die of physical damage or poisoning, and typically the cells swell and burst, spilling their contents over their neighbours. PCD is in fact a tidy process, creating no mess. The most common form of PCD is apoptosis, in which the cell nucleus becomes condensed and the DNA is fragmented, generating characteristic "ladders" upon gel analysis, the cell shrivels, and the shrunken corpse is generally engulfed and digested by neighbouring cells. This process is mediated by a class of cysteine proteases called caspases, which cleave key cellular proteins, inducing the typical morphological features described above. Specific caspase inhibitors can sometimes block or delay PCD, but not in all cases. This will be discussed later (see 1.2.4.3.3).

PML expression or POD localisation is altered in a number of situations involving abnormal cell survival, including virus infections, senescence or other human cancers. What is more, *Pml-/-* mice are protected from the lethal effects of radiation and anti-Fas antibody (Wang *et al.*, 1998). A possible explanation for these findings is that PML is involved in the control of cell survival or death, and that disruption of PML results in inappropriate cell survival. Recent evidence indicates that PML may in fact be implicated in several different cell-death pathways. PML has been shown to act as a transcriptional co-activator with p53, colocalising with the protein in the PODs, defining a PML-dependent, p53-regulatory pathway for apoptosis (Guo *et al.*, 2000). PML has also been shown to be essential for the induction of apoptosis by multiple

stimuli such a DNA damage, Fas, TNF, ceramide and IFNs, by a p53-independent pathway (Wang *et al.*, 1998). Further research suggests that PML overexpression induces rapid cell death in a caspase-independent death process, independently of *de novo* transcription and cell cycling (Quignon *et al.*, 1998). Taken together, these results suggest that PML is essential for multiple PCD pathways.

1.2.4.3.1. PML in p53-dependent apoptosis

As has previously been discussed, p53 is a tumour-suppressor protein that has functions in regulation of cell growth and cell death in response to cellular stress (see 1.1.5.2.). In thymocytes, DNA-damage-induced apoptosis in response to γ-irradiation is dependent on normal p53 function (Lowe *et al.*, 1993; Clarke *et al.*, 1993). Wild-type and *Pml-/-* thymocytes were compared, and a marked reduction in the level of apoptosis in *Pml*-deficient cells observed (Guo *et al.*, 2000; Wang *et al.*, 1998). PML was found to markedly increase the level of transcriptional activity at p53 response elements, but was unable to act directly upon them. In this case, PML was found to co-activate the *Bax* and *GADD45* promoters. GST-pulldown experiments demonstrated that PML and p53 physically interact through the p53 DNA-binding domain, and the C-terminal domain of PML. Interestingly, in about 10% of U2OS cells, p53 was found to colocalize with PML to the POD. Using PML mutants for POD localisation but still capable of p53 interaction, it was shown that localisation of PML in the PODs was necessary for the enhancement of transcriptional activation by p53 (Guo *et al.*, 2000).

These results demonstrated that PML was involved in regulation of p53-dependent apoptosis in cells such as thymocytes, and bone marrow haemopoietic cells. The protein acts in this pathway as a p53 transcriptional co-activator, that is necessary for correct p53-DNA binding and induction of p53 target genes following γ-irradiation. It is likely that this effect is mediated through the post-translational modification of p53 by acetylation, by which it is made transcriptionally active. While PML has no intrinsic acetyltransferase activity, it nevertheless is found in close association with CBP (La Morte *et al.*, 1998), a known acetyltransferase of p53. This is another POD-associated protein, and the observation that PML, CBP and p53 all co-localise to PODs supports the hypothesis that the reciprocal interactions between these three proteins are important for stabilising the p53-CBP acetylation complex.

Recently, Fogal *et al.* (2000), demonstrated that p53 is recruited into the PODs specifically by sumolated PML isoform IV (previously termed PML3 in Fogal *et al.*, 2000), resulting in a marked increase in transcription from certain p53 responsive promoters. Interestingly, SUMO-1, required for PML localisation to PODs, was found to modify p53 directly (Gostissa *et al.*, 1999; Rodriguez *et al.*, 1999; Müller *et al.*, 2000), and when coexpressed with hUbc9 (the sumolation enzyme) localised p53 to POD-like nuclear structures. However, Fogal *et al.* showed that this effect did not depend on the direct sumolation of the protein, since a conjugation-deficient mutant was efficiently targeted to the PODs. They went on to demonstrate that p53 recruitment to PODs was specifically mediated by the PML IV splice variant, in comparison with an alternate splice variant, PML III (previously termed PML-L in Fogal *et al.*, 2000). This specificity was shown to be due to a region of the PML variant outside the central domain and therefore the known sumolation sites of the protein. As overexpression of hUbc9 and SUMO-1 had the same effect, it is likely that this was achieved via enhanced sumolation of endogenous PML, augmenting the PODs. Overexpression of PML IV resulted in significantly reduced cell survival, dependent upon the presence of p53. PML III did not have any effect upon cell-survival in this assay. These results demonstrate that not only do PML and the PODs affect cell survival in a p53-dependent manner, but that this is specific to a subset of PML types, perhaps only one type. Co-expression of p53 and PML III confirmed that this isoform strongly increased the transcriptional activity of p53 at the well-established p53 responsive promoter PIG3, (p53 induced gene 3) involved in apoptosis (Polyak *et al.*, 1997; Venot *et al.*, 1998). Interestingly, activity of p53 at another well-known p53 responsive promoter, p21 (El-Deiry *et al.*, 1993) was not greatly enhanced, demonstrating that PML IV is able to enhance p53-dependent transactivation in a promoter-specific manner. Worth noting is that PIG3 is involved in the induction of apoptosis in response to oxidative stress (Polyak *et al.*, 1997), consistent with a role for the PODs in p53-dependent apoptosis. Where PML IV mutants deficient in sumolation and consequently POD localisation were used, p53 transcriptional activity was not significantly increased. Thus, interaction of p53 with PML IV is not alone enough to enhance transcriptional activity, it must also be relocated to the PODs.

Further evidence for the importance of PML in p53 activity comes from the observation that the p53-PML binding site is the location of the majority of p53

inactivating mutations observed in naturally occurring tumours. It is possible that functional inactivation of PML through a failure to properly colocalise p53, results in tumour formation.

1.2.4.3.2. PML in p53-independent (Bcl2-inhibitable) apoptotic pathway

In mice and cells in which *Pml* was ablated by homologous recombination, Wang *et al.* (1998) demonstrated that PML antagonised the initiation, promotion and progression of tumours of various histological origins, acting as a cell-growth and tumour suppressor. They went on to demonstrate that haemoglobin concentrations and red blood cell counts following γ-irradiation were reduced to a lesser extent in *Pml-/-* mice as compared with their *Pml+/+* littermates. DNA-damage-induced apoptosis was reduced in splenocytes, and reduced lethality was observed in the irradiated *Pml-/-* group, where death following irradiation is generally due to anaemia following acute bone marrow aplasia. Their studies also demonstrated that PML is active in Fas- and caspase-dependent apoptosis. This is a p53-independent (Bcl2-inhibitable) pathway, involving the induction of Fas and its ligand (Fasl). This results in the activation of a cascade of caspase cysteine proteases, ultimately causing apoptosis. T-lymphocyte activation causes the upregulation of the Fas receptor and caspases, while DNA damage triggers the production of Fasl, again resulting in caspase activation and programmed cell death.

In situ TUNEL, cell viability and 3H-thymidine incorporation assays have shown that *in vitro, Pml-/-* splenocytes and thymocytes were protected from Fas-induced apoptosis (Wang *et al.*, 1998). In addition, *Pml-/-* mice were protected from lethality that otherwise results from massive apoptosis in the liver, consequent to administration of an anti-Fas antibody that is known to engage with and activate the Fas receptor. This protection from lethality was shown not to be the result of impaired Fas and Fasl induction. Finally, caspase 1 and caspase 3 activation was reduced in *Pml-/-* splenocytes upon γ-irradiation; inhibition of these caspases is sufficient to block Fas-induced apoptosis and DNA-damage-induced apoptosis of mitogen treated splenocytes (Nagata, 1997; Enari *et al.*, 1995; Enari *et al.*, 1996).

Taken together, these results demonstrate that PML is essential for Fas-induced cell death, acting downstream of Fas, and suggest that PML is required for caspase 1 and 3 activation.

1.2.4.3.3. PML induction of a caspase-independent death process

While the most common form of PCD is apoptosis, mediated by caspases, certain cell death processes exist that are not blocked by the broad caspase inhibitors such as zVAD-fmk (zVAD) or BD-fmk (BD) (Xiang *et al.*,1996; de Maria *et al.*, 1997; Miller *et al.*, 1997; McCarthy *et al.*, 1997). In particular, the continued induction of cell death in the presence of these inhibitors by the proapoptotic protein, Bax, which is known to trigger caspase activation, suggests that cell-death executioners other than the caspases exist.

Transfection of a PML expression vector into an SV40-transformed rat embryonic fibroblast (RET) cell line, resulted in morphological changes suggestive of apoptosis, yielding a positive TUNEL assay result and some DNA cleavage. However this cell death was not associated with the typical nuclear morphological features of apoptosis such as internucleosomal DNA laddering, chromatin condensation and nuclear fragmentation In addition, poly(ADP-ribose)polymerase (PARP) and lamin B remained uncleaved unlike during normal apoptosis when they are cleaved by activated caspase 3 (Quignon *et al.*, 1998). Together with the observation that basal levels of caspase substrates were not increased following PML transfection (in contrast to IFN treatment), this result suggests that caspases are not activated during PML-triggered cell death in this system. Moreover, using zVAD to eliminate caspase activation in IFNα-treated cells not only failed to inhibit cell death, but was found to increase PML expression and enhance IFN-triggered cell death (Quignon *et al.*, 1998).

BAX is a nuclear protein that has been shown to induce caspase-independent cell death, and which, upon induction of apoptosis, is targeted to the mitochondria (Miller *et al.*, 1997; Wolter *et al.*, 1997). Double labelling of BAX and PML has shown that a nucleoplasmic portion of BAX colocalizes with PML to the PODs. Interestingly, not only does overexpression of PML induce the recruitment of BAX to PODs in HeLa cells, but in APL cells, BAX shows a similar diffuse, speckled pattern of distribution to PML, shifting to a normal pattern after retinoic acid or arsenic treatment. Similar observations have been made for the cdk inhibitor p27KIP1, which is partially POD-associated (Quignon *et al.*, 1998).

PML may be implicated in known instances of caspase-independent cell death, induced by BAX or MYC expression, adenovirus E4orf4, ceramides and inhibition of

the ubiquitin degradation pathway. Recruitment of BAX or other proteins may constitute the death signal. SUMO-1 binding to PML may be involved, as overexpression has been linked to modulation of apoptosis (Okura *et al.*, 1996).

1.2.4.4. The PODs in transcriptional regulation

The PML protein has variously been described as both an inhibitor and an enhancer of transcription. Other RING finger family members are also implicated in transcriptional control. Two further RING finger proteins, XNF7 and pWA33, both amphibian maternal factors, associate with lampbrush chromosome loops suggesting an involvement in transcription. The localisation of CBP to the PODs also implicates these structures in transcriptional regulation, as CBP acts as coactivator to several regulatory transcriptional events (Chrivia *et al.*, 1993; Kamei *et al.*, 1996; Chakravati *et al.*, 1996) and possesses acetyl-transferase activity, implicating it in the remodelling of chromosomes/histones for active transcription (Bannister and Kouzarides., 1997; Ogryzko *et al.*, 1996). Indeed, cotransfection of PML increased transactivation by a Gal4-CBP fusion protein *in vivo* in a dose-dependent manner (Doucas *et al.*, 1999). Deletions in PML affecting its binding with CBP not only abolished transactivation of the Gal4-CBP construct, but slightly reduced basal levels of activity. These results suggest that PML binds to CBP, acting as a cofactor to increase transcriptional activity. Further, PML was found to be a potent cofactor in the hormone stimulated interaction of CBP with steroid hormone nuclear receptors (NRs), driving hormone-dependent transcription. While PML does not interact directly with NRs, cotransfection of PML and the glucocorticoid receptor (GR) into cells undergoing hormone stimulation, showed that at the lowest doses, PML increased GR activity more than tenfold (Doucas *et al.*, 1999). These data show that PML can act in transcriptional regulation as a potent cofactor for CBP. The interaction of PML and CBP with other proteins at the PODs might represent, in part, a large coactivation complex, directly participating in transcriptional regulation.

If the PODs and/or PML were involved in transcription, one might expect to find them in proximity to nascent or newly transcribed RNA. However, work utilising Br-UTP labelling of newly transcribed RNA failed to identify any colocalisation with PML or PODs (Jackson *et al.*, 1993; Wansink *et al.*, 1993). To eliminate the possibility that RNA localising to PODs is inaccessible to antibodies to Br-UTP or that the membrane permeabilisation required for Br-UTP labelling disrupts proper

RNA synthesis, LaMorte *et al.* (1998) employed a new approach involving the direct microinjection of a fluorescenated nucleotide (FITC-UTP) into HEp-2 cells. The localisation of newly synthesised RNA incorporating the stain was then visualised by immunofluorescence microscopy. By co-staining using an anti-PML antibody, it was shown that the vast majority of FITC-UTP foci localised to the PODs but that a small number also colocalized with the coiled-bodies. This group went on to argue using immunoelectron microscopy data, that nascent RNA exists within PODs, suggesting their direct involvement in the regulation of gene expression. The findings of LaMorte *et al.* (1998) were challenged, however, when electron microscopic imaging (ESI) revealed that PODs did not contain nascent RNA or chromatin, nor did they stain with antibodies recognising highly acetylated histones, a diagnostic feature of actively transcribed genes (Boisvert *et al.*, 2000). By ESI, the presence of RNA or DNA is observed as small fibres or granules rich in phosphorus. In contrast, the core of the nuclear body appeared to be protein based, being a phosphorus-depleted structure. However, phosphorus-rich fibres were observed at the periphery of the core of the POD, and, using fluorine-substituted uridine (FU) as a marker, these were shown to consist of nascent RNA. Using an antibody to the highly acetylated, transcription-associated species of histone H3 (Boggs *et al.*, 1996), it was demonstrated that highly acetylated chromatin surrounded the PODs, even if it was not found within them. Some PODs were found in association with multiple blocks of acetylated chromatin. Taken together, these results suggest that, while the core of the POD may not in fact have a direct association with transcriptionally active DNA, they may nevertheless be involved in some aspect of transcriptional regulation, perhaps creating a transcription permissible microenvironment within the nucleus. The high concentrations of CBP at the PODs might provide a suitable environment for chromatin remodelling and transcriptional activity. Additional support for POD involvement in transcription was provided by the finding that PODs are often embedded in the SC35-enriched nuclear domains where transcriptionally active genes are often localised (Ishov *et al.*, 1997; Smith *et al.*, 1999). This role for the POD would explain the observation that certain viral genomes and transcripts localise next to this structure (Ishov and Maul, 1996; Ishov *et al.*, 1997).

Immunofluorescence *in situ* hybridisation (immuno-FISH) was used to determine the three-dimensional organisation of gene-rich and gene-poor regions of DNA in the nucleus in relation to the PODs. The major histocompatibility complex (MHC) on

chromosome 6, and the epidermal differentiation complex (EDC) on chromosome 1, were examined for association with the POD in comparison with each other and a third region, 6p24 of chromosome 6, containing no known genes and flanked by two genes (Olavesen *et al.*, 1997), neither of which is expressed in human fibroblasts (Ebisawa *et al.*, 1999; Huang and Domann, 1999). Probes hybridising to the LMP/TAP genes of the MHC region, the SPRR genes of the EDC, and a 500bp sub-region of 6p24, allowed visualisation of the genomic regions, and a rabbit polyclonal anti-PML antibody was used to relate their locations to that of PML under confocal microscopy analysis.

Using this technique, Shiels *et al.* (2001) demonstrated that PODs were found localising with MHC-probes in ~42% of nuclei. In comparison, PODs colocalised with EDC probes in ~24%, and with 6p24 probes in ~20% of nuclei respectively. Statistical analysis confirmed that these observations represented a significant difference in POD association between the MHC and other regions. These results indicate that the PODs can form specific associations with chromosomal regions. To test whether this MHC-POD association reflected transcriptional activity of the locus, cells were treated with known regulators of MHC transcription. Treatment with IFNγ stimulates activity at the MHC (Boehm *et al.*, 1997), and also induces PML expression. Despite this upregulation, no statistically significant alteration to the MHC-PML association was observed.

While not completely clarifying the role of PODs in transcription, the above-outlined results do suggest that in at least some cases, the PODs or surrounding regions are involved in nascent RNA synthesis. It has been suggested that PODs might associate with specific gene-rich regions such as the MHC to form a functional compartment involved in the regulation of transcription of that region. While a direct role for PODs in transcription of genes other than those involved in growth suppression and/or apoptosis would appear to be at variance with these processes, it may be that the functional state of the structure is delicately balanced between inhibition or enhancement of specific gene expression, dependent upon external or internal stimuli.

1.2.4.5. PML interactions with cyclin D1 and eIF-4E

Cyclins were originally discovered as a result of their intense synthesis following the fertilisation of marine invertebrate eggs (Rosenthal *et al.*, 1980). DNA replication and

mitosis are dependent on the activity of heterodimers comprising a catalytic cyclin-dependent kinase (cdk) subunit, with a cyclin subunit. There are several different types of cyclin and cdk that are involved at different stages in the cell cycle. Cell cycle progression is driven by the coordinated regulation of the activities of cdks in response to external signals, achieved by the post-translational modification of cdks by phosphorylation-dephosphorylation cascades, and by changing rates of transcription or proteolysis of individual cyclins, with consequent changes in the substrates of cdk through the cell cycle (reviewed by John *et al.*, 2001; Obaya and Sedivy, 2002). The process is regulated by protein kinases and phosphatases such as Wee1 and Cdc25 (reviewed by Niwa and Walter, 2000; John *et al.*, 2001).

The cyclin D1 protein functions at the G1/S transition of the cell cycle (Hunter and Pines, 1994) and is found in complex with Cdc28 to initiate the expression of other cyclins and genes involved in DNA replication. Because expression of cyclin D1 is strongly influenced by conditions affecting cell growth, it has been suggested to play a central role in coupling growth rate to cell cycle progression (Neufeld and Edgar, 1998). Overexpression of eukaryotic translation initiation factor 4E (eIF-4E) was demonstrated to increase cyclin D1 levels (Rousseau *et al.*, 1996). This translation factor has been shown to promote growth and oncogenic potential, playing well defined biochemical roles as the limiting component in translation initiation (Sonenberg and Gingras, 1998). eIF4E binds the 5'm^7G cap of mRNA, and this cap-binding is essential for the initiation of cap-dependent translation and the regulation of mRNA stability (Marcotrigiano *et al.*, 1997; Keiper and Rhoads, 1997; Dehlin *et al.*, 2000) Overexpression of eIF4E has been linked to increased nucleocytoplasmic transport and increased cytoplasmic levels of cyclin D1 (Rousseau *et al.*, 1996; Lai and Borden, 2000). The resultant increase in cyclin D1 protein levels has been linked to the transformation activity of eIF4E (Rousseau *et al.*, 1996).

Interestingly, immuno-staining experiments demonstrated that a large proportion of eIF4E colocalised with PML to a subset of PODs (Lai and Borden, 2000; Cohen *et al.*, 2001). Immunopurification assays were used to demonstrate a direct and specific interaction between the two proteins, and it was later shown that this interaction occurred at the RING finger of PML (Cohen *et al.*, 2001). These observations, and the known roles of the PODs in apoptosis and cell-cycle regulation, suggested a potential connection between these structures and cyclin D1 regulation. Lai and Borden (2000) went on to determine the significance of the observed interaction between PML and

eIF4E by transfecting NIH3T3 cells with PML and monitoring the production of the cyclin D1 and glyceraldehyde 3 phosphate deydrogenase (GAPDH) proteins. GAPDH was chosen as a control as the level of the protein product had previously been shown to be unaffected by overexpression of eIF4E (Rousseau *et al.*, 1996). They demonstrated that PML overexpression specifically reduced the production of cyclin D1, via increased retention of mRNA in the nucleus, mediated by the PML-eIF4E interaction. This effect could be abrogated by the coexpression of eIF4E with PML, which caused an increase in the nuclear-cytoplasmic transport of cyclin D1 mRNA. PML was found to modulate the mRNA transport function of eIF4E by reducing its affinity for the m^7G cap substrate (Cohen *et al.*, 2001). These results provide a mechanism for the previous observation that cyclin D1 protein levels were reduced by PML overexpression in breast cancer cells (Le *et al.*, 1998).

Further studies have shown that eIF4E forms nuclear bodies independently of PML. In an APL-derived cell line where the PODs were disrupted, eIF4E formed nuclear bodies, which became the sites for POD formation upon ATRA treatment of the cells (Cohen *et al.*, 2001). Dispersal of eIF4E from the nuclear structures by treatment with an analogue of its substrate, m^7GpppG resulted in the disruption of the PODs via the dissociation of PML (Cohen *et al.*, 2001). These results suggest that eIF4E may be ancestral to PML and have important implications for the role of the PODs. These structures may have evolved as an elaboration of eIF4E regulation. This idea is supported by the conservation of eIF4E among eukaryotes from unicellular yeast to mammals (Sonenberg and Gingras, 1998) whereas PML is present only in mammals, and the observations that *PML-/-* mice are morphologically normal (Wang *et al.*, 1998) whereas deletion of the *eIF4E* gene appears impossible due to its essential function in cellular metabolism.

1.2.4.6. Other POD associated proteins

SUMO-1 and CBP have already been discussed in relation to PML, but several other proteins are commonly found in association with PODs and may have a bearing on their function. Of major importance is Sp100 and its variants, and others include ISG20, Int-6 and LYSP100/Sp140.

Sp100 is an acidic protein that is known to transactivate a number of promoters, although the mechanism by which this is achieved is presently unclear (reviewed by Sternsdorf *et al.*, 1997; Dent *et al.*, 1996). Like PML, Sp100 is highly interferon-

inducible. Several different isoforms are generated by alternative splicing at the C-terminus and are designated SpAlt or Sp100B (Dent *et al.*, 1996; Guldner *et al.*, 1999). The Sp100 variants of the SpAlt family, contain a high mobility group 1 (HMG1) protein sequence, called an HMG-box, as a C-terminal domain (Guldner *et al.*, 1999). Indeed, SpAlt-HMG has the highest homology to HMG1 thus far observed in any HMG-box protein. Proteins of this superfamily have been shown to bind directly to DNA, some with high sequence specificity (reviewed by Grosschedl *et al.*, 1994), and have been shown to be involved in processes as diverse as activation of rRNA transcription, sex determination in mammals or determination of fungal mating type (Laudet *et al.*, 1993).

Lysp100-A, B and Sp140 are splice variants from the same gene, taken by some to represent a leukocyte-specific class of POD component (Bloch *et al.*, 1996). Others debate the exact localization of these proteins, one group reporting only partial overlap with PODs in novel domains termed LANDS (Lymphocyte Associated Nuclear Domains) (Dent *et al.*, 1996). The proteins have several structural similarities to Sp100 and SpAlt/SP100-B, but the LYSP100B/Sp140 proteins contain two additional motifs not present in any known Sp100 splice variant. These constitute a RING-finger like, cysteine/histidine rich PHD domain, and a bromodomain. The pairing of these domains is common to several cellular co-activators including CBP (Arany *et al.*, 1995). Thus it is possible that LYSP100B/Sp140 act as transcriptional co-activators, and it is thought that they may play a role in lymphocyte differentiation (Bloch, 1996). While limited to lymphocytes, the postulated role of these proteins is, given their similarity to standard POD components, consistent with a role for PODs as centres for the accumulation and regulation of factors important in cell growth, differentiation and transcriptional regulation.

ISG20 (interferon-stimulated gene product of 20kDa) was identified by differential screening of a cDNA library from an IFN treated-human lymphoblastoid cell line, in a search for unknown IFN-inducible proteins. It was observed by confocal immunofluorescence analysis to localise to the PODs although yeast two-hybrid study showed no direct interaction between ISG20 and PML or Sp100 (Gongora *et al.*, 1997). Sequence analysis of the ISG20 cDNA suggests a very basic protein with a relative molecular mass of 20.4kDa. Interestingly, it is predicted to form a coiled-coil domain and, as these structures are known to mediate protein:protein interactions, it is likely that ISG20 acts as part of a multiprotein complex.

The function of ISG20 is not yet known, but certain pieces of evidence support the idea that it may act as a negative regulator of cell division. The subcellular localisation of ISG20 is predominantly nuclear and punctate, but varies from one cell to another. This presumably reflects the cell-cycle dependent state of the PODs. ISG20 may have a direct role in the cell cycle, or simply be shuffled about as the PODs undergo alterations. In addition, ISG20 has significant homologies to the *Xenopus laevis* XPMC2 gene product, which has been shown to rescue a fission yeast mitotic catastrophe mutant defective in both Wee1 and Mik1 kinases (Su and Maller, 1995). While ISG20 did not achieve similar complementation, the protein appears truncated in the N-terminal half in comparison with XPMC2, and it is possible that the protein requires additional interactions via the coiled-coil domain to mimic the function of the amphibian gene product in humans.

The *Int-6* gene was originally identified as one of the integration sites of the murine mammary tumour virus (MMTV) (Marchetti *et al.*, 1995), and has been shown to colocalise to the PODs, probably through interaction with the Ret finger protein (Rfp) (Desbois *et al.*, 1996). It has been shown to encode the p48 component of the eukaryotic translation initiation factor-3 (eIF3-p48) and to play a role in the control of cell growth (Asano *et al.*, 1997; Akiyoshi *et al.*, 2001). Disruption of the Int-6 locus by integration of the MMTV virus results in expression of a truncated protein, and has been speculated to be the crucial event in the virus-induced transformation process (Marchetti *et al.*, 1995). More recently, a reduction in Int-6/eIF3-p48 expression has been observed in certain malignancies (Marchetti *et al.*, 2001). In summary, the role of Int-6 is currently poorly understood, but it is possibly another negative regulator of cell growth and division.

Daxx is a Fas-binding protein that has been shown to promote Fas-mediated apoptosis through activation of the Jun NH_2-terminal kinase (JNK) and JNK kinase ASK1 (apoptosis signal-regulating kinase 1) (Yang *et al.*, 1997; Chang *et al.*, 1998) and is a strong repressor of basal transcription, appearing to interact directly with histone deacetylases. It was demonstrated that Daxx resided primarily in colocalisation with PML in the nucleus at the PODs (Li *et al.*, 2000). Interestingly, recruitment of Daxx to the PODs was shown correlate with enhanced Fas-mediated cell death (Torii *et al.*, 1999) and with the inhibition Daxx-mediated transcriptional repression (Li *et al.*, 2000). SUMO-1 modification of PML was shown to be required for this effect (Ishov *et al.*, 1999; Li *et al.*, 2000). That PML interacts with Daxx in this manner, suggests a

role for the PODs in suppression of transcriptional repression, and again implicates these structures in the regulation of Fas-mediated apoptosis.

1.2.4.7. PODs and virus infection

As previously mentioned, the PODs are dynamic sub-nuclear structures that can be altered by any of several factors. Among these, infection by certain viruses can bring about changes in the appearance, distribution or composition of these bodies, notably human influenza A, human T-cell leukaemia virus (HTLV), herpes simplex virus (HSV), human cytomegalovirus (CMV), Epstein-Barr virus (EBV), and adenovirus (reviewed by Sternsdorf *et al.*, 1997). Taken with the highly interferon-inducible nature of PML and other POD proteins, the propensity of viruses to disrupt these structures make it likely they have a role in the early or late antiviral response, which the viruses are seeking to evade.

1.2.4.7.1. PODs and RNA virus infections

Infection with the RNA virus, influenza A, causes an increase in the number and staining intensity of PODs in HeLa cells when using Sp100 antibodies (Guldner *et al.*, 1992) similar to that observed upon interferon treatment of cells. Interestingly, it has been reported that overexpression of PML confers resistance to infection by both influenza A and vesicular stomatitis virus (VSV), both RNA viruses whose infections are sensitive to interferon (Chelbi-Alix *et al.*, 1998). PML expression was found to interfere with VSV mRNA and protein synthesis. The inhibition of viral multiplication by PML was found not to be common to all RNA viruses, and was not as strong as that conferred by the IFN mediator protein, MxA. However, these results suggest that elevated PML expression can contribute to the antiviral state induced in IFN-treated cells.

HTLV is the human retrovirus responsible for adult T cell leukaemia. The viral oncoprotein Tax, interacts with the cellular protein Int-6, which has been reported to localise to the PODs. Expression of the Tax oncoprotein of HTLV I from a Herpesvirus saimiri vector, was shown to induce a diffuse, cytoplasmic redistribution of Int-6 from the PODs. Tax binds to Int-6, causing it to be retained in the cytoplasm and preventing its localisation to PODs (Desbois *et al.*, 1996). Expression of Tax is necessary and sufficient for transformation of primary human T cells (Grassman *et*

al., 1992) and since no other POD proteins are affected by Tax, this suggests that Int-6 redistribution is significant to this process.

1.2.4.7.2. PODs and herpes virus interactions

During infection with the various herpes viruses, the parental viral genomes migrate to the periphery of the PODs, components of which are then dispersed or relocated (Kelly *et al.*, 1995; Korioth *et al.*, 1996; Maul and Everett, 1994; Ishov and Maul, 1996).

The HSV-1 viral immediate-early (IE) protein, Vmw110 (also known as ICP0) is a positive regulator of gene expression that is required for the disruption of the PODs during HSV infection (Maul *et al.*, 1993; Maul and Everett, 1994). This disruption was found to correlate with the loss of several PML isoforms, dependent upon Vmw110 and active proteasomes (Everett *et al.*, 1998). HSV-1 infection of HEp-2 cells caused the rapid loss of those higher molecular-weight isoforms of PML thought to be SUMO-1 modified. Indeed, transfection of a SUMO-1 expressing plasmid (pCIPIC1) and subsequent SDS-Page and Western blot analysis, produced a multitude of high molecular weight polypeptides corresponding to SUMO-1 conjugates. These included a major band at 90kDa corresponding to a form of RanGAP1 known to be covalently attached to SUMO-1 (Mahajan *et al.*, 1997; Matunis *et al.*, 1997). Upon superinfection with wild-type virus, many of these higher molecular weight SUMO-1 conjugate bands disappeared. However, superinfection with Vmw110-deficient mutant viruses did not result in the loss of any SUMO-1 conjugates, demonstrating that this process is dependent upon Vmw110 and the integrity of its RING finger. As certain of the conjugate bands were not reduced (including that for RanGAP1), this would appear to be a specific process.

An HSV-1 mutant deficient in POD modification was used to determine the location of viral DNA replication compartments relative to the PODs in HEp-2 cells. Using the Vmw110 RING finger deletion mutant FXE, Ishov and Maul (1996) demonstrated that while the replication compartments developed away from the PODs, later in infection (8 hr p.i.) the two were adjacent. The use of wild-type virus demonstrated that this was not mutant-specific behaviour, and that even at 3 hours after infection, HSV-1 input DNA and transcripts could be observed preferentially localising to the periphery of the PODs. These results paralleled findings obtained from the study of the relationship between adenovirus 5 DNA and the PODs by the same group.

In addition, human cytomegalovirus (HCMV) and Epstein-Barr virus have also been demonstrated to disperse POD-associated proteins.

Upon infection with HCMV, PML and Sp100 were rapidly dispersed from the PODs, as occured during HSV-1 infection (Kelly *et al.*, 1995; Korioth *et al.*, 1996). This was induced by expression of the immediate-early gene IE-1 (Korioth *et al.*, 1996).

In the case of Epstein-Barr virus, the redistribution of POD proteins occurred in a markedly different manner. Bell *et al.* (2000) found that in latently infected Burkitt's lymphoma and lymphoblastoid cells, the PODs remained intact, with no association between these structures and the viral genomes. Interestingly, upon lytic activation, the POD-associated proteins were sequentially dispersed at different stages of the lytic cycle, with Sp100 and Daxx being dispersed before the onset of viral replication, and PML dispersed after. The EBV genome associated with the remnants of the POD, which were retained until the early stages of lytic replication (Bell *et al.*, 2000). Although EBV has developed an alternative method of replication by remaining latent in cells, it would appear from the results shown above, that dispersal of POD proteins is important for the more "aggressive" process of lytic replication.

1.2.4.7.3. PML, PODs and adenovirus infection

The replication domains of adenovirus 5 are visible as round or goblet shaped, viral DNA-binding protein (DBP)-positive sites, within the nucleus of infected cells (Pombo *et al.*, 1994). Early in infection, replication domains are found in association with sites of high nuclear factor-1 (NF-1) accumulation (Ishov and Maul, 1996). NF-1 is a cellular, single-stranded DNA-binding protein that is present throughout the nucleus but is highly concentrated in a few domains numbering one to six in HEp-2 cells. Later in Ad5 infection, when the replication sites have expanded, the protein is targeted to the viral replication domains where it is used to aid assembly of the nucleoprotein complex at the viral origin of replication (Bosher *et al.*, 1992). Replication sites are also often found in close proximity to coiled bodies. However, not all sites of viral replication are associated with an NF-1 site or coiled body (Ishov and Maul, 1996), indicating that these cellular structures are not of primary importance in Ad5 DNA replication.

During adenovirus type 5 infection, the POD-associated proteins PML and Sp100 were shown to be redistributed into track-like structures. These "tracks" had no obvious spatial relationship with the viral replication domains early in infection

(Ishov and Maul, 1996). More detailed analysis revealed that while Sp100, PML and other POD-associated proteins were distributed to the tracks prior to viral DNA replication, most of these proteins (notably Sp100) eventually segregated from the tracks and joined the replication domains upon DNA replication. Interestingly, of the antigens tested, only PML did not at any point join the replication domains as determined by immunofluorescence microscopy, remaining at all times in tracks. In contrast, while adenovirus relocates the majority of POD proteins to viral replication domains, HSV-1 does not (Maul *et al.*, 1993; Maul and Everett, 1994). The significance of these relocations to the progress of adenovirus infection is as yet not known. The distribution of POD-associated proteins to viral replication domains might indicate a positive role for these proteins in viral replication, or might be an element of the host antiviral response. Ishov and Maul (1996) went on to use an *in situ* nuclear run-on procedure incorporating BrUTP, to demonstrate by confocal microscopy that the distribution of the POD-associated proteins within the viral replication domains did not correlate with viral transcription.

By identifying a mutant adenovirus defective in track formation, it was possible to assign responsibility for POD reorganisation to a single viral gene product. Distinct deletion mutants of the E4 region were infected into HeLa cells, representing deletions of ORFs 1 and 2 (H5dl 1005), ORFs 1, 2 and 3 or just ORF3. The results showed that the viruses lacking E4orf3 did not form PML tracks (Carvalho *et al.*, 1995). These observations were mirrored by the work of Doucas *et al.* (1996), who demonstrated the requirement for E4orf3 in track formation by using an insertion mutant of E4orf3 (inorf3), where the number of infected cells scoring positive for track formation was drastically reduced. Nevertheless, Sp100 was still found to locate to the viral replication domains, albeit after a delay. In a reciprocal experiment, an E4 mutant expressing only E4orf3 was shown to induce POD reorganisation at a similar efficiency to wild-type Ad5. It was shown by immunofluorescence microscopy that the E4orf3 protein colocalized to these filamentous tracks with PML. Transient transfection of both HeLa and Hep-2 cells with a pCMV E4orf3 expression vector also resulted in the formation of PML/E4orf3 co-staining tracks (Carvalho *et al.*, 1995; Ishov and Maul, 1996; this thesis), demonstrating that E4orf3 was necessary and sufficient for track formation. Overexpression of PML by cotransfection antagonised track formation, generating unusually large PODs. Co-expression of

E4orf3 and PMI Δlz, deleted in the 60 amino acids constituting the main dimerization domain, resulted in a diffuse nuclear and cytoplasmic PML stain, where E4orf3 did not associate with the mutant PM protein, but was found at the PODs with endogenous PML.

Mutants for the E1A, E1B and E3 regions had wild-type phenotypes in respect to POD reorganisation, other than that onset of track formation was delayed from ~8hr to ~24 hrs p.i. where cells were infected with the E1A deleted mutant (Ishov and Maul, 1996). This is an interesting observation, as the E1A protein can be found in association with the PODs following infection or transfection of the protein, though it does not appear to affect the integrity of the structures. It may more simply reflect delayed expression of E4orf3 in the absence of E1A transactivation.

Use of the deletion mutant H5 1004 which expresses only ORF1 from the E4 gene region, enabled retention of the PODs during infection, and here it was possible to demonstrate that viral replication domains located adjacent to or closely associated with PODs. Further, using wtAd5, it was shown that while at early stages in infection (1.5hr p.i), adenoviral DNA had no obvious correlation with PODs, at later times (4hrs p.i.) ~50% of the input viral DNA was found close to the PODs. As the PODs only occupy <0.05% of the total nuclear volume, this is undoubtedly significant and represents a preferential association of viral DNA with PODs. This association was found to be independent of new transcription and protein synthesis.

POD disruption is common to several different viruses suggesting that it plays a crucial role in the success of infection. However, the fact that E4orf3 is absolutely required for track formation while E4orf3 deficient mutants grow in a similar manner to wild-type viruses, at least in standard cell cultures, argues that track formation is not a necessity for viral replication. However, while not essential, the reorganisation of the PODs may be linked to more efficient viral replication. It has been demonstrated, in an otherwise completely E4-deficient background, that E4orf3 stimulates the efficiency of viral propagation >2000-fold (Huang and Hearing, 1989a). Cell lines engineered to stably overexpress PML showed an inhibition of track formation by E4orf3 (using dl366*+ORF3), concomitant with a decrease in replication of the virus (Doucas *et al.*, 1996). This result argues that the function of E4orf3 in POD reorganisation is responsible at least in part, for the ability of the protein to enhance viral propagation.

The biochemical status of PML following Ad5 infection was analysed by Leppard and Everett (1999), using Western blotting with the PML specific monoclonal antibody, 5E10 (Sturman *et al.,* 1992). Uninfected cells had the typical array of PML isoforms with SUMO-1 modified and unmodified forms present (see fig 1.4.). By 16 hours p.i., two new bands had formed, and a third intensified, at the apparent expense of intensity in the major PML bands at about 120 and 140kDa. At a later stage in infection, the isoforms generally held to represent SUMO-1 modified PML were reduced or absent, as were the two slower migrating infection-specific bands. However, the third band generated by Ad5 infection (indicated in lane 10 of fig 4.1. by the filled arrow), became more intense.

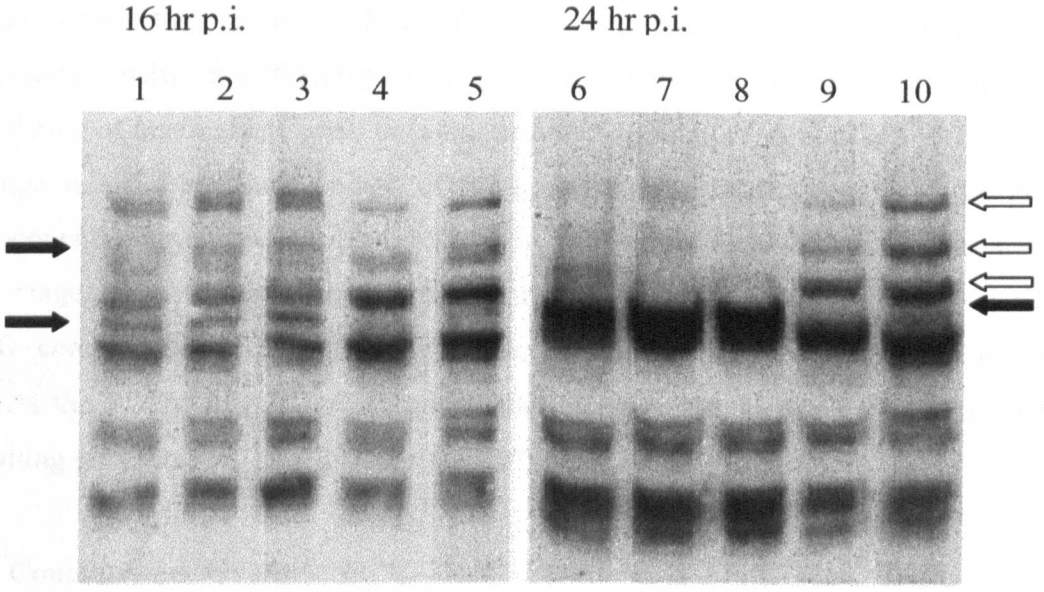

Fig 1.4. PML isoforms in infected HEp-2 cells. HEp-2 cells were infected with adenovirus *dl*309 (lanes 1, 6), *dl*338 (2, 7), *dl*355 (3, 8), *dl*1-3 (4, 9) or mock infected (5, 10) at 37°C. Extracts were separated on a 6% SDS-Page gel, blotted and probed for PML with mAb 5E10. The filled arrows show virus specific PML isoforms when infected with E4orf3 *wt* virus. Open arrows point out SUMO-1-conjugated isoforms lost during infection with E4orf3 *wt* virus (from Leppard and Everett, 1999).

In comparison, extracts of cells infected with various deletion mutants demonstrated that the same changes to the PML species occurred in the absence of either E4orf6 or E1B-55kDa. However, cells infected with a deletion mutant lacking E4 Orfs1-3 showed the same PML staining pattern as uninfected cells (Leppard and Everett, 1999). These results demonstrated that either E4orf1, 2 or 3 proteins or a combination of all three, was required for the PML biochemical alteration underlying this change

in banding pattern. As E4orf3 has been shown to be necessary and sufficient for POD reorganisation as determined by immunofluorescence, it seems likely that these phenomena are two aspects of the same, Orf3-dependent process.

Interestingly, the major novel PML species observed subsequent to wild-type adenovirus infection has marked similarity to the new species observed during the normal cell-cycle at mitosis when the PODs temporarily disperse (see 1.2.4.2.). Also, the slower migrating SUMO-1 modified PML isoforms are reduced or lost as occurs during mitosis. It would appear that adenovirus might make use of a similar mechanism, potentially hijacking the cell's own components to deregulate cell cycle progression and prevent cell-suicide upon infection.

1.2.4.7.4. POD redistribution after non-virological stress

In attempting to gain an insight into the role of the PODs, it is worth noting other stress factors that result in abnormal POD appearance. Heat shock or cadmium treatment results in redistribution of the PODs into a microspeckled appearance consisting of hundreds of small dots amongst the chromatin (Maul *et al.*, 1995). This change is rapid and independent of protein synthesis. During recovery, the POD components regroup into discrete structures, passing through an intermediate track-like stage. These observations might result from a process of active transport with POD components travelling along nuclear filaments. Amino acid starvation also affects the PODs, in this case reducing their number but increasing their size (the resulting structures are called "large bodies") (Kamei, 1996).

1.3. Conclusions

The importance of the cellular structures known as PODs and their associated proteins has become increasingly clear as research in diverse biological fields has converged on these subnuclear domains and their functions. Currently, they appear to be involved in several distinct cellular and viral processes, leading to a certain degree of confusion as to their prime function in the cellular environment. However, perhaps it will be possible to relate these seemingly disparate functions to a coherent whole, by gaining a greater insight into each separate process. It already seems apparent that, through negative regulation, the defining POD component, PML, plays important roles in cell-cycle regulation and PCD. While these are separate processes, it is not difficult to see how these two functions are related, in that both involve altered

patterns of transcription; indeed they are linked processes, failure of one resulting in the other. The model of the POD as the centre of a cell cycle "braking" and apoptosis mechanism, fits comfortably with the observed disruption of the structures in several malignancies and by virus infections, where unregulated cell proliferation is necessary or advantageous to the progression of the disease.

Although, simplistically, this hypothesis might imply that PODs negatively regulate gene expression, work focusing on the transcriptional significance of the PODs suggests a more positive role. CBP is a coactivator of several regulatory transcriptional events, Sp100 is a known transcriptional transactivator, and even PML has been reported to act as a transcriptional co-activator. In addition, certain viral transcripts localise next to these structures (Ishov and Maul, 1996; Ishov *et al.*, 1997), and PODs seem to associate preferentially with transcriptionally active chromatin.

These observations, taken with the apparent identification of nascent RNA at the peripheries of the PODs, seem to strongly indicate a role for these structures in transcriptional activation where the POD may enhance transcription of target genes through recruitment of activators, and also the inhibition of transcriptional repressors such as Daxx. Until the exact function of each POD-associated protein is known, it is entirely possible that the role of the POD in transcription is still an inhibitory one. PML after all is required for localization of CBP to the POD, and suppresses production of the cyclin D1 protein by interaction with eIF4E at the POD. Perhaps the PODs exist to concentrate antagonistic factors in one location, where they can be released as is appropriate. This may be a complex interaction of multiple sub-units, not requiring direct association of all components with PML. Instead, each may be sensitive to the state of others, thus providing a framework for the establishment of feedback loops and potentially quite complex responses to numerous stimuli. This would also explain why, during adenovirus infection, the PODs are dispersed, but the majority of the associated proteins ultimately localise to the nearby viral replication domains, while PML is excluded.

1.4. Aims of this Thesis

The main aim of this thesis was to further investigate the role of the PODs, using a virological approach to study several aspects of virus-host interaction between Ad5 E4orf3 and PML and the PODs. Specifically, the objectives were:

- To identify regions of the Orf3 gene necessary for POD component reorganisation and PML modification by expressing the gene in eukaryotic cells, using eukaryotic expression vectors
- To determine the relevance of those functions to the infection process
- To mutate single amino acids within Orf3 using PCR techniques and examine any resultant modification of function in POD organisation/PML modification
- To determine whether POD reorganisation and PML modification functions of Orf3 could be separated in our system
- To relate structural information to observed interactions between E1B-55K, Orf3 and POD components in both mutant and wild-type virus/viral elements, making use of immunofluorescence analysis and western blotting techniques
- To determine a phenotype for Orf3 mutants using whole virus

2. Materials and Methods

2.1. Materials

2.1.1. Common buffers and solutions

Chloroform/iso-amyl alcohol: 96% (v/v) chloroform, 4% (v/v) iso-amyl alcohol.

LB: 1% (w/v) bactotryptone, 1% (w/v) NaCl, 0.5% (w/v) yeast extract.

LB agar: LB containing 1.5% (w/v) bacto-agar.

Miniprep solution I: 25mM Tris.HCl adjusted to pH 8.0 with HCl, 10mM EDTA, 50mM glucose (5mg/ml lysozyme added just prior to use).

Miniprep solution II: 200mM NaOH, 1.0% (w/v) SDS.

Miniprep solution III: 600mM potassium acetate, 11.5% (v/v) glacial acetic acid, pH 4.8 with acetic acid if required.

Phenol/chloroform: 50% (v/v) Tris-buffered phenol, 48% (v/v) chloroform, 2% (v/v) iso-amyl alcohol.

Phosphate buffered saline (PBS): 137 mM NaCl, 2.7 mM Na_2HPO_4, 1.4 mM KH_2PO_4.

1 X SDS-PAGE loading buffer: 10% (v/v) glycerol, 50mM Tris.HCl pH 6.8, 4% (w/v) Sodium Dodecyl Sulphate (SDS), 0.01% (v/v) bromophenol blue, then add 200mM Diothiothreitol (DTT) just prior to use.

TBE: 89 mM Tris base, 89 mM boric acid, 1 mM ethylenediaminetetra-acetic acid (EDTA) pH 8.0.

TD: 25 mM Tris.HCl pH 7.5, 137 mM NaCl, 5 mM KCl, 0.7 mM Na_2HPO_4.

TE: 10 mM Tris.HCl pH 8.0, 1 mM EDTA.

TFB I: 100mM RbCl, 50 mM $MnCl_2$, 10 mM $CaCl_2$, 30 mM potassium acetate, 10% (w/v) glycerol, adjusted to pH 5.8 with 1M HAc.

TFB II: 10 mM 3-[N-Morpholino]propanesulphonic acid (MOPS), 10 mM RbCl, 75 mM $CaCl_2$, 19% (w/v) glycerol, adjusted to pH 7.0 with 4M NaOH.

TNE: 10mM Tris.HCl pH 8.0, 100 mM NaCl, 1 mM EDTA.

TS: 25 mM Tris.HCl pH 7.5, 137 mM NaCl, 5 mM KCl, 0.7 mM Na_2HPO_4, 0.9 mM $CaCl_2$, 1 mM $MgCl_2$.

2.1.2. Bacterial strains

Escherichia coli strain	Phenotype
XL-1 Blue	*RecA1 endA1 gyrA96 thi-1 hsdR17 supE44 relA1 lac* [F'*proAB lacI*^{q}*ZΔM15* Tn*10* (Tet^{r})]. (Used for all cloning steps)

2.1.3. Adenovirus strains

Virus strain	Phenotype
*Wt*300	Wild type (Jones and Shenk, 1979)
*dl*355	Inactivation of E4-Orf6 product (Halbert *et al.*, 1985)
inorf3	Inactivation of E4orf3 product (Huang and Hearing, 1989)

2.1.4. Cell lines

Cell line	Origin
293	Adenovirus-transformed human embryonic kidney (Graham *et al.*, 1977)
HeLa	Human cervical epitheloid carcinoma (Scherer *et al.*, 1953)
HEp-2	Human epidermoid carcinoma (Moore *et al.*, 1955)

2.1.5. Antibodies and conjugates

	Protein recognised		Dilution used	
			Western	I.F
Primary antibodies	PML	Mouse monoclonal 5E10 (Stuurman *et al.*, 1992)	1:20	1:10
	PML	Mouse monoclonal PG-M3 (Santa Cruz Biotechnology Inc.)	1:500	1:500
	E2a DNA-binding protein (DBP)	Mouse monoclonal B6-8 (Reich *et al.*, 1983)	N/A	1:10
	E1b 55K	Mouse monoclonal 2A6 (Sarnow *et al.*, 1982)	N/A	1:100
	E1b 55K	Rat monoclonal 9C10 (Zantema *et al.*, 1985)	N/A	1:10
	E4orf3	Mouse monoclonal A4-7 (Carvalho *et al.*, 1995)	1:5000	1:1000
	E4orf3	Rat monoclonal 6A11 (Nevels *et al.*, 1999)	1:20	1:10
Secondary antibodies	Mouse Ig	Biotinylated goat (Amersham Pharmacia Biotech)	1:400	N/A
	Mouse Ig	Horseradish-peroxidase linked goat A4416 (Sigma)	1:500-1000	N/A
	Mouse Ig	Horseradish-peroxidase linked goat (Chemicon International)	1:500	N/A
	Mouse Ig	Fluorescene isothiocyanate (FITC)-conjugated goat (Calbiochem)	N/A	1:100
	Rat Ig	Biotinylated goat (Amersham Pharmacia Biotech)	1:400	N/A
	Rat Ig	Horseradish-peroxidase-linked goat (Chemicon International)	1:500-1000	N/A
	Rat Ig	Rhodamine-conjugated goat (Calbiochem)	N/A	1:100

2.1.6. Oligonucleotides

All oligonucleotides were obtained from Life Technologies (now Invitrogen) and are shown 5' to 3'.

2.1.6.1. PCR Primers

Primer JD1: GGCCAGATATACGCGTTGACATTG

Primer JD2: CGCCACTGTGCTGGATATCTGC

Primer JD3: TATTTGGCTATGGTTGAAGGTGCTGGAATG

Primer JD4: CAGCACCTTCAACCATAGCCAAATAATTCTC

Primer JD5: GCGAGGCCGTTCACTTAATAGATCTTC

Primer JD6: TATTAAGTGAACGGCCTCCCCTCC

Primer JD7: ACGTGGCCGCCGTTTGCCTTTTG

Primer JD8: AAAAGGCAAACGGCCGCCACGTCCAAGT

Primer JD11: GACCACGCCGTTCACTTAATAGATCTTC

Primer JD12: AGTGAACGGCGTGGTCAAACTCTACAGC

Primer JD13: GCGAGATATGGTTGAAGGTGCTGGAATG

Primer JD14: CCTTCAACCATATCTCGCCACCTTC

Primer JD15: GAGGCTGAAGGAGCAGATTTTTACAATGGCCGGACT

Primer JD16: CTGCTCCTTCAGCCTCAAGCAGCGAATC

Primer JD17: TTTGACCACGCCGCCGGAG

Primer JD18: TCCGGCGGCGTGGTCAAA

Primer JD19: CCACCGCCGGGGAGCGCGTTCACTTAATA

Primer JD20: TCCCCGGCGGTGGCGTGGTCAAA

Primer JD21: ACCGGAGCCGAGCGCGTTCACTTAAT

Primer JD22: TATTAAGTGAACGCGCTCGGCTCCGGTG

Primer JD23: ATTAAGTGAACGCGGGCCCCTCC

Primer JD24: GGAGGGGCCCGCGTTCACTTAATAG

Primer JD25: TCGAGTAATACGACTCACTATAGGGCGAG

Primer JD26: TCGACTCGCCCTATAGTGAGTCGTATTAC

Primer JCD27: CTGGAACAATGACAGTGGAGAG

Primer JCD28: CATTATGACTCCGGACATGACC

2.1.6.2. Sequencing primers

Primer JD9: GCACAGTCGAGGCTGAT

Primer JD10: CACTGCTTACTGGCTTATCG

Primer JCD29: CCACCACCGCAGAATAAGCC

Primer JCD30: GCAGACCTGCACGATTATGT

2.2. Suppliers

All chemicals of analytical or molecular biology grade were supplied by Sigma (Poole, Dorset, UK) or BDH Laboratory supplies (Merck Ltd, Poole, Dorset, UK) unless otherwise stated below.

Amersham Pharmacia Biotech (Bucks., UK).

Biotinylated goat α-mouse IgG, Streptavidin-biotinylated horseradish peroxidase complex, Hybond C membrane, SDS-PAGE molecular weight markers.

Becton-Dickinson (Cockeysville, USA).

Yeast extract.

BioRad (Hemel Hempsted, Herts., UK).

Acrylamide, N,N'-methylene-bis-acrylamide, ammonium persulphate, electrophoresis grade SDS.

BOC (Surrey, UK)

CO_2, dry ice.

Calbiochem (Nottingham, UK).

Goat α-mouse IgG fluorescein isothiocyanate (FITC)-conjugate, goat α-rat IgG rhodamine conjugate.

Chemicon International (Harrow, UK).

Goat α-mouse IgG horseradish-peroxidase conjugate, goat α-rat IgG horseradish-peroxidase conjugate.

Difco Laboratories (Hants., UK).

Bacto-agar, bactotryptone, Noble agar.

Fisher Scientific (Loughborough, UK).

Caesium chloride, SDS.

Fuji Photo Film Co.Ltd. (Dusseldorf, Germany).

Super RX X-ray film.

Gibco BRL Life Technologies Ltd. (Renfrewshire, Scotland).

Restriction enzymes, 1kb DNA ladder, calf intestinal alkaline phosphate (CIAP), Taq DNA polymerase, T4 DNA ligase, Dulbecco's modified Eagles medium (DMEM), newborn calf serum (NCS), foetal calf serum (FCS), trypsin, versene.

Kodak (London, UK).

X-ray developing fluid, X-ray fixative.

New England Biolabs (Hearts., UK).

Restriction enzymes.

Premiere Beverages (Stafford, UK).

Dried milk powder (Marvel).

Promega UK (Southampton, UK).

Wizard® PureFection plasmid purification kit.

Qiagen (Hilden, Germany).

Qiaprep miniprep reagents, Qiaprep midiprep reagents.

University of Warwick media preparation service.

Sterile PBS, distilled H_2O.

Vector Laboratories (Burlingame, CA).

Vectashield® mounting medium.

2.3. Methods

2.3.1. DNA manipulations

2.3.1.1. Restriction enzyme digestion

All DNA was digested in the buffers supplied by the manufacturer at the recommended temperature, typically in a volume of 20-100 µl. Digestion of DNA with multiple enzymes was performed in the buffer which gave the optimum activity of all enzymes. Reactions were stopped by the addition of EDTA to 25 mM or heat inactivation where appropriate.

2.3.1.2. Dephosphorylation of DNA

Dephosphorylation reactions were performed in 50mM Tris.HCl pH 8.0, 10mM $MgCl_2$, 100mM NaCl, using calf intestinal alkaline phosphatase (CIAP). DNA fragments with protruding 5' termini were incubated at 37°C for 30 min with 1 unit of

CIAP, followed by a repeat incubation with a further aliquot of CIAP. Reactions were stopped by heat inactivation (65°C, 15 min). Electrophoresis and electroelution were used to purify the dephosphorylated DNA prior to its use in cloning steps.

2.3.1.3. Ligation of DNA molecules

DNA fragments with cohesive ends were ligated for 16 hr. at 16°C, using 2 units of T4 DNA ligase in the supplied buffer (50mM Tris.HCl pH 7.6, 10mM $MgCl_2$, 1mM ATP, 1mM dithiothreitol (DTT), 5% (w/v) polyethylene glycol (PEG) 8000). Typically a 3-fold molar excess of insert over vector DNA fragments was used.

2.3.1.4. Gel electrophoresis of DNA molecules

DNA fragments were separated on type I agarose (0.6-1.4% w/v), TBE gels, containing 0.5mg/ml ethidium bromide. Samples were loaded in 30% glycerol, 0.04% bromophenol blue. Electrophoresis was performed in TBE at 70mA until the required degree of separation was achieved. Bands were then visualised by transillumination with UV light, and photographed using computerised gel imaging equipment (Prior Laboratory supplies, UK). DNA fragment sizes were estimated by comparison to a DNA ladder of known fragment size (1kb ladder, GibcoBRL).

2.3.1.5. Electroelution of DNA molecules from agarose gels

The DNA to be purified was excised from the gel and eluted into 500µl TBE in sealed dialysis tubing (molecular weight cut-off, 16,000) by electrophoresis in 0.5 X TBE at 150V for 30min. The eluate was then extracted twice with phenol/chloroform, followed by ethanol precipitation.

Alternatively, DNA was purified from agarose gel slices using the Qiagen DNA purification kit. This DNA did not require phenol-chloroform extraction or ethanol precipitation.

2.3.1.6. Phenol/chloroform extraction

An equal volume of phenol/chloroform prewarmed to 37°C was added to the DNA solution and mixed by repeated inversion. Phase separation was achieved by centrifugation in a microcentrifuge at 2300 x g for 2 min; the less dense aqueous phase was removed to a clean tube.

2.3.1.7. Ethanol precipitation

DNA was precipitated from aqueous solution by the addition of sodium acetate to 300mM, plus 2 volumes of ethanol. This was placed at -70°C for 1hr (or -20°C overnight), after which the DNA was pelleted by centrifugation in a microcentrifuge at 16,000 x g for 15 min, washed with 70% (v/v) ethanol and re-centrifuged for 5 min. The pellet was dried briefly in a vacuum dessicator and resuspended in 10mM Tris.HCl pH 7.5.

2.3.1.8. Spectrophotometric quantification of DNA

The concentration and purity of DNA in aqueous solution was determined by absorbancies at 260nm and 280nm. An absorbance of 1.0 at 260nm indicates a concentration equal to 50µg/ml for double stranded DNA. Purity was assessed by the ratio of absorbance at 260nm to that at 280nm, a ratio of 1.7-1.8 indicating purity.

2.3.1.9. Automated DNA sequencing

Automated DNA sequencing was performed by Mrs L.Ward, Department of Biological Sciences, University of Warwick, using an Applied Biosystems sequencer (model 373a).

2.3.1.10. Polymerase chain reaction (PCR) (after Mullis *et al.*, 1986)

Target DNA was amplified by PCR; all reactions were optimised but a typical 50µl reaction mix consisted of 100ng target DNA, 200ng each of forward and reverse primers, 1mM each of dATP, dCTP, dGTP, dTTP, optimum concentration of $MgCl_2$, 1 unit Taq polymerase (non-proof reading) in the buffer supplied by the manufacturer. Reaction conditions were:

94°C, 1 min; 60°C, 1 min; 74°C, 3 min x 19 cycles, then 94°C, 1 min; 60°C, 1 min; 74°C, 7 min x 1 cycle, followed by a 4°C soak until the sample could be removed for processing.

A typical 50µl mutational PCR mix for the primary reaction, would consist of 200ng target DNA, 1mM each of dATP, dCTP, dGTP, dTTP, the optimum concentration of $MgCl_2$, 1 unit Taq polymerase in the buffer supplied by the manufacturer and 200ng of each primer. Reaction conditions used were:

94°C, 1 min; 55°C, 1 min; 74°C, 3 min x 19 cycles, then 94°C, 1 min; 55°C, 1 min; 74°C, 7 min x 1 cycle, followed by a 4°C soak.

In a typical 50µl mutational PCR second stage amplification reaction, approximately 500ng of each product of two complementary primary PCR reactions would be mixed, in a total volume of 10µl. To this was added 1mM each of dATP, dCTP, dGTP, dTTP, the optimum concentration of $MgCl_2$ and 1 unit Taq polymerase in the buffer supplied by the manufacturer. This mixture underwent one cycle at 94°C, 1 min; 60°C, 1 min; 74°C, 7 min, then 200ng of each outside primer was added, and DNA amplified by the usual PCR method.

2.3.2. Bacteriological techniques

2.3.2.1. Culture and storage of bacteria

Escherichia coli (E.coli) XL1-Blue were cultured in LB containing 15µg/ml tetracycline at 37°C with shaking. Transformed bacteria were grown on LB agar plates or as liquid cultures, both containing 100µg/ml ampicillin (LBamp) and incubated at 37°C with shaking.

Cultures were maintained in long-term storage as a 50% (v/v) mix of glycerol and exponential phase liquid culture, at –70°C.

2.3.2.2. Transforming bacteria, and rendering competent for transformation

5ml of LB was inoculated with a single colony of *E.coli* strain XL1-Blue, and cultured to stationary phase at 37°C. 50µl of this was used to inoculate 25ml of LB which was cultured to OD_{550} 0.3-0.4. This was split equally between two flasks, each containing 250ml of LB, and cultured to OD_{550} 0.4-0.5. The cultures were cooled on ice for 15 min. Then the cells were harvested by centrifugation (1,300 x g, 10 min, at 4°C). Pellets were resuspended gently in 100ml of ice-cold TFB I and re-centrifuged. The supernatant was discarded and the pellet resuspended in 10ml of ice-cold TFB II. 0.5ml aliquots were rapidly frozen in a dry ice/ethanol bath and stored at -70°C.

To transform competent bacteria, DNA (10ng control plasmid or 15µl ligation reaction) was diluted in 100µl of sterile distilled water and placed on ice. Competent bacteria were thawed rapidly and 150µl added to the DNA solution, which was left on

ice for 1hr, subjected to heat-shock (42°C, 2 min) then placed on ice for 5 min. 300µl of LB was then added and the cells incubated at 37°C for 30 min prior to plating on LB agar plates containing 100µg/ml ampicillin, which were then incubated for 16 hrs at 37°C.

2.3.2.3. Small scale preparation of plasmid DNA

5ml of LBamp was inoculated with a single bacterial colony and grown overnight at 37°C with shaking. Plasmid DNA was isolated from 1.5ml of bacterial culture using a Qiagen Miniprep plasmid purification kit, following the manufacturer's instructions. This DNA was suitable for restriction enzyme analysis and cloning.

Alternatively, the alkaline lysis method was used. 1.5ml of bacterial culture was centrifuged in a microcentrifuge for 1 min at 2300 x g. The medium was aspirated, and the pellet resuspended in 100µl of ice cold miniprep solution I. This was vortexed, and left for 5 min at room temperature with an open lid. Then 200µl of freshly made, ice cold miniprep solution II was added and the mixture inverted rapidly 2-3 times before being placed on ice. After 5 min, 150µl of ice cold solution III was added and the mixture vortexed gently in an inverted position for 10 sec. This was then placed onto ice for a further 5 min, before centrifuging at 13,400 x g for 5 min at 4°C. The supernatant was transferred to a fresh tube, to which was added an equal volume of phenol/chloroform. These were mixed by vortexing, and centrifuged at 2300 x g for 2 min. The aqueous phase was removed and 2 volumes of ethanol added. This was vortexed, and left to stand at room temperature for 2 min. The DNA was pelleted by micro-centrifugation (16,000 x g, 5 min, room temperature), the supernatant removed, and the pellet washed by addition of 1ml of 70% ethanol followed by brief vortexing, and recentrifugation for 5 min at 16,000 x g. The supernatant was then removed, and the pellet briefly dried in a vacuum. The DNA pellet was resuspended in 50µl TE (pH 8.0) containing DNase-free pancreatic RNaseA (20µg/ml). The DNA in solution was stored at -20°C.

2.3.2.4. Large scale preparation of plasmid DNA

A single bacterial colony containing the plasmid of interest was used to inoculate 1.5ml of LBamp and cultured to stationary phase. 50µl of this was used to inoculate 25ml of LBamp, which was cultured to OD_{600} of 0.6. This culture was then used to

inoculate 500ml of LBamp and cultured to OD_{600} of 0.4. Chloramphenicol was then added at 100μg/ml to amplify the plasmid, and the culture was incubated for a further 16 hrs. All incubations were carried out at 37°C unless stated otherwise in the relevant results chapter.

Cells were collected by centrifugation (1,600 x g, 30 min, 4°C) and resuspended in 10ml of cold 25% sucrose, 50mM Tris.HCl pH 8.0. 4ml of cold 0.25 M EDTA was added, mixed gently and placed on ice for 5 min. 20mg of lysozyme dissolved in 2ml of TNE was then added, mixed gently and placed on ice for 15 min. Following this, 16ml of cold Triton lysis mixture (0.1% (v/v) Triton X-100, 62.5mM EDTA, 50mM Tris.HCl pH 8.0) was added, mixed gently and placed on ice for a further 5 min. Cellular debris was then removed by centrifugation (35,000 x g, 40 min, 4°C). The supernatant was then extracted by mixing vigorously with 7ml Tris-buffered phenol and 1ml chloroform/iso-amyl alcohol, allowed to stand for 10 min and then centrifuged (18,000 x g, 10 min, 4°C). The aqueous phase was removed and further extracted by the addition of 20ml chloroform/iso-amyl alcohol, vigorous mixing and centrifugation as before. The aqueous phase was removed and the DNA precipitated by the addition of 2 volumes of 95% (v/v) ethanol at -70°C for 1hr. The DNA was pelleted by centrifugation (18,000 x g, 20 min, 4°C) and dried in a vacuum dessicator for 15 min. The pellet was resuspended in 4.5 ml TNE to which was added 4.72g CsCl and 320μl ethidium bromide solution (10mg/ml). Plasmid DNA was purified by equilibrium density gradient centrifugation in a Beckman Vti65 rotor (200,000 x g, 16hrs, 20°C). Ethidium bromide was removed from the DNA by repeated extraction with an equal volume of NaCl-saturated isopropanol. 3 volumes of TNE were then added and the DNA precipitated at -70°C using 95% (v/v) ethanol. Plasmid DNA was recovered by centrifugation (15,900 x g, 30 min, 4°C), washed in 70% (v/v) ethanol, then dried and resuspended in 0.5ml 10mM Tris.HCl pH 8.5, containing 10μg RNaseA.

2.3.3. Tissue culture techniques

2.3.3.1. Maintenance of cell lines

All cell lines were cultured in 90mm γ-irradiated tissue culture dishes at 37°C in a 5% CO_2 atmosphere and passaged when confluent. HEp-2, HeLa and 293 cells (and

derivatives) were maintained in DMEM/10% newborn calf serum (NCS) (v/v). Cells were passaged as follows: monolayers were washed with 0.02% v/v versene, then cells detached by adding 2.5ml of 0.02% (v/v) versene containing 1.25mg trypsin, for 3-5 min. Cells were removed into 0.5ml NCS and centrifuged at 600 x g for 4 min. The pellet was resuspended in medium and cells seeded at the required density.

2.3.3.2. Long term storage of mammalian cells in liquid nitrogen

Sub-confluent 90 mm dishes of cells were trypsinised for passage and the cell pellet resuspended in 1ml of 92% (v/v) NCS, 8% (v/v) dimethyl sulphoxide (DMSO). The cell suspension was frozen in 0.5ml aliquots by cooling slowly to -70°C overnight. Frozen vials were subsequently transferred to liquid nitrogen.

2.3.3.3. Recovery of frozen cell stocks from liquid nitrogen storage

Cells were thawed rapidly at 37°C then transferred to 10ml of pre-warmed medium in a 90mm dish. The medium was replaced the following day to remove residual DMSO.

2.3.3.4. Transfection of mammalian cells with dsDNA

2.3.3.4.1. Calcium phosphate transfection

Cells to be transfected were grown to the required density (usually 70% confluency) in tissue culture dishes (size of dish depended upon assay). The volumes used were scaled up or down for larger or smaller dishes. The total volume of mix was always 10% of that of the medium in the dish. The calcium phosphate/DNA precipitate was prepared as follows, for a 60mm dish containing 5ml DMEM: 0.5ml of mix A (250mM $CaCl_2$) containing the DNA to be precipitated was added dropwise to 0.5ml of mix B (0.05mM Na_2HPO_4, 10mM KCl, 270 mM NaCl, 0.2% (w/v) N-2-hydroxyethylpiperazine-N'-2-ethanesulphonic acid (Hepes), pH 7.08-7.12) whilst bubbling air through mix B. This was left at room temperature for 30 min then added dropwise to the cell cultures, 0.5ml per 60mm dish containing 5ml growth medium. Cells were incubated at 37°C for 4hrs and the medium replaced. Cells were subsequently incubated at 37°C/5% CO_2 for the desired period.

2.3.3.4.2. Liposome mediated transfection

Cells were transfected with LIPOFECTAMINE™ (Gibco BRL, Renfrewshire, Scotland) according to the manufacturer's instructions.

2.3.4. Virological techniques

2.3.4.1. Virus infection of mammalian cells

Infections were initiated by removing the growth medium and adding an amount of virus calculated to give the desired multiplicity of infection, diluted in DMEM without serum. Cells were incubated at 37°C and rocked every 15 min. After 1hr, full growth medium containing serum was added and the cells incubated at 37°C for the time appropriate to the experiment.

2.3.4.2. Large scale preparation of virus stocks and DNA

90% confluent dishes of cells were infected with virus (m.o.i. of 2 pfu/cell) and harvested at full cytopathic effect. Cells were collected by centrifugation (500 x g, 5 min) and resuspended in cold 0.1 M Tris.HCl pH 8.0, to a final volume of 5ml for up to 4 dishes. This suspension was sonicated on ice using a Jencons sonicator with a 3mm tip, using two sets of ten, one second, pulses separated by 30 seconds. Cell debris was removed by centrifugation (5,600 x g, 10 min, 4°C) and the supernatant layered over a two-step CsCl gradient (2ml 1.4 g/ml CsCl, 3ml 1.25 g/ml CsCl, both final density in TD). Gradients were centrifuged (150,000 x g, 1 hr, 15°C) in a Beckman SW 41 rotor and the virus band collected by puncturing the tube and collecting the relevant part of the flow-through. This was then diluted with 1.35g/ml CsCl/TD and centrifuged to equiibrium (150,000 x g, 16hrs, 15°C) in a Beckman SW 50.1 rotor. The virus band was collected as before and either used to prepare a purified virus stock or viral DNA.

(i). Purified virus stock

A small sample of the collected virus was diluted 1 in 500 with TE/0.1% (w/v) SDS and the optical density measured. Virus particle concentration was determined using the formula, A_{260} of 1.0 = 1 x 10^{12} particles/ml. The remaining virus stock was then diluted five-fold with stabilising buffer (0.1% (w/v) bovine serum albumin (BSA),

50% (v/v) glycerol, 10 mM Tris.HCl pH 8.0, 100 mM NaCl, 2mM $MgCl_2$) and stored at -20°C.

(ii). Viral DNA

Collected virus was diluted with two volumes of H_2O and precipitated with 2 volumes of ethanol at -70°C for 30 min. Virions were pelleted by centrifugation (7,600 x g, 20 min, 4°C), dried briefly and resuspended in 2ml TNE with the addition of 120µl 10% (w/v) SDS, 40µl 250mM EDTA and 200µg proteinase K. This was incubated at 37°C for 1hr, then extracted twice with an equal volume of phenol/chloroform. The aqueous phase was collected and NaCl added to a final concentration of 0.1M. Viral DNA was precipitated by addition of 2 volumes of ethanol at -70°C for 30 min. DNA was pelleted by centrifugation (15,900 x g, 30 min, 4°C), washed in 70% ethanol, dried and resuspended in 0.5ml TE pH 8.0 at + 4°C.

2.3.4.3. Adenovirus reconstruction by *in vivo* recombination

293 cells were plated at 50% confluence one day before use. The medium was replaced with DMEM/10% FCS 3 hrs prior to use. The DNA/$Ca_3(PO_4)_2$ precipitate was prepared 30 min prior to use as follows (volumes correct for one 60mm dish): (a) A mix of 50µl 2 x Hepes buffer, approximately 1µl 100 x PO_4, and the DNA solutions made up to 90µl total with H_2O was prepared. (b) 10µl of 1.25M $CaCl_2$ was added to (a), while bubbles were blown gently through the suspension. This was then left for 30 min at room temperature. The DNA solutions were in TE and comprised 1µl of 1mg/ml salmon sperm DNA (unsheared), 1-3 µg plasmid DNA with the viral sequences liberated by digestion at least at the 0 map unit end, and 0.5-1.0µg viral genomic DNA (permitting overlap with plasmid sequences, to regenerate full length genome). The medium was removed from the cells, 0.9ml of DMEM/5% FCS was added to the DNA precipitate, and this was then layered over the cells. The inoculum was left on the cells for 3hrs, with rocking at frequent intervals. After this incubation, 1.0ml TS + 20% glycerol was gently added to the monolayer for 1 min only. The TS/glycerol was then removed, and the monolayer washed twice gently with TS. Following the wash, liquid or solid media was added as required.

2.3.4.4. Standard amplification of viral plaques

The infected cell monolayer was overlayed with solid medium. Each plaque was picked with a sterile pasteur and transferred to 0.5ml TS/2% NCS, and then freeze/thawed 3 times. The lysate was subsequently used to infect a 60mm dish of cells. After 1 week, or at full cytopathic effect (whichever was sooner), the cells were harvested from the 60mm dish in the medium and freeze/thawed 3 times. Of this lysate, 0.5ml was used to infect a 90mm dish of cells. The remainder of the lysate was reserved as a stock. The infected 90mm culture was processed for viral DNA by the rapid preparation procedure (see below) to verify the identity of the starting plaque before proceeding further. After selecting an appropriate plaque from which to grow a final stock, about 0.2ml of the reserved 4.5ml of lysate was used to infect 10 dishes of cells (HeLa or 293 as appropriate). At or prior to full c.p.e, these cultures could be processed for virions.

2.3.4.5. Adenovirus DNA rapid preparation

The cells from a 90mm dish were harvested at full c.p.e and pelleted at 160 x g for 5min. The supernatant was removed completely and the pellet was resuspended in 0.4ml TE pH 9.0, 10mM spermine, then 0.4ml DOC lysis buffer (20% EtOH, 100mM Tris pH 9.0, 0.4% sodium deoxycholate) was added. This was gently mixed without vortexing and then centrifuged (12,000 x g, 15min, 4°C) in a Beckman JA21 rotor. The supernatant was then supplemented with 60µl 10% SDS, 40µl 0.25M EDTA and 20µl of 20mg/ml proteinase K in a 1.5ml microfuge tube. This was incubated for 1hr at 37°C then extracted once in an equal volume of phenol/chloroform. The aqueous phase was collected and 30µl of 5M NaCl added. The tube was filled with isopropanol at room temperature, mixed, and the DNA pelleted by centrifugation (15,900 x g, 15 min). Following centrifugation, the supernatant was discarded and the DNA dried and resuspended in 50µl TE. RNAse was added if required.

2.3.4.6. Viral miniprep

Cells from each well of a 12 well dish were harvested at full c.p.e. and transferred to a 1.5ml microfuge tube. These were centrifuged at 1000 rpm for 5 min, the supernatant removed, and the pellets stored at -20°C. The cell pellet was resuspended in 100µl TE

pH 9.0, 10mM spermine. This was mixed, then 100µl DOC lysis buffer added. The mixture was centrifuged in a benchtop microfuge. The supernatant was transferred to a clean microfuge tube, to which was added 15µl 10% SDS, 10µl 0.25M EDTA and 5µl of 20mg/ml proteinase K. This was incubated for 1hr at 37°C then extracted once in a equal volume of phenol/chloroform. The aqueous phase was collected and 7.5µl of 5M NaCl added. 200µl of room temperature isopropanol was added to the tube, and the contents mixed before the DNA was pelleted by centrifugation. Following centrifugation, the supernatant was discarded and the DNA resuspended in 12µl dH_2O. RNAse was added to a final concentration of 20µg/ml.

2.3.5. Analysis of protein expression

2.3.5.1. Extraction of total cellular protein from mammalian cells

The medium was aspirated from tissue culture dishes and the cells harvested directly into a small volume of 1 X SDS-PAGE loading buffer. The volume of buffer depended upon the size of the assay. A typical volume would be 100µl loading buffer for 10^6 cells. Samples were stored at -20°C.

2.3.5.2. SDS polyacrylamide gel electrophoresis (SDS-PAGE)

Protein samples were denatured and reduced by boiling in SDS-PAGE loading buffer for 5 min. Proteins were separated by electrophoresis in discontinuous SDS-polyacrylamide gels according to the method of Laemmli (1970). Gels consisted of a 5% stacking gel, and resolving gels of various percentages (as noted in the relevant results chapters). Electrophoresis was performed using the Bio-Rad mini-PROTEAN II electrophoresis system according to the manufacturer's instructions.

2.3.5.3. Western blotting

Proteins were separated by SDS-PAGE and transferred to nitrocellulose membrane according to the method of Towbin *et al.* (1979). The gel and membrane were equilibrated in transfer buffer (25 mM Tris base, 192 mM glycine, 20% methanol) for 30 min. Electroblotting was performed in the Bio-Rad Mini Trans-Blot® Electrophoretic Transfer Cell, at 350mA for 1 hr, or at 90mA overnight. The membrane was blocked in PBS/0.1% (v/v) Tween 20 (PBST)/5% (w/v) milk powder

overnight at 4°C, before being probed with antibodies (see 2.1.5. for dilutions used). The membrane was incubated with primary antibody for 2 hr, followed by a 1 hr incubation with secondary antibody and a 1 hr incubation with enzyme conjugate (if required). All antibodies were diluted in PBST/5% milk and incubations performed at room temperature with vigorous shaking. Between each incubation membranes were washed four times (>5 min per wash) in PBST. Membranes were developed using Chemiluminescence Reagent *Plus* Western Blotting detection reagents (NEN™ Life Sciences Products) according to the manufacturer's instructions.

2.3.5.4. Immunofluorescence microscopy

Cells grown on coverslips were washed twice in PBS, fixed for 15 min with a solution of 3.7% (v/v) formaldehyde in PBS and then washed again with PBS. They were then permeabilised by incubation for 10 min in 0.5% NP40 in PBS, washed again in PBS and then stored immersed in PBS at 4°C. Before analysis, coverslips were incubated in PBS/1% bovine serum albumin (BSA) for 1hr and all reagents used subsequently were diluted in this solution. To detect specific antigens, coverslips were incubated with the relevant primary antibody for 1 hr, followed by three washes in PBS. Bound primary antibody was then detected by incubating coverslips for 1 hr with species-specific secondary antibody conjugates (see section 2.1.5. for details and dilutions used) for 1 hr and washed as before. If staining of nuclei was required, 4,6-diamidino-2-phenylindole (DAPI) was added to the final PBS wash at 1μg/ml. Coverslips were mounted in Vectashield® mounting medium, then viewed and photographed using a Nikon optiphot microscope and single lens reflex (SLR) 35mm camera loaded with slide film (typically ASA 1600).

3. Construction of recombinant plasmids to express wild-type E4orf3 in eukaryotic cells

In order to investigate any effects of Orf3 alone upon the eukaryotic cell, it was decided to generate an eukaryotic expression vector capable of expressing Orf3 in isolation from other viral products. A suitable vector would amplify the DNA of interest in prokaryotic cells, and upon transfection into eukaryotic cells, would drive expression of E4orf3. Expression of Orf3 would be visualised using Western-blotting and immunofluorescence microscopy techniques on samples taken from transfected cells.

3.1. Construction of pEXP4.Orf3

The plasmid pEXP4 (from Keith Leppard) (fig.3.1) fitted the criteria for the vector, having an *amp*R region for selection of recombinants, and the promoter/enhancer region from the SV40 genome, capable of driving expression in the eukaryotic environment.

The plasmid contains a pUC18 polylinker region, or multiple cloning site, which contains several restriction target sites, facilitating insertion of the gene in the correct orientation between the promoter and a poly-A region.

To simplify the cloning procedure, an existant plasmid, pGEM.Orf3 was used as a source of E4orf3 (fig.3.2). In this plasmid, the gene of interest was flanked by restriction sites, which allowed one step excision of the region using a double digest.

3.1.1. Double digest of pGEM.Orf3 by EcoRI and BamHI

The restriction enzymes BamHI and EcoRI were used in double digest to excise E4orf3 from the pGEMOrf3. The total plasmid is 2.8 kbp, and Orf3 is encoded by a 430bp section. Consequently a successful digest would generate fragments of approximately 2.4kbp and 0.4kbp. If the reaction had not gone to completion, a band of 2.8kbp representing undigested parental DNA would also be present. The double digest generates a linear fragment with two differently cut ends (see fig.3.3). This prevents self-annealing of the fragments, as the two ends are incompatible.

Samples of the digest products were loaded onto a 1.4% agarose gel, along with DNA 1kbp marker ladder, allowing sizing of the DNA fragments generated (see fig.3.4)

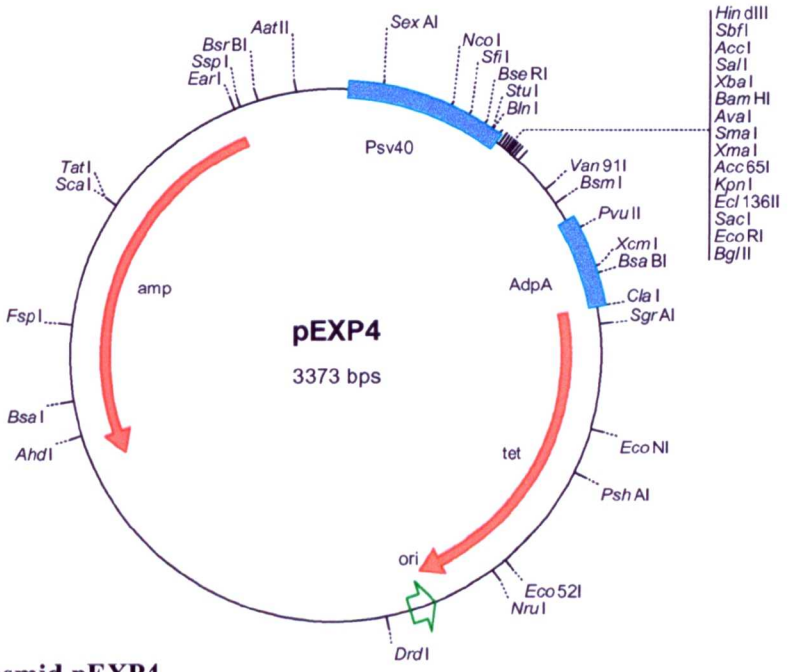

Fig.3.1. Plasmid pEXP4.

Map shows unique restriction sites. Abbreviations: amp, ampicillin resistance gene; tet, tetracycline resistance gene; Psv40, SV40 promoter region ; AdpA, adenovirus polyadenylation site; ori, plasmid origin of replication.

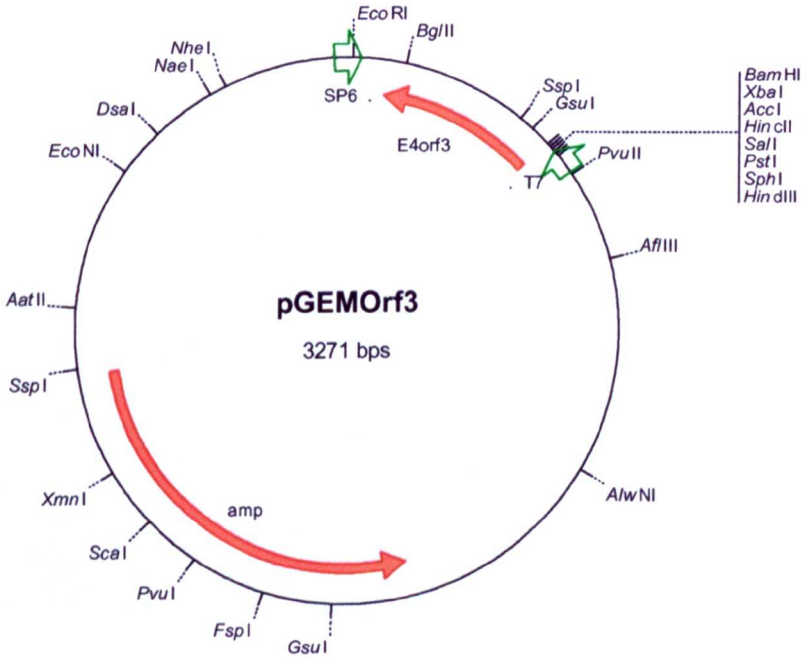

Fig.3.2. Donor plasmid pGEM.Orf3.

Plasmid bearing the Ad5 E4Orf3 gene sequence. Map shows unique restriction sites. Abbreviations : amp, ampicillin resistance gene; SP6, SP6 RNA polymerase transcription initiation site; T7, T7 RNA polymerase transcription initiation site.

Fig.3.3. Diagramatic representation of the generation of sticky-ended fragments by EcoRI/BamHI double digest

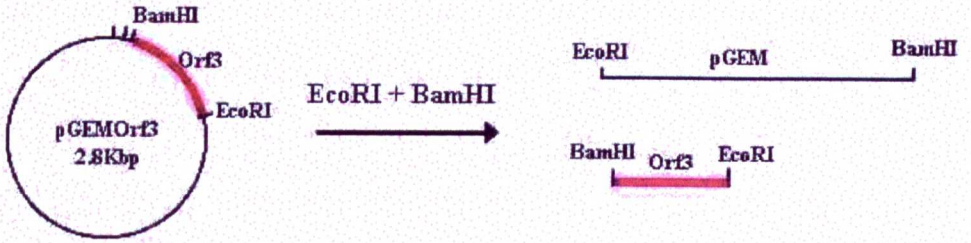

3.1. 2. Restriction digest of Vector pEXP4

In order to linearise the plasmid and allow insertion of E4orf3 in the correct orientation, the same pair of restriction enzymes was used as above and a sample of the fragment produced was run on agarose gel (fig.3.4).

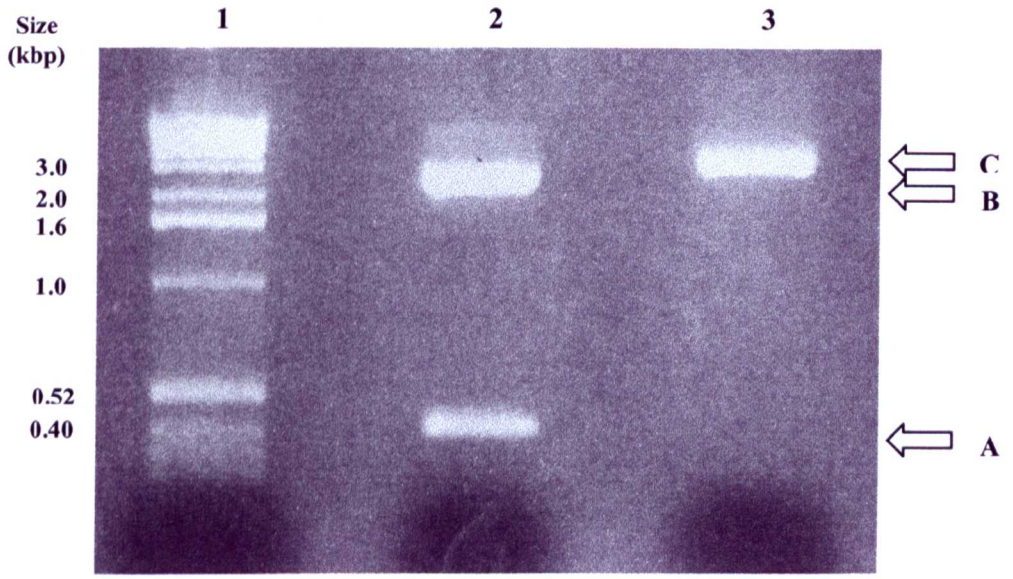

Fig.3.4: BamHI/EcoRI double digest products of pGEMOrf3 and pEXP4. DNA samples were analysed on a 1.4% TBE/agarose gel. Lane 1 is loaded with 1Kb ladder. Lane 2 shows the products of EcoRI/BamHI digest of pGEMOrf3, where arrow B indicates pGEM, and arrow A indicates excised E4orf3. Lane 3 show the double digest products of pEXP4, where arrow C indicates linearised plasmid, and the cut-out fragment is not visible.

3.1.3. Ligation of E4orf3 and linearised pEXP4

The digest products of pGEMOrf3 and pEXP4 were separated on individual gels and slices containing the desired fragments cut away from the rest of the gel. The DNA was purified from the gel by electroelution. The purified E4orf3 and linearised pEXP4 fragments were then ligated together. Cut pEXP4 alone was ligated to provide a negative control for transformation. After overnight incubation, the ligation mixes were used to transform *E.coli* XL1Blue. A positive control for transformation of uncut vector DNA was included.

Colonies obtained were used to prepare small scale DNA preparations (minipreps), samples of which were subjected to analytical restriction digest, to confirm the presence of an Orf3-sized fragment in the correct orientation, in the pEXP4 vector. An EcoRI and BamHI digest was performed on DNA prepared in this manner from twelve picked clones, and the products separated on a 1.4% agarose gel (fig.3.5).

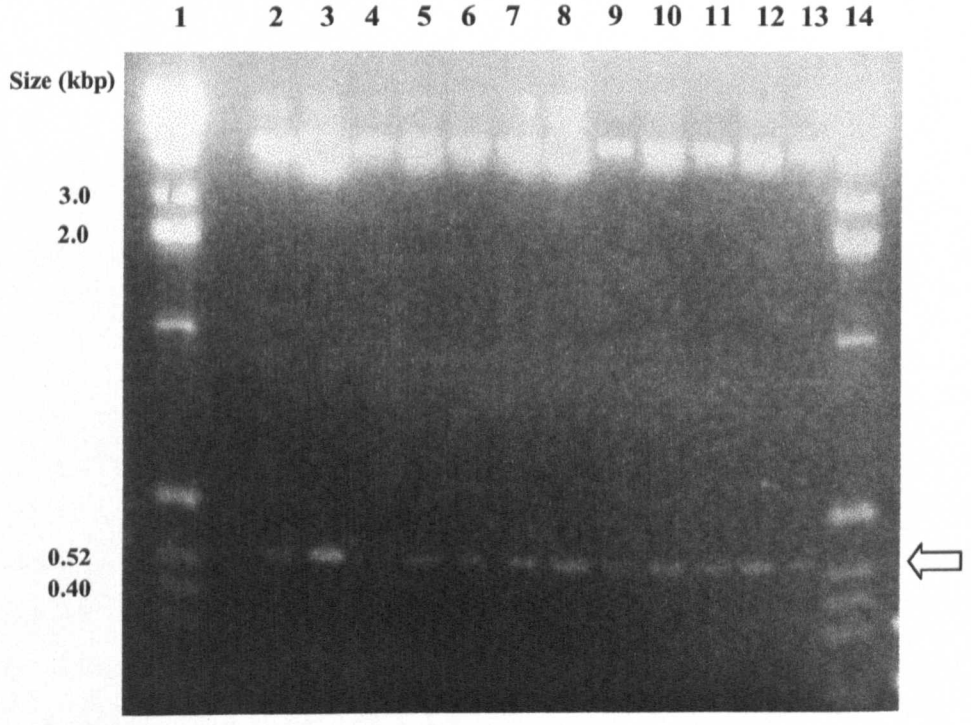

Fig.3.5: EcoRI/BamHI digest products of miniprep DNA of candidate clones of pEXP4.Orf3.DNA samples were loaded on a 1.4% agarose/TBE gel. Lanes 1 and 14 were loaded with 1Kb ladder. Lanes 2 to 13 show the digest products of 12 candidate clones of E4orf3 in pEXP4. The arrow indicates the approximately 0.4Kb band, indicating the presence of E4orf3 in these clones.

These digests confirmed the presence of a cloned fragment of the correct size in the vector. However despite the use of two different restriction enzymes, it was still possible that Orf3 might have inserted in the wrong orientation or in multiple copies. To ensure this was not the case, two of the above samples were digested using different enzymes, chosen to generate a junction fragment characteristic of a correctly oriented insert. A BamHI/BglII digest would be expected to yield a 3.5kbp and a 317bp fragment in a correctly aligned pEXP4.Orf3 plasmid. If Orf3 had inserted "backwards", the same digest would yield 3.7kbp and 99bp fragments. If the insert joined end to end to form tandem repeats before insertion into the vector, we would expect the 3.5kbp vector DNA band, and smaller bands of 226bp, and 317bp. Accordingly, this digest was performed on samples 2 and 7. A band of the correct size was seen in the digest of miniprep 2, indicating an insert in the correct orientation. Clone 2 was used to prepare a large scale plasmid DNA preparation. This plasmid was named pEXP4.Orf3 (fig.3.6).

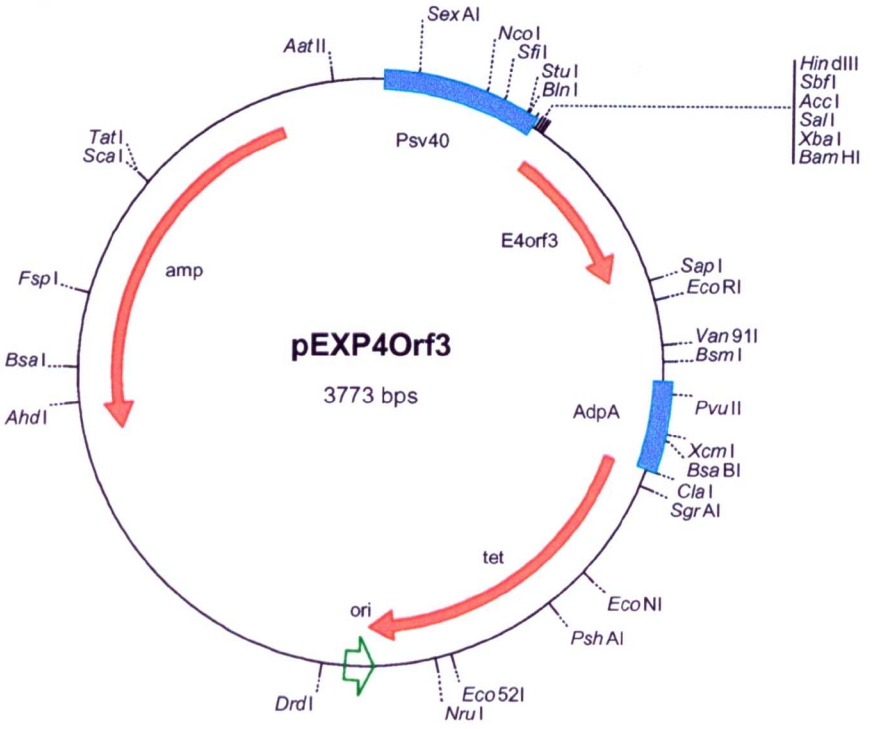

Fig.3.6. Plasmid pEXP4.Orf3

PEXP4-based plasmid bearing the Ad5 E4Orf3 gene sequence. Map shows unique restriction sites. Abbreviations: amp, ampicillin resistance gene; Psv40, SV40 promoter region; AdpA, adenovirus polyadenylation site; tet, tetracycline resistance gene; ori, plasmid origin of replication.

3.1.4. Transient transfection and Immunofluorescence using pEXP4.Orf3

To assess the suitability of pEXP4.Orf3 as a eukaryotic expression vector for E4orf3, it was decided to perform transient transfection assays in mammalian cells. The Hep-2 cell line is a readily available laboratory cell line derived from human epithelial tissue in which Ad5-dependent rearrangement of the ND10s and the altered PML isoform pattern had previously been described. (Leppard and Everett, 1999). Transfection was performed by the calcium phosphate method upon cells grown on glass coverslips. The cells were fixed 24 hrs post-transfection and then probed for Orf3 expression. It was not possible to detect any Orf3 expression in the transfected cells under immunofluorescence microscopy as compared with cells infected with *wt* Ad5, in which Orf3 tracks are clearly visible (compare panels A and B, fig.3.7).

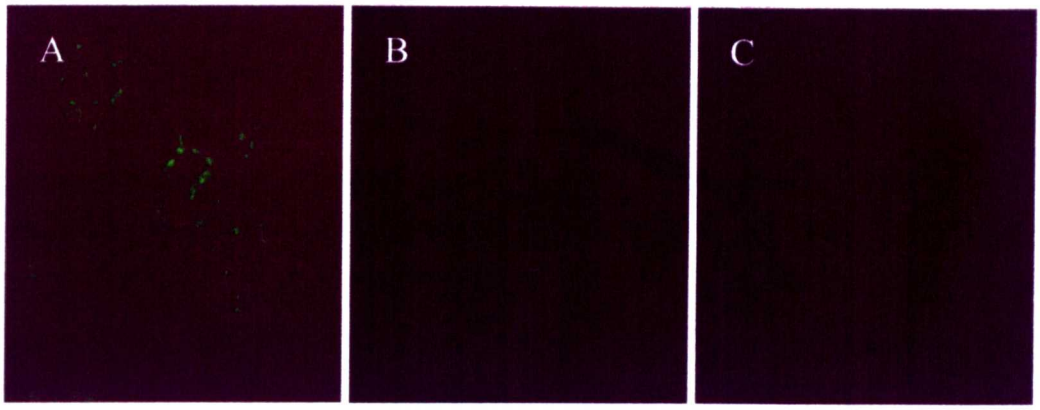

Fig.3.7: E4orf3 expression in transfected or infected HEp-2 cells. Fluorescence microscope images taken using a x100 viewing objective. All panels show HEp-2 cells probed with antibody A4-7 against E4 Orf3, showing green fluorescence where Orf3 is expressed.
Panel A shows Ad5 wt300 infected cells (at m.o.i. 10), panel B shows pEXP4.Orf3 transfected cells and panel C shows mock-infected cells.

3.2. Construction of pcDNA3.1/Orf3*wt*

Vector pEXP4 had been used previously to express heterologous proteins in COS1 cells. However, the vector replicates in these cells in contrast to the situation in HEp-2 cells. In the absence of this replication, expression appears to be too weak to detect. It was therefore decided to construct a second eukaryotic expression system, placing E4orf3 under the transcriptional regulation of a stronger promoter. To this end, pcDNA3.1/HisB/*lacZ* (fig.3.8.) was chosen. While this plasmid is actually a positive control for the parent vector, pcDNA3.1/HisB, rather than a vector *per se*, it was possible to adapt it for use here. Like pEXP4, the plasmid contains an *amp*R region, as well as a polylinker region. Unlike pEXP4 however, pcDNA3.1/HisB/*lacZ* has been designed to place inserts under the control of the human cytomegalovirus immediate early promoter region. This confers strong, constitutive expression in many mammalian cells. The plasmid, pGEMOrf3 was again used as the donor of E4orf3.

3.2.1. Double digest of pGEMOrf3 with EcoRI and HindIII

The desired vector in this case did not contain the restriction site BamHI. Consequently, a different cloning approach had to be devised. Fortunately, it was still possible to generate compatible sticky ended fragments, as both the donor and vector had EcoRI and HindIII restriction sites in suitable positions (see fig.3.2. and fig.3.8.). A double digest using these two enzymes was carried out in standard conditions.

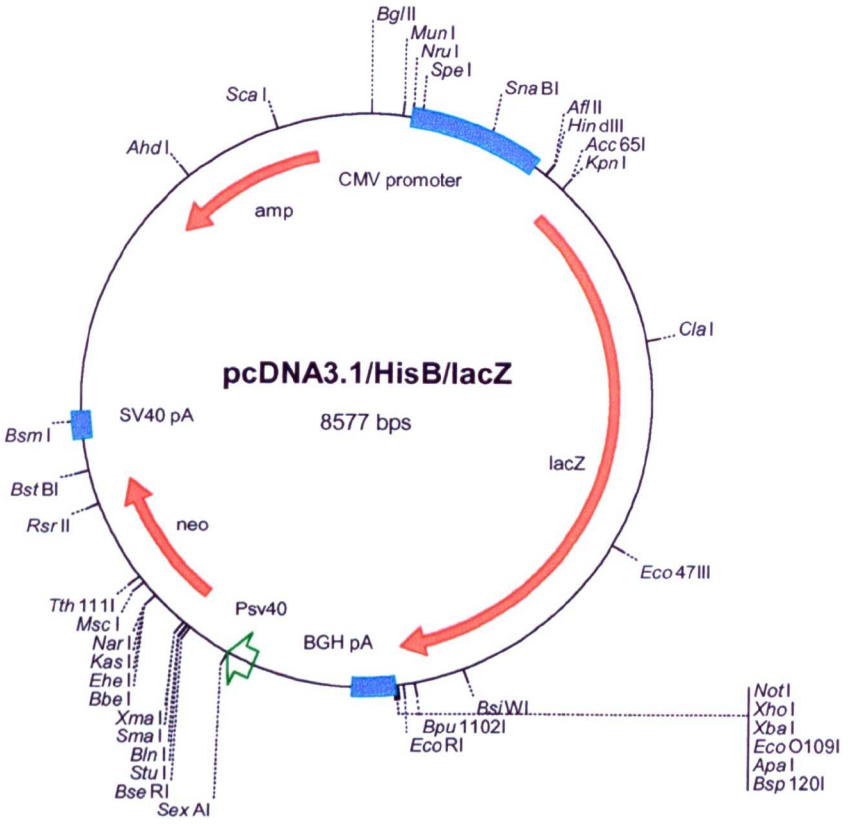

Fig.3.8. Plasmid pcDNA3.1/HisB/*lacZ* (Invitrogen).
Plasmid containing *lacZ* reporter gene. Map shows unique restriction sites. Abbreviations: amp; ampicillin resistance gene; neo, neomycin resistance gene; CMV promoter, cytomegalovirus immediate early promoter; Psv40, SV40 promoter region; SV40 pA, SV40 polyadenylation region.

3.2.2. Double digest of pcDNA3.1/HisB/*lacZ*

It was possible to digest the vector to generate a linear fragment with ends compatible with the insert fragment, but at the loss of certain elements of the plasmid. pcDNA3.1/HisB is designed to enable the formation of a fusion protein between an inserted fragment of DNA of interest and a six histidine tag sequence, allowing affinity purification on immobilised nickel ion columns. It also contained a *lacZ* gene. Cells expressing the product of this gene turn blue in the presence of Xgal (a chromogenic substitute for β galactosidase). Cleavage with HindIII and EcoRI

restriction enzymes flanked the region containing both of these elements. Use of these enzymes to linearise would remove all these elements. This was useful as *lacZ* effectively constituted a previous and unwanted insert into the vector. The HindIII/EcoRI digest was expected to produce two bands. The desired, vector fragment, was expected to be approximately 5.4Kbp, while the fragment containing the histidine "tag" and *lacZ* gene was expected to be around 3.1Kbp (fig.3.9.).

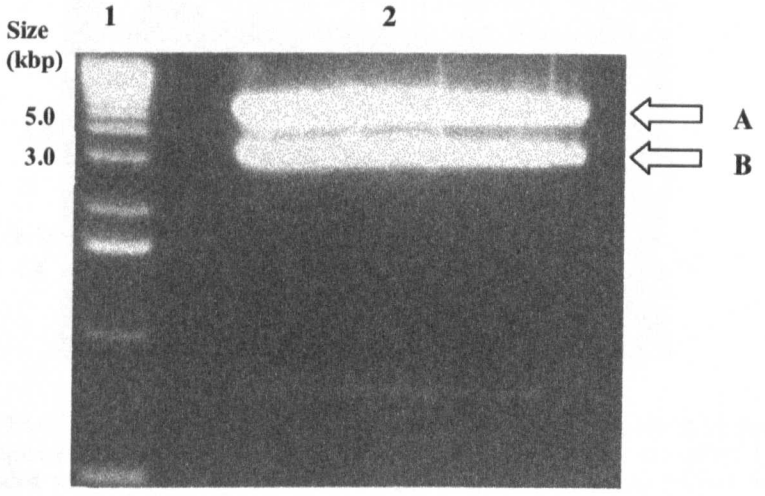

Fig.3.9: 0.8% agarose gel of EcoRI + HindIIIdigest of pcDNA3.1/HisB/*lacZ*. Lane 1 shows 1Kb marker. Wide lane 2 shows the fragments generated by EcoRI + HindIII double digest of pcDNA3.1/HisB/*lacZ*, where arrow A indicates the approximately 5.4Kbp pcDNA3.1 fragment. Arrow B indicates the approximately 3.1Kbp fragment containing the $(His)_6$ tag region and *lacZ* gene.

3.2.3. Ligation of pcDNA3.1 and E4Orf3

The digest products of pGEMOrf3 and pcDNA3.1/HisB/*lacZ* were separated on individual gels and the desired fragments purified by electroelution. These were then ligated together and were used to transform bacteria. Small scale DNA preparations were performed on 8 clones, and these were then subjected to analytical restriction digest, to confirm the presence of an Orf3-sized fragment in the pcDNA3.1 vector (fig.3.10.). Here the arrow indicates E4orf3 coding region as a drop out fragment of approximately 0.4Kbp in each of the clones tested. Again, it was necessary to confirm that, where present, the insert was in the correct orientation. Two samples were chosen and BglII/HindIII double digests performed. This digest was expected to yield fragments of approximately 4.6Kbp, 0.9Kbp and 0.35 Kbp from the desired recombinant (see fig.3.11.). These fragments are identified by arrows A, B and C

respectively in figure 3.11, and were present in both samples, thus both bacterial clones contain the insert in the correct orientation. Therefore, these analytical digests demonstrated the insertion of E4Orf3 into the pcDNA3.1 vector in the correct orientation, to generate pcDNA3.1/Orf3*wt* (fig.3.12.).

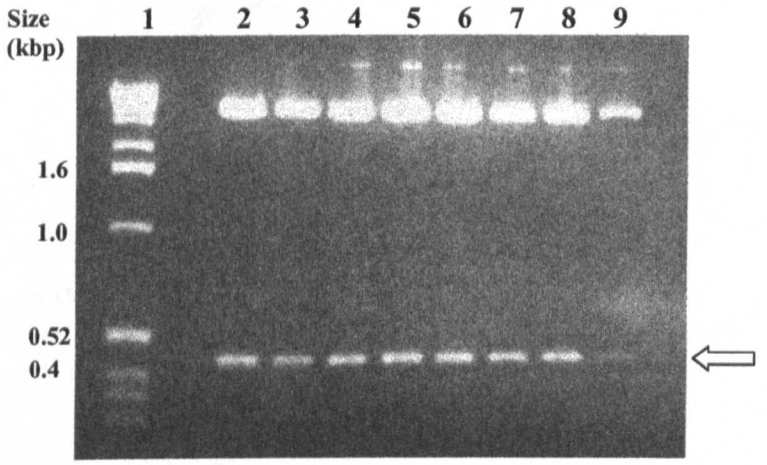

Fig.3.10: EcoRI/HindIII digest products of miniprep DNA of candidate pcDNA3.1/Orf3 clones. DNA samples were analysed on a 1.4% agarose/TBE gel. Lane 1 shows 1Kb ladder. Lanes 2 to 9 are loaded with EcoRI + HindIII double digested samples of plasmid DNA from eight different bacterial clones.

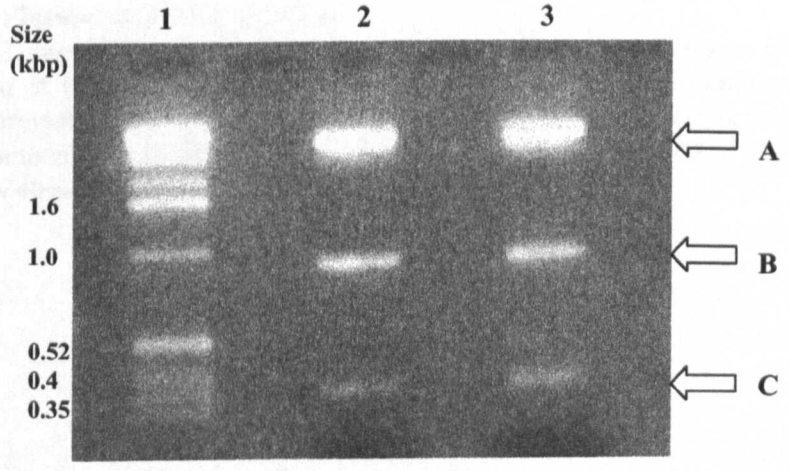

Fig.3.11: HindIII/BglII digest products of miniprep DNA of candidate pcDNA3.1/Orf3 clones. Lane 1 shows 1Kb marker. Lanes 2 and 3 are loaded with HindIII + BglII double digests of samples 1 and 5 from fig.3.11 respectively. Arrow A indicates a band of approximately 4.6Kbp, arrow B indicates a band of approximately 0.9Kbp, and arrow C indicates a band of approximately 0.35 Kbp.

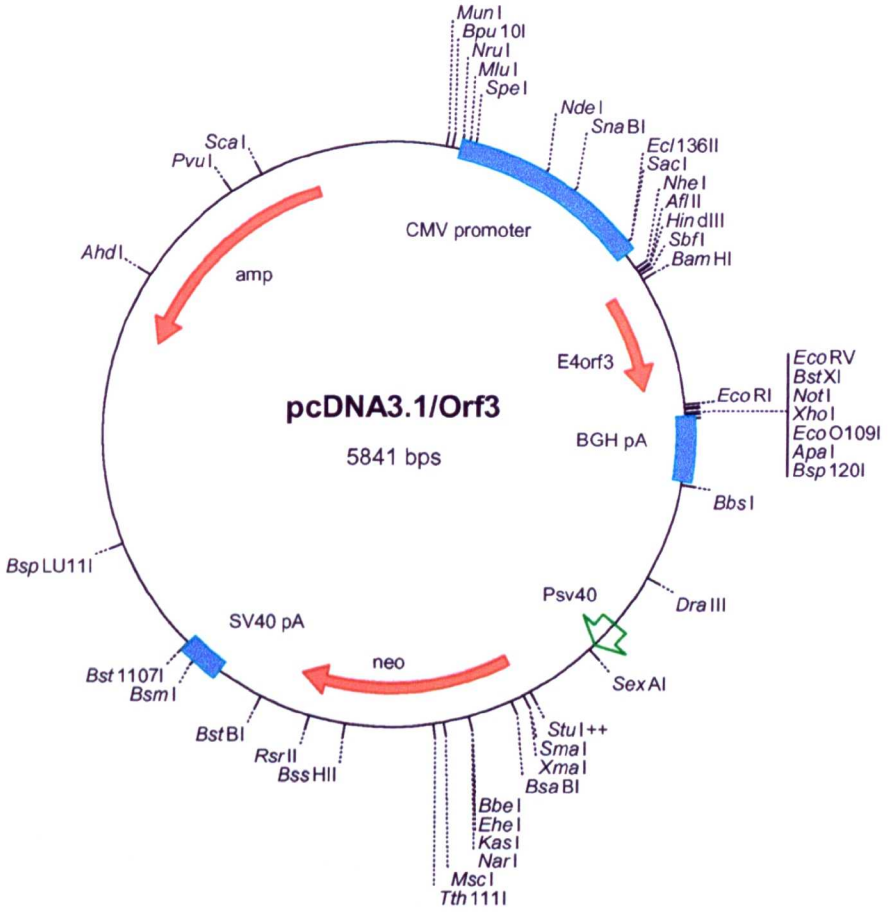

Fig.3.12. Plasmid pcDNA3.1/Orf3*wt*.
PcDNA3.1-based plasmid bearing the Ad5 E4Orf3 gene sequence. Constitutive expression of Orf3 is driven by the CMV promoter. Map shows unique restriction sites. Abbreviations: amp, ampicillin resistance gene; neo, neomycin resistance gene; CMV promoter, cytomegalovirus immediate early promoter; Psv40, SV40 promoter region; SV40 pA, SV40 polyadenylation region.

3.3. Expression of pcDNA3.1/Orf3*wt* in HEp-2 cells detected by Immunofluorescence

As before, transfection was performed by the calcium/phosphate method upon the HEp-2 cells grown on glass coverslips. In contrast to the results obtained using pEXP4.Orf3 (fig.3.8 panel B), Orf3 was clearly visible in cells transfected with pcDNA3.1/Orf3*wt*, and formed nuclear "tracks" in a subset of cells, similar to those observed during Ad5 infection (compare fig.3.13. panels A and B). Indeed, using similar exposure times, E4orf3 appears to be overexpressed in many cells transfected with pcDNA3.1/Orf3*wt* relative to infected cells. This could be due to the high activity of the CMV promoter, and/or multiple transfections into single cells.

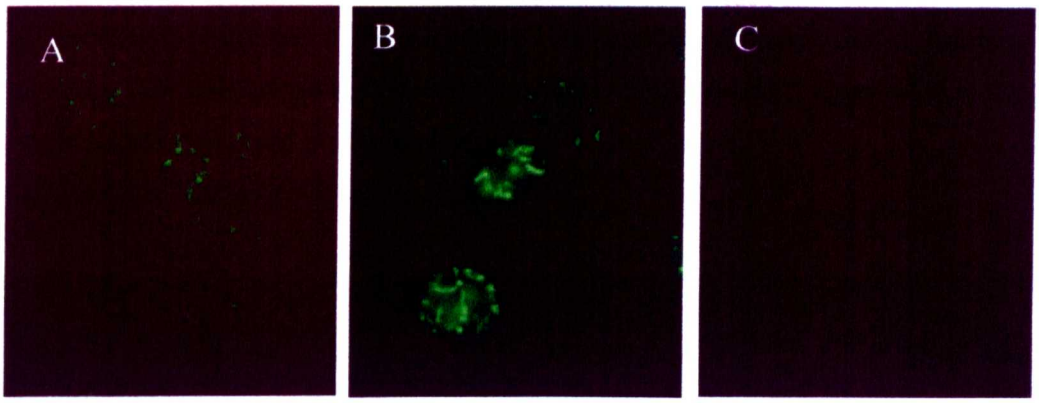

Fig.3.13: E4orf3 expression in transfected or infected HEp-2 cells. Fluorescence microscope images taken using a x100 viewing objective. All panels show HEp-2 cells probed with antibody A4-7 against E4 Orf3, showing green fluorescence where Orf3 is expressed.
Panel A shows Ad5 wt300 infected cells (at m.o.i. 10), panel B shows pcDNA3.1/Orf3 transfected cells and panel C shows mock-infected cells.

To determine whether these structures stained for Orf3 colocalised with PML, cells transfected with pcDNA3.1/Orf3*wt* were co-stained for both Orf3, and endogenous PML. The specificity of secondary antibodies used was tested to prove species specificity (data not shown). These cells were also DAPI stained, (fig.3.14.). Panel A shows cells probed with antibody 5E10 against PML generating green fluorescence where PML is localised. Panel B shows the same cells probed with antibody 6A11 against E4orf3, generating red fluorescence where E4orf3 is present. Panel C shows both stains overlaid to generate yellow fluorescence where the two proteins co-localise, plus DAPI-staining, to help determine the outline of the nucleus and the relation of Orf3 expression to this structure. As can be seen, these results confirmed

that E4orf3 expressed from pcDNA3.1/Orf3*wt* was detectable in the nucleus of HEp-2 cells (panel B), and that it appeared to form nuclear structures that colocalised with and reorganised endogenous PML into track-like structures, similar to those observed during wild-type Ad5 infection (panels A and C). Often, in transfected cells, the green fluorescence equated with the presence of PML, was apparently stronger than that of surrounding, non-transfected cells. As it is unlikely that expression of Orf3 causes a corresponding overexpression of PML in transfected cells, it seems probable that the apparent increase in green fluorescence represents a "bleed-through" of fluorescence from the red spectrum. This was not usually problematic to our assay, as the formation of PML tracks and the loss of the discrete PODs can be unambiguously visualised in infected cells and those expressing E4orf3*wt* with or without co-staining for E4orf3. However, when interpreting immunofluorescence data, it was necessary to be aware that some of the apparent PML staining, might in fact correspond to a very bright E4orf3 signal and not PML at all.

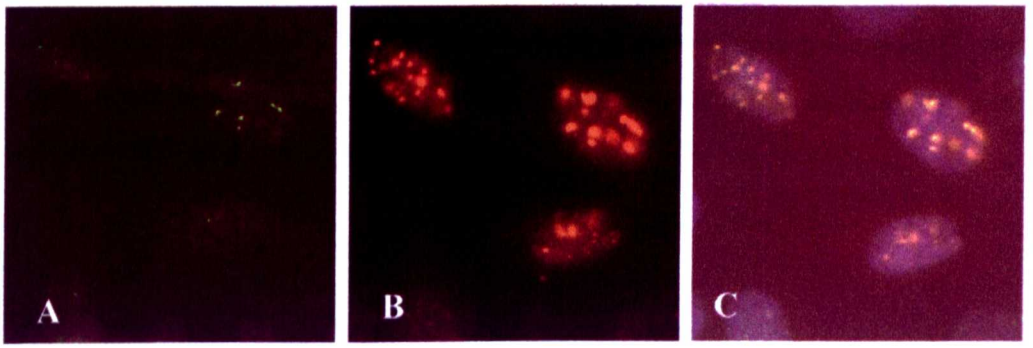

Fig.3.14: E4orf3 and PML costaining in transfected HEp-2 cells. Fluorescence microscope images taken using a x100 viewing objective. All panels show the same field of HEp-2 cells transfected with pcDNA3.1/Orf3*wt*. Panel A shows cells probed with mAb 5E10 against PML. Panel B shows the same cells probed with 6A11 against E4orf3. In panel C both stains are overlaid. Additionally, the cells in panel C are DAPI stained.

3.4. Discussion

By cloning the wild-type E4orf3 gene from the donor plasmid, pGEMOrf3, into pcDNA3.1/HisB/*LacZ*, it was possible to drive expression of this viral protein in eukaryotic HEp-2 cells. Earlier experiments attempting to drive expression of Orf3 from the plasmid, pEXP4, proved unsuccessful. It would appear that in this system,

the CMV promoter of the pcDNA3.1 plasmid backbone is a more potent means of driving expression of E4orf3 than the SV40 promoter provided by pEXP4.

Through the use of Immunofluorescence microscopy, it was possible to demonstrate that a subset of HEp-2 cells transfected with pcDNA3.1/Orf3*wt* were expressing Orf3 in detectable quantities, using antibody 6A11 to detect the Orf3 protein. By staining transfected cells with DAPI, it was possible to define the nuclei of cells, and so demonstrate that E4orf3 localised exclusively to these structures and was not present in the cytoplasm. By co-staining cells for Orf3 and endogenous PML (using mAb 5E10), it was possible to demonstrate that these two proteins apparently colocalised within the nuclei. What is more, the PML staining pattern appeared to be altered in cells expressing Orf3 as compared to neighbouring cells where the presence of Orf3 was not in evidence. In transfected cells, PML was reorganised from the usual "nuclear dots" into track-like structures, and Orf3 apparently colocalised with PML, to these nuclear "tracks". This pattern of PML redistribution is characteristic of alterations consequent to wild-type Ad5 infection. Indeed, the use of adenoviruses lacking the E4orf3 region have demonstrated that this protein is necessary for track formation (Carvalho *et al.*, 1995; Doucas *et al.*,1996).

These experiments, making use of pcDNA3.1/Orf3*wt* to deliver Orf3 to HEp-2 cells in isolation from other viral proteins, were able to demonstrate that the E4orf3 protein is not only necessary, but also sufficient for an alteration in PML localisation, similar to that observed during infection.

4. Construction and expression of mutants in pcDNA3.1/Orf*wt*

Having demonstrated by immunofluorescence that the vector, pcDNA3.1/Orf3*wt*, was capable of expressing E4orf3 in eukaryotic cells to give a pattern of localisation essentially indistinguishable from that seen for Ad5-infected cells, it was of interest to try and identify the regions of the protein necessary for nuclear localisation and track formation, and to use this information to explore the nature of the interaction with the cell in general and PML in particular through the construction of mutant Orf3 expressing plasmids.

4.1. Generation of Orf3 mutants in pcDNA3.1 Vector

The E4orf3 sequences from five adenovirus serotypes were obtained from the Genbank database and aligned and examined for conserved sequences. Since these proteins are expected to have similar functions during their respective virus infections, sequence conservation would be predicted to indicate a gene region important to correct functioning of the protein product. In this way, four conserved regions were identified as potential candidates for functional analysis (see fig.4.1.). It was decided to investigate the significance of each of these regions in E4orf3 function, by mutational analysis of individual bases within these regions. Initially, three Orf3 point mutants and three deletion mutants were generated by mutational PCR (fig.4.2.). All point mutations were designed to substitute alanine for the existing residue. Alanine is a relatively small and non-reactive amino acid, and consequently is commonly used in this way to investigate loss of function without interfering in a positive manner. The mutants were as follows; Orf3G42A, Orf3R68A, Orf3R100A, Orf3del9-13, Orf3del38-42 and Orf3del96-100. The E4orf3 gene was amplified from pcDNA3.1/Orf3, rather than from the viral genome. This was advantageous, as it preserved convenient restriction sites in proximity to the gene, for cloning of the final product back into the vector. Mg^{2+} concentrations needed to be optimised for each reaction. An example of this optimisation is shown in figure 4.3, which illustrates the priming results for primer pairings JD1/JD4 and JD2/JD3, to generate Orf3G42A.

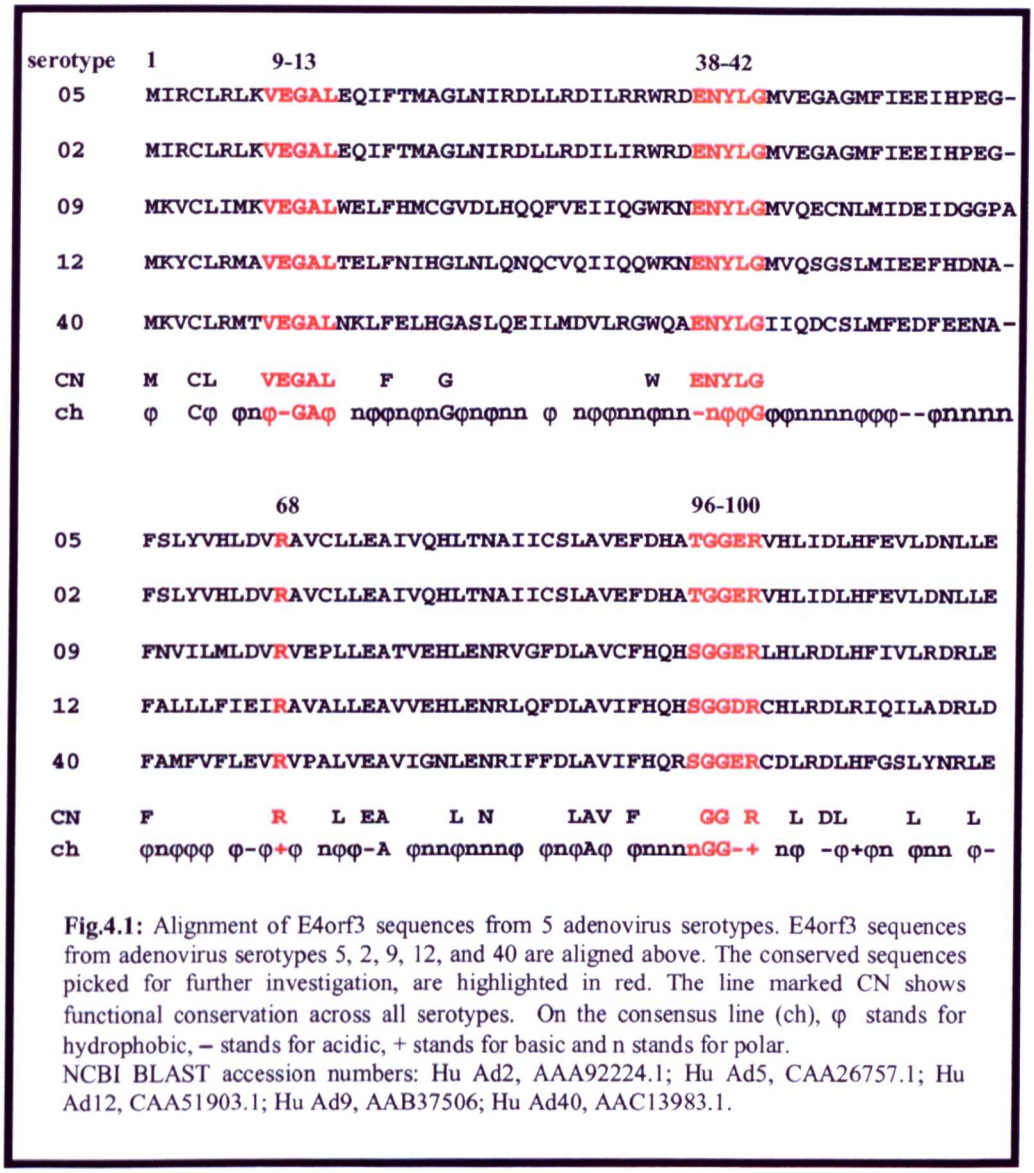

Fig.4.1: Alignment of E4orf3 sequences from 5 adenovirus serotypes. E4orf3 sequences from adenovirus serotypes 5, 2, 9, 12, and 40 are aligned above. The conserved sequences picked for further investigation, are highlighted in red. The line marked CN shows functional conservation across all serotypes. On the consensus line (ch), φ stands for hydrophobic, – stands for acidic, + stands for basic and n stands for polar.
NCBI BLAST accession numbers: Hu Ad2, AAA92224.1; Hu Ad5, CAA26757.1; Hu Ad12, CAA51903.1; Hu Ad9, AAB37506; Hu Ad40, AAC13983.1.

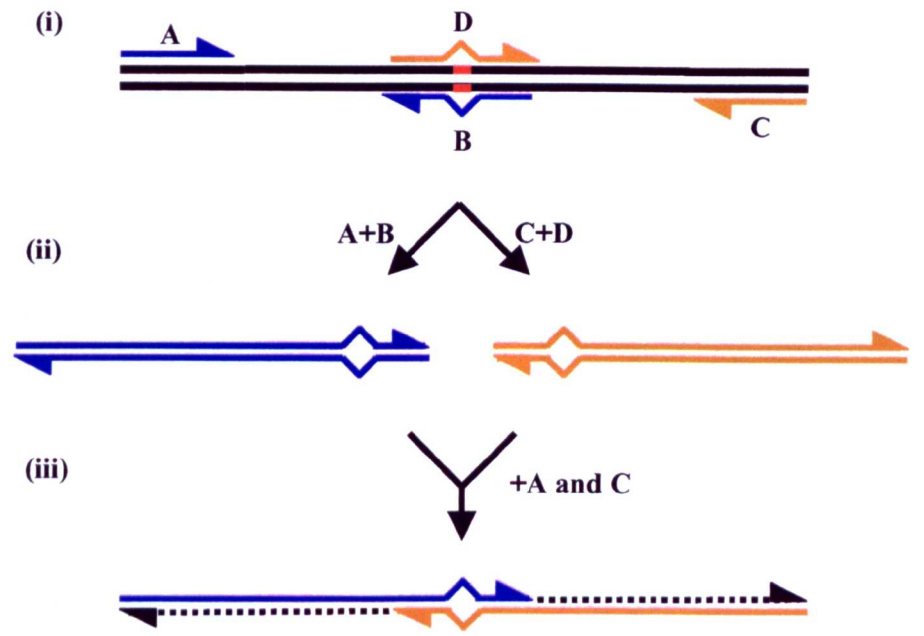

Fig.4.2: Schematic diagram of mutational PCR. Mutational PCR is a two step PCR reaction. In the primary PCR reaction (i), an internal primer spanning the region of interest and carrying the desired mutation (B or D), is paired with an appropriate outside primer (A or C, matching colours denotes a primer pairing). This reaction generates truncated copies of the template, carrying the mutation (ii). A second, similar primary PCR reaction is carried out in the other direction. The internal primers are designed to provide some overlap at this point between both products of the primary PCR reactions. The products of these primary reactions are mixed, and annealed at the point of overlap by heating and cooling of the mix (iii). These paired strands then use their partner as the template during strand lengthening (broken line arrow indicates direction of lengthening), generating double stranded DNA fragments bearing the mutated gene of interest. PCR with primers A and C is then used to amplify the DNA as usual.

Lanes 2 and 3 of panel A show that at suboptimal $MgCl_2$ concentrations there is no PCR product for this reaction, while lane 4 shows that at optimal conditions the desired product is generated. The sizes of the primary reaction products were expected to be different for each primer pair used. The primers used to generate each mutation, and their expected primary reaction product are listed in a table in Appendix I. Samples of the 1° PCR reactions containing the desired fragments were used in the second stage amplification.

The products of the 2° PCR reactions were loaded onto agarose gels (fig.4.4.).

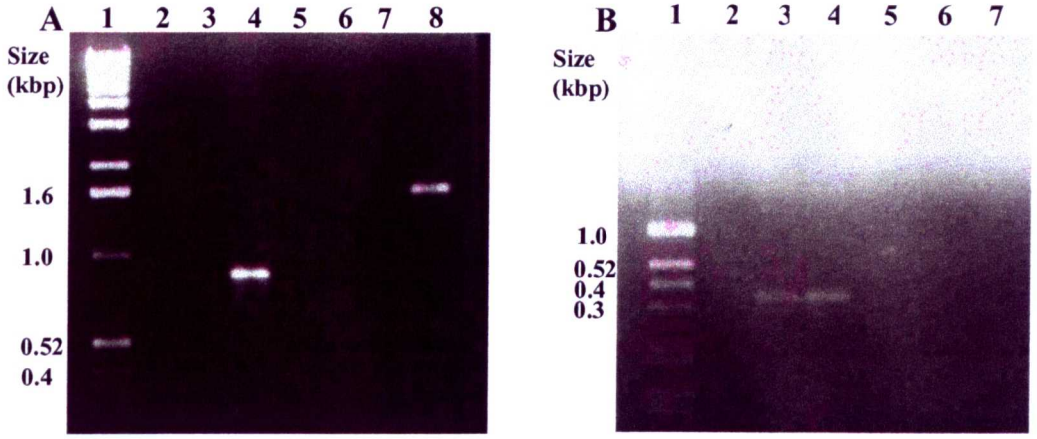

Fig.4.3: Agarose gels showing an example of mutational PCR 1° products. Panel A shows a 1% agarose gel. Lane 1 shows 1Kb ladder. Lanes 2 to 4 show PCR products generated using primer pair JD1 and JD4 at increasing $MgCl_2$ concentrations. Lanes 5 to 7 show the negative controls for the reaction. Lane 8 is loaded with the product of an adenoviral DNA positive control. Panel B shows a 2% agarose gel loaded with the complementary PCR reaction products. Lane 1 shows 1Kb ladder. Lanes 2 to 4 show PCR products generated using primer pair JD 2 and JD3 at increasing $MgCl_2$ concentrations. Lanes 5 to 7 are loaded with the negative controls for this reaction.

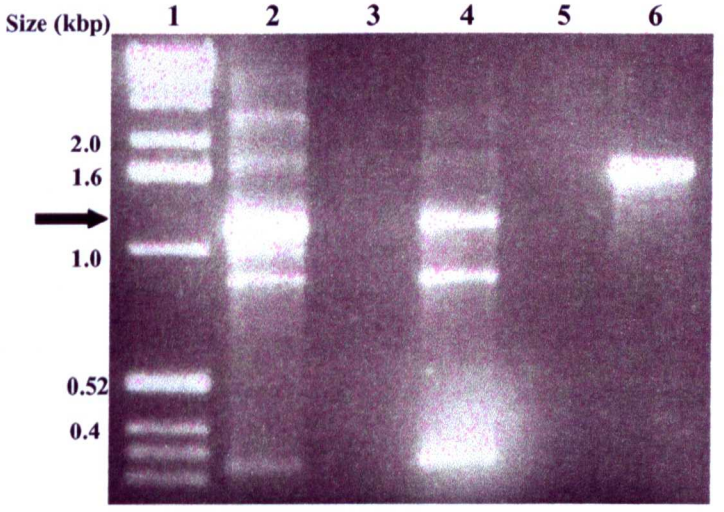

Fig.4.4: A 1.4% agarose gel showing mutational PCR 2° products. Lane 1 shows 1Kb ladder. Lanes 2 and 4 show the products of different 2°PCR reactions, each using the 1° PCR reaction products shown in fig.3.17, lane 4 of both panel A and panel B. Lanes 3 and 5 show negative controls, and lane 6 is loaded with the standard positive control for PCR. The position of the desired Orf3G42A product is indicated with an arrow.

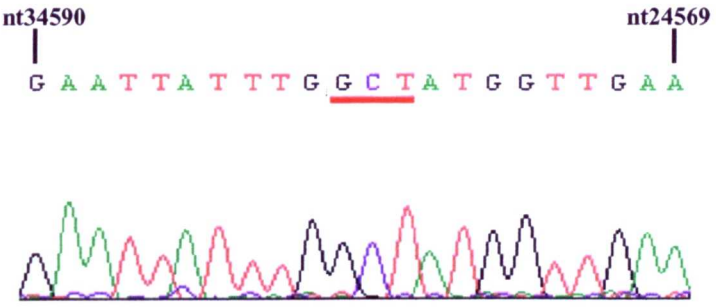

Fig.4.5: A Section of a sequencing chromatogram of the mutant E4orf3 plasmid, pcDNA3.1/Orf3G42A is shown here. The numbers above the chromatogram denote the position of the indicated nucleotide in the Ad5 sequence. The triplet comprising nt34578-34580 (underlined in red) has been mutated from GGC, coding for Glycine, to GCT, coding for Alanine. Sequence chromatograms are presented in Appendix II-XII.

The desired fragments were excised and electroeluted from the agarose gels, phenol/chloroform purified and resuspended in H_2O. The purified DNA was then "trimmed" using EcoRI and HindIII restriction enzyme digestion, to generate fragments suitable for cloning into the pcDNA3.1 plasmid backbone. Cloning of the fragments into the vector was carried out using standard procedures as described above (see section 3.2) and plasmid amplified in bacteria, and purified for analysis by the maxiprep method. All plasmids were sequenced across the E4orf3 gene to ensure that they carried the desired mutation, and that no additional alterations had occurred to the gene (see appendices II-XII). An example of sequence data obtained from the plasmid, pcDNA3.1/G42A (refer to figs.4.3 and 4.4), is shown in figure 4.5.

4.2. Transient transfection of HEp-2 cells and Immunofluorescence using eukaryotic expression vectors of E4orf3 mutants

In order to determine whether any of the E4orf3 mutants resulted in an abnormal phenotype when expressed in eukaryotic cells, the mutant Orf3 expressing plasmids were transfected by the calcium-phosphate method into HEp-2 cells grown on glass coverslips, as before. These were then fixed, double-labelled for E4orf3 and PML, and examined under immunofluorescence microscopy (fig.4.6). In the cells transfected with each of the point mutants (4.6A), E4orf3 could be seen as a nuclear stain in track-like formations, as had previously been observed using pcDNA3.1/Orf3*wt* (4.6A) and by wild-type infection (4.6C). However, the remaining deletion mutants showed aberrant staining for Orf3.

Fig.4.6 A.

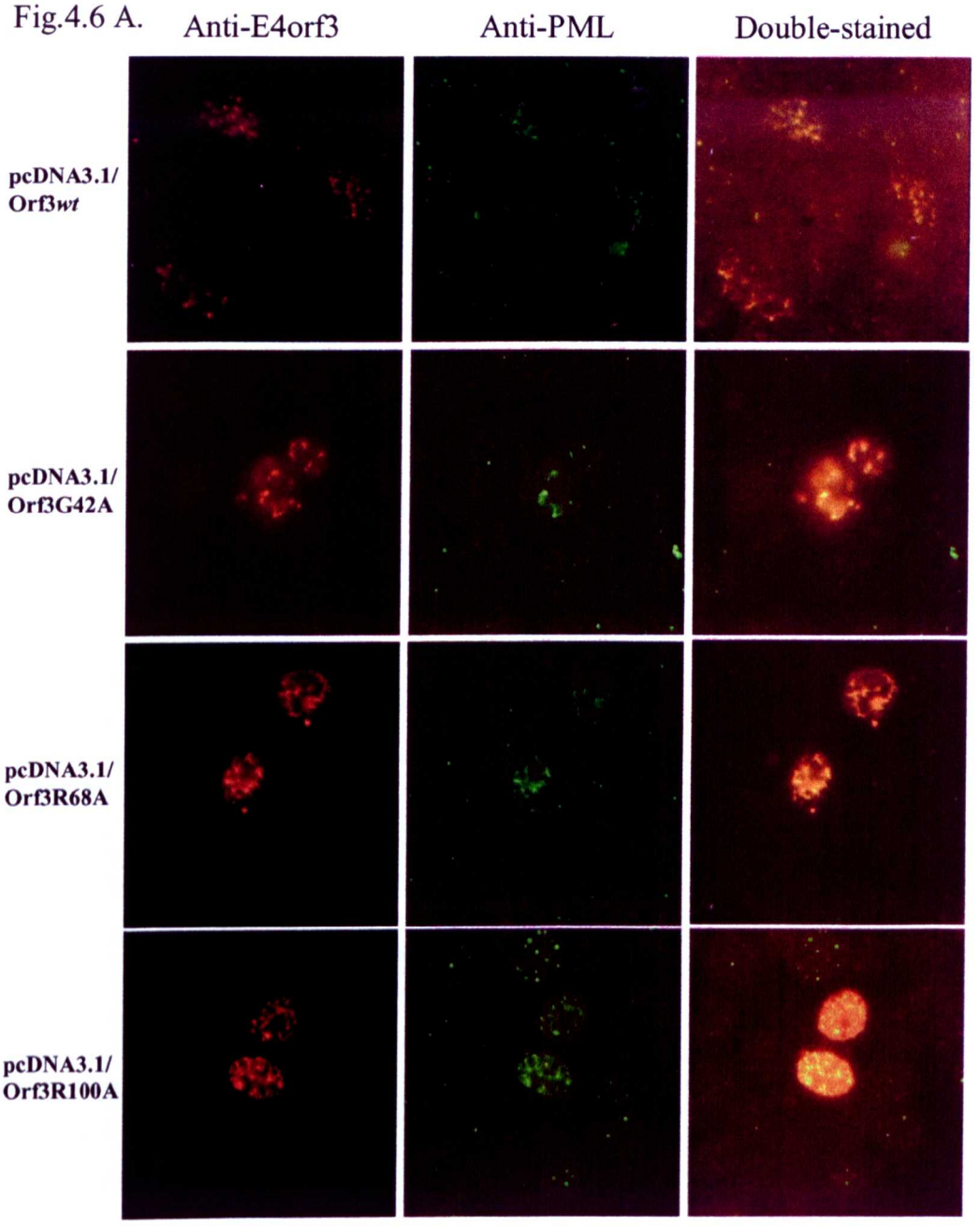
Anti-E4orf3
Anti-PML
Double-stained
pcDNA3.1/
Orf3wt
pcDNA3.1/
Orf3G42A
pcDNA3.1/
Orf3R68A
pcDNA3.1/
Orf3R100A

Fig.4.6 B.

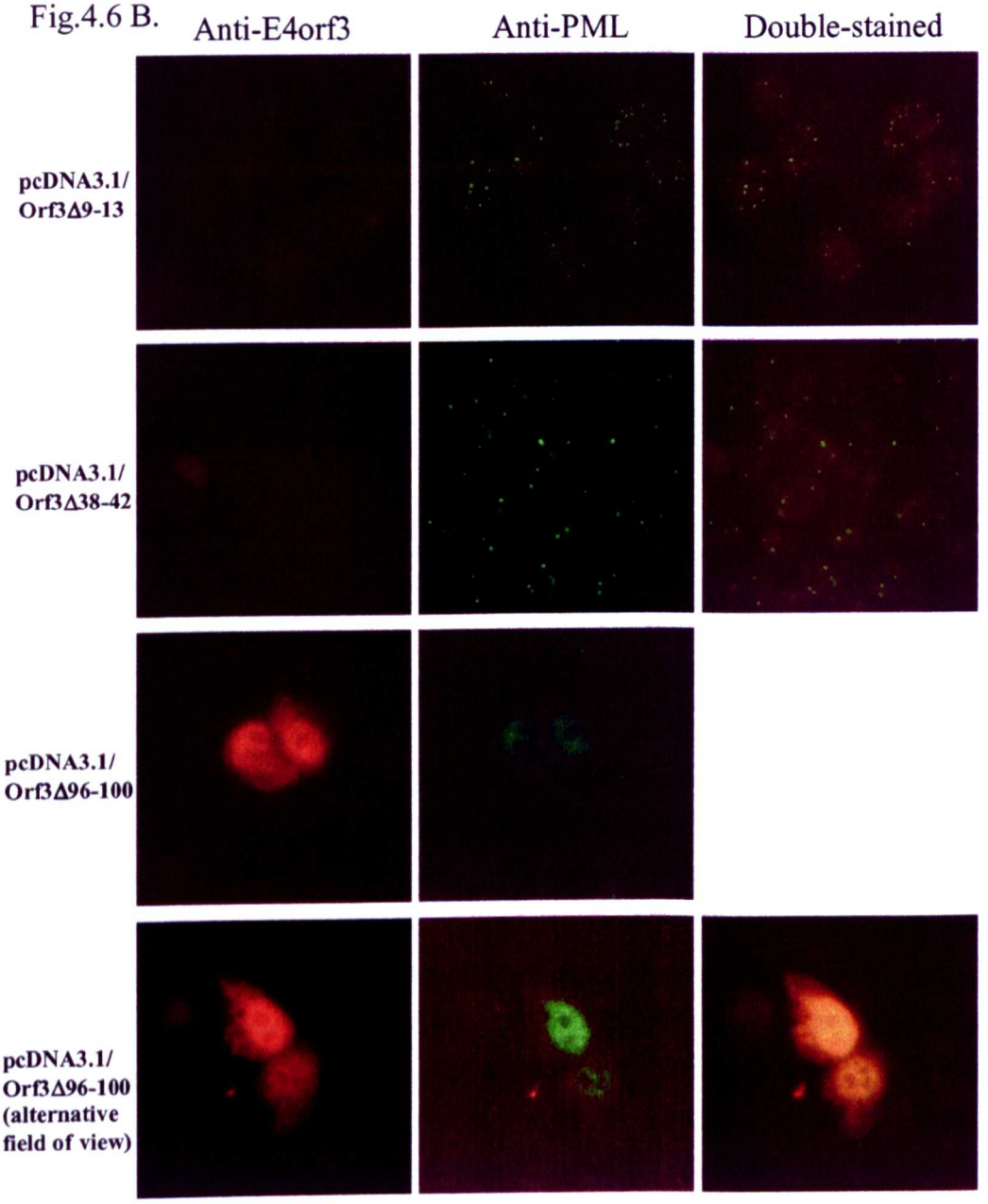
Anti-E4orf3
Anti-PML
Double-stained
pcDNA3.1/
Orf3Δ9-13
pcDNA3.1/
Orf3Δ38-42
pcDNA3.1/
Orf3Δ96-100
pcDNA3.1/
Orf3Δ96-100
(alternative
field of view)

Fig.4.6 C.

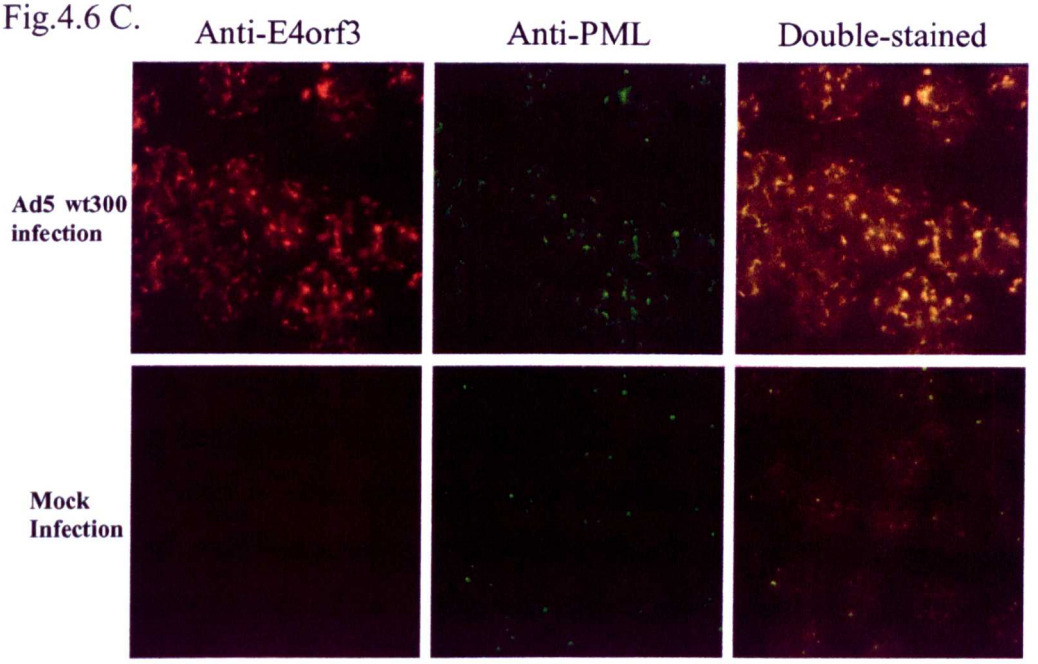

Fig.4.6: E4orf3 and PML co-staining in transfected HEp-2 cells, compared with Ad5*wt*300 and mock infected controls.Fluorescence microscope images were taken using a x100 viewing objective. Each series of panels from left to right show the same field of HEp-2 cells transfected/infected as indicated on the left, and probed as indicated at the top. Cells were probed with mAb 5E10 against PML and with 6A11 against E4orf3.

Transfection with pcDNA3.1/Orf3del9-13 or pcDNA3.1/Orf3del38-42, did not produce any visible Orf3 stain (4.6 B, upper six panels). This was perhaps to be expected, as these deletions could have significantly disrupted the tertiary structure, destabilising the protein or concealing the antibody-binding site. Nevertheless, the GOR secondary structure prediction method (version IV, Garnier *et al.,* 1996), does not predict these regions to be in structurally important alpha helical regions and consequently, these deletions might not be thought to have a major impact on protein structure and function. It was also possible that these deletions directly impacted on the antibody epitope. Transfection with the Orf3del96-100 mutant was however, more interesting, in that E4orf3 staining was visible, but in contrast to the well defined nuclear tracks previously observed, it was found in both cytoplasmic and nuclear compartments as a diffuse stain (4.6B, lower six panels). In cells expressing this protein, green fluorescence was observed as a diffuse signal, apparently overlaying discrete, nuclear foci of green fluorescence. In transfected cells, the green fluorescence equated with the presence of PML, is apparently stronger than that of surrounding, non-transfected cells. As it is unlikely that expression of Orf3 causes a

corresponding overexpression of PML in transfected cells, it seems probable that the apparent increase in green fluorescence represents a "bleed through" of fluorescence from the red spectrum. This was not usually problematic to our assay, as the formation of PML tracks, and the loss of the discrete PODs can clearly be seen in infected cells, and in those expressing E4orf3*wt*. However, where cells were transfected with pcDNA3.1/Orf3del96-100, the bright, diffuse green signal corresponding to bleed-through of red signal, did to some extent obscure the localisation of PML. Nevertheless it is possible, referring to fig.4.6B, to distinguish discrete structures beneath the diffuse green stain. These represent PODs that have not undergone reorganisation, and are features not observed in infected cells, or those transfected with plasmids that generate Orf3 tracks. Seemingly, PML did not colocalise with the diffuse E4orf3 mutant, and the PODs were not disrupted to generate PML tracks or other structures. This would suggest that in order to interact with PML, Orf3 must first localise to the PODs. That is to say, PML interaction with Orf3 cannot occur outside of the PODs, and E4orf3 must be concentrated in discrete subnuclear regions to associate with PML.

4.3. Generation of further Orf3 mutants in pcDNA3.1 Vector

The immunofluorescence microscopy data on the initial panel of six mutants for E4orf3, revealed that one deletion mutant, Orf3del96-100, displayed aberrant Orf3 localisation when expressed in eukaryotic HEp-2 cells, implicating residues 96-100 in the correct localisation of Orf3. In an attempt to further characterise the motif responsible for this phenotype, further point mutants were designed to substitute alanine for each amino acid in this region. Orf3R100A had already been constructed, so only the following four mutants had to be constructed; Orf3T96A, Orf3G97A, Orf3G98A and Orf3E99A. As before, DNA fragments coding for mutant Orf3s were generated by using mutational PCR, and these were subsequently cloned into the pcDNA3.1 vector backbone, and amplified in bacteria. Again, all final constructs were sequenced across the Orf3 gene region (see appendices II-XII).

4.4. Transient transfection of HEp-2 cells and Immunofluorescence using E4orf3 point mutants spanning residues 96-100

The four plasmids, pcDNA3.1/Orf3T96A, G97A, G98A and E99A were transfected into HEp-2 cells grown on glass coverslips, as before. These were fixed and stained

for E4orf3 expression, 24 hrs post-transfection, and observed by immunofluorescence microscopy. In all cases, Orf3 staining was observed in the nuclei of transfected cells in track-like structures (Fig.4.7A.). In the case of cells expressing E4orf3T96A, there also appeared to be notable concentrations of Orf3 outside the nucleus in several cells, in addition to the tracks within. This phenotype is demonstrated in figure 4.7B, where DAPI staining was used to stain the DNA and define the boundaries of the nucleus. Here, Orf3 staining appears as a punctate stain apparently outside of the nuclei of any of the surrounding cells. This point mutant appeared to share a milder version of the phenotype observed when the deletion mutant, Orf3del96-100, was expressed. However, an inherent difficulty with the technique used, is the variability in expression from cell to cell as can be seen by comparing the apparent pattern of Orf3 expression between the pcDNA3.1/Orf3T96A transfected cells shown in figures 4.7A and 4.7B. One cell may have been transfected with more plasmids than its neighbour, and consequently express the protein to a greater extent. This can render results misleading. It may have been the case that Orf3 was only present in the cytoplasm of cells expressing T96A because the cells observed were greatly overproducing the protein in comparison with other transfections. In this case, despite a fully functional protein, some Orf3 might have "leaked" or been transported into cellular compartments where it might not normally be found in these quantities. A number of cells were viewed, and only those considered representative of the "average" cell in a transfection were recorded. By this means, it was hoped to eliminate out the effects of overexpression. However, the problems associated with achieving consistent and standard expression of Orf3 were inherent to the transient transfection method.

Fig.4.7 A.

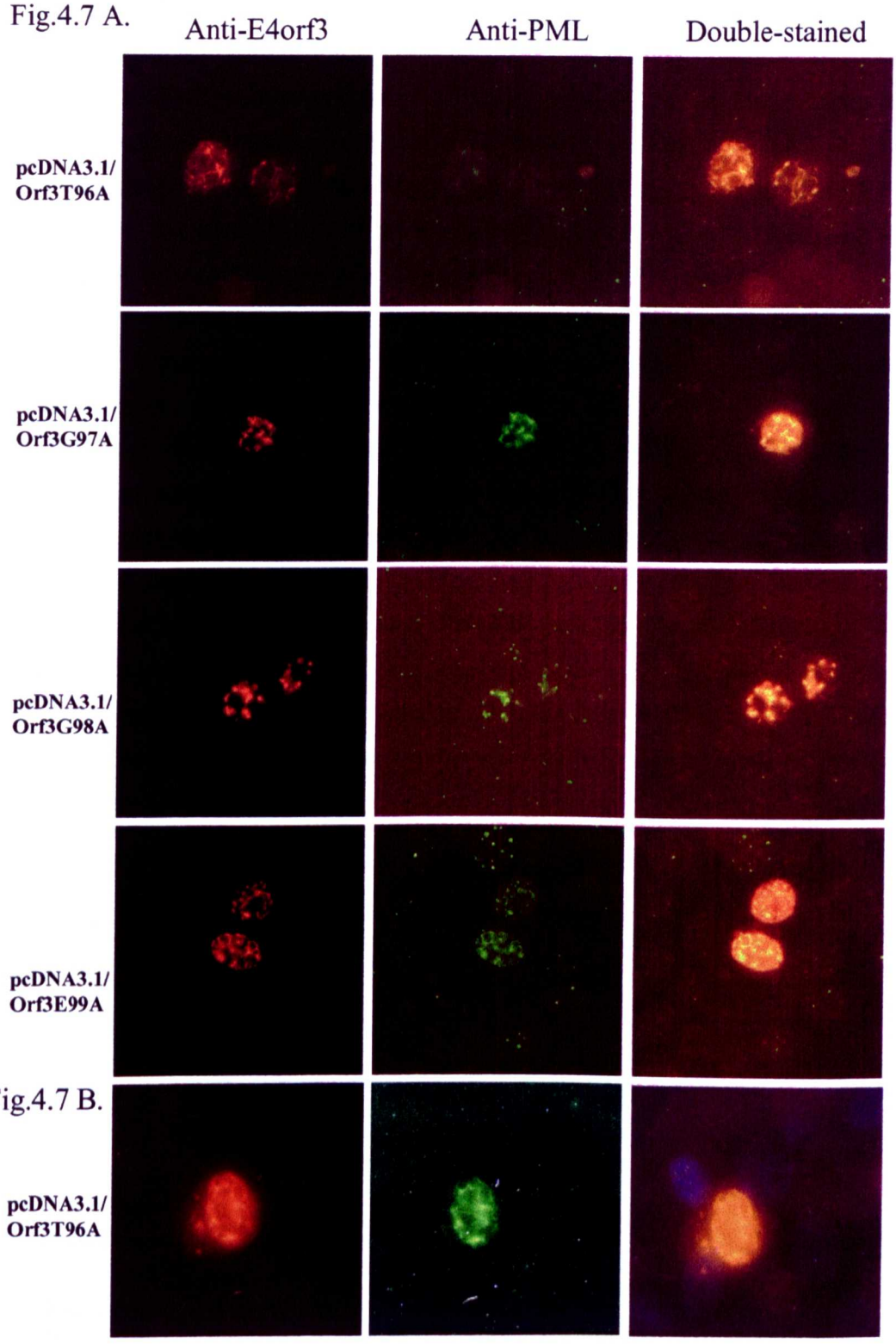

Fig.4.7 B.

Fig.4.7. E4orf3 and PML costaining in transfected HEp-2 cells. Fluorescence microscope images were taken using a x100 viewing objective. Each series of panels from left to right show the same field of HEp-2 cells transfected with the plasmid indicated on the left, and probed as indicated at the top. Cells were probed with mAb 5E10 against PML and with 6A11 against E4orf3.
In figure 4.7B, DAPI staining was also used to stain DNA and define the boundaries of the nucleus.

4.5. Western Blotting of HEp-2 derived samples with pcDNA3.1/Orf3*wt*

Having demonstrated that it was possible to detect E4orf3 expression in eukaryotic HEp-2 cells by IF microscopy using the vector, pcDNA3.1/Orf3*wt*, it was of interest to determine whether this plasmid system could be used as the basis for a western blotting assay into effects of Ad5 E4orf3 upon the biochemical properties of PML. As previously discussed, it has been demonstrated that E4orf3 is necessary for the generation of an infection-specific PML banding pattern in Western blot assays, and it has been postulated that this biochemical alteration of PML is necessary for, or results from the formation of PML "tracks". The immunofluorescence microscopy results shown above, confirmed the observation that E4orf3 alone was necessary and sufficient for the formation of "tracks" (Carvalho *et al.,* 1995; Doucas *et al.,* 1996). A biochemical alteration of PML in the same system would link the two phenomena.

Firstly, it was necessary to determine whether Orf3 could be detected by Western blot in samples derived from transfected HEp-2 cells, with samples from Ad5-infected cells as positive controls. An Ad5inorf3 infection was included as a negative control for orf3 expression. This mutant virus does not produce Orf3, but is otherwise wild-type. Accordingly, samples were taken at 24 hours post-transfection and infection, and run on 15% SDS-PAGE. The protein was then blotted onto nitrocellulose, and detected using antibody to E4orf3 (Fig.4.8.)

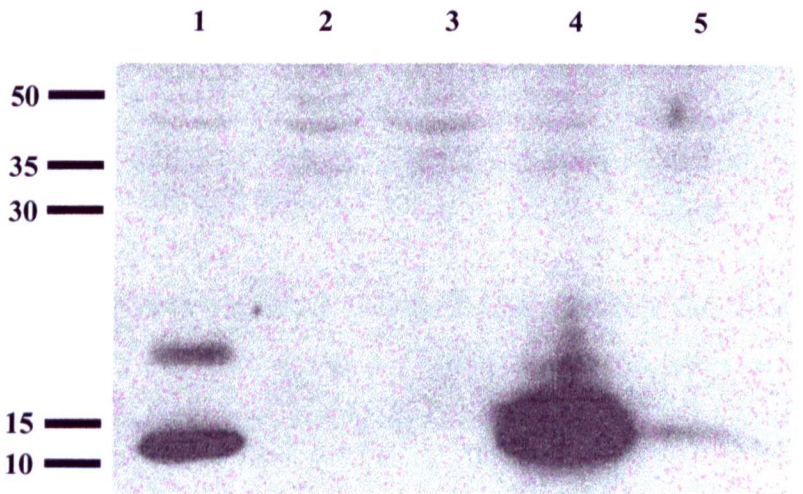

Fig.4.8: Presence of E4orf3 in transfected and infected HEp-2 cells. Approximately 3.5 x 10^4 HEp-2 cells were transfected with pcDNA3.1/Orf3wt (lane 1), pcDNA3.1/HisB/*lacZ*, mock-transfected (lane 2), infected with wt300 (lane 4), Ad5inorf3 (lane 5) or mock-infected (lane 3) at 37°C. Total cell extracts were prepared at 24 hours post-transfection and infection. Extracts were separated by SDS-PAGE on a 15% gel, blotted and probed for E4orf3 with antibody 6A11. The positions to which proteins of known molecular mass migrated are shown at the left (kDa).

As can be seen in lane 4 of figure 4.8, a band of approximately 11K corresponding to E4orf3 is clearly discernible in cells infected with wild-type adenovirus (wt300). A band of similar mobility is also present in lane 1, comprising the contents of cells transfected with pcDNA3.1/Orf3*wt*. This band is not present in either the mock-infection, Ad5inorf3 infection, or mock-transfection (lanes 3, 2 and 5, respectively). The faint banding in lane 5 is probably due to "spillover" from lane 4. Note the lower mobility band in lane 1 (approx. 20K). This may be an artefact, or represent an altered, possibly SUMO-1 modified form of E4orf3. These results demonstrated that the E4orf3 protein was produced in HEp-2 cells transfected with pcDNA3.1/Orf3wt however, repeat experiments using standard conditions showed that this system was unreliable in generating a strong Orf3 signal from transfected cells (see fig.4.9). Here, despite a strong E4orf3 signal in samples taken from HEp-2 cells infected with wild-type adenovirus (lane 4 of both blots), cells transfected with pcDNA3.1/Orf3*wt* only yielded a very weak E4orf3 signal (fig.4.9 panel A, lane 1) or none at all (panel B, lane 1).

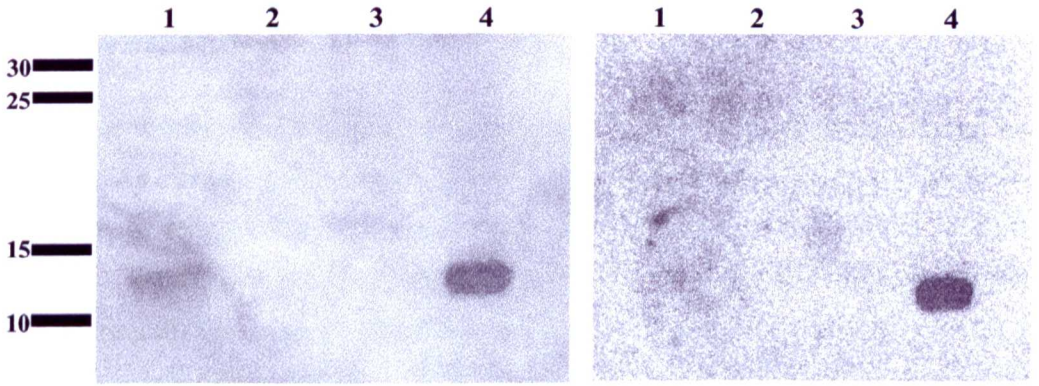

Fig.4.9: Two separate Western blot assays of total protein samples taken from HEp-2 cells transfected with pcDNA3.1/Orf3*wt*, compared with cells infected with wild-type Ad5. Approximately 2 x 10^4 HEp-2 cells were transfected with pcDNA3.1/Orf3wt (lane 1 of blots A and B) or mock-transfected (lane 2 of blots A and B). Approximately 1 x 10^4 cells were mock-infected (lane 3 of blots A and B) or infected with Ad5 wt300 (lane 4 of blots A and B). The positions to which proteins of known molecular mass migrated are shown at the left (kDa).

Despite the difficulties involved in maintaining comparable Orf3 expression levels between transient transfections, it was decided to attempt a blot of transfected samples, probing against PML. Samples of HEp-2 cells transfected with

pcDNA3.1/Orf3*wt* were loaded on 7.5% SDS-PAGE gels along with Ad5 infected controls and transferred onto nitrocellulose membranes (fig.4.10).

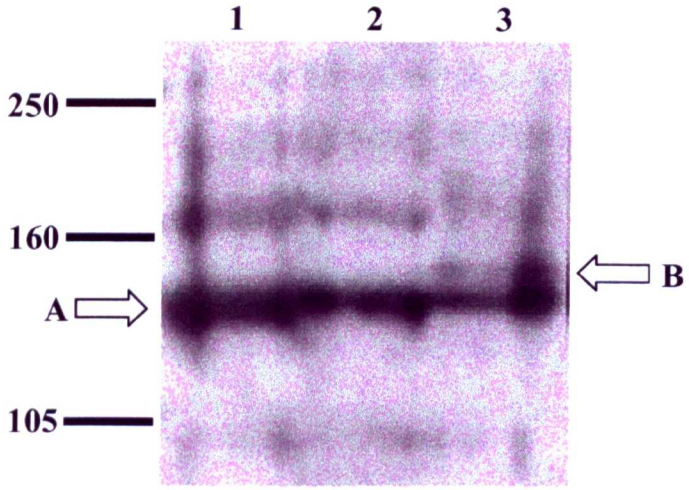

Fig.4.10: PML isoforms in transfected and infected HEp-2 cells. Extracts were separated by SDS-PAGE on a 7.5% gel, blotted and probed for PML with antibody 5E10. Each lane is loaded with the equivalent of 4 x 10^4 HEp-2 cells. Lane 1 is loaded with a sample of cells transfected with pcDNA3.1/Orf3*wt*. Lane 2 is loaded with mock infected samples. Lane 3 is loaded with samples derived from cells infected with wild type 300 Ad5. Arrow A indicates the major PML band at approximately 140kDa. Arrow B indicates the infection specific PML isoform just above the 140kD band. The positions to which proteins of known molecular mass migrated are shown at the left (kDa).

The best results were obtained when the blot was carried out overnight using low current. As can be seen in samples taken from cells infected with Ad5 wt300, it was possible to recreate the distinctive, adenovirus infection-specific pattern of PML species distribution previously demonstrated by Leppard and Everett (1999). Comparing the extracts of infected cells (lane 3), with mock infected cells (lane 2), it can be seen that three low mobility PML bands were lost and a novel band, indicated by arrow B appeared, migrating just above the major 140kD band, indicated by arrow A. However, those lanes loaded with extracts of pcDNA3.1/Orf3*wt* transfected HEp-2 cells (lane 1) do not show this distinctive PML banding pattern, displaying a similar pattern to mock-derived samples in this assay. Taken on face value, these results suggest that E4orf3 alone is not sufficient for the observed biochemical alteration of PML upon infection, and thus this process and track formation are not directly related. However, due to the variable nature of transfection efficiency in these assays, it is difficult to argue that the above results are meaningful. More importantly, an obvious criticism of this experiment is simply that even at its best, transfection efficiency is still too low to generate meaningful results. At best, transfection efficiency was

probably below 5%, as determined by immunofluorescence microscopy on cells processed in parallel. The relatively high total levels of Orf3 observed in a "successful" transfection by western blotting, actually only represents a subset of cells, which are vastly overexpressing E4orf3 in relation to infected cells. As surplus Orf3 is not transported outside of the producing cell to its neighbours, total Orf3 protein level in this assay is not related to the number of cells exposed to the effects of Orf3. Thus, if only 1 in 20 cells are transfected, only 1 in 20 cells might be expected to contain "infection specific" PML species. This amount of altered protein could well be lost amongst the vast majority of unmodified PML. Indeed, it was never likely that transfection would visibly reduce the levels of the three low mobility isoforms as occurs during infection, but it was hoped that it might be possible to visualise the appearance of the novel band above 140kD. However, this was not the case, and the results of this experiment were consequently inconclusive.

4.6. Western blotting of HEp-2 derived samples using the panel of pcDNA3.1/Orf3 mutants

Despite the discouraging results obtained from SDS-PAGE and Western blotting using samples taken of HEp-2 cells transfected with pcDNA3.1/Orf3*wt*, it was hoped that it would be possible to visualise Orf3 in samples taken from cells transfected with the panel of Orf3 mutants, and relate this to any biochemical alterations observed in PML in the same samples. For example, it would useful to determine that the novel, infection-specific PML band appeared when tracks were generated (by the majority of mutants), but that PML was not altered where Orf3 localisation was disrupted (using del96-100). It would have been interesting to note whether any of the constructs when expressed were mutant for PML biochemical alteration, but not track formation. It was hoped that these results would help tie track formation and PML modification together, or demonstrate that the two were indeed separate processes. Unfortunately it proved difficult to visualise Orf3 on the blots and impossible to visualise it for all transfections at the same time, thus there were no grounds for comparison between samples. Figure 4.11 is typical of such a result. Here, a band corresponding to E4orf3 can only be visualised in cell extracts of Ad5-infected HEp-2 cells. Analysis of PML banding pattern in the same samples did not show any modification, other than in the virus infected samples. As Figure 4.12 shows, extracts of HEp-2 cells transfected with Orf3 expressing plasmids appeared to be in all ways similar to extracts of mock

transfected cells. Three SUMO-1-modified PML isoforms were visible above the major band of 140kDa (arrow A), and no novel bands had appeared. However, where HEp-2 cells were Ad5-infected, these three lower-mobility PML isoforms were lost, and in addition, the infection-specific band appeared above 140kDa (labelled with arrow B).

As before, these results were largely inconclusive, due to the lack of consistency between assays and the low overall transfection efficiency. Multiple approaches were utilised to address this problem. One was to try and improve transfection efficiency to a level where the novel, infection-specific PML isoform, if produced, would be present in sufficient quantities to be visualised by western blotting. The other approach was to assume that E4orf3 was present in sufficient quantities to generate the novel band, but had not done so as Orf3 alone was not sufficient for this phenomenon, but required additional viral input. If this could be shown to be the case, it would not be necessary to elaborate on the existing technique. In addition, it was considered desirable to construct recombinant Ad5 viruses substituting selected E4orf3 mutants for the wild-type gene, so that 100% of cells in a culture could be made to express mutant Orf3 and overcome the problems of transfection.

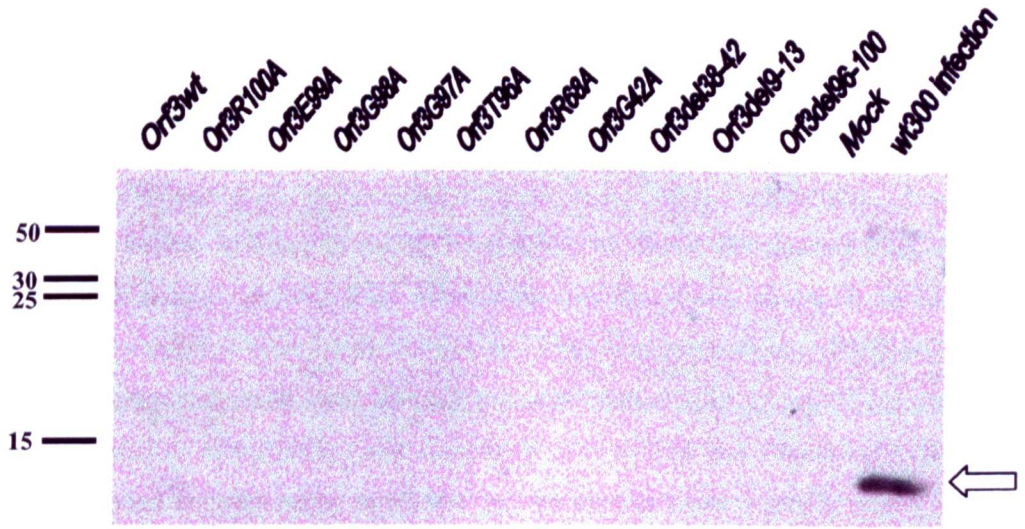

Fig.4.11: Each of the mutant E4orf3 expressing plasmids was transfected into 2 x 10^5 HEp-2 cells at 37°C and total cell extracts prepared at 24 hours post-transfection. HEp-2 cells were infected with Ad5 wt300 as a positive control for E4orf3 expression. Extracts were separated by SDS-PAGE on a 15% gel, blotted and probed for E4orf3 with antibody 6A11. E4orf3 expression can only be visualised in samples infected with Ad5 wt300 (indicated by the arrow). The positions to which proteins of known molecular mass migrated are shown at the left (kDa).

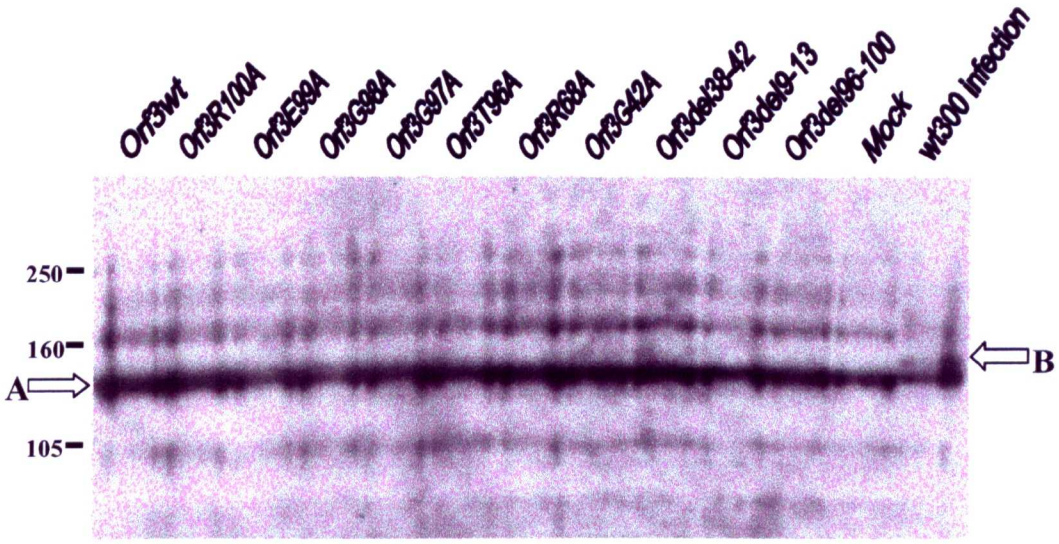

Fig.4.12: PML isoforms in transfected and infected HEp-2 cells. Each of the mutant E4orf3 expressing plasmids was transfected into 2 x 10^5 HEp-2 cells at 37°C and total cell extracts prepared at 24 hours post-transfection. HEp-2 cells were infected with Ad5 wt300 as a positive control for E4orf3 expression. Extracts were separated by SDS-PAGE on a 7.5% gel, blotted and probed for PML with antibody 5E10. Arrow A indicates the major PML band at approximately 140kDa.The positions to which proteins of known molecular mass migrated are shown at the left (kDa).

4.7. The use of 293 cells in transfection and infection assays

It was decided to investigate the suitability of using 293 cells rather than HEp-2 cells as a potential means of increasing transfection efficiency. 293 cells are adenovirus-transformed human embryonic kidney cells expressing the adenoviral E1b-55K product (Graham *et al.*, 1977), and are known to be highly transfectable. However, it was not known whether it would be possible to detect the desired PML banding pattern in samples derived from these cells. Initially, it was necessary to perform a simple comparison between the E4orf3 and PML banding patterns of 293 and HEp-2 cells in samples derived from infected and non-infected cells. Using Western blotting, it was possible to visualise Orf3 expression in both 293 and HEp-2 cells (fig.4.13). Here, a band corresponding to E4orf3 can be seen in lanes 2 and 5, where 293 and HEp-2 cells respectively, were infected with Ad5 wt300. This band is not visible in the mock infections (lanes 3 and 6) or infections with the virus inorf3 which carries an insertional mutation of E4orf3, rendering the gene non-functional (lanes 1 and 4).

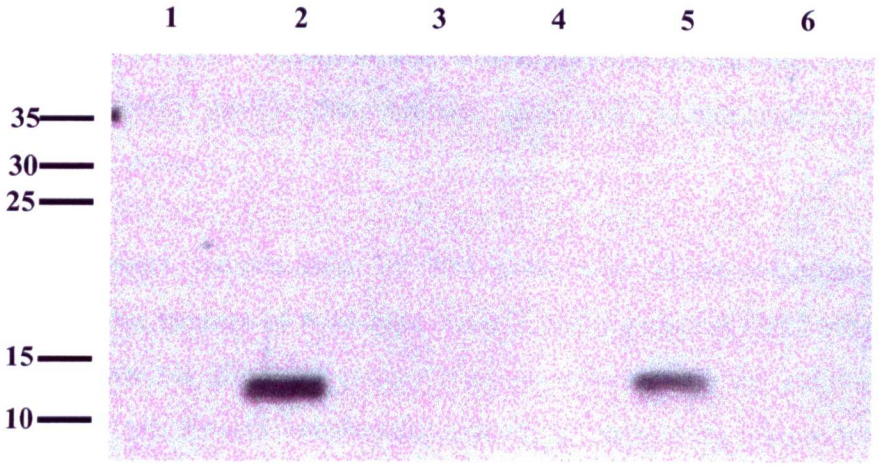

Fig.4.13: The presence of E4orf3 in infected 293 or HEp-2 cells. 2 x 10^5 cells were infected with Ad5 wt300 (lanes 2 and 5), Ad5 inorf3 (lanes 1 and 4) or mock infected (lanes 3 and 6) at 37°C and total cell extracts prepared at 24 h p.i. Extracts were separated by SDS-PAGE on a 15% gel, blotted and probed for E4orf3 with antibody 6A11. Lanes 1 to 3 show samples derived from 293 cells. Lanes 4 to 6 show samples derived from Hep-2 cells. The positions to which proteins of known molecular mass migrated are shown at the left (kDa).

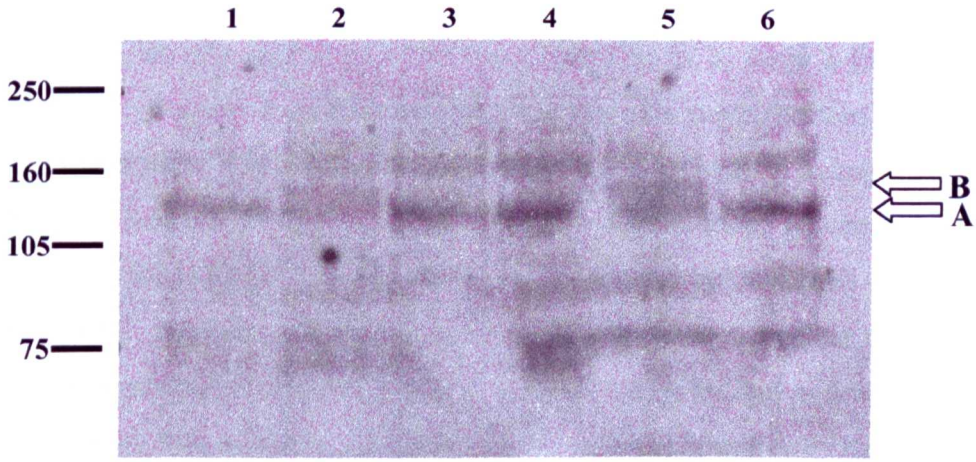

Fig.4.14: PML isoforms in infected HEp-2 or 293 cells. 2 x 10^5 cells were infected with Ad5 wt300 (lanes 2 and 5), Ad5 inorf3 (lanes 1 and 4) or mock infected (lanes 3 and 6) at 37°C and total cell extracts prepared at 24 h p.i. Extracts were separated by SDS-PAGE on a 7.5% gel, blotted and probed for PML with antibody 5E10. Lanes 1 to 3 show samples derived from 293 cells. Lanes 4 to 6 show samples derived from Hep-2 cells. Arrow A indicates the major 140kDa PML band. Arrow B indicates the adenovirus infection specific isoform just above 140kDa. The positions to which proteins of known molecular mass migrated are shown at the left (kDa).

Probing of the same samples for PML demonstrated that 293 and HEp-2 cells were equivalent in relation to this protein (fig.4.14.). The diagnostic infection-specific band (indicated by arrow B) just above 140kDa could be seen in the content of wt300 infected cells of both types (lanes 2 and 5), but not in mock infections (lanes 3 and 6), or infections with inorf3 (lanes 1 and 4). The absence of the infection-specific band in cells infected with inorf3, demonstrates that Orf3 is necessary for this PML modification to occur.

4.7.1. Transient transfection of 293 cells and Immunofluorescence using plasmids vectors of wild-type E4orf3 and a panel of Orf3 mutants

293 cells grown on glass coverslips were transfected by the calcium phosphate method, with all E4orf3 expressing plasmids previously described, alongside appropriate controls. At 24hrs post infection, these were formaldehyde fixed, blocked and probed with mAb 5E10 against PML, and rat 6A11 against E4orf3. The results are shown in figure 4.15. Here, the results essentially mirrored those obtained using HEp-2. Again, Orf3 is visualised as nuclear tracks for all mutants except for del96-100, and to a lesser extent in Orf3T96A. Importantly, 293 cells proved to be much more transfectable than HEp-2 cells, giving a typical transfection efficiency of 20-25%. This made 293 cells much more suitable for the Western blot assay of PML isoforms. With relatively high levels of Orf3 expression in as large a fraction as a quarter of cells, we might expect to see the presence of a novel protein isoform in addition to unmodified PML reflected in blots. The drawback of using 293 cells proved to be a weaker PML stain under immunofluorescence. Nevertheless, the important properties of Orf3/PML colocalisation could still be discerned. It is worth noting that E4orf3 has been shown to bind to and colocalise at nuclear tracks with E1B-55kDa, also present in 293 cells. Recent evidence suggests that in doing so, Orf3 liberates p53 from 55K induced inhibition of transcriptional activity (Konig *et al.*, 1999). While, it is worth considering the effect 55K might have on the experimental system being studied, it seems unlikely that the presence of this viral protein would adversely affect our assay when we consider that both viral proteins are present in the wild-type Ad5-infected cells in which the alteration of PML banding patterns and ND10s was characterized.

Interestingly, IF microscopy analysis of 293 cells transfected with pcDNA3.1/Orf3del38-42, revealed nuclear Orf3 "tracks" similar to those observed in

cells expressing wild-type Orf3. It had previously not been possible to observe expression of this protein in transfected Hep-2 cells, suggesting that some intrinsic property of 293 cells may have been stabilising the protein in some way. One obvious difference between Hep-2 cells and 293 cells is the presence of the adenovirus protein, E1b-55kDa in the latter. This protein is known to form a complex with E4orf3 at early stages in infection, and it was of interest to determine whether 55K was responsible for stabilising Orf3 in 293 cells. To test this, HEp-2 cells were co-transfected with both pcDNA3.1/Orf3del38-42, and the E1b-55kDa expressing plasmid, XhoI-C (fig 4.16). These cells were then co-stained against Orf3 and 55K (fig.4.17). In this assay, the Orf3del38-42 protein appeared to be present, forming the typical nuclear tracks. These Orf3 tracks apparently colocalise with the 55K protein. On the basis of this result, it would appear that Orf3del38-42 was indeed "stabilised" in some way by the presence of ElB55kDa.

Fig.4.15 A.

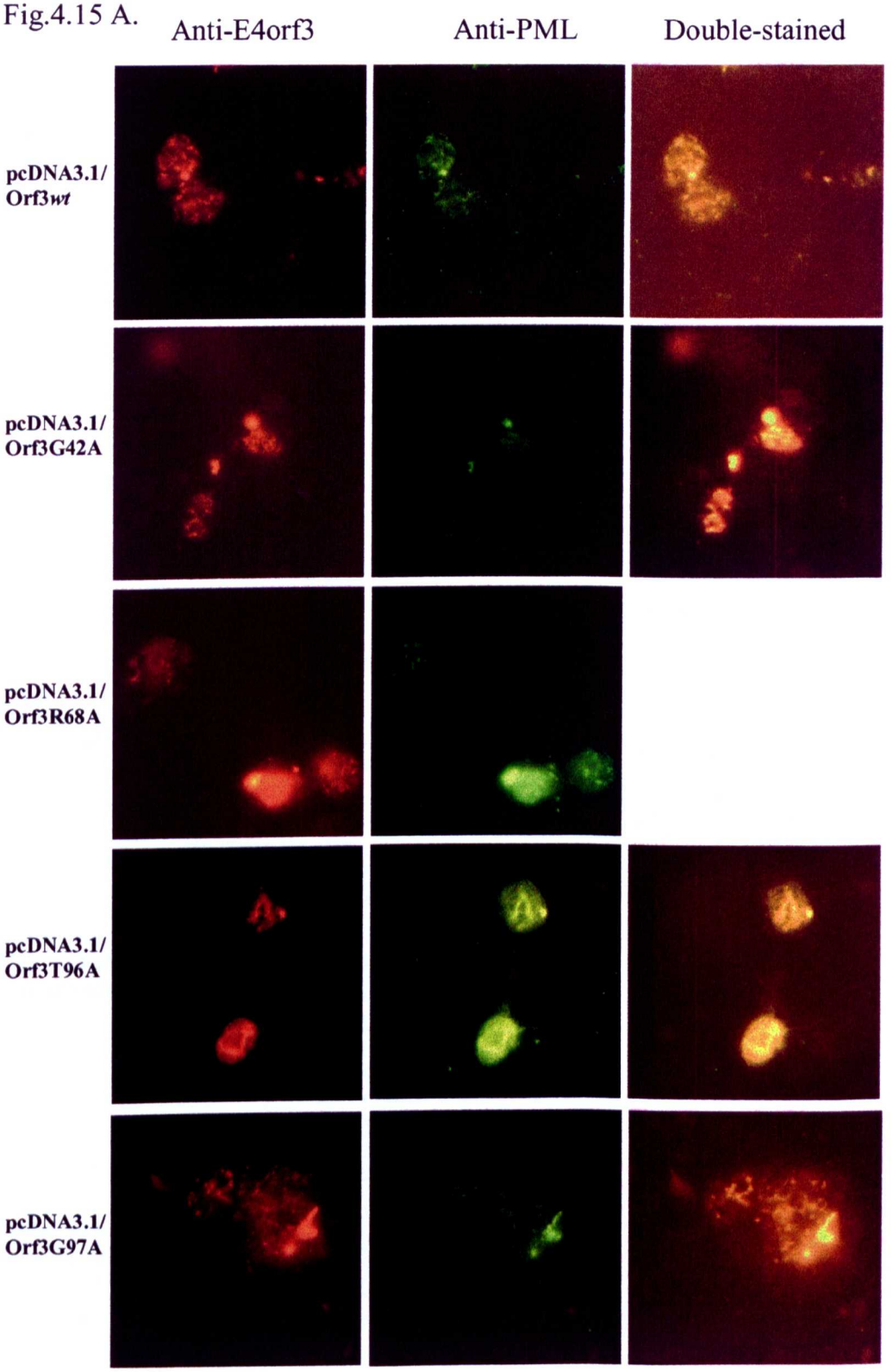
Anti-E4orf3
Anti-PML
Double-stained
pcDNA3.1/ Orf3wt
pcDNA3.1/ Orf3G42A
pcDNA3.1/ Orf3R68A
pcDNA3.1/ Orf3T96A
pcDNA3.1/ Orf3G97A

Fig.4.15 B.

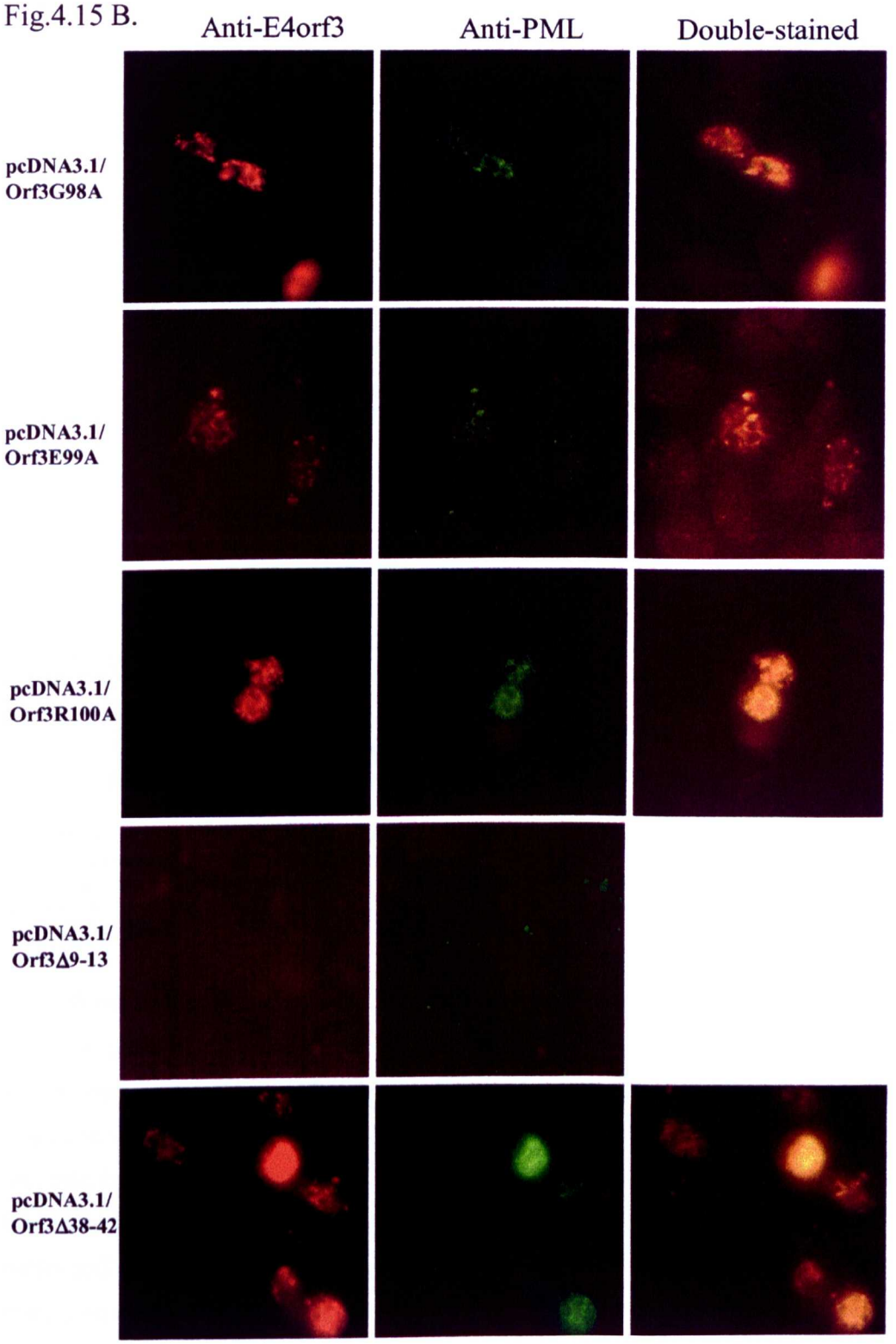
Anti-E4orf3
Anti-PML
Double-stained
pcDNA3.1/
Orf3G98A
pcDNA3.1/
Orf3E99A
pcDNA3.1/
Orf3R100A
pcDNA3.1/
Orf3Δ9-13
pcDNA3.1/
Orf3Δ38-42

Fig.4.15 C.

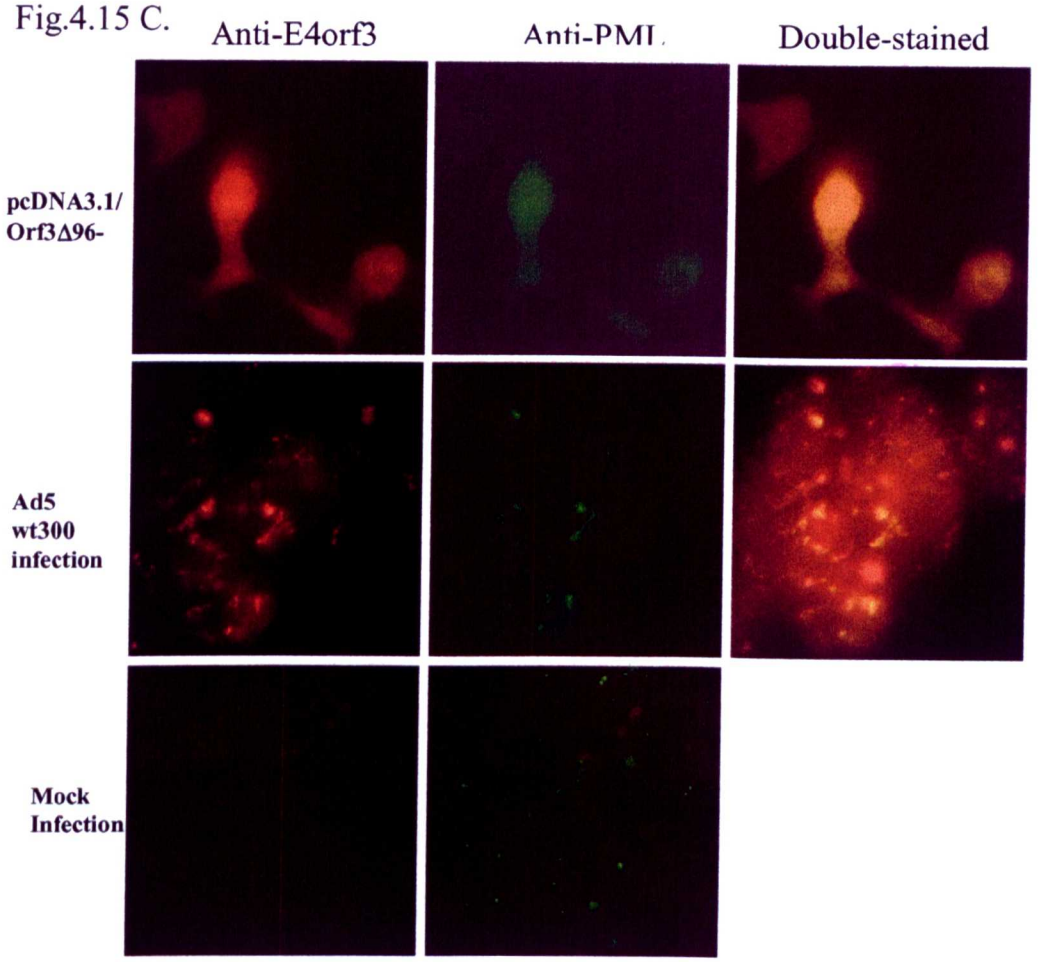

Fig.4.15: E4orf3 and PML costaining in transfected 293 cells, compared with Ad5*wt*300 and mock infected controls. Fluorescence microscope images were taken using a x100 viewing objective. Each series of panels from left to right show the same field of 293 cells transfected/infected as indicated on the left, and probed as indicated at the top. Cells were probed with mAb 5E10 against PML and with 6A11 against E4orf3.

4.7.2. Western blotting of 293-derived samples using the panel of pcDNA3.1/Orf3 mutants

Having demonstrated expression of E4orf3 in 293 cells by immunofluorescence, it was of interest to repeat the Western blot assays described above (section 4.5.) using this cell line. Again, cells underwent calcium-phosphate transfection, and total cell lysates were harvested at 24 hours post transfection or infection in SDS-PAGE lysis buffer and analysed on 15% minigels for E4orf3 and 7.5% minigels for PML. The protein was then blotted onto nitrocellulose, and detected with antibodies 5E10 and 6A11 against PML and E4orf3 respectively (figs.4.18 and 4.19).

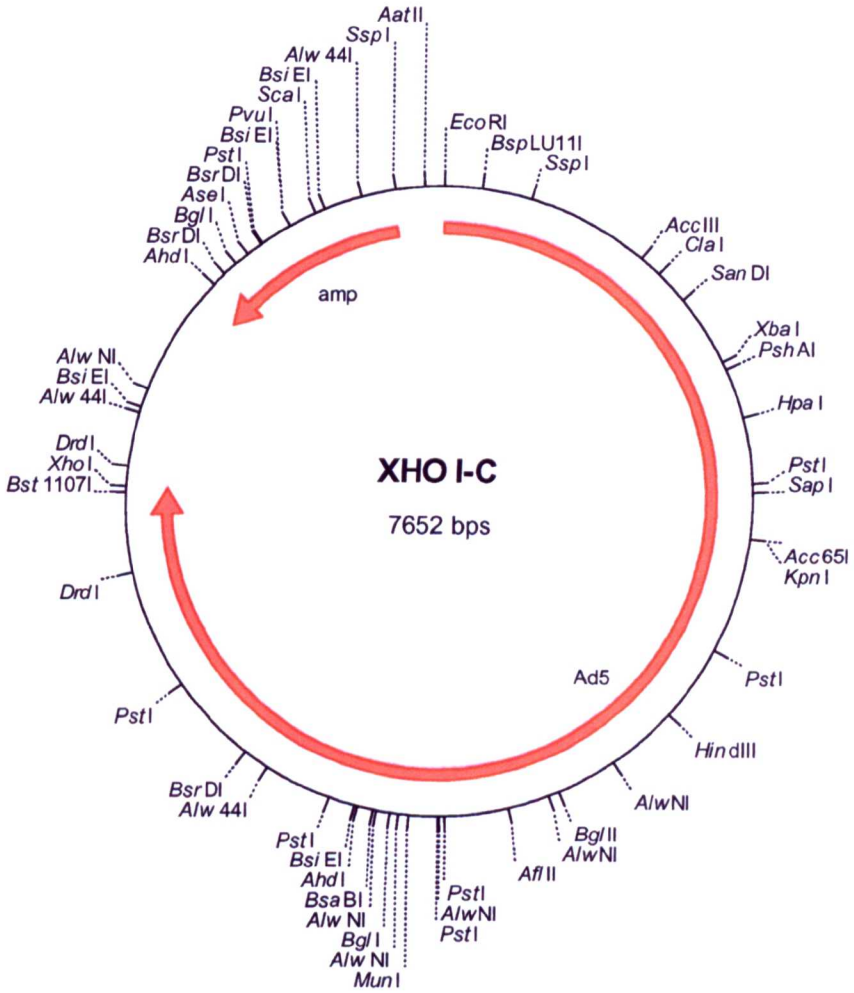

Figure 4.16. Plasmid Xho I-C.
pBR322-based plasmid, bearing Ad5 sequences from 1-5788 of Ad5. The tetracyclin resistance gene *tet* is lost from parental BR322. Abbreviations: amp, ampicillin resistance gene.

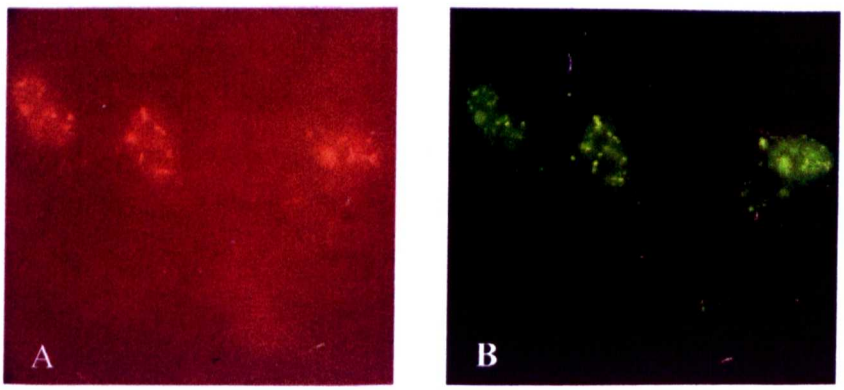

Fig.4.17: E4orf3 and E1B55kDa staining in transfected Hep-2 cells. Fluorescence microscope images were taken using a x100 viewing objective. Panel A shows cells probed with mAb 2A6 against E1B55kDa. Panel B shows the same cells probed with 6A11 against E4Orf3.

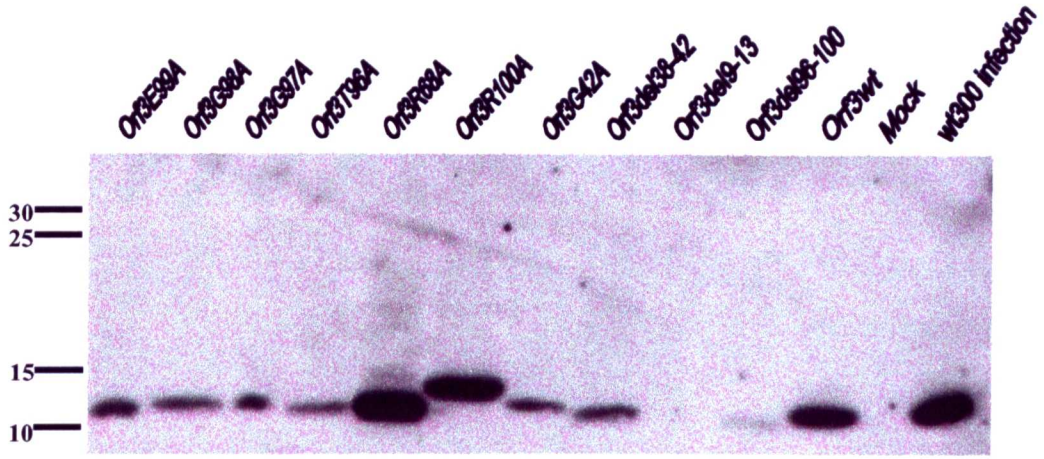

Fig 4.18: Each E4orf3 expressing plasmid was transfected into 2 x 10^5 293 cells at 37°C. Mock transfections and infections with Ad5 wt300 were carried out in parallel, to provide negative and positive controls for E4orf3 expression, respectively. Total cell extracts were prepared 24 h p.i. Extracts were separated by SDS-PAGE on a 15% gel, blotted and probed for E4orf3 with antibody 6A11. The positions to which proteins of known molecular mass migrated are shown at the left (kDa).

As figure 4.18 illustrates, E4orf3 expression can be visualised in all samples other than those transfected with pcDNA3.1/Orf3del9-13, and the mock transfection. In addition, the Orf3R100A protein, which falls within the deletion region of interest, appears to have a markedly different electrophoretic mobility than wild-type Orf3. The absence of a band corresponding to E4orf3 in cells transfected with pcDNA3.1/Orf3del9-13 tallies with the observations by microscopy, in which it was not possible to detect the presence of Orf3 in cells transfected with this construct using the same anti-Orf3 antibody. Possible explanations for this observation would be that the gene is so disrupted by this deletion, that no stable protein is produced, or that the antibody epitope is concealed, altered or deleted. Also of interest is the visibly reduced level of detectable protein where cells are expressing Orf3del96-100. This reduction in staining intensity might represent less efficient Orf3 expression, reduced protein stability, or reduced affinity with the antibody. Perhaps Orf3del96-100 is targeted for degradation upon losing the association to the PODs.

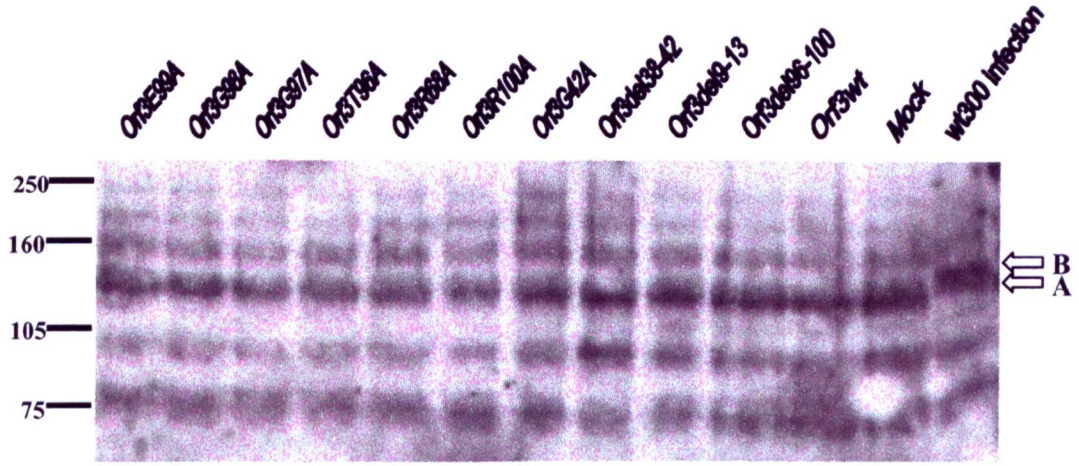

Fig.4.19: Each E4orf3 expressing plasmid was transfected into 2 x 10^5 293 cells at 37°C. Mock transfections and infections with Ad5 wt300 were carried out in parallel, to provide negative and positive controls for E4orf3 expression, respectively. Total cell extracts were prepared 24 h p.i. Extracts were separated by SDS-PAGE on a 7.5% gel, blotted and probed for PML with antibody 5E10. The positions to which proteins of known molecular mass migrated are shown at the left (kDa).

As can be seen in figure 4.19, the PML banding pattern of transfected 293 cells was not visibly modified in comparison to mock transfected cells despite achieving high levels of E4orf3 expression (fig.4.18), and approximately 25% transfection efficiency. In comparison with cells transfected with pcDNA3.1/Orf3*wt*, only the extracts of infected cells have the diagnostic band (arrow A) just above the major 140kDa PML band (arrow B). The three SUMO-1 modified PML isoforms between approximately 150 and 250kDa can be seen in extracts of E4orf3 and mock transfected 293 cells, but have been reduced or lost where cells were Ad5-infected. These observations can be explained if the transfection efficiency was still too low to generate enough modified PML for visualisation, or if E4orf3 alone was not sufficient for this effect. In short, despite the increase in transfection efficiency made possible by the use of 293 cells, it was still not possible to say whether E4orf3 was sufficient for the PML biochemical modification observed in infection.

4.7.3. Transfection and superinfection of 293 cells

To address the question as to whether too few cells were expressing E4orf3 in a transfection to generate visible levels of infection specific PML, or whether E4orf3 required extra viral input, 293 cells were transfected with the panel of Orf3 expressing

plasmids as before, and subsequently superinfected with Ad5inorf3. This mutant virus does not produce Orf3, but is otherwise wild-type. Following a successful transfection and subsequent infection with inorf3, a cell would be provided with the full complement of viral proteins. It was to be expected that the infection specific PML band would be visualised in Western blots of these samples, if enough cells expressed Orf3 but if other viral factors were also required (fig.4.20). As can be seen, neither cells transfected with pcDNA3.1/Orf3*wt* (lane 1), nor those transfected and superinfected with inorf3 (lane 2), showed any alteration in the pattern of PML isoform distribution, in comparison with mock infected 293 cells (lane 4). Cells infected with inorf3 alone did not demonstrate any PML biochemical alteration (lane 3), demonstrating that the Orf3 protein is necessary for the generation of the infection specific isoform. Given that a successfully transfected/superinfected cell would be expected to contain all adenovirus proteins, this result demonstrated that the transfection efficiency was not high enough to enable the observation of the infection specific band by this method. Consequently, it was not possible to determine whether or not E4orf3 alone was sufficient to generate the altered distribution of PML isoforms, and whether this PML biochemical alteration was linked directly to the generation of PML tracks, observed upon expression of Orf3 in HEp-2 or 293 cells.

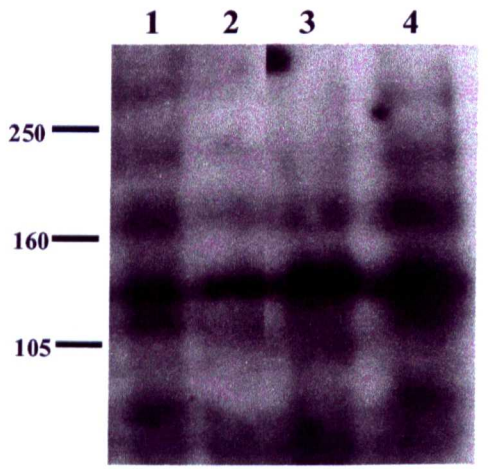

Fig.4.20. Each lane is loaded with the equivalent of 4 x 10^4 293 cells grown at 37°C. Lane 1 was loaded with the lysate of cells transfected with pcDNA3.1/Orf3*wt*. Lane 2 was loaded with the lysate of cells transfected with pcDNA3.1/Orf3*wt* and superinfected with Ad5 inorf3. Lane 3 is loaded with the lysate of cells infected with Ad5 inorf3. Lane 4 is loaded with mock infected cells. Extracts were separated by SDS-PAGE on a 7.5% gel, blotted and probed for PML with antibody 5E10. The positions to which proteins of known molecular mass migrated are shown at the left (kDa).

4.8. Discussion

Having demonstrated that the successful expression of E4orf3*wt* in eukaryotic HEp-2 cells resulted in the redistribution of endogenous PML from nuclear "dots" to "tracks" similar to those observed during wild-type Ad5 infection, it was of interest to determine which regions of the protein were important for this function. Using mutational PCR, the E4orf3 gene was amplified from the viral genome, and point and deletion mutants of certain conserved regions were incorporated into the amplified DNA strands. These were then cloned into the pcDNA3.1 plasmid backbone to place expression of these modified genes under the control of the same CMV promoter used successfully in pcDNA3.1/Orf3*wt*. These mutants were transfected into HEp-2 cells, and these were then viewed for Orf3 expression and PML localisation under immunofluorescence microscopy. The results generated showed that in most cases, the point mutations had no discernible effect upon Orf3 expression and colocalisation with PML. However, the deletion mutants of Orf3 demonstrated markedly different patterns of Orf3 distribution. In HEp-2 cells, neither the deletion spanning residues 9 to 13, nor that spanning residues 38 to 42 expressed any detectable E4orf3. In these cases, it was possible that the deletions had a major impact on the structure or stability of the protein, possibly even compromising the antibody-binding site. The deletion spanning residues 96 to 100 was interesting, representing a shift in the pattern of Orf3 localisation from nuclear tracks, to a diffuse stain apparently present throughout the cell. Further point mutants were made to cover the region represented by this deletion mutant. Of these, Orf3T96A appeared to demonstrate to a lesser extent, something of the phenotype of Orf3del96-100, with discernible extranuclear localisation. However, due to the inadequacies of transient transfection, it was not possible to unequivocally identify this phenotype. Nevertheless, this mutant was flagged for further investigation, having potentially interesting characteristics.

It was of interest to try and determine whether the presence of Orf3 alone, while sufficient for PML track formation and POD disruption, was sufficient for the biochemical alteration of PML also seen during infection, and whether this process was linked to POD disruption. The biochemical alteration of PML is determined by Western blotting. No alteration in the distribution of PML isoforms could be detected in samples from transfected HEp-2 cells, however, Western blotting revealed that Orf3 was difficult to detect in these same samples, suggesting a poor transfection rate, and providing an potential explanation for the lack of observable PML alteration.

Consequently, in an attempt to improve transfection efficiency, 293 cells were used as an alternative to HEp-2 cells. These assays proved much more successful, and Western blotting confirmed that Orf3 was routinely and reliably detectable in samples derived from 293 cells, at levels roughly equivalent to those obtained from samples infected with wild-type adenovirus. Immunofluorescence microscopy analysis of transfected 293 cells revealed much the same pattern of Orf3 distribution and PML localisation as those using HEp-2 cells, although Orf3T96A did not seem to generate a mutant phenotype in these cells. One notable exception was the clear presence of Orf3/PML colocalisation to nuclear tracks in 293 cells transfected with pcDNA3.1/Orf3del38-42. Orf3 protein was not detectable by IF in HEp-2 cells transfected with this plasmid, and these results suggest that perhaps in the case of this mutation, an unstable protein was produced which required an additional protein to stabilise the structure. 293 cells have been engineered to express the adenovirus E1b-55kDa protein, which is known to be capable of complex formation with E4orf3. Interestingly, when cotransfected with a 55K expressing plasmid, Orf3del38-42 was detectable in Hep-2 cells, exhibiting apparently wild-type characteristics. This suggests a mechanism whereby 55K is capable of stabilising this mutant Orf3 protein, perhaps within a complex.

Despite enhanced Orf3 expression using 293 cells, it was not possible to detect any alteration in the distribution of PML isoforms by Western blotting. This could mean that despite high levels of Orf3, the number of individual cells expressing Orf3 was not sufficient to generate detectable levels of "infection-specific" PML, as Orf3 is not apparently transported between neighbouring cells. Alternatively, these results could indicate that although known to be necessary for the generation of the infection specific PML species (Leppard and Everett, 1999), Orf3 is not sufficient to drive this alteration without extra viral input. In this scenario, the disruption of the PODs and PML biochemical alteration would represent separate processes. To attempt to address this question, 293 cells were first transfected with pcDNA3.1/Orf3*wt*, and then superinfected with Ad5 inorf3. Cells infected with inorf3 alone would not be exposed to the effects of Orf3. Those both transfected and infected, would have the full complement of viral proteins. In these experiments, the infection- specific PML band could not be visualised by Western blotting, supporting the suggestion that transient transfection efficiency was simply too low to generate meaningful results relating to the effect of Orf3 upon transfected cells.

5. Construction of cell cultures permanently expressing adenovirus serotype 5 E4orf3 protein

In an attempt to address some of the limitations of our transient transfection assay, it was decided to attempt to generate mixed cell cultures enriched for E4orf3 expressing cells and, later, cell lines that were permanently expressing Orf3. It would be advantageous to generate a cell line in which every cell expressed levels of Orf3 comparable to those expressed during an infection. This would allow us to characterise with confidence the phenotype of each mutant. It would also be simple to extract total cell lysates from these cells and examine the PML banding pattern in Western blots to determine whether Orf3 alone had an effect on the distribution of PML species. If this proved not to be the case, the Orf3 expressing cell line could be used in subsequent infection or transfection experiments to determine which other viral protein(s) acted as partner(s) in this modification and to investigate other E4orf3:virus:host interactions.

5.1. Cell cultures "enriched" for E4orf3 expressing cells.

It was first decided to generate cell cultures "enriched" for E4orf3 expressing cells. In this case, each cell in the culture would not be equivalent, in that they would be the products of multiple transfection events. This was deemed sufficient for our needs, provided that a large proportion of the cells expressed high levels of E4orf3. Indeed, this approach had the advantage that effects on PML due to the selection of a specific host cell variant would not have to be excluded as an explanation for any effects observed. This was achieved by transfecting pcDNA3.1/Orf3*wt* into HEp-2 cells as before, by the calcium-phosphate method. This vector contains a neomycin resistance marker, allowing the use of G-418 to select cells which are expressing proteins from the vector in eukaryotic cells, in much the same way as ampicillin resistance is used to select for transformed bacterial cells. Accordingly, G-418 was added to the growth medium of transfected cells, approximately 24 hours after infection. Subsequently, the medium was replaced every 3 days with DMEM/10% NCS containing G-418. After optimisation, G-418 was always added to yield a final concentration of 500μg/ml. At this concentration, non-transfected Hep-2 failed to plate successfully after 5-6 days. After approximately two weeks of G-418 treatment, surviving clones had become established, and these were all trypsinized and pooled onto smaller dishes ie. the

equivalent of a transfected 90mm dish was eventually pooled onto one well of a 6 well dish. Often, these cells required further concentrating onto smaller wells yet. This mixed culture was then grown on a larger scale, and samples were taken for SDS-PAGE, and cells were also grown on glass coverslips for immunofluorescence microscopy (IF) analysis.

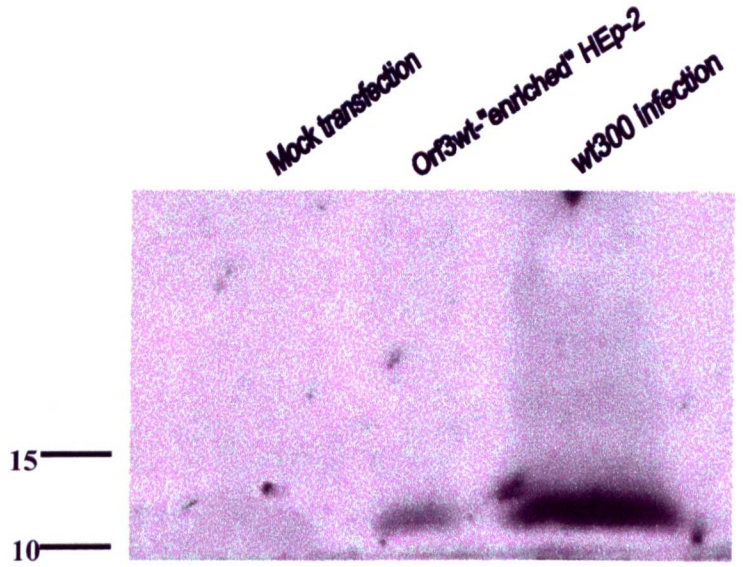

Fig.5.1: Extracts of mock transfected, *Orf3wt*-enriched and Ad5 wt300 infected HEp-2 cells were separated by SDS-PAGE on a 15% gel, blotted and probed for E4orf3 with antibody 6A11. The positions to which proteins of known molecular mass migrated are shown at the left (kDa).

In the first instance, Western blotting analysis confirmed expression of E4orf3 in cells transfected with pcDNA3.1/Orf3*wt* and enriched as above, (fig.5.1) and IF analysis confirmed that a very high percentage of cells were expressing E4orf3 in high quantities (fig.5.2). In panel A of figure 5.2, endogenous PML can be seen in the track-like structures observed during wild-type Ad5 infection and transient E4orf3 expression. Panels B and C show colocalisation of Orf3 in tracks with PML. A high level of Orf3 expression was observed, corresponding with a somewhat diffuse stain outside of the nuclei (panel D) in addition to the nuclear tracks. This may reflect a positive selection for stronger expression from the plasmid, corresponding to demands for cellular survival in the presence of G-418. The IF results also showed the cells to be piled up on top of each other, in contrast to the usual cell monolayer. This might have been a phenotype consequent to continual E4orf3 expression, or may have been

an artefact. However, as this cell line was not sustainable in culture (see below), the former explanation perhaps deserves further investigation.

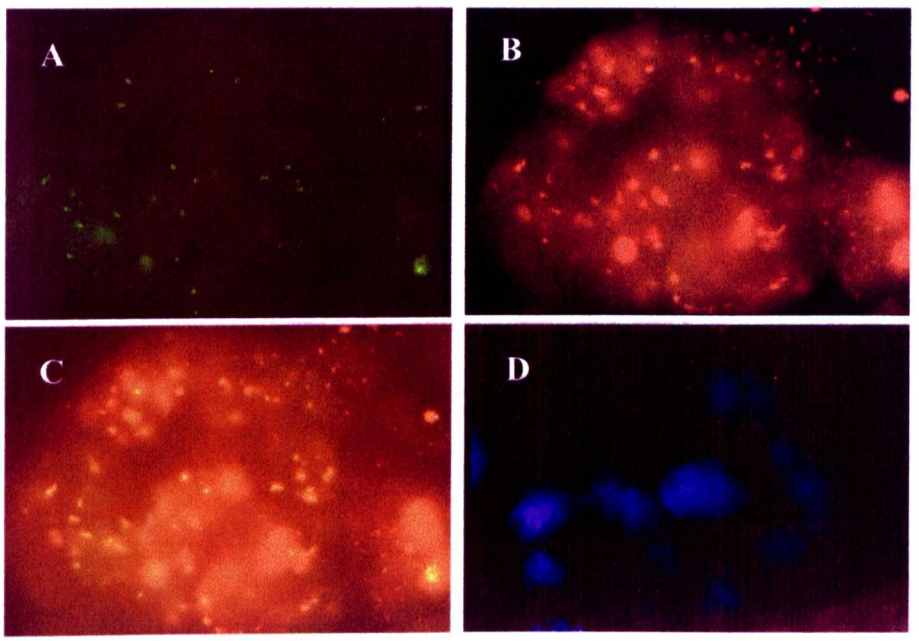

Fig.5.2: Immunofluorescence micoscopy data of HEp-2 cells enriched for those permanently expressing E4orf3. The data above show a representative sample of HEp-2 cells selected with G-418 for those with active and permanent expression from pcDNA3.1/Orf3*wt* DNA. Panel A shows cells stained with 5E10 anti-PML. Panel B shows strong E4orf3 expression in the same cells, using antibody 6A11. Panel C is double stained for both PML and Orf3. Panel D is DAPI stained to show the locations of the nuclei of the cells in this field of vision.

Approximately 5 weeks after initial treatment with G-418, the Orf3*wt*-expressing mixed culture generated by this method began to become less healthy, and ultimately it was not possible to maintain these cells in culture. Cells that had been frozen as soon as the mixed culture was established were successfully revived, but these only survived for a short period of time. There were no obvious signs of contamination. A possible explanation for the lack of survival would be that cumulative G-418 treatments at the concentration used ultimately inhibit cell survival, or perhaps permanently high levels of E4orf3 disrupt cellular function to such an extent that, eventually, they can no longer survive. Subsequent attempts to generate Orf3 expressing mixed cultures were less successful. The same high percentage of Orf3 expressing cells was not recreated. Essentially the same technique was used to generate cell cultures derived from HEp-2 cells transfected with the panel of mutant Orf3 expressing plasmids, and total cell lysates from these G-418 selected cultures and the original wild-type Orf3 expressing culture were analysed for PML banding

pattern by Western blotting (fig.5.3). As can be seen, all samples have a similar PML banding pattern as the mock infection, none having the Ad5 infection specific band just above 140kDa. IF microscopy analysis showed that these later attempts to generate Orf3 expressing mixed cultures were less successful than the first attempt (data not shown). Although it was possible to grow these later cultures indefinitely, they did not have a similar, high percentage of Orf3 expressing cells.

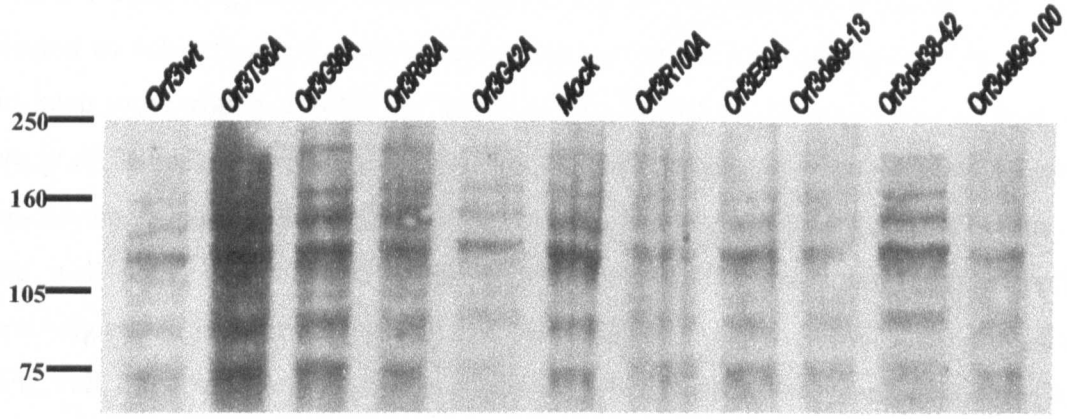

Fig.5.3: Western blot showing distribution of PML species in Hep-2 cells enriched for permanent Orf3 expression using G-418 selection. The positions to which proteins of known molecular mass migrated are shown at the left (kDa).

This supports the idea that continuous Orf3 expression is detrimental to cell health. This could explain the apparent loss of Orf3 expression over time in the mixed culture. Individual cells might incorporate varying and partial sections of the plasmid DNA, and this DNA could incorporate into different regions of the HEp-2 genome during individual events, influencing the strength of expression from the insert, and also potentially disrupting certain cellular processes. It is not difficult to envision a scenario whereby certain cells acquire resistance to G-418 without the potentially disadvantageous Orf3 gene. These cells might then have a selective advantage over cells expressing. Alternatively, strength of expression from the incorporated DNA might have an effect on cell viability. There may be a limit of tolerance up to which point increasing expression from the insert would be advantageous by increasing resistance to G-418, but beyond which the relatively higher levels of Orf3 would inhibit cell survival.

5.2. HEp-2 cell lines stably expressing E4orf3*wt* and E4orf3R68A

As it was not possible to develop mixed cell cultures containing a high percentage of Orf3 expressing cells, it was decided to grow clones of individual cells, picked subsequent to transfection and primary G-418 selection. Assuming that each cell in the colony was equivalent in terms of Orf3 expression, an Orf3 expressing cell line would have the advantage of eliminating competition between cells expressing more, less or no Orf3. Cells were transfected as before on 60mm dishes with pcDNA3.1/Orf3*wt* and pcDNA3.1/Orf3R68A. It was not deemed necessary at this point to attempt to generate cell lines expressing all the Orf3 mutants, and R68A was selected as subjectively, it had appeared that mixed cultures expressing this protein had been more viable. G-418 was added to the medium to a final concentration of 500μg/ml. After approximately three weeks, individual clones were picked using trypsin/versene sterile cloning disks. These were then dropped into individual wells of a 96 well plate, and allowed to grow in G-418 selective medium for one week. Surviving cell lines were then plated into individual wells of a 24 well dish. After this point, cell lines were trypsinized and plated onto larger dishes as appropriate. Cell lines were maintained in the wells of 6 well dishes. These clones were analysed for Orf3 expression by immunofluorescence microscopy, and cell lines expressing appreciable levels of Orf3 were maintained (data not shown). Other cell lines were discarded. SDS-PAGE samples of the selected cell lines were prepared at approximately five weeks after initial IF screening. These samples analysed by Western blotting (see fig.5.4). These data show that E4orf3 could not be visualised by this technique in samples derived from any of these clones. A band in lane 13 just above the 10kD marker is an artifact and does not represent Orf3.

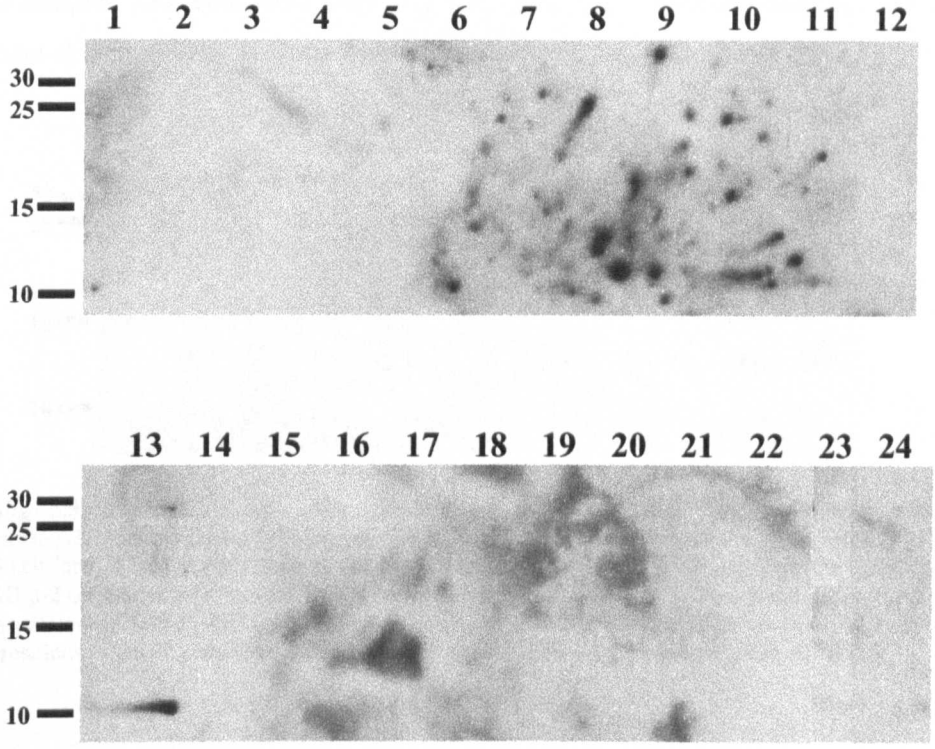

Fig 5.4: Extracts of cell lines developed from HEp-2 cells transfected with either pcDNA3.1/Orf3*wt* (lanes 1-20), or pcDNA3.1/Orf3R68A (lanes 21-24), and selected with G-418. Each lane is loaded with the equivalent of 4 x 10^4 cells. Extracts were separated by SDS-PAGE on a 15% gel, blotted and probed for E4orf3 with antibody 6A11. The positions to which proteins of known molecular mass migrated are shown at the left (kDa). Blots were overexposed to allow for weak signals. Apparent "band" in lane 13 is an artifact.

Despite these results, it was still thought possible that Orf3 was present in each clone, even if in minimal quantities. Accordingly, if Orf3 was sufficient for the observed PML modification, some modified PML would also be present. If this were true, and assuming that all cells were equal, it was thought possible to detect modified PML in samples of these cells. Thus, three "Orf3*wt* expressing" and three "Orf3R68A expressing" cell lines were retained, and samples harvested in SDS-PAGE sample buffer. These samples were analysed for E4orf3 expression by Western blotting analysis (fig.5.5). As can be seen, there is a faint band corresponding to the Orf3 protein in samples derived from one of the HEp-2.Orf3*wt* cell lines (lane 3), and in samples derived from one of the HEp-2.Orf3R68A cell lines (lane 6). While the level of Orf3 expression was much lower than that obtained during transient transfection, every cell in these cell lines should have been equivalent, and any alterations to endogenous proteins would be expected to be present in all cells, rather than a subset.

The samples with detectable Orf3 (fig 5.5, lanes 3 and 6), were analysed for PML species distribution by Western blotting analysis (fig.5.6, lanes 1 and 2).

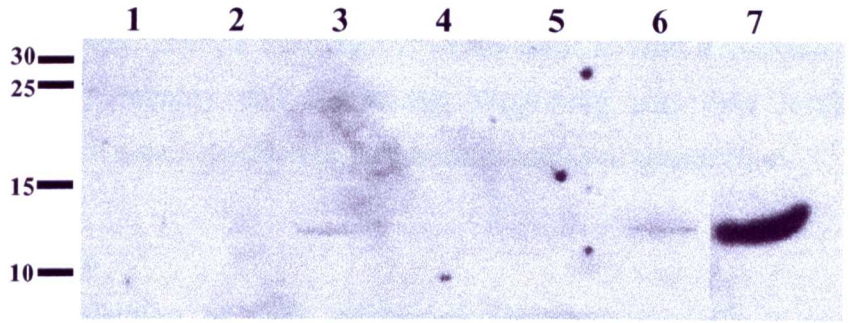

Fig 5.5: Extracts of cell lines developed from HEp-2 cells transfected with either pcDNA3.1/Orf3*wt* (lanes 1-3), or pcDNA3.1/Orf3R68A (lanes 4-6), and selected with G-418. Each lane is loaded with the equivalent of 4 x 10^4 cells. Lane 7 is loaded with the extract of HEp-2 cells infected with Ad5 wt300, as a positive control for E4Orf3 expression. Extracts were separated by SDS-PAGE on a 15% gel, blotted and probed for E4orf3 with antibody 6A11. The positions to which proteins of known molecular mass migrated are shown at the left (kDa).

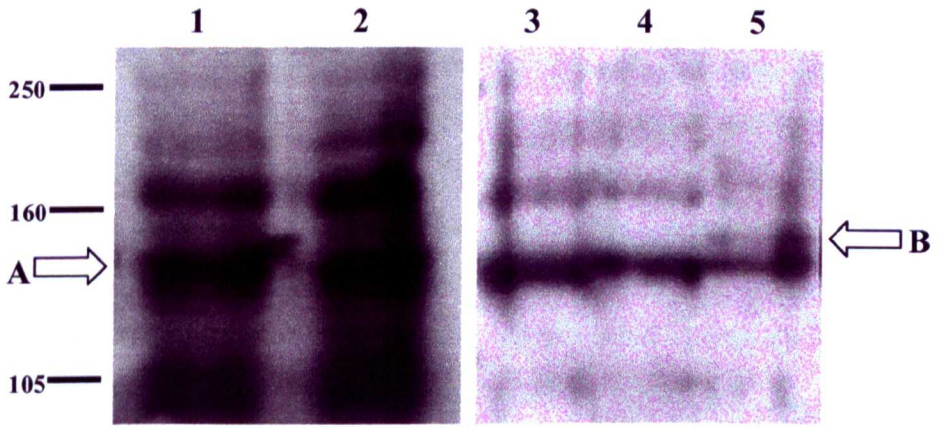

Fig 5.6: Extracts of cell lines developed from HEp-2 cells transfected with either pcDNA3.1/Orf3*wt* (lane 1), or pcDNA3.1/Orf3R68A (lane 2), and selected with G-418, compared with samples derived from transfected, infected or mock infected cells. Each lane is loaded with the equivalent of 4 x 10^4 cells. Lane 3 is loaded with the extract of HEp-2 cells transfected with pcDNA3.1/Orf3*wt*. Lane 4 is loaded with mock infected samples. Lane 5 is loaded with samples derived from cells infected with Ad5 wt300. Arrow A indicates the major PML band at approximately 140kDa. Arrow B indicates the infection specific PML isoform just above the 140kD band. Extracts were separated by SDS-PAGE on a 15% gel, blotted and probed for Orf3 with antibody 6A11. The positions to which proteins of known molecular mass migrated are shown at the left (kDa).

Comparison of the PML banding patterns of the "Orf3*wt* expressing" and "Orf3R68A expressing" cell lines with the banding pattern of pcDNA3.1/Orf3*wt* transiently transfected, mock infected or wt300 infected HEp-23 cells (provided in lanes 3-5), reveals that the pattern of PML isoform distribution was not altered in these cell lines. This suggests that either the level of Orf3 expression was too low to alter PML biochemistry, or that Orf3 alone is not sufficient to generate the altered pattern. The former explanation appears more likely, as the level of Orf3 expression was too low to be detected reliably and repeatedly, suggesting very low levels indeed in comparison with either a wild-type infection, or transient transfection.

5.3. Discussion

Transient transfection of Orf3 expressing plasmids into HEp-2 and 293 cells, confirmed that Orf3 expression was capable of producing PML and Orf3 colocalisation in nuclear structures, similar to the "tracks" observed during infection with wild-type adenovirus. An Orf3 mutant of this function was identified, and it was desirable to investigate any links between Orf3 function, POD reorganisation and PML biochemical modification. However, due to the relatively low percentage of cells in a culture exposed to the effects of Orf3 when comparing transient transfections with infections, this technique could not be used to answer these questions. It was hoped that the problem could be addressed by producing cell cultures in which all cells expressed E4orf3, and that this could be achieved by selecting against those cells which had not successfully incorporated plasmid DNA into their genomes and which therefore did not express E4orf3. Initially, this seemed to be an effective tactic, and a mixed culture was produced in which a high percentage of cells expressed E4orf3. However, this culture could not be sustained, and subsequent attempts to repeat this experiment failed to produce high percentages of Orf3 expressing cells. It was thought possible that even G-418 resistant cells might eventually succumb to the detrimental effects of the chemical. However, it was possible to produce cultures that remained resistant to the effects of G-418 indefinitely, despite the lack of high, or even detectable Orf3 expression. This observation would argue against G-418 induced "slow-death". Rather, it seems likely that the Orf3 protein itself is antagonistic to continued cell survival, or at least, can only be tolerated for any length of time at low concentrations. It had been suggested that within the environment of a mixed culture, cells expressing a higher level of Orf3

might have a selective disadvantage in competition with other cells expressing less of the protein. If this were the case, it might still have been possible to generate a culture expressing high levels of Orf3, if this element of competition was removed. Accordingly, cell lines were developed from individual clones. However, in this instance only those expressing low or undetectable levels of Orf3 survived. This observation, coupled with the demise of the first mixed culture to successfully produce high levels of stable Orf3 expression, argue that the protein, in high levels, is not mildly detrimental, but lethal to cell survival.

Western blotting analysis of samples taken early in the selection process revealed that at this stage, certain cell lines were expressing Orf3 at detectable, if low, levels. Further Western blotting analysis of these samples could not identify any alteration in the distribution of PML species when compared with samples taken from standard HEp-2 cells. This pattern is similar to that observed in samples taken from HEp-2 and 293 cells transiently transfected with the plasmids, and together, these results would suggest that, while capable of POD disruption, Orf3 alone cannot bring about the alteration in PML observed during infection. However, the mixed cultures and cell-lines constructed to express Orf3 did not, ultimately, address the concerns associated with transient transfection. All the cells in a culture were not necessarily equivalent and exposed to the Orf3 protein. The evidence suggests that the Orf3 protein was detrimental to cell survival. Accordingly, individual cells within a clone, or clones within a mixed culture, that expressed little or no Orf3 would have had a competitive advantage over surrounding cells, providing resistance to G-418 was retained. Therefore cells expressing and exposed to Orf3 may have been in the minority, even in a supposed cell "line".

The inability to maintain high levels of Orf3 expression in these cell-lines, means that the above results cannot be used as the basis of any hypothesis regarding the potential link between Orf3 function, POD redistribution and PML biochemical alteration.

6. Construction of whole, infectious virus, expressing mutant E4orf3 protein.

A further method of addressing some of the limitations inherent to transient transfection would be to generate whole infectious viruses expressing the mutant forms of E4orf3. A virus generated in this method would provide an efficient means of expressing the desired protein in every cell in a monolayer, and in addition would enable a more meaningful evaluation of the role of the protein in an environment more closely approximating that observed in nature. A gross disruption of the normal Orf3 nuclear localisation pattern had been observed by IF microscopy in cells expressing the del96-100 mutation. A similar, if less well defined phenotype had been observed in cells expressing the Orf3T96A mutation into eukaryotic cells (see sections 4.1, 4.3 and 4.6.1), although this was not an unambiguous result. Accordingly, it was attempted to construct two recombinant viral genomes, one carrying each of the above mutations.

6.1. Reconstruction of mutant adenovirus by *in vivo* recombination.

A schematic diagram of the steps involved in the *in vivo* reconstruction of a mutant adenovirus genome is provided in figure 6.1 (panels A and B).

Initially, a 4850bp fragment between Nde I (Ad5 31088) and Cla I (added at end of viral genome in plasmid, relative position 35938) sites was cloned by restriction digest from the right hand end of the viral genome, into the vector, pBR322 (fig 6.2). The resultant construct of approximately 7Kbp was amplified in bacteria, and designated pBR322Ndefrag (see fig 6.3). Oligonucleotides were designed to amplify a region containing the E4orf3 region from the viral genome, ensuring that BstE II (Ad5 35233) and EcoR V (Ad5 33754) restriction sites were retained at either side of the gene. These outside primers were coupled with the mutational primers already used (see sections 4.0 and 4.2), to generate complementing DNA fragments containing E4orf3del96-100 or E4orf3T96A by primary mutational PCR reactions. Samples of these reactions were analysed on agarose gels prior to further steps. Bands of 735bp and 877bp were expected from the primary reactions during construction of E4orf3T96A, and these can be seen in lanes 2 and 3 of the gel shown in fig.6.4, respectively. Several extraneous DNA fragments were generated during the PCR used to generate the 735bp fragment (lane 2). These can result from false-priming, where

the annealing temperature used during PCR is too low to eliminate all non-specific hybridisation between primer and template. Nevertheless, the desired fragment was by far the most common product, and samples of the 1° PCR reactions containing the desired fragments were used in the second stage amplification as before. The products of the 2° PCR reactions were loaded onto agarose gels. Figure 6.5, shows the 2° PCR product of a reaction using the 1° PCR products shown in lanes 2 and 3 of figure 6.4.

Fig.6.1 A: Schematic of adenovirus reconstruction by *in vivo* recombination.

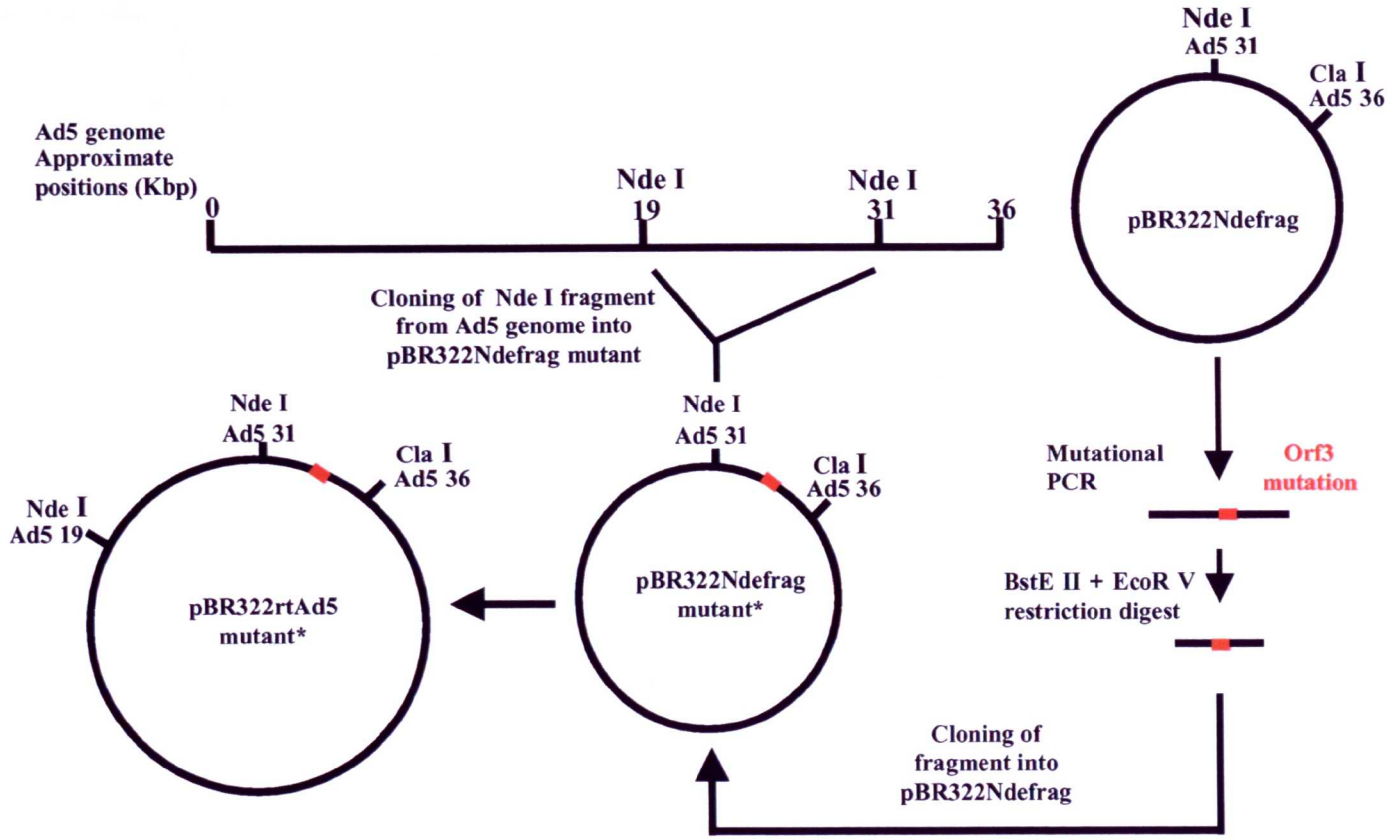

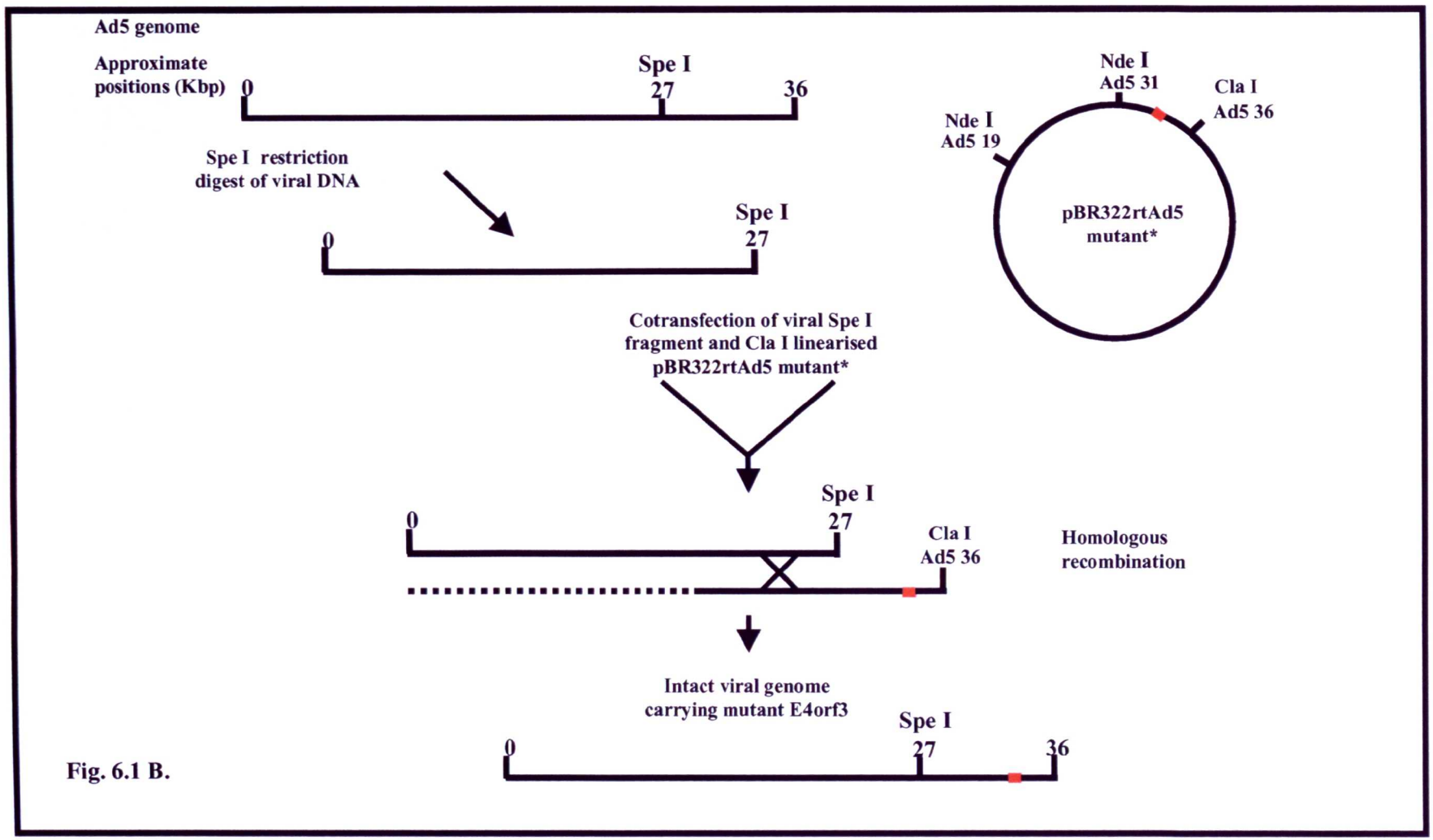
Ad5 genome
Approximate positions (Kbp)
0
Spe I
27
36
Spe I restriction digest of viral DNA
0
Spe I
27
Nde I
Ad5 31
Cla I
Ad5 36
Nde I
Ad5 19
pBR322rtAd5 mutant*
Cotransfection of viral Spe I fragment and Cla I linearised pBR322rtAd5 mutant*
0
Spe I
27
Cla I
Ad5 36
Homologous recombination
Intact viral genome carrying mutant E4orf3
0
Spe I
27
36

Fig. 6.1 B.

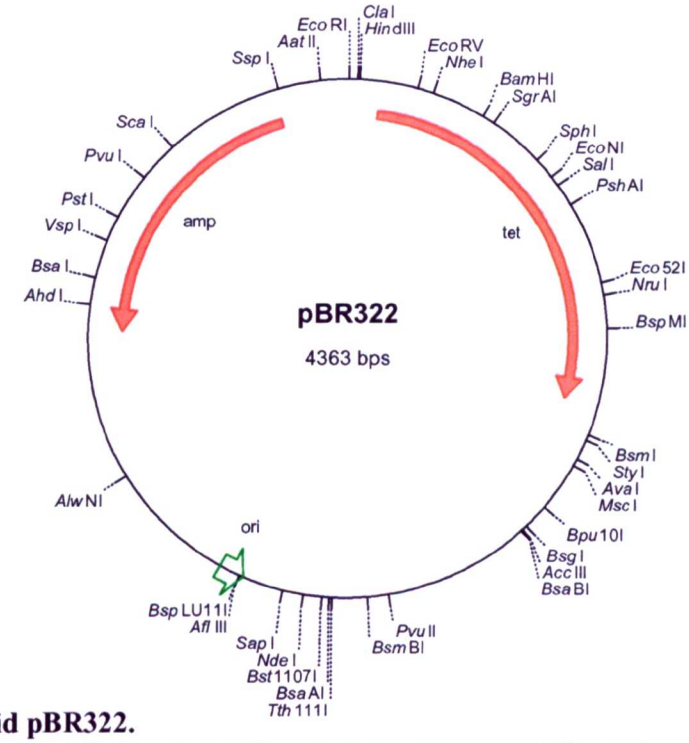

Fig.6.2. Plasmid pBR322.
Map show unique restriction sites. Abbreviations: amp, ampicillin resistance gene; tet, teracyclin resistance gene; ori, plasmid origin of replication.

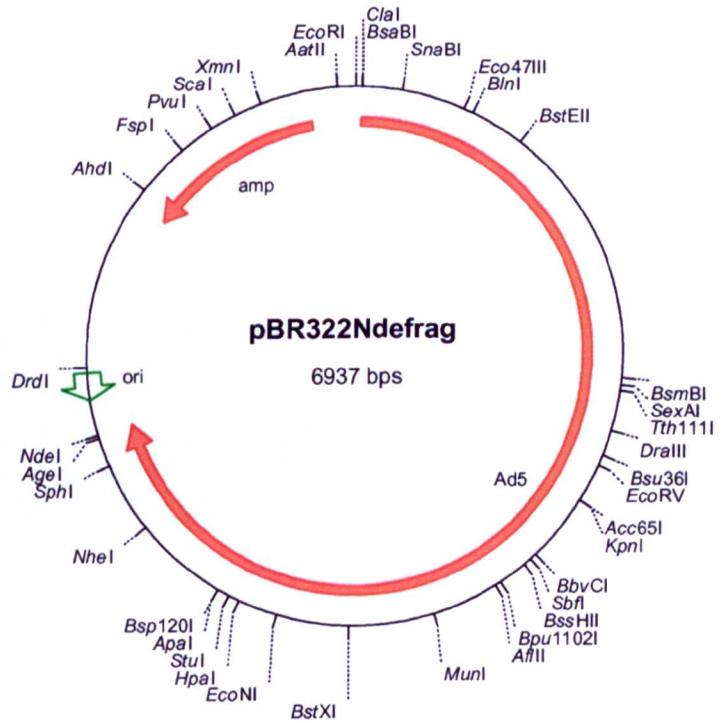

Fig. 6.3. Plasmid pBR322Ndefrag.
pBR322-based plasmid containing adenovirus serotype-5 sequences between virus base-pair positions 31088 and 35938. Abbreviations: amp, ampicillin resistance gene; Ad5, cloned Ad5 sequences; ori, plasmid origin of replication.

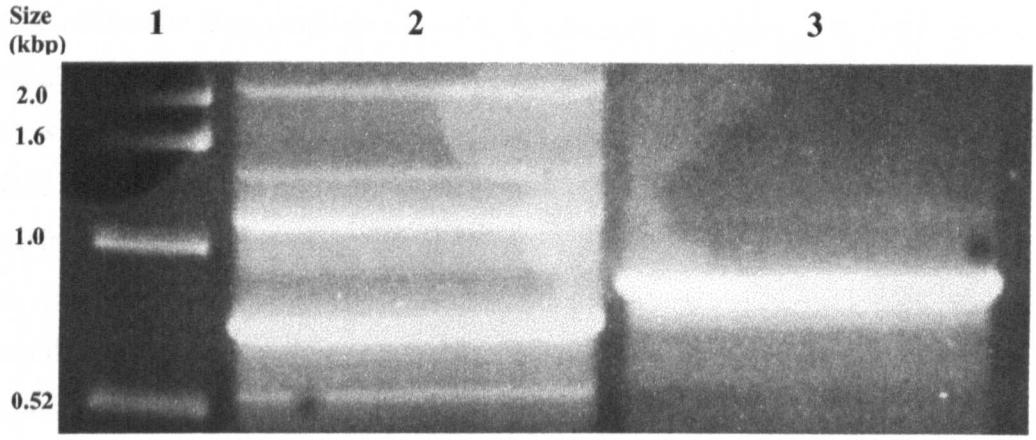

Fig.6.4: 0.8% agarose gel showing an example of mutational PCR 1° products. Lane 1 shows 1Kb ladder. Wide lanes 2 and 3 show 1° PCR products.

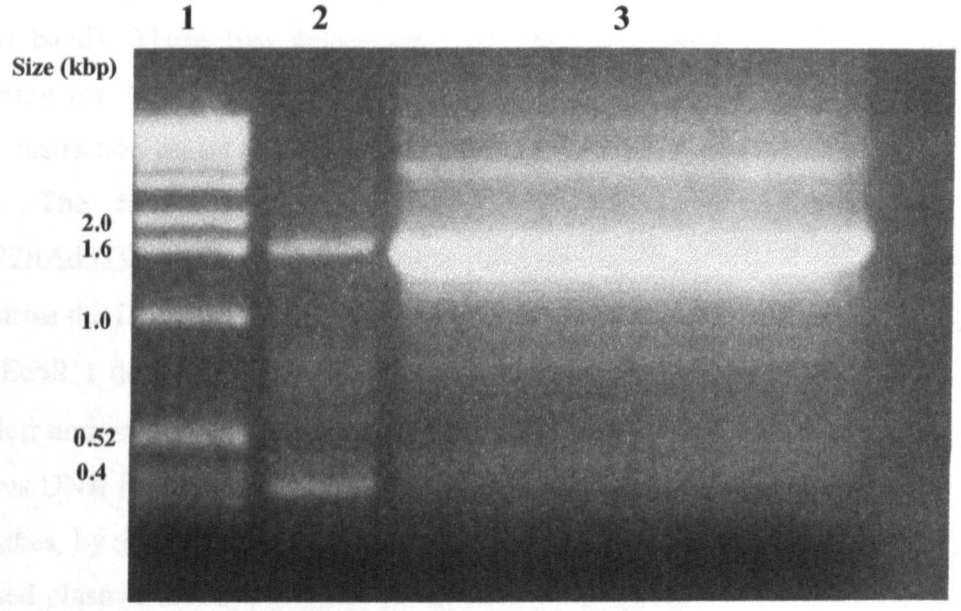

Fig.6.5: 1% agarose gel showing an example of mutational PCR 2° products. Lane 1 shows 1Kb ladder. Lane 2 is loaded with negative control for 2° PCR. Wide lane 3 shows 2° PCR products.

A band of approximately 1.6 kbp was expected, and this can be seen in lane 3. However, a band of this size can also be seen in the negative control, loaded in lane 2. The negative control comprised of the 1° PCR product shown in lane 2 of fig.6.4, without the complementary fragment shown in lane 3. This 1° reaction would have

carried forward some full length template into the 2° reaction, and so could have given a 1.6 kbp fragment with the pair of outside primers used. This is not desirable, and could be eliminated by reducing the input of 1° reaction product into the 2° reaction. In this instance, that was not found to be necessary. A BstE II and EcoR V double restriction digest was then used to excise a region spanning the Orf3 gene from pBR322Ndefrag, and the products of the secondary PCR reactions were cut at the same sites The vector and insert thus prepared were ligated together to generate pBR322Ndefrag96-100 and pBR322NdefragT96A. These plasmids were amplified in bacteria, and sequencing reactions performed to verify that the desired mutations had been generated in an otherwise intact region of the viral genome within the vector plasmid. Having shown that plasmids carrying the desired stretches of mutant viral genome were successfully cloned into pBR322, these plasmids underwent Nde I restriction digest to linearise the DNA, and CIAP treatment to prevent self-ligation. The linearised DNA was then purified from agarose gels. Intact viral genome underwent a Nde I restriction digest to liberate a 11540bp fragment between positions 19548 and 31088 from the viral genome (Sca I was also used to help resolve the desired band). These two fragments were ligated together to generate plasmids containing the Ad5 genome between 19548bp and 35938bp. An Eco RI and Pvu I double restriction digest was used at this stage to ensure the correct orientation of the inserts. The resultant plasmids were designated pBr322rtAd5del96-100 and pBR322rtAd5T96A (fig.6.6). Next, each plasmid underwent Cla I restriction digest, to linearise the DNA at the end of the viral insert. Viral genomic DNA underwent Spe I and EcoR I double restriction digest, to generate a DNA fragment spanning the entire left end of viral genome as far as position 27082. The linearised plasmid DNA and virus DNA fragments were purified, and the two co-transfected into 293 cells in 6 well dishes, by a modified calcium-phosphate transfection method (see methods). The linearised plasmid and 27083bp viral fragment share a 7534bp region of overlapping sequence between positions 19548 and 27082. In principle, these two DNA fragments, when co-transfected into a recipient cell, would recombine at the region of homology, to generate full-length viral genome, as well as a by-product containing plasmid DNA. The intact viral genome thus generated would contain the mutated gene of interest, and would be capable of replication and the synthesis of new virus particles, as the lack of Orf3 function does not significantly impair virus growth

(Huang and Hearing, 1989a). In this manner it would be possible to harvest virus particles mutant for the gene of interest, and amplify these further in HEp-2 cells. Approximately 24 hours post-transfection, the liquid medium was removed and replaced with solid noble agar containing medium. Staining overlay was added to the cells 10 days post transfection, and a sterile pasteur pipette was used to remove any plaques to 0.5ml TS/2% CS. These were then placed at -70°C. The presence of plaques is indicative of replicating virus. As plaques were observed in co-transfected wells, it was possible that viral recombination had successfully occurred. However, negative controls consisting of cells transfected only with "cut" virus fragments also produced similar numbers of plaques, indicating that viable virus DNA was present in the mock control and therefore that the digest of viral DNA had not gone to completion. Nevertheless, it was decided to progress with the "recombinant virus" plaques, in the hope that some recombinant viruses were present.

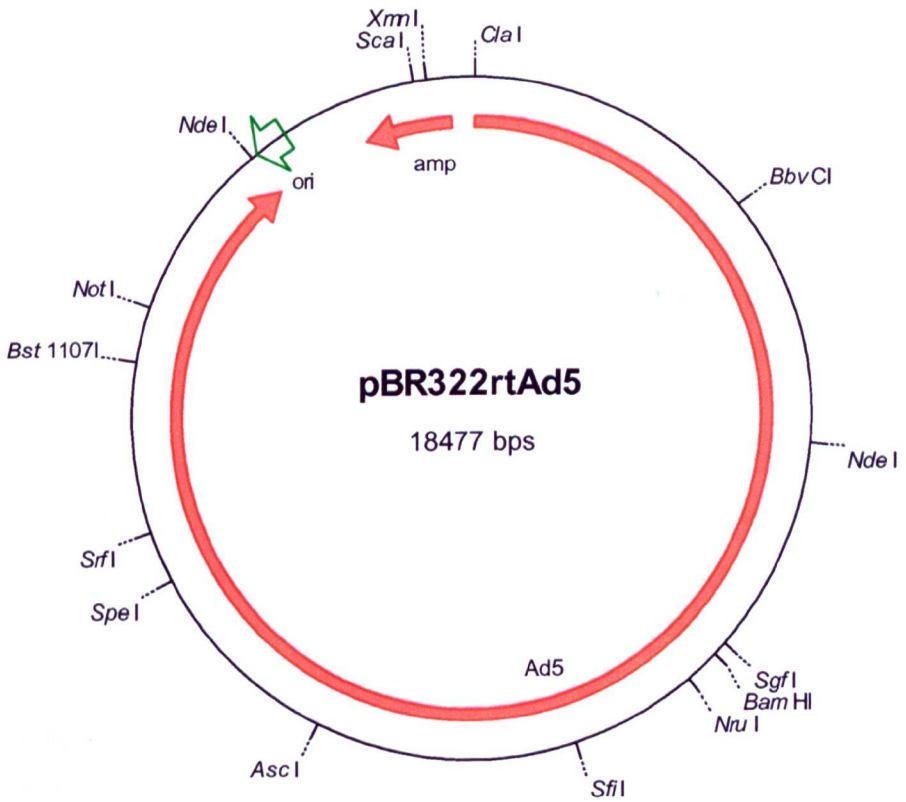

Fig.6.6. Plasmid pBR322rtAd5.
pBR322-based plasmid containing Adenovirus serotype-5 sequences between virus base-pair positions 19548-35938. Abbreviations: amp, ampicillin resistance gene; Ad5, cloned Ad5 sequences; ori, plasmid origin of replication.

The plaques in TS/CS were freeze thawed three times to liberate virus particles from the cells. 0.2ml of each lysate was used to infect a well of a 12 well dish of HEp-2 cells. The cells reached full c.p.e. 4 days later, and were harvested into a microfuge tube. These samples were used to purify DNA for sequencing (see methods, 2.3.5.6). However, insufficient DNA was obtained by this method for sequencing. To obtain more viral DNA, 90mm dishes of HEp-2 cells were infected with 0.2ml of the plaque containing lysates. These cells were harvested at full c.p.e. 8 days post infection, and the DNA purified by the adenovirus DNA rapid preparation method (see methods, 2.3.5.5). Samples were prepared for sequencing reactions, but once again no results were obtainable. Whether this was due to low DNA concentration, or a low quality DNA preparation is not known. The sequencing reactions have not currently been repeated, and no further experiments have been performed using these viruses due to lack of time.

6.2. Discussion

In order to investigate the effect of E4orf3 upon the distribution of PML isoforms in eukaryotic cells, it was necessary to express these viral proteins in a high percentage of cells in a culture. It would then be possible to further characterise the nature of the Orf3del96-100 mutation that resulted in a loss of the typical Orf3 nuclear localisation. Transient transfection was effective at generating high levels of Orf3 expression, but this was limited to a small subsection of the cells in a culture. Further, it was not possible to generate cell lines permanently expressing sufficiently high levels of Orf3. A viable third alternative was to engineer whole infectious virus, in which Orf3 mutants of interest were substituted for the wild-type protein. This technique would not however, permit the study of Orf3 in isolation from all other viral proteins. Nevertheless, it would have been interesting to determine whether the Orf3del96-100 mutant was capable of restoring the infection specific PML banding pattern, lost in Ad5 mutants lacking a functional Orf3. A virus carrying this mutation would help to address the question as to whether the typical Orf3 nuclear localisation pattern was linked to PML biochemical modification, and important to Orf3 function in infection. The initial steps in the process of construction were successful, and plasmids containing 16.4Kbp of the adenovirus genome including the chosen mutants of E4orf3, were generated. Unfortunately, early attempts to use these plasmids for *in vivo* reconstruction of whole viral genome were not successful. Nevertheless, these

constructs could be used to complete construction of mutant viruses, which could then be used as described above to investigate the exact nature of the localisation mutants of Orf3, in a setting closely related to that found in nature.

7. General Discussion

7.1. Introduction

Recently, it has become clear that the PODs and the PML protein, may play important roles in several cell processes, including regulation of the levels of active proteins in the nucleus, transcriptional regulation, suppression of growth and transformation, antiviral response, cell-cycle regulation and apoptosis (see 1.2.3.). Disruption of the PODs, and redistribution of PML from the PODs, is observed in several malignant tissues, at the beginning of mitosis, as a result of non-virological stress such as heat-shock and during infection with several viruses (see 1.2.4.).

During wild-type adenovirus infection, PML is redistributed from the normal punctate, nuclear bodies, into "track-like" structures, which colocalise with the viral protein, E4orf3. Early in infection, the viral protein E1B-55K, implicated in the deregulation of cell cycle control and viral mRNA transport (see 1.1.5.2.), also localises to these tracks. The E4orf3 protein was found to be necessary and sufficient for redistribution of PML into these nuclear tracks. Interestingly, E4orf3 was shown to stimulate the efficiency of viral propagation >2000-fold, and cell lines engineered to stably overexpress PML showed an inhibition of track formation by E4orf3, concomitant with a decrease in replication of the virus (Doucas *et al.*, 1996). These results suggested that the function of E4orf3 in POD reorganisation is responsible at least in part, for the ability of the protein to enhance viral propagation.

Analysis of the biochemical status of PML by Western blotting, demonstrated a similar redistribution of PML species during mitosis and adenovirus infection. Three, lower mobility isoforms, generally held to represent SUMO-1 conjugated isoforms, were reduced or lost, and a novel band migrating just above the major 140kDa isoform, appeared (see 1.2.4.2. and 1.2.4.7.3). The E4orf3 protein was found to be necessary for these alterations, through the use of virus mutants lacking functional E4orf3 (Everett *et al.*, 1999).

It was of interest to determine whether PML biochemical modification and POD redistribution were directly linked, the one leading to the other, and to determine the role E4orf3 played in these processes. This thesis aimed primarily to determine whether E4orf3 alone was capable of generating the infection-specific PML banding pattern, and which regions of the protein were responsible for POD protein

redistribution and/or PML biochemical alteration. By first developing a technique to express E4orf3 alone in eukaryotic cells, and then generating mutants of E4orf3 for use in this system, it was hoped that it would be possible to investigate aspects of the function of this protein in relation to the cellular protein, PML, in an environment free of other viral factors.

7.2. Transient transfection assays and IF analysis

Using a eukaryotic expression vector, it was possible to express wild-type E4orf3 in eukaryotic HEp-2 cells using calcium-phosphate transient transfection. IF microscopy analysis demonstrated that transfected cells were expressing the Orf3 protein, and that this resulted in PML/Orf3 track formation, similar to that observed during wild-type infection. This observation reinforced the work of Carvalho *et al.* (1995) and Ishov and Maul (1996), demonstrating that E4orf3 was not only necessary, but also sufficient for PML redistribution into nuclear tracks.

In an attempt to identify regions of the protein important to this function, several point and deletion mutants were generated in conserved regions of the gene, by mutational PCR. These mutant E4orf3 proteins were then expressed in HEp-2 cells as before by transient transfection. IF microscopy analysis demonstrated that in the majority of cases, these mutations had no observable effect upon the pattern of Orf3 and PML distribution when compared to wild-type Orf3. The regions these mutations represented were effectively ruled out as singularly important to this aspect of Orf3 function. However, at least one mutation caused a significant alteration in the normal pattern of Orf3 distribution. The Orf3del96-100 mutation, when expressed in eukaryotic cells generated a diffuse, cytoplasmic stain. The alteration in Orf3 localisation appeared to affect colocalisation with PML. The PML protein appeared to remain in punctate, nuclear bodies, rather than form nuclear tracks, or colocalise with Orf3del96-100 as a diffuse, cytoplasmic stain. This was not an unambiguous result, as the strong Orf3 stain seemed to result in some "bleed-through" into the green spectrum where PML staining is observed. Nevertheless, punctate bodies could be observed beneath the diffuse stain, suggesting that the PODs had not, in fact, been redistributed.

This result provides an insight into how E4orf3 functions in relation to PML, and perhaps as to how the various potential processes involving this protein could be co-ordinated and regulated. It would appear that Orf3 must first localise near to or at the

PODs, before commencing to interact with PML. Orf3 is well below the diffusion limit for nuclear pores, and consequently does not require a nuclear localisation signal (NLS) to enter the nucleus. However, it would be observed as a diffuse, cellular component were there not some interaction, tethering the protein to the nucleus. Perhaps the Orf3del96-100 mutant lacks this ability to interact with the appropriate nuclear components and thus is not retained in the nucleus. This would be consistent with experimental observations. If regions of Orf3 required for the nuclear retention of the protein were intact, we would expect nuclear localisation, even if a further interaction with PML was compromised. It is possible that the interaction with PML results in the nuclear localisation of Orf3. Interestingly, the region spanning residues 96-99 of the gene was identified by ScanProsite as a potential casein kinase II phosphorylation site. This is of interest, considering the central role of phosphorylation in control of POD related processes. For example, the tumour suppressor pRB, will only localise to PODs in the inactive, phosphorylated form (Alcalay *et al.,* 1998). Also, SUMO-1 is covalently linked to a subset of PML in a phosphorylation-dependent manner. Phosphatase inhibitors such as calyculin A, inhibit SUMO-1 and PML conjugation, resulting in the stabilisation of the PML isoform typically only present during mitosis, and possibly, Ad5 infection (Müller *et al.,* 1998). Perhaps phosphorylation at this region of the Orf3 protein is necessary for nuclear localisation to the tracks, as is the case for pRb.

It must be stated, however, that the assertion that residues 96-99 comprise a casein kinase II phosphorylation site is by no means unequivocal. The combination of residues identified is not an uncommon one, and the presence of glycine in this region, commonly found at turns in the secondary structure of proteins, might suggest that the deletion in this region simply caused a gross structural deformity. In this case, we might expect to identify the protein with antibodies assuming the antibody-binding site remains intact, but could to all intents and purposes, be identifying a completely non-functional protein, without identifying any active sites. Nevertheless, the GOR secondary structure prediction method (version IV, Garnier *et al.,* 1996), indicated that this deleted region is likely to comprise a random coil region of the protein. Only the last residue (R100A), is predicted by this method to be part of an alpha helical, structural region. If the predictions of this method were true, we might not expect the deletion of residues 96-100 to have a major impact on the structural integrity of the protein. In addition, proteins that misfold are normally recognised and degraded by

the cell. The high level of protein detected by Western blotting argues that this is not the case.

Each of the Orf3 expressing plasmids was also transfected into 293 cells in an attempt to increase transfection efficiency (see 7.3). Interestingly, IF microscopy analysis of these cells upon transfection with Orf3del38-42, revealed a difference between HEp-2 and 293 cells. It was not possible to visualise this protein in Hep-2 cells, and yet when expressed in 293 cells, the protein was visible and formed nuclear tracks. This suggested that some intrinsic property of 293 cells may have been stabilising the protein in such a manner as to reveal the antibody binding site for detection by antibody. One obvious difference between Hep-2 cells and 293 cells is the presence of the adenovirus protein, E1b-55kDa in the latter. This protein is known to form a complex with E4orf3 at early stages in infection, and it was of interest to determine whether 55K was responsible for stabilising this Orf3 mutant in 293 cells. To test this, HEp-2 cells were co-transfected with both pcDNA3.1/Orf3*wt*, and a plasmid expressing E1b-55kDa. These cells were then co-stained for Orf3 and 55K, and it was found that the presence of 55K enabled detection of the Orf3 protein in HEp-2 cells. These observations suggest that the region spanning residues 38-42 was not directly linked to Orf3 nuclear localisation and POD disruption, as the protein was still capable of generating tracks. In addition, they demonstrate that this region of Orf3 was not required for interaction with the E1b-55kDa protein, as this protein was redistributed from a diffuse, cytoplasmic distribution, to colocalise with Orf3 at nuclear tracks. This mutation might, however, be implicated in antibody binding or the structural stability of the protein. Although not predicted to be within a structurally important alpha-helical region by the GOR secondary structure prediction model (version IV, Garnier *et al.,* 1996) this deletion might cause a modification in protein structure, concealing the antibody-binding site. If this were the case, binding of 55K could cause a conformational change, resulting in the exposure of the antibody-binding site, ultimately allowing detection of Orf3 in our assay.

As well as the E1b-55kDa protein, 293 cells also express the adenovirus E1A protein, known to localise to the PODs (Carvalho *et al.,* 1995). Although this protein was not investigated in this research, a possible link with the altered expression of the mutant Orf3 protein in 293 cells and expression of E1A cannot be discounted, and further work to look at potential E1A/Orf/PML interactions in this system would be valuable.

7.3. Western blotting analysis of transiently transfected cells

In an attempt to determine whether Orf3-induced track formation was directly linked to an altered distribution of PML biochemical species, Western blotting was used to analyse samples derived from HEp-2 cells transfected with all E4orf3 expressing plasmids. The results obtained did not demonstrate the loss of those PML isoforms generally considered to be SUMO-1-conjugated, nor was the infection-specific band migrating just above 140kDa identifiable. These results however were flawed, in that only a low transfection efficiency was obtainable. Other than the major band migrating at approximately 140kDa, both the SUMO-conjugated isoforms of PML, and the infection-specific band are relatively uncommon and difficult to detect by this method. With a low transfection efficiency, the difficulties of detecting any alterations in the status of these isoforms are amplified, and indeed, proved insurmountable.

Through replacing HEp-2 cells with 293 cells in this system, it was possible to greatly improve the transfection efficiency. Nevertheless, samples of transfected 293 cells yielded the same pattern of PML species as mock controls. Once again, though the transfection efficiency was improved, it was not possible to draw positive conclusions here from negative results.

7.4. Problems associated with permanent cell lines expressing E4orf3

One of the major drawbacks of transient transfection, was that only a small percentage of cells in a sample could be considered to be expressing and exposed to E4orf3. In earlier experiments investigating the biochemical alteration of PML during the progress of the cell cycle, Everett *et al.* (1999) found it necessary to synchronise cells to ensure that a high proportion of the cells under observation had the same PML species. Only then was it possible to observe the mitosis-specific band by Western blotting. The infection-specific PML isoform of interest is similar in mobility and abundance to the mitosis-specific isoform, and it was to be expected that a similar percentage of cells would need to have this PML isoform in order that it could be observed by Western blotting analysis, as was required during the studies of Everett *et al.* Therefore, in order to determine whether or not E4orf3 could generate the infection-specific PML band, it was necessary to increase the percentage of cells in a sample that might be expected to have this PML isoform. To address this problem, cell lines were developed to permanently express the viral protein. It was hope that this measure would facilitate observation by Western blotting of any Orf3 induced

biochemical alteration of PML. Unfortunately, this technique encountered several problems that proved unsolvable.

Several cell-lines and mixed cultures enriched for "Orf3-expressing" cells were developed on the basis of resistance to G-418, provided by the vector plasmid. Mixed cultures enriched for G-418 resistant cells, and cell-lines developed from resistant clones, were tested by Western blotting analysis and IF microscopy for the presence of Orf3.

A mixed culture was developed which successfully expressed Orf3 in a high percentage of cells. However, this failed to persist in culture beyond 5-6 weeks (approximately 10 passages), and frozen stocks could not successfully be maintained after thawing. One possible explanation for this phenomenon could be that the cells were exposed to bacterial or fungal contamination. Contamination of the Orf3 expressing mixed culture would explain why these cells failed to plate down and why frozen stocks could not be successfully resurrected. However, contaminants could not be visualised under microscopy, and the addition of *penicillin* and *streptomycin* to the media had no effect. This would argue that contamination was not the cause of the problem.

At early stages in the assay, Orf3 could be detected by IF microscopy, and to a lesser extent by Western blotting, in certain of the cell-lines derived from single clones. Over time and numerous passages however, any expression of Orf3 appears to have been lost from these lines. Western blotting analysis of the PML isoforms present in these cells revealed no discernible difference in comparison with "normal" HEp-2 cells. Nevertheless, the cells were resistant to the effects of G-418, apparently indefinitely. This suggests that resistance to this toxin had been incorporated from the vector plasmid into the HEp-2 genome. The fact that Orf3 was not also expressed in these cells is revealing. Insertion events have a random quality, and foreign DNA may incorporate into the cellular genome at various locations, and to differing extents. Therefore all insertions are not equivalent, and different sections of foreign DNA may be incorporated. It could be that the gene conferring G-418 resistance simply incorporated more successfully into the HEp-2 genome, whether due to some intrinsic qualities of this stretch of DNA, or simply bad luck. Perhaps repetition of these experiments would produce viable cell-lines permanently expressing Orf3. A more likely explanation, would be that Orf3 has a deleterious effect on cell survival. This would explain the preferential survival of cells with resistance to G-418, but not

expressing Orf3. This too would explain how, in a clone of "identical" cells, expression of E4orf3 was lost over time. Cells carrying incorporated DNA have a tendency to expel this DNA from their genome over time. The continual application of selection (in this case G-418), is designed to limit this, by putting these cells at a selective disadvantage in comparison with cells maintaining the insert. Despite this pressure, expression from Orf3 was lost. In this case, it appears that selection favoured cells maintaining certain portions of the foreign DNA, but rejecting Orf3. If this is the case, it will not be possible to generate cell lines from HEp-2 cells, to permanently express E4orf3. It is, however, possible that other cell types will prove resistant to the effects of the viral protein, and can be used to develop cell-lines permanently expressing Orf3.

This conjecture leads one to consider how the Orf3 protein could cause such effects in eukaryotic cells, and whether these effects are linked to the function of the protein during infection. For example, it has been demonstrated in this thesis and elsewhere, that transient expression of E4orf3 alone in eukaryotic cells reorganises endogenous PML from the spherical PODs into track-like structures. As previously mentioned, PML and the PODs have been implicated in several cellular processes, including cell-cycle regulation and apoptosis (see 1.2.3.). The reorganisation of the PODs by Orf3 may have an important role in the deregulation of the cell cycle, helping to provide an environment suitable for viral replication. Perhaps those cells permanently expressing Orf3 cannot, ultimately, sustain themselves in culture without the normal, discrete PODs. If this was effected through a deregulation of cell cycle control, we might expect the accumulation of high levels of p53 in the nucleus, as occurs consequent to expression of Ad E1A proteins (McMahon *et al.*, 1998; Fuchs *et al.*, 2001; Rikitake and Moran, 1992; Barbeau *et al.*, 1994; Shenk, 1996). These high levels of p53 can then induce apoptosis. Perhaps Orf3 has a less-severe, but similar effect on cells over time. If this were the case, we would expect to see evidence of a deregulated cell-cycle. In effect, the cells might be expected to multiply in an uncoordinated fashion and not as a monolayer. In the only culture to express high levels of Orf3 in a large percentage of cells (the mixed culture, see fig.5.2), cells did indeed appear to be growing on top of each other, rather than as a well-defined monolayer. It was not possible to maintain this enriched culture for study, but these results are intriguing, suggesting that Orf3 may indeed act to transform cells if expressed strongly enough,

before ultimately causing apoptosis, through the deregulation of PML and POD function and cell cycle regulation.

Of note, is the work of Nevels *et al.* (1999), in which cell lines were developed which permanently expressed E4orf3. While the successful development of these cell lines would appear to be at variance with the observations made above, there were several key differences in experimental approach, and the results presented in this thesis perhaps go some way to help elucidate their observations. Of primary importance, the transformed lines developed by Nevels *et al.*, were designed to express not only E4orf3, but also various combinations of the adenovirus E1A, E1B and E4orf6 products. The E1A/E1B products alone were found to be sufficient for cell transformation, and it was within this environment that Orf3 was expressed. Indeed, in support of the observations made in this thesis, Nevels *et al.* observed that high levels of E4orf3 were deleterious to cell survival, and concluded that the activities of this protein may be modulated in the presence of other viral products, particularly those of the E1B gene. Cell lines expressing E1A, E1B and E4orf3 gene products exhibited higher growth rates and saturation densities, and induced tumours more frequently than transformed cells expressing E1A and E1B only. Under these conditions therefore, it would appear that E4orf3 has growth-promoting activities. However, the presence of E4orf3 did not appear to have any effect on the steady-state levels of p53 in cell lines expressing the E1A, E1B and E4orf3 gene products, in comparison with cell lines expressing the E1A and E1B gene products only. Thus it would appear that any effects on cell survival and growth rates consequent to high levels of E4orf3 expression, are not due to modification of p53. Nevertheless, the levels of this tumour suppressor protein have not been observed in cells expressing only E4orf3. Nevels *et al.* demonstrated that unlike E4orf6, the Orf3 gene product was not capable of reducing steady-state levels of p53, but did not convincingly demonstrate that Orf3 did not increase the levels of p53 when expressed alone. The E1A product greatly increased the steady-state levels of p53, and in cells expressing both this protein and Orf3, it may have been the case that an Orf3-induced p53 increase went unnoticed. This is certainly worth investigation, although once again, the deleterious effects of Orf3 on cell-survival would make any such investigation problematic.

Recent work by Stracker *et al.* (2002), has demonstrated that the E4orf3 protein is responsible for the redistribution and inactivation of the cellular Mre11-Rad50-NBS1

DNA repair complex. This multiprotein complex is important in double-strand break repair, meiotic recombination and telomere maintenance in mammalian cells, but was also shown by Stracker *et al.* (2002) to be required for the formation of the adenovirus DNA concatomers seen upon infection with virus mutants lacking either functional Orf3 or Or6/55K complexes (see section 1.1.5.5.). In uninfected cells, Mre11, Rad50 and NBS1 were shown to be present throughout the nucleoplasm, but concentrated at sites of replication and at the PODs. During a wild-type infection, the complex was redistributed into speckles, followed by a decrease in abundance of the constituent proteins. Upon infection with an E4 deleted virus, Mre11, Rad50 and NBS1 were shown to locate to viral replication centres, with the consequent generation of concatemeric adenoviral DNA. Through the use of virus mutants, and the expression of individual E4 proteins in eukaryotic cells, Stracker *et al.* demonstrated that the E4orf6/55K complex was responsible for the degradation of Mre11 and Rad50, but that Orf3 was responsible for the redistribution of the proteins to the cytoplasm and to nuclear speckles partially overlapping with the PML tracks of the redistributed PODs. This redistribution was sufficient for the inactivation of the Mre11-Rad50-NBS1 complex in the formation of concatemeric viral DNA, and reflects a requirement for the inactivation of this complex for viral reproduction. In addition however, these results provide a mechanism by which Orf3 could affect the long term survival of cells expressing the protein. The Mre11-Rad50-NBS1 complex has been implicated as an important regulator of genome stability, preventing normal cells from becoming malignant. If expression of Orf3 alone is sufficient to disrupt the normal functioning of the complex, it is likely that host cells would not persist in the long term, as such DNA repair mechanisms are crucial to cell survival.

7.5. Construction of whole virus

Given the problems encountered during attempts to express Orf3 in a large enough percentage of cells to enable the study of any alterations in the Western blot banding pattern for PML, it was decided to generate whole, infectious virus, substituting mutant E4orf3 for wild-type Orf3 in the virus genome. Initially, it was decided to generate two mutants, expressing Orf3del96-100 and Orf3T96A. These would have enabled investigation of the effects of the altered pattern of Orf3 localisation upon the PML banding pattern. A virus with aberrant localisation of Orf3 would help to address the question as to whether the typical Orf3 nuclear localisation pattern was

linked to PML biochemical modification, and important to Orf3 function in infection. Of course, the deletion mutant may have represented a non-functional Orf3 protein, as alluded to above, in which circumstance infection with Ad5del96-100 would not tell us more about Orf3 function than existant mutants lacking Orf3 entirely. Nevertheless, using whole virus expressing these mutants, it would be possible to determine whether other known Orf3 interactions, such as with the viral protein, E1B-55K were also affected.

55K has a diffuse, cytoplasmic distribution in the absence of other viral proteins, but during co-transfection experiments, complexes with Orf3 to colocalise at the PODs. This process is mirrored early in infection, until 55K apparently preferentially complexes with E4orf6 to localise at the periphery of the viral replication centres (Ornelles *et al.*, 1991). Localisation mutations of Orf3 might still complex with 55K, assuming that protein structure is not disrupted in the protein region required for this activity. If this were the case, it would be of interest to observe any subsequent alterations in 55K localisation and/or function.

Attempts to generate the desired mutant viruses were not completed. Nevertheless, the plasmids necessary to *in vivo* recombination were successfully constructed, facilitating any future attempts to generate infectious viruses expressing these E4orf3 mutations.

7.6. Concluding remarks

Using plasmid vectors to express the adenovirus protein, E4orf3, in eukaryotic cells, these studies have demonstrated that this protein is necessary and sufficient to reorganise the PODs from discrete, spherical structures, into track-like structures colocalising Orf3 and PML, similar to those observed during infection. By generating point mutations and deletion mutations in the Orf3 gene, and expressing the proteins in eukaryotic cells, it has been possible to eliminate several conserved regions of the gene as necessary for the interaction between Orf3 and PML, and nuclear track formation. However, one deletion mutant, Orf3del96-100, was identified which resulted in an unusual, diffuse cytoplasmic Orf3 localisation when expressed in eukaryotic cells and observed by IF microscopy. It was possible that the disruption in Orf3 localisation caused by this, relatively large, deletion (5 residues), was caused by a gross conformational change of the protein, and not through modification of an active site involved in track formation. Further point mutations of the residues in this

region were generated, but none of the expressed proteins demonstrated a similar protein distribution to the deletion. These results would appear to support the idea that deletion of residues 96-100 simply disrupts the Orf3 protein, while leaving the antibody-binding site intact. Nevertheless, one point mutation within this region (Orf3T96A), did seem under IF microscopy, to have an extranuclear component, as well as forming the "normal" nuclear tracks. While this observation was consistent, it was not convincing, due to the inherent variability in levels of protein expression using transient transfection. This method can result in wildly varying expression levels from one cell to the next, and high expression of Orf3 from any plasmid, usually resulted in some extranuclear protein. While an extranuclear component was usually, rather than occasionally, present in cells expressing Orf3T96A, the observation was too vague and inconsistent to be considered "true".

It was also attempted to try and ascertain any link between the Orf3-inducible PML "tracks", and the PML biochemical alteration observed during infection. Once again, transient transfection proved to be an unsuitable method for these studies, as the transfection efficiency in two cell types, was simply too low to allow the reliable interpretation of results.

Accordingly, other methods were used to attempt to elucidate the phenotype of the two mutants and to determine whether Orf3 alone was responsible for the PML biochemical alteration, by generating stable cell lines or whole, mutant virus. Unfortunately, it was not possible to generate cell lines permanently expressing E4orf3, and the construction of mutant virus was not completed. Interestingly, it was not possible to generate cell lines permanently expressing E4orf3del96-100, suggesting that either the method used to generate these cell-lines was faulty and Orf3 may not, as earlier suggested, be deleterious to cell survival, or that to some extent Orf3del96-100 was still functional and selected against in culture.

It would be of interest to generate further point mutations in the Orf3 gene, covering other conserved residues that have not, so far, been investigated. Namely, these are V9, E10, G11, A12, E38, N39, Y40 and *L41*. Using the same methods, these could initially be screened by transient transfection and IF analysis in eukaryotic cells, for any abnormalities in interaction with PML and the PODs, and nuclear track formation. Such studies may identify a single residue necessary for these interactions, which could help to characterise the nature of the interaction between Orf3 and PML. For example, are nuclear localisation to the PODs and track formation two, separable

processes, or two aspects of a single interaction? It is also possible that no single residue is crucial to track formation, in which case, the deletion of residues 96-100 may yet point towards a crucial site. It would be of interest to express a protein with an additional point mutation, adjacent to T96A, perhaps G97A, and determine whether this would result in an altered Orf3 distribution, without resorting to deletions or mutations that we might expect to result in gross, conformational changes.

The nature of the interaction between Orf3 and E1b-55kDa is also of interest, and the plasmids already constructed could be used in future investigations to explore the importance of these conserved regions to this, second interaction. The regions represented in the panel of Orf3 expressing plasmids are conserved across adenovirus serotypes, suggesting some functional significance. If, as suggested by these studies, they are not implicated in POD redistribution and track formation, they might be expected to be important in other functions of the protein, such as the formation of a complex with 55K. It would be a relatively simple matter to screen these Orf3 proteins for 55K colocalisation mutants, by co-transfecting the two proteins into eukaryotic cells. Previous work has demonstrated the utility of this approach, showing that when co-expressed in HEp-2 cells with Orf3, the E1b-55kDa protein is reorganised from a diffuse, cytoplasmic stain, to colocalise at the nuclear tracks (data not shown). This simple procedure could be utilised to identify any Orf3 mutations that did not reorganise 55K.

It is becoming increasingly clear that the PODs and PML are integral to many cellular processes and therefore have implications for many fields of interest. By gaining greater insights into the function of these structures we will better understand complex cellular processes such as apoptosis, transcriptional regulation and the antiviral response. This will inevitably have an impact on research into and the successful treatment of conditions involving inappropriate cell growth and survival such as APL and other malignancies, and may impact on treatment strategies for degenerative disorders involving inappropriate cell death such as Alzheimer's disease and Parkinson's disease. By studying the interactions of virus and host in this manner, it may become possible to harness viruses as tools for the treatment of disease by gene delivery, and through the measured control of the processes of cell death, to treat or prevent those illnesses brought about from within consequent to the deregulation of our own, cellular processes.

8. Bibliography

Ahn MJ, Nason-Burchenal K, Moasser MM and Dmitrovsky E. (1995). Growth suppression of acute promyelocytic leukemia cells having increased expression of the non-rearranging alleles: RARα or PML. *Oncogene* **10**, 2307-2314.

Akiyoshi Y, Clayton J, Phan L, Yamamoto M, Hinnebusch AG, Watanabe Y and Asano K. (2001). Fission yeast homolog of murine *int-6* protein, encoded by mouse mammary tumor virus integration site, is associated with the conserved core subunits of eukaryotic translation initiation factor 3. *Journal of Biological Chemistry* **276**, 10056-10062.

Alcalay M, Tomassoni L, Colombo E, Stoldt S, Grignani F, Fagioli M, Szekely L, Helin K and Pelicci PG. (1998). The promyelocytic leukemia gene product (PML) forms stable complexes with the retinoblastoma protein. *Molecular and Cellular Biology* **18**, 1084-1093.

Arany Z, Newsome D, Oldread E, Livingston DM and Eckner R. (1995). A family of transcriptional adapter proteins targeted by the E1A oncoprotein. *Nature* **375**, 81-84.

Arrand JR and Roberts RJ. (1979). The nucleotide sequences at the termini of adenovirus-2 DNA. *Journal of Molecular biology* **128**, 577-594.

Asano K, Merrick WC and Hershey JWB. (1997). The translation initiation factor eIF3-p48 subunit is encoded by *int-6*, a site of frequent integration by the mouse mammary tumor virus genome. *Journal of Biological Chemistry* **272**, 23477-23480.

Babiss LE, Ginsberg HS and Darnell JE Jr. (1985). Adenovirus E1B proteins are required for accumulation of late viral mRNA and for effects on cellular mRNA translation and transport. *Molecular and Cellular Biology* **5**, 2552-2558.

Bannister AJ and Kouzarides T. (1996). The CBP co-activator is a histone acetyltransferase. *Nature* 384, 641-643.

Barbeau D, Charbonneau R, Whalen SG, Bayley ST and Branton PE. (1994). Functional Interactions within adenovirus E1A protein complexes. *Oncogene* **9**, 359-373.

Bell P, Lieberman PM and Maul GG. (2000). Lytic but Not Latent Replication of Epstein-Barr Virus Is Associated with PML and Induces Sequential Release of Nucclear Domain 10 Proteins. *The Journal of Virology* **74**, 11800-11810.

Beltz GA and Flint SJ. (1979). Inhibition of HeLa cell protein synthesis during adenovirus infection. Restriction of cellular messenger RNA sequences to the nucleus. *Journal of Molecular Biology* **131**, 353-373.

Bergelson JM, Cunningham JA, Droguett G, Kurt-Jones EA, Krithivas A, Hong JS, Horwitz MS, Crowell RI and Finberg RW. (1997). Isolation of a common receptor for coxsackie B viruses and adenoviruses 2 and 5. *Science* **275**, 1320-1323.

Bernstein RM, Neuberger JM, Bunn CC, Callender ME, Hughes GR and Williams R. (1984). Diversity of autoantibodies in primary biliary cirrhosis and chronic active hepatitis. *Clinical and Experimental Immunology* **55**, 553-560.

Bhattacharya S, Eckner R, Grossman S, Oldread E, Arany Z, D'Andrea A and Livingston DM. (1996). Cooperation of Stat2 and p300/CBP in signalling induced by interferon-alpha. *Nature* **383**, 344-347.

Blair Zajdel ME and Blair GE. (1988). The intracellular distribution of the transformation-associated protein p53 in adenovirus-transformed rodent cells. *Oncogene* **2**, 579-584.

Bloch DB, delaMonte SM, Guigaouri P, Filippov A and Bloch KD. (1996). Identification and characterization of a leukocyte-specific component of the nuclear body. *Journal of Biological Chemistry* **271**, 29198-29204.

Boddy MN, Howe K, Etkin LD, Solomon E and Freemont PS. (1996). PIC 1, a novel ubiquitin-like protein which interacts with the PML component of a multiprotein complex that is disrupted in acute promyelocytic leukaemia. *Oncogene* **3**, 971-982.

Bodnar JW, Hanson PI, Polvino-Bodnar M, Zempsky W and Ward DC. (1989). The terminal regions of adenovirus and minute virus of mice DNAs are preferentially associated with the nuclear matrix in infected cells. *Journal of Virology* **63**, 4344-4353.

Boehm U, Klamp T Groot M and Howard JC. (1997). Cellular responses to interferon-gamma. *Annual Review of Immunology* **15**, 749-795.

Boggs BA, Connors B, Sobel RE, Chinaud AC and Allis CD. (1996). Reduced levels of histone H3 acetylation on the inactive X chromosomes as shown by histone acetylation. *Chromosoma* **104**, 41-49.

Boisvert FM, Hendzel MJ and Bazett-Jones DP. (2000). Promyelocytic Leukemia (PML) Nuclear Bodies Are Protein Structures that Do Not Accumulate RNA. *The Journal of Cell Biology* **148**, 283-292.

Bondesson M, Öhman K, Mannervik M, Fan S and Akusjärvi G. (1996). Adenovirus E4 open reading frame 4 protein autoregulates E4 transcription by inhibiting E1A transactivation of the E4 promoter. *Journal of Virology* **70**, 3844-3851.

Borden KLB, Campbelldwyer EJ, Carlile GW, Djavani M and Salvato MS. (1998). Two RING finger proteins, the oncoprotein PML and the arenavirus Z protein, colocalize with the nuclear fraction of the ribosomal P proteins. *Journal of Virology* **72**, 3819-3826.

Bosher J, Dawson A and Hay RT. (1992). Nuclear factor I is specifically targeted to discrete subnuclear sites in adenovirus type 2-infected cells. *Journal of Virology* **66**, 3140-3150.

Bridge E and Ketner G. (1989). Redundant control of adenovirus late gene expression by early region 4. *Journal of Virology* **63**, 631-638.

Bridge E, Carmo-Fonseca M, Lamond A and Pettersson U. (1993). Dynamic organization of splicing factors in adenovirus-infected cells. *Journal of Virology* **69**, 281-290.

Burgert HG and Blusch JH. (2000). Immunomodulatory functions encoded by the E3 transcription unit of adenoviruses. *Virus Genes* **21**, 13-25.

Cao TY, Duprez E, Borden KLB, Freemont PS and Etkin LD. (1998). Ret finger protein is a normal component of PML nuclear bodies and interacts directly with PML. *Journal of Cell Science* **111**, 1319-1329.

Capco DG, Wan KD and Penman S. (1982). The nuclear matrix: Three-dimensional architecture and protein composition. *Cell* **29**, 847-858.

Carmo-Fonseca M, Pepperkok R, Carvalho MT and Lamond AI. (1992). Transcription-dependent colocalization of the U1, U2, U4/U6, and U5 snRNPs in coiled bodies. *The Journal of Cell Biology* **117**, 1-14.

Carvalho T, Seeler J, Ohman K, Jordan P, Petterson U, Akusjarvi G, Carmo-Fonseca M and Dejean A. (1995). Targeting of adenovirus E1A and E4ORF3 proteins to nuclear matrix-associated PML bodies. *The Journal of Cell Biology* **131**, 45-56.

Chakravarti D, LaMorte VJ, Nelson MC, Nakajima T, Schulman IG, Juguilon H, Montminy M and Evans RM. (1996). Role of CBP/P300 in nuclear receptor signalling. *Nature* **383**, 99-103.

Challberg MD, Desiderio SV, and Kelly TJ Jr. (1980). Adenovirus DNA replication in vitro: characterization of a protein covalently linked to nascent DNA strands. *Proceedings of the National Academy of Sciences, USA* **77**, 5015-5109.

Challberg MD, Ostrove JM and Kelly TJ Jr. (1982). Initiation of adenovirus DNA replication: detection of covalent complexes between nucleotide and the 80-kilodalton terminal protein. *Journal of Virology* **41**, 265-270.

Chan EK, Takano S, Andrade LE, Hamel JC and Matera AG. (1994). Structure, expression and chromosomal localization of human p80-coilin gene. *Nucleic Acids Research* **22**, 4462-4469.

Chang HY, Nishitoh H, Yang XL, Ichijo H and Baltimore D. (1998). Activation of apoptosis signal regulating kinase 1 (ASK1) by the adapter protein Daxx. *Science* **281**, 1860-1863.

Chatterjee PK, Vayda ME and Flint SJ. (1986). Adenoviral protein VII packages intracellular viral DNA throughout the early phase of infection. *The EMBO Journal* **7**, 1633-1644.

Chao DT and Korsmeyer SJ. (1998). BCL-2 family: regulators of cell death. *Annual Review of Immunology* **16**, 395-419.

Chelbi-Alix MK, Pelicano L, Quignon F, Koken MHM, Venturini L, Stadler M, Pavlovic J, Degos L and de Thé H. (1995). Induction of the PML protein by interferons in normal and APL cells. *Leukemia* **9**, 2027-2033.

Chelbi-Alix MK, Quignon F, Pelicano L, Koken MHM and de Thé H. (1998). Resistance to Virus Infection Conferred by the Interferon-Induced Promyelocytic Leukemia Protein. *Journal of Virology* **72**, 1043-1051.

Chinnadurai G. (1998). Control of apoptosis by human adenovirus genes. *Seminars in Virology* **8**, 399-408.

Chrivia JC, Kwok RPS, Lamb N, Hagiwara M, Montminy MR and Goodman RH. (1993). Phosphorylated Creb binds specifically to the nuclear-protein CBP. *Nature* **365**, 855-859.

Clarke AR, Purdie CA, Harrison DJ, Morris RG, Bird CC, Hooper ML and Wyllie AH. (1993). Thymocyte apoptosis induced by p53-dependent and independent pathways. *Nature* **362**, 849-852.

Cohen N, Sharma M, Kentsis A, Oerez J M, Strudwick S and Borden K L B. (2001). PML RING suppresses oncogenic transformation by reducing the affinity of eIF4E for mRNA. *The EMBO Journal* **20**, 4547-4559.

Commission on Acute Respiratory Disease. (1947). Experimental transmission of minor respiratory illness to human volunteers by filter-passing agents. Demonstration of two types of illness characterized by long and short incubation periods and different clinical features. *Journal of Clinical Investigation* **26**, 957-973.

Dales S and Chardonnet Y. (1973). Early events in the interaction of adenoviruses with HeLa cells. IV. Association with microtubules and the nuclear pore complex during vectorial movement of the inoculum. *Virology* **56**, 465-483.

Davison E, Diaz R M, Hart I R, Santis G and Marshall J F. (1997). Integrin $\alpha_v\beta_1$-mediated adenovirus infection is enhanced by the integrin-activating antibody TS2/16. *Journal of Virology* **71**, 6204-6207.

Davison E, Kirby I, Elliot T and Santis G. (1999). The human HLA-A*0201 allele, expressed in hamster cells, is not a high-affinity receptor for adenovirus type 5 fiber. *Journal of Virology* **73**, 4513-4517.

Dehlin E, Wormington M, Korner CG and Wahle E. (2000). Cap-dependent deadenylation of mRNA. *EMBO Journal* **19**, 1079-1086.

De Jong JC, Wermenbol AG, Verweij-Uijterwaal MW, Slaterus KW, Wertheim-Van Dillen P, Van Doornum GJ, Khoo SH and Hierholzer JC. (1999). Adenoviruses from human immunodeficiency virus-infected individuals, including two strains that represent new candidate serotypes Ad50 and Ad51 of species B1 and D, respectively. *Journal of Clinical Microbiology* **37**, 3940-3945.

De Maria R, Lenti L, Malisan F, d'Agostino F, Tomassini B, Zeuner A, Rippo MR and Testi R. (1997). Requirement for GD3 ganglioside in CD95- and ceramide-induced apoptosis. *Science* **277**, 1652-1655.

Dent AL, Yewdell J, Puviondutilleul F, Koken MHM, de Thé H and Staudt LM. (1996). LYSP1-associated nuclear domains (LANDs): Description of a new class of subnuclear structures and their relationship to PML nuclear bodies. *Blood* **88**, 1423-1436.

Desbois C, Rousset R, Bantignies F and Jalinot P. (1996). Exclusion of Int-6 from PML nuclear bodies by binding to the HTLV-1 tax oncoprotein. *Science* **273**, 951-953.

Desiderio SV and Kelly TJ Jr. (1981). Structure of the linkage between adenovirus DNA and the 55,000 molecular weight terminal protein. *Journal of Molecular Biology* **145**, 319-337.

De Thé H, Chomienne C, Lanotte M, Degos L and Dejean A. (1990). The t(15; 17) translocation of acute promyelocytic leukaemia fuses the retinoic acid receptor alpha gene to a novel transcribed locus. *Nature* **347**, 558-561.

Dingle JH and Langmuir AD. (1968). Epidemiology of acute, respiratory disease in military recruits. *American Review of Respiratory Diseases* **97**, Suppl:1-65.

Dix I and Leppard K N. (1995). Expression of adenovirus type 5 E4 Orf2 protein during lytic infection. *Journal of General Virology* **76**, 1051-1055.

Dobbelstein M, Roth J, Kimberley WT, Levine AJ and Shenk T. (1997). Nuclear export of the E1B 55-kDa and E4 34-kDa adenoviral oncoproteins mediated by a rev-like signal sequence. *The EMBO Journal* **16**, 4276-4284.

Donehower LA, Harvey M, Slagle BL, McArthur MJ, Montgomery CA Jr, Butel JS and Bradley A. (1992). Mice deficient for p53 are developmentally normal but susceptible to spontaneous tumours. *Nature* **356**, 215-221.

Dosch T, Horn F, Schneider G, Krätzer F, Dobner T, Hauber J and Stauber RH. (2001). The Adenovirus Type 5 E1B-55K Oncoprotein Actively Shuttles in Virus-Infected Cells, Whereas Transport of E4orf6 Is Mediated by a CRM1-Independent Mechanism. *Journal of Virology* **75**, 5677-5683.

Doucas V, Ishov AM, Romo A, Juguilon H, Weitzman MD, Evans RM and Maul GG. (1996). Adenovirus replication is coupled with the dynamic properties of the PML nuclear structure. *Genes and Development* **10**, 196-207.

Doucas V, Tini M, Egan DA and Evans RM. (1999). Modulation of CREB binding protein function by the promyelocytic (PML) oncoprotein suggests a role for nuclear bodies in hormone signaling. *Proceedings of the National Academy of Sciences, USA* **96**, 2627-2632.

Dyck JA, Maul GG, Miller WJ, Chen JD, Kakizura A and Evans RM. (1994). A novel macromolecular structure is a target of the promyelocyte-retinoic acid receptor oncoprotein. *Cell* **76**, 333-343.

Ebisawa T, Tada K, Kitajima I, Tojo K, Sampath TK, Kawabata M, Miyazono K and Imamura T. (1999). Characterization of bone morphogenetic protein-6 signaling pathways in osteoblast differentiation. *The Journal of Cell Science* **112**, 3519-3527.

El-Deiry WS, Tokino T, Velculescu VE, Levy DB, Parsons R, Trent JM, Lin D, Mercer WE, Kinzler KW and Vogelstein B. (1993). WAF1, a potential mediator of p53 tumor suppression. *Cell* **75**, 817-825.

Enari M, Hugh H and Nagata S. (1995). Involvement of an ICE-like protease in Fas-mediated apoptosis. *Nature* **375**, 78-81.

Enari M, Talanian RV, Wong WW and Nagata S . (1996). Sequential activation of ICE-like and CPP32-like proteases during Fas-mediated apoptosis. *Nature* **380**, 723-726.

Everitt E, Lutter L and Philipson L. (1975). Structural proteins of adenoviruses. XII. Location and neighbor relationship among proteins of adenovirion type 2 as revealed by enzymatic iodination, immunoprecipitation and chemical cross-linking. *Virology* **67**, 197-208.

Everett RD, Freemont P, Saitoh H, Dasso M, Orr A, Kathoria M and Parkinson J. (1998). The Disruption of ND10 during Herpes Simplex Virus Infection Correlates with the Vmn110- and Proteasome-Dependent Loss of Several PML Isoforms. *Journal of Virology* **72**, 6581-6591.

Everett RD, Lomonte P, Sternsdorf T, Van Driel R and Orr A. (1999). Cell cycle regulation of PML modification and ND10 composition. *Journal of Cell Science* **112**, 4581-4588.

Fey EG, Krochmalnic G and Penman S. (1986). The nonchromatin substructures of the nucleus: the ribonucleoprotein (RNP)-containing and RNP-depleted matrices analyzed by sequential fractionation and resinless section electron microscopy. *Journal of Cell Biology* **102**, 1654-1665.

Field J, Gronostajski RM and Hurwitz J. (1984). Properties of the Adenovirus DNA-polymerase. *Journal of Biological Chemistry* **259**, 9487-9495.

Fogal V, Gostissa M, sandy P, Zacchi P, Sternsdorf T, Jensen K, Pandolfi PP, Will H, Schneider C and del Sal G. (2000). Regulation of p53 activity in nuclear bodies by a specific PML isoform. *The EMBO Journal* **19**, 6185-6195.

Fredman JN and Engler JA. (1993). Adenovirus precursor to terminal protein interacts with the nuclear matrix in vivo and in vitro. *Journal of Virology* **67**, 3384-3395.

Freemont PS, Hanson IM and Trowsdale J. (1991). A novel cysteine-rich sequence motiv. *Cell* **64**, 483-484.

Fuchs M, Gerber J, Drapkin R, Sif S, Ikura T, Ogryzko V, Lane WS, Nakatani Y and Livingston DM. (2001). The p400 Complex is an Essential E1A Transformation Target. *Cell* **106**, 297-307.

Gasser SM, Amati BB, Cardenas ME and Hofmann JFX. (1989). Studies on scaffold attachment sites and their relation to genome function. *InternationalReview of Cytology* **119**, 57-96.

Gerace L and Burke B. (1988). Functional organization of the nuclear envelope. *Annual Review of Cell Biology* **4**, 335-374.

Giaccia AJ and Kastan MB. (1998). The complexity of p53 modulation: emerging patterns from divergent signals. *Genes and Development* **12**, 2973-2983.

Ginsberg HS, Gold E, Jordan WS Jr, Katz S, Badger GF and Dingle JH. (1955). Relation of the new respiratory agents to acute respiratory diseases. *American Journal of Public Health* **45**, 915-922.

Ginsberg HS, Pereira HG, Valentine RC and Wilcox WC. (1966). A proposed terminology for the adenovirus antigens and virion morphological subunits. *Virology* **28**, 782-783.

Goddard AD, Borrow J, Freemont PS and Solomon E. (1991). Characterization of a zinc finger gene disrupted by the t(15; 17) in acute promyelocytic leukaemia. *Science* **254**, 1371-1374.

Gongora C, David G, Pintard L, Tissot C, Hua TD, Dejean A and Mechti N. (1997). Molecular Cloning of a New Interferon-induced PML Nuclear Body-associated Protein. *The Journal of Biological Chemistry* **272**, 19457-19463.

Goodrum FD, Shenk T and Ornelles DA. (1996). Adenovirus early region 4 34-kilodalton protein directs the nuclear localization of the early region 1B 55-kilodalton protein in primate cells. *Journal of Virology* **70**, 6323-6335.

Garnier J, Gibrat JF and Robson B. (1996). GOR secondary structure prediction method version IV. *Methods in Enzymology* **266**, 540-553.

Gooding LR, Aquino L, Duerksen-Hughes PJ, Day D, Horton TM, Yei SP and Wold WS. (1991). The E1B 19,000-molecular-weight protein of group C adenoviruses prevents tumor necrosis factor cytolysis of human cells but not of mouse cells. *Journal of Virology* **65**, 3083-3094.

Gostissa M, Hengstermann A, Fogal V, Sandy P, Schwarz SE, Scheffner M and Del Sal G. (1999). Activation of p53 by conjugation to the ubiquitin-like protein SUMO-1. *The EMBO Journal* **18**, 6462-6471.

Graham FL, Smiley J, Russell WC and Nairn R. (1977). Characteristics of a human cell line transformed by DNA from human adenovirus type 5. *Journal of General Virology* **56**, 59-72.

Grassmann R, Berchtold S, Radant I, Alt M, Fleckenstein B, Sodroski JG, Haseltine AW and Ramstedt U. (1992). Role of human T-cell leukemia virus type 1 X region in immortalization of primary human lymphocytes in culture. *Journal of Virology* **66**, 4570-4575.

Greber UF, Suomalainen M, Stidwell RP, Boucke K, Ebersold MW and Helenius A. (1997). The role of the nuclear pore complex in adenovirus DNA entry. *The EMBO Journal* **16**, 5998-6007.

Grötzinger T, Sternsdorf T, Jensen K and Will H. (1996). Interferon-modulated expression of genes encoding the nuclear-dot-associated proteins Sp100 and promyelocytic leukemia protein (PML). *European Journal of Biochemistry* **238**, 554-560.

Guldner HH, Szostecki C, Grötzinger T and Will H. (1992). IFN enhance expression of Sp100, an autoantigen in primary biliary cirrhosis. *Journal of Immunology* **149**, 4067-4073.

Guldner HH, Szostecki C, Schroder P, Matschl U, Jensen K, Luders C, Will H and Sternsdorf T. (1999) Splice variants of the nuclear dot-associated Sp100 protein contain homologies to HMG-1 and a human nuclear phosphoprotein-box motif. *Journal of Cell Science* **112**, 733-747.

Guo A, Salomoni P, Luo J, Shih A, Zhong S, Gu W and Pandolfi PP. (2000). The function of PML in p53-dependent apoptosis. *Nature Cell Biology* **2**, 730-736.

Halbert DN, Cutt JR and Shenk T. (1985). Adenovirus early region-4 encodes functions required for efficient DNA-replication, late gene-expression, and host-cell shutoff. *Journal of Virology* **56**, 250-257.

Hasegawa N, Iwashita T, Asai N, Murakami H, Iwata Y, Isomura T, Goto H, Hayakawa T and Takahashi M. (1996). A RING finger motif regulates transforming activity of the frp/ret fusion gene. *Biochemical and Biophysical Research Communications* **225**, 627-631.

Han JH, Modha D and White E. (1998). Interaction of E1B 19K with Bax is required to block Bax-induced loss of mitochondrial membrane potential and apoptosis. *Oncogene* **17**, 2993-3005.

He DC, Nickerson JA and Penman S. (1990). Core Filaments of the Nuclear Matrix. *Journal of Cell Biology* **110**, 569-580.

Hierholzer JC. (1973). Further subgrouping of the human adenoviruses by differential hemagglutination. *Journal of Infectious Diseases* **128**, 541-550.

Hierholzer JC, Wigand R, Anderson LJ, Adrian T and Gold JW. (1988). Adenoviruses from patients with AIDS: a plethora of serotypes and a description of five new serotypes of subgenus D (types 43-47). *Journal of Infectious Diseases* **158**, 804-813.

Hodges M, Tissot C and Freemont PS. (1998). Protein regulation: tag wrestling with relatives of ubiquitin. *Current Biology* **8**, R749-752.

Hollstein M, Rice K, Greenblatt MS, Soussi T, Fuchs R, Sorlie T, Hovig E, Smith-Sorensen B, Montesano R and Harris CC. (1994). Database of p53 gene somatic mutations in human tumors and cell lines. *Nucleic Acids Research* **22**, 3551-3555.

Hong SS, Karayan L, Tournier J, Curiel DT and Boulanger PA. (1997). Adenovirus type 5 fiber knob binds to MHC class I alpha2 domain at the surface of human epithelial and B lymphoblastoid cells. *EMBO Journal* **16**, 2294-2306.

Horne RW, Bonner S, Waterson AP and Wildy P. (1959). The icosahedral form of an adenovirus. *Journal of Molecular Biology* **1**, 84-86.

Huang M and Hearing P. (1989a). Adenovirus early region 4 encodes two gene products with redundant effects in lytic infection. *Journal of Virology* **63**, 2605-2615.

Huang M and Hearing P. (1989b). The adenovirus open reading frame 6/7 protein regulates the DNA binding activity of the cellular transcription factor E2F, through a direct complex. *Genes and Development* **3**, 1699-1710.

Huang S and Spector DL. (1991). Nascent pre-mRNA transcripts are associated with nuclear regions enriched in splicing factors. *Genes and Development* **5**, 2288-2302.

Huang Y and Domann FE. (1999). Transcription factor AP-2 mRNA and DNA binding activity are constitutively expressed in SV40-immortalized but not normal human lung fibroblasts. *Archives of Biochemistry and Biophysics* **364**, 241-246.

Hunter T and Pines J. (1994). Cyclins and cancer .2. Cyclin-D and cdk inhibitors come of age. *Cell* **79**, 573-582.

Ishibashi M and Maizel JV Jr. (1974). The polypeptides of adenovirus. VI. Early and late glycopolypeptides. *Virology* **58**, 345-361.

Ishov AM and Maul GG. (1996). The Periphery of Nuclear Domain 10 (ND10) as Site of DNA Virus Deposition. *The Journal of Cell Biology* **134**, 815-826.

Ishov AM, Stenberg RM and Maul GG. (1997). Human cytomegalovirus immediate early transcription with host nuclear structures: definition of an immediate transcript environment. *The Journal of Cell Biology* **138**, 5-16.

Ishov AM, Sotnikov AG, Negorev D, Vladimirova OV, Neff N, Kamitani T, Yeh ETH, Strauss JF and Maul GG. (1999). PML is critical for ND10 formation and recruits the PML-interacting protein Daxx to this nuclear structure when modified by SUMO-1. *The Journal of Cell Biology* **147**, 221-233.

Jackson DA and Cook PR. (1985). Transcription occurs at a nucleoskeleton. *The EMBO Journal* **4**, 919-925.

Jackson DA and Cook PR. (1986). Replication occurs at a nucleoskeleton. *The EMBO Journal* **5**, 1403-1410.

Jackson DA, Dickinson P and Cook PR. (1990). The size of chromatin loops in HeLa cells. *The EMBO Journal* **9**, 567-571.

Jackson DA, Hassan AB, Errington RJ and Cook PR. (1993). Visualization of focal sites of transcription within human nuclei. *The EMBO Journal* **12**, 1059-1065.

Javier R, Raska K and Shenk T. (1992). Requirement for the Adenovirus Type-9 E4 Region in Production of Mammary Tumors. *Science* **257**, 1267-1271.

Javier R T. (1994). Adenovirus type 9 open reading frame 1 encodes a transforming protein required for the production of mammary tumours in rats. *Journal of Virology* **68**, 3917-3924.

Jawetz E. (1959). The story of shipyard eye. *British Medical Journal* **1**, 873-878.

JimenezGarcia IF, Seguravaldez MD, Ochs RL, Rothblum LI, Hannan R and Spector DL. (1994). Nucleologenesis - U3 snRNA-containing prenucleolar bodies move to sites of active pre-ribosomal-RNA transcription after mitosis. *Molecular Biology of the Cell* **5**, 955-966.

John PCL, Mews M and Moore R. (2001) Cyclin/Cdk complexes: their involvement in cell cycle progression and mitotic division. *Protoplasma* **216**, 119-142.

Johnson PR and Hochstrasser M. (1997). SUMO-1: ubiquitin gains weight. *Trends in Cell Biology* **7**, 408-413.

Jones N and Shenk T. (1971). Isolation of adenovirus type 5 host range deletion mutants defective for transformation of rat embryo cells. *Cell* **17**, 683-689.

Jones N and Shenk T. (1979). An adenovirus type 5 early gene function regulates expression of other early viral genes. *Proceedings of the National Academy of Sciences, USA* **76**, 3665-3669.

Jornvall H, Luka J, Klein G and Appella E. (1982). A 53-kilodalton protein common to chemically and virally transformed-cells shows extensive sequence similarities between species. *Proceedings of the National Academy of Sciences, USA* **79**, 287-291.

Kalvakolanu DVR, Bandyopadhyay SK, Harter ML and Sen GC. (1991). Inhibition of interferon-inducible gene-expression by adenovirus E1a proteins - block in transcriptional complex-formation. *Proceedings of the National Academy of Sciences, USA* **88**, 7459-7463.

Kamei Y, Xu L, Heinzel T, Torchia J, Kurokawa R, Gloss B, Lin SC, Heyman RA, Rose DW, Glass CK and Rosenfeld MG. (1996). A CBP integrator complex mediates transcriptional activation and AP-1 inhibition by nuclear receptors. *Cell* **85**, 403-414.

Keiper BD and Rhoads RE. (1997). Cap-independent translation initiation in Xenopus oocytes. *Nucleic Acids Research* **25**, 395-402.

Kelly C, Van Driel R and Wilkinson GWG. (1995). Disruption of PML-associated nuclear bodies during human cytomegalovirus infection. *Journal of General Virology* **76**, 2887-2893.

Ko LJ and Prives C. (1996). p53: puzzle and paradigm. *Genes and Development* **10**, 1054-1072.

Kogan SC, Hong SH, Schultz DB, Privalsky ML and Bishop JM. (2000). Leukemia initiated by PMLRARalpha: the PML domain plays a critical role while retinoic acid-mediated transactivation is dispensable. *Blood* **95**, 1541-1550.

Koken MHM, Puvion DF, Guillemin MC, Viron A, Linares-Cruz G, Stuurman N, De Jong L, Szostecki C, Calvo F, Chomienne C, Degos L, Puvion E and De Thé H. (1994). The t(15; 17) translocation alters a nuclear body in a retinoic acid-reversible fashion. *The EMBO Journal* **13**, 1073-1083.

Koken MHM, Linares-Cruz G, Quignon F, Viron A, Chelbi-Alix MK, sobczak-Thepot J, Juhlin L, Degos L, Calvo F and De Thé H. (1995). The PML growth-suppressor has an altered expression in human oncogenesis. *Oncogene* **10**, 1315-1324.

König C, Roth J and Dobbelstein M. (1999). Adenovirus type 5 E4orf3 Protein Relieves p53 Inhibition by E1B-55-Kilodalton Protein. *Journal of Virology* **73**, 2253-2262.

Korioth F, Maul GG, Plachter B, Stamminger T and Frey J. (1996). The nuclear domain 10 (ND10) is disrupted by the human cytomegalovirus gene product IE1. *Experimental Cell Research* **229**, 155-158.

Kratzer F, Rosorius O, Heger P, Hirschmann N, Dobner T, Hauber J and Stauber RH. (2000). The adenovirus type 5 E1B-55K oncoprotein is a highly active shuttle protein and shuttling is independent of E4orf6, p53 and Mdm2. *Oncogene* **19**, 850-857.

Kurz A, Lampel S, Nickolenko JE, Bradl J, Benner A, Zirbel RM, Cremer T and Lichter P. (1996). Active and inactive genes localize preferentially in the periphery of chromosome territories. *Journal of Cell Biology* **135**, 1195-1205.

Laemmli UK. (1970). Cleavage of Structural Proteins during the Assembly of the Head of Bacteriophage T4. *Nature* **226**, 680-685.

Lai HK and Borden KLB. (2000). The promyelocytic leukemia (PML) protein suppresses cyclin D1 protein production by altering the nuclear cytoplasmic distribution of cyclin D1 mRNA. *Oncogene* **19**, 1623-1634.

La Morte VJ, Dyck JA, Ochs RL and Evans RM. (1998). Localization of nascent RNA and CREB binding protein with the PML-containing nuclear body. *Proceedings of the National Academy of Sciences, USA* **95**, 4991-4996.

Larsson S, Bellet A and Akusjarvi G. (1986). VA RNAs from avian and human adenoviruses: dramatic differences in length, sequence and gene localization. *Journal of Virology* **58**, 600-609.

Laudet V, Stehelin D and Clevers H. (1993). Ancestry and Diversity of the HMG box superfamily. *Nucleic Acids Research* **21**, 2493-2501.

Lavau C, Marchio A, Fagioli M, Jansen J, Falini B, Lebon P, Grosveld F, Pandolfi PP, Pelicci PG and Dejean A. (1995). The acute promyelocytic leukaemia-associated PML gene is induced by interferon. *Oncogene* **11**, 871-876.

Le HF, Yang P and Chang KS. (1996). Analysis of the growth and transformation suppressor domains of promyelocytic leukemia gene, PML. *The Journal of Biological Chemistry* **271**, 130-135.

Le XF, Vallian S, Mu ZM, Hung MC and Chang KS. (1998). Recombinant PML adenovirus suppresses growth and tumorigenicity of human breast cancer cells by inducing G1 cell cycle arrest and apoptosis. *Oncogene* **16**, 1839-1849.

Le Douarin B, Zechel C, Garnier JM, Lutz Y, Tora L, Pierrat B, Heery D, Gronemeyer D, Chambon P and Losson R. (1995). The N-terminal part of TIF1, a putative mediator of the ligand-dependent activation function (AF-2) of nuclear receptors, is fused to B-*raf* in the oncogenic protein T18. *EMBO Journal* **14**, 2020-2033.

Lefebvre S, Burglen L, Reboullet S, Clermont O, Burlet P, Viollet L, Benichou B, Cruaud C, Millasseau P, Zeviani M, Lepaslier D, Frezal J, Cohen D, Weissenbach J, Munnich A and Melki J. (1995). Identification and characterization of a spinal muscular atrophy-determining gene. *Cell* **89**, 155-165.

Leppard KN. (1997). E4 gene function in adenovirus, adenovirus vector and adeno-associated virus infections. *Journal of General Virology* **78**, 2131-2138.

Leppard KN. (1998). Regulated RNA processing and RNA transport during adenovirus infection. *Seminars in Virology* **8**, 301-307.

Leppard KN and Everett RD. (1999). The adenovirus type 5 E1b 55K and E4 Orf3 proteins associate in infected cells and affect ND10 components. *Journal of General Virology* **80**, 997-1008.

Levine AJ. (1997). p53, the cellular gatekeeper for growth and division. *Cell* **88**, 323-331.

Li G, Sudlow G and Belmont A. (1998). Interphase cell cycle dynamics of a late-replicating, heterochromatic homogeneously staining region: precise choreography of condensation/decondensation and nuclear positioning. *Journal of Cell Biology* **140**, 975-989.

Li SJ and Hochstrasser M. (1999). A new protease required for cell-cycle progression in yeast. *Nature* **398**, 246-251.

Li H, Leo C, Zhu J, Wu X, O'Neil J, Park E and Don Chen J. (2000). Sequestration and Inhibition of Daxx-Mediated Transcriptional Repression by PML. *Molecular and Cellular Biology* **20**, 1784-1796.

Lichy JH, Horwitz MS and Hurwitz J. (1981). Formation of a covalent complex between the 80,000 dalton adenovirus terminal protein and 5' dCMP *in vitro*. *Proceedings of the National Academy of Sciences, USA* **79**, 2678-2682.

Liu Q and Dreyfuss G. (1996). A novel nuclear structure containing the survival of motor neurons protein.*The EMBO Journal* **15**, 3555-3565.

Lovering R, Hanson IM, Borden KL, Martin S, O'Reilly NJ, Evan GI, Rahman D, Pappin DJ, Trowsdale J and Freemont PS. (1993). Identification and preliminary characterization of a protein motif related to the zinc finger. *Proceedings of the National Academy of Sciences, USA* **90**, 2112-2116.

Lowe SW, Schmitt E, Smith S, Osborne B and Jacks T. (1993). p53 is required for radiation-induced apoptosis in mouse thymocytes. *Nature* **362**, 847-849.

Mahajan R, Delphin C, Guan T, Gerace L and Melchior F. (1997). A small ubiquitin-related polypeptide involved in targeting RanGAP1 to nuclear pore complex protein RanBP2. *Cell* **88**, 97-107.

Maizel JV Jr, White DO and Scharff MD. (1968). The polypeptides of adenovirus. I. Evidence for multiple protein components in the virion and a comparison of types 2, 7 and 12. *Virology* **36**, 115-125.

Marchetti A, Buttitta F, Miyazaki S, Gallahan D, Smith GH and Callahan R. (1995). Int-6, a highly conserved, widely expressed gene, is mutated by mouse mammary tumor virus in mammary preneoplasia. *Journal of Virology* **69**, 1932-1938.

Marchetti A, Buttitta F, Pellegrini S, Bertacca G and Callahan R. (2001). Reduced expression of INT-6/eIF3-p48 in human tumors. *International Journal of Oncology* **18**, 175-179.

Marcotrigiano J, Gingras AC, Sonenberg N and Burley SK. (1997). Cocrystal structure of the messenger RNA 5' cap-binding protein (eIF4E) bound to 7-methyl-GDP. *Cell* **89**, 951-961.

Matunis MJ, Couvavas E and Bloebel G. (1997). A novel ubiquitin-like modification modulates the partitioning of the Ran-GTPase-activating protein RanGAP1 between the cytosol and the nuclear pore complex. *Journal of Cell Biology* **135**, 1457-1470.

Maul GG, Guldner HH and Spivack JG. (1993). Modification of discrete nuclear domains induced by herpes simplex virus type 1 immediate early gene 1 product (ICP0). *Journal of General Virology* **74**, 2679-2690.

Maul GG and Everett RD. (1994). The nuclear localisation of PML, a cellular member of the C3HC4 zinc-binding domain protein family, is rearranged during herpes simplex virus infection by the C3HC4 viral protein ICP0. *The Journal of General Virology* **75**, 1223-1233.

Maul GG, Yu E, Ishov AM and Epstein AL. (1995). Nuclear domain 10 (ND10) associated proteins are also present in nuclear bodies and redistributed to hundreds of nuclear sites after stress. *Journal of Cell Biochemistry* **59**, 498-513.

Maul GG, Jensen DE, Ishov AM, Herlyn M and Rauscher FJ. (1998). Nuclear redistribution of BRCA1 during viral infection. *Cell Growth and Differentiation* **9**, 743-755.

McCarthy NJ, Whyte MK, Gilbert CS and Evan GI. (1997). Inhibition of Ced-3/ICE-related proteases does not prevent cell death induced by oncogenes, DNA damage, or the Bcl-2 homologue Bak. *The Journal of Cell Biology* **136**, 215-227.

McMahon SB, Van BH, Dugan KA, Copeland TD and Cole MD. (1998). The novel ATM-related protein TRRAP/PAF400 is an essential cofactor for the c-Myc and E2F oncoproteins. *Cell* **94**, 363-374.

Miller TM, Moulder KL, Knudson CM, Creedon DJ, Deshmukh M, Korsmeyer SJ and Johnson EM Jr. (1997). Bax deletion further orders the cell death pathway in cerebellar granule cells and suggests a caspase-independent pathway to cell death. *Journal of Cell Biology* **139**, 205-217.

Mirkovitch J, Mirault ME and Laemmli UK. (1984). Organization of the higher-order chromatin loop: specific DNA attachment sites on nuclear scaffold. *Cell* **39**, 223-232.

Mirza MA and Weber J. (1982). Structure of adenovirus chromatin. *Biochimica et Biophysica Acta* **696**, 76-86.

Moore AE, Sabachewski L and Toolan HW. (1955). Culture characteristics of four permanent lines of human cancer cells. *Cancer research* **15**, 598-602.

Moore MA, Horikoshi N and Shenk T. (1996). Oncogenic potential of the adenovirus E4orf6 protein. *Proceedings of the National Academy of Sciences, USA* **93**, 11295-11301.

Morris CA, Flewett TH, Bryden AS and Davies H. (1975). Virus particles in gastroenteritis? Epidemic viral enteritis in a long-stay children's ward. *Lancet* **1**, 4-5.

Muda M, Boschert U, Smith A, Antonsson B, Gillieron C, Chabert C, Camps M, Martinou I, Ashworth A and Arkinstall S. (1997). Molecular cloning and functional characterization of a novel mitogen-activated protein kinase phosphatase, MKP-4. *Journal of Biological Chemistry* **272**, 5141-5151.

Müller S, Matunis M J and Dejean A. (1998). Conjugation with the ubiquitin-related modifier SUMO-1 regulates the partitioning of PML within the nucleus. *The EMBO Journal* **17**, 61-70.

Müller S, Berger M, Lehembre F, Seeler JS, Haupt Y and Dejean A. (2000). c-Jun and p53 activity is modulated by SUMO-1 modification. *Journal of Biological Chemistry* **275**, 13321-13329.

Mullis K, Faloona F, Scharf S, Saiki R, Horn G and Erlich H. B. (1986). Specific enzymatic amplification of DNA in vitro: the polymerase chain reaction. *Cold Spring Harbour Symposium on Quantitative Biology* **51**, 263-73.

Nakayasu H and Berezney R. (1989). Mapping replicational sites in the eucaryotic cell nucleus. *Journal of Cell Biology* **108**, 1-11.

Nagata S. (1997). Apoptosis by death factor. *Cell* **88**, 355-365.

Neill S D, Hemstrom C, Virtanen A and Nevins J R. (1990). An adenovirus E4 gene product trans-activates *E2* transcription and stimulates stable E2F binding through a direct association with E2F. *Proceedings of the National Academy of Sciences, USA* **87**, 2008-2012.

Neufeld TP and Edgar BA. (1998). Connections between growth and the cell cycle. *Current opinion in Cell Biology* **10**, 784-890.

Nevels M, Tauber B, Kremmer E, Spruss T, Wolf H and Dobner T. (1990). Transforming potential of the adenovirus type 5 E4orf3 protein. *Journal of Virology* **73**, 1591-1600.

Nevels M, Rubenwolf S, Spruss T, Wolf H and Dobner T. (1997). The adenovirus E4orf6 protein can promote E1A/E1B-induced focus formation by interfering with p53 tumor suppresor function. *Proceedings of the National Academy of Sciences, USA* **94**, 1206-1211.

Nevels M, Täuber B, Kremmer E, Spruss T, Wolf H and Dobner T. (1999). Transforming Potential of the Adenovirus Type 5 E4orf3 Protein. *Journal of Virology* **73**, 1591-1600.

Niwa M and Walter P. (2000). Pausing to Decide. *Proceedings of the National Academy of Sciences, USA* **97**, 12396-12397.

Norrby E. (1966). The relationship between soluble antigens and the virion of adenovirus type 3. I. Morphological characteristics. *Virology* **28**, 236-248.

Norrby E. (1969). The structural and functional diversity of adenovirus capsid components. *Journal of General Virology* **5**, 221-236.

Obaya AJ and Sedivy JM. (2002). Regulation of cyclin-Cdk activity in mammalian cells. *Cellular and Molecular Life Sciences* **59**, 126-142.

Ogryzko VV, Schiltz RL, Russanova V, Howard BH and Nakatani Y. (1996). The transcriptional coactivators p300 and CBP are histone acetyltransferases. *Cell* **87**, 953-959.

Ohi N, Tokonuga A, Tsunoda H, Nakano K, Haraguchi K, Oda K, Motoyama N and Nakajima T. (1999). A novel adenovirus E1B19K-binding protein B5 inhibits apoptosis induced by Nip3 by forming a heterodimer through the C-terminal hydrophobic region. *Cell Death and Differentiation* **6**, 314-325.

OkuraT, Gong L, Kamitani T, Wada T, Okura I, Wei C F, Chang H M and Yeh ET. (1996). Protection against Fas/APO-1- and tumor necrosis factor-mediated cell death by a novel protein, sentrin. *Journal of Immunology* **157**, 4277-4281.

Olavesen MG, Bentley E, Mason RV, Stephens RJ and Ragoussis J. (1997). Fine mapping of 39 ESTs on humam chromosome 6p23-p25. *Genomics* **46**, 303-306.

Ornelles D A and Shenk T. (1991). Localization of the adenovirus early region 1B 55-kilodalton protein during lytic infection: association with nuclear viral inclusions requires the early region 3 34-kilodalton protein. *Journal of Virology* **65**, 424-429.

Phelan A, Carmo-Fonseca M, McLaughlan J, Lamond AI and Clements JB. (1993). A herpes simplex virus type 1 immediate-early gene product, IE63, regulates small nuclear ribonucleoprotein distribution. *Proceedings of the National Academy of Sciences, USA* **90**, 9056-9060.

Pilder S, Moore M, Logan J and Shenk T. (1986). The adenovirus E1B-55K transforming polypeptide modulates transport or cytoplasmic stabilization of viral and host cell mRNAs. *Molecular and Cellular Biology* **6**, 470-476.

Polyak K, Xia Y, Zweier JL, Kinzler KW and Vogelstein B. (1997). A model for p53-induced apoptosis. *Nature* **389**, 300-305.

Pombo A, Ferreira J, Bridge E and Carmo-Fonseca M. (1994). Adenovirus replication and transcription sites are spatially separated in the nucleus of infected cells. *EMBO Journal* **13**, 5075-5085.

Powell F, Schroeter AL and Dickson ER. (1984). Antinuclear antibodies in primary biliary cirrhosis. *Lancet* **1**, 288-289.

Querido E, Marcellus A, Lai A, Rachel C, Teodoro JG, Ketner G and Branton PE. (1997). Regulation of p53 levels by the E1B 55-kilodalton protein and E4orf6 in adenovirus-infected cells. *Journal of Virology* **71**, 3788-3798.

Quignon F, De Bels F, Koken M, Feunteun J, Ameisen JC and De Thé H. (1998). PML induces a novel caspase-independent death process. *Nature Genetics* **20**, 259-265.

Raska I, Ochs RL, Andrade LE, Chan EK, Burlingame R, Peebles C, Gruol D and Tan EM. (1990). Association between the nucleolus and the coiled body. *Journal of Structural Biology* **104**, 120-127.

Raychaudhuri P, Bagchi S, Neill SD and Nevins JR. (1990). Activation of the E2F transcription factor in adenovirus-infected cells involves E1A-dependent stimulation of DNA-binding activity and induction of cooperative binding mediated by an E4 gene product. *Journal of Virology* **64**, 2702-2710.

Reich NC, Sarnow P, Duprey E and Levine AJ. (1983). monoclonal-antibodies which recognize native and denatured forms of the adenovirus DNA-binding protein. *Virology* **128**, 480-484.

Rikitake Y and Moran E. (1992). DNA-binding properties of the E1A-associated 300-kilodalton protein. *Molecular and Cellular Biology* **12**, 2826-2836.

Robinett CC, Straight A, Li G, Willhelm C, Sudlow G, Murray A and Belmont AS. (1996). In vivo localization of DNA sequences and visualization of large-scale chromatin organization using lac operator/repressor recognition. *Journal of Cell Biology* **135**, 1685-1700.

Rodriguez MS, Desterro JM, Lain S, Midgley CA, Lane DP and Hay RT. (1999). SUMO-1 modification activates the transcriptional response of p53. *The EMBO Journal* **18**, 6455-6461.

Rodriguez MS, Dargemont C and Hay RT. (2001). SUMO-1 Conjugation *in Vivo* Requires Both a Consensus Modification Motif and Nuclear Targeting. *The Journal of Biological Chemistry* **276**, 12654-12659.

Roelvink PW, Lizonova A, Lee JGM, Li Y, Bergelson JM, Finberg RW, Brough DE, Kovesdi I and Wickham TJ. (1998). The coxsackievirus-adenovirus receptor protein can function as a cellular attachment protein for adenovirus serotypes from subgroups A, C, D and F. *Journal of Virology* **72**, 7909-7915.

Rosen I. (1960). A hemagglutination-inhibition technique for typing adenoviruses. *American Journal of Hygiene* **71**, 120-128.

Rousseau D, Kaspar R, Rosenwald I, Gehrke L and Sonenberg N. (1996). Translation initiation of ornithine decarboxylase and nucleocytoplasmic transport of cyclin D1 mRNA are increased in cells overexpressing eukaryotic initiation factor 4E. *Proceedings of the National Academy of Sciences, USA* **93**, 1065-1070.

Ruthardt M, Orleth A, Tomassoni L, Puccetti E, Riganelli D, Alcalay M, Mannucci R, Nicoletti I, Grignani F, Fagioli M and Pelicci PG. (1998). The acute promyelocytic leukaemia specific PML and PLZF proteins localize to adjacent and functionally distinct nuclear bodies. *Oncogene* **16**, 1945-1953.

Sarnow P, Sullivan CA and Levine AJ. (1982). A monoclonal-antibody detecting the adenovirus type-5 E1B-58kD tumor-antigen - characterization of the E1B-58kD tumor-antigen in adenovirus-infected and adenovirus-transformed cells. *Virology* **120**, 510-517.

Sarnow P, Hearing P, Anderson CW, Halbert DN, Shenk T and Levine AJ. (1984). Adenovirus early region 1B 58,000-dalton tumor antigen is physically associated with an early region 4 25,000-dalton protein protein in productively infected cells. *Journal of Virology* **49**, 692-700.

Schaack J, Ho WY, Freimuth P and Shenk T. (1990). Adenovirus terminal protein mediates both nuclear matrix association and efficient transcription of adenovirus DNA. *Genes and Development* **4**, 1197-1208.

Schardin M, Cremer T, Hager HD and Lang M. (1985). Specific staining of human chromosomes in Chinese hamster x man hybrid cell lines demonstrates interphase chromosome territories. *Human Genetics* **71**, 281-287.

Scherer WF, Syverton JT and Gey GO. (1953). Studies on the propogation *in vitro* of poliomyelitis viruses. *Journal of Experimental medicine* **97**, 695-710.

Schroder HC, Bachmann M, Diehl-Seifert B and Muller WE. (1987). Transport of mRNA from nucleus to cytoplasm. *Progress in Nucleic Acid Research and Molecular Biology* **34**, 89-142.

Shenk T. (2001). *Adenoviridae*: The viruses and their replication. *Fields Virology, 4th edition*, 2265-2300.

Shiels C, Islam SA, Vatcheva R, Sasieni P, Sternberg MJE, Freemont PS and Sheer D. (2001). PML bodies associate specifically with the MHC gene cluster in interphase nuclei. *Journal of Cell Science* **114**, 3705-3716.

Smart J and Stillman BW. (1982). Adenovirus terminal protein precursor. Partial amino acid sequence and the site of covalent linkage to virus DNA. *Journal of Biological Chemistry* **257**, 13499-13506.

Smith HC, Harris SG, Zillmann M and Berget SM. (1989). Evidence that a nuclear matrix protein participates in premessenger RNA splicing. *Experimental Cell Research* **182**, 521-533.

Smith KP, Moen PT, Wydner KL, Coleman JR and Lawrence JB. (1999). Processing of endogenous pre-mRNAs in association with SC-35 domains is gene specific. *The Journal of Cell Biology* **144**, 617-629.

Sonenberg N and Gingras AC. (1998). The mRNA 5' cap-binding protein eIF4E and control of cell growth. *Current Opinion in Cell Biology* **10**, 268-275.

Stadler M, Chelbi-Alix MK, Koken MH, Venturini L, Lee C, Saib A, Quignon F, Pelicano L, Guillemin MC, Schindler C and De Thé H. (1995). Transcriptional induction of the PML growth suppressor gene by interferons is mediated through an ISRE and a GAS element. *Oncogene* **11**, 2565-2573.

Steegenga WT, Riteco N, Jochemsen AG, Fallaux FJ and Bos JL. (1998). The large E1B protein together with the E4orf6 protein target p53 for active degradation in adenovirus infected cells. *Oncogene* **16**, 349-357.

Sternsdorf T, Grötzinger T, Jensen K and Will H. (1997). Nuclear Dots: Actors on many stages. *Immunobiology* **198**, 307-331.

Stewart PL, Burnett RM, Cyrklaff M and Fuller SD. (1991). Image reconstruction reveals the complex molecular organization of adenovirus. *Cell* **67**, 145-154.

Stillman BW, Lewis JB, Chow LT, Mathews MB and Smart E. (1981). Identification of the gene and mRNA for the adenovirus terminal protein precursor. *Cell* **23**, 497-508.

Stuurman N, De Graaf A, Floore A, Josso A, Humbel B, De Jong L and Van Driel R. (1992). A monoclonal antibody recognizing nuclear matrix-associated nuclear bodies. *Journal of Cell Science* **101**, 773-784.

Su JY and Maller JL. (1995). Cloning and expression of a Xenopus gene that prevents mitotic catastrophe in fission yeast. *Molecular and General genetics* **246**, 387-396.

Suomalainen M, Nakano MY, Keller S, Boucke K, Stidwell RP and Greber UF. (1999). Microtubule-dependent plus- and minus end-directed motilities are competing processes for nuclear targeting of adenoviruses. *Journal of Cell Biology* **144**, 657-672.

Szekely L, Pokrovskaja K, Jiang WQ, De Thé H, Ringertz N and Klein G. (1996). The Epstein-Barr virus-encoded nuclear antigen EBNA-5 accumulates in PML-containing bodies. *Journal of Virology* **70**, 2562-2568.

Tamanoi F and Stillman BW. (1982). Function of adenovirus terminal protein in the initiation of DNA replication. *Proceedings of the National Academy of Sciences, USA* **79**, 2221-2225.

Terris B, Baldin V, Dubois S, Degott C, Flejou J F, Henin D and Dejean A. (1995). PML nuclear bodies are general targets for inflammation and cell proliferation. *Cancer Research* **55**, 1590-1597.

Tomko R P, Xu R and Philipson L. (1997). HCAR and MCAR: The human and mouse cellular receptors for subgroup C adenoviruses and group B coxsackieviruses. *Proceedings of the National Academy of Sciences, USA* **94**, 3352-3356.

Tomko RP, Johansson CB, Totrov M, Abagyan R, Frisen J and Philipson L. (2000). Expression of the adenovirus receptor and its interaction with the fiber knob. *Experimental Cell Research* **255**, 47-55.

Toogood CI, Crompton J and Hay RT. (1992). Antipeptide antisera define netralizing epitopes on the adenovirus hexon. *Journal of General Virology* **73**, 1429-1435.

Torii S, Egan DA, Evans RA and Reed JC. (1999). Human Daxx regulates Fas-induced apoptosis from nuclear PML oncogenic domains (PODs). *EMBO Journal* **18**, 6037-6049.

Towbin H, Staehelin T and Gordon J. (1979). Electrophoretic transfer of proteins from polyacrylamide gels to nitrocellulose sheets: procedures and some applications. *Proceedings of the National Academy of Sciences, USA* **76**, 4350-4354.

van der Vliet PC and Levine AJ. (1973). DNA-binding proteins specific for cells infected by adenovirus. *Nature* **246**, 170-174.

van Oostrum J and Burnett RM. (1985). The molecular composition of the adenovirus type 2 virion. *Journal of Virology* **56**, 439-448.

Venot C, Maratrat M, Dureuil C, Conseiller E, Bracco L and Debussche L. (1998). The requirement for the p53 proline-rich functional domain for mediation of apoptosis is correlated with specific PIG3 gene transactivation and with transcriptional repression. *The EMBO journal* **17**, 4668-4679.

Verheijen R, van Verooij W and Ramaekers F. (1988). The nuclear matrix: Structure and composition. *Journal of Cell Science* **86**, 173-190.

Wang ZG, Ruggero D, Ronchetti S, Zhong S, Gaboli M, Rivi R and Pandolfi PP. (1998). Pml is essential for multiple apoptotic pathways. *Nature genetics* **20**, 266-271.

Wanker EE, Rovira C, Scherzinger E, Hasenbank R, Walter S, Tait D, Colicelli J and Lehrach H. (1997). HIP-I: a huntingtin interacting protein isolated by the yeast two-hybrid system. *Human Molecular genetics* **6**, 487-495.

Wanker EE. (2002). Hip1 and Hippi participate in a novel cell death-signaling pathway. *Developmental Cell* **2**, 126-128.

Wansink DG, Schul W, Vanderkraan I, Vansteensel B, Vandriel R and Dejong L. (1993). Fluorescent labeling of nascent RNA reveals transcription by RNA polymerase-II in domains scattered throughout the nucleus. *The Journal of Cell Biology* **122**, 283-293.

Wansink DG, Sibon OC, Cremers FF, van Driel R and de Jong L. (1996). Ultrastructural localization of active genes in nuclei of A431 cells. *Journal of Cell Biochemistry* **62**, 10-18.

Wasylyk B, Hahn SL and Giovane A. (1993). The Ets family of transcription factors. *European Journal of Biochemistry* **211**, 7-18.

Watkins JF, Sung P, Prakesh L and Prakesh S. *(1993). The Saccharomyces* cerevisiae DNA repair gene RAD23 encodes a nuclear protein containing a ubiquitin-like domain required for biological function. *Molecular and Cellular Biology* **13**, 7757-7765.

Weiden MD and Ginsberg HS. (1994). Deletion of the E4 region of the genome produces adenovirus DNA concatemers. *Proceedings of the National Academy of Sciences, USA* **91**, 153-157.

Weiss RS, McArthur MJ and Javier RT. (1996). Human adenovirus type 9 E4 open reading frame 1 encodes a cytoplasmic transforming protein capable of increasing the oncogenicity of CREF cells. *Journal of Virology* **70**, 862-872.

White E. (1995). Regulation of p53-dependent apoptosis by E1A and E1B. *Current Topics in Microbiology and Immunology* **199**, 34-58.

Wickham TJ, Mathias P, Cheresh DA and Nemerow GR. (1993). Integrins alpha v beta 3 and alpha v beta 5 promote adenovirus internalization but not virus attachment. *Cell* **73**, 309-319.

Wold WS. (1993). Adenovirus genes that modulate the sensitivity of virus-infected cells to lysis by TNF. *Journal of Cell Biochemistry* **53**, 329-335.

Wolter KG, Hsu YT, Smith CL, Nechushtan A, Xi XG and Youle RJ. (1997). Movement of Bax from the cytosol to mitochondria during apoptosis. *Journal of Cell Biology* **139**, 1281-1292.

Xiang J, Chao D T and Korsmeyer S J. *(1996).* BAX-induced cell death may not require interleukin 1 β-converting enzyme-like proteases. *Proceedings of the National Academy of Sciences, USA* **93**, 14559-14563.

Xing YG and Lawrence JB. (1991). Preservation of specific RNA distribution within the chromatin-depleted nuclear demonstrated by in situ hybridization coupled with biochemical fractionation. *Journal of Cell Biology* **112**, 1055-1063.

Yang XL, KhosraviFar R, Chang HY and Baltimore D. (1997). Daxx, a novel Fas-binding protein that activates JNK and apoptosis. *Cell* **89**, 1067-1076.

Yolken RH. (1982). Gastroenteritis associated with enteric type adenovirus in hospitalized infants. *Journal of Pediatrics* **101**, 21-26.

Zantema A, Fransen JAM, Davis-Olivier A, Ramaekers FCS, Voojis GP, DeLeys B and van der Eb AJ. (1985). Localization of the E1B proteins of adenovirus 5 in transformed cells as revealed by interaction with monoclonal antibodies. *Virology* **142**, 44-58.

Zeitlin S, Wilson RC and Efstratiadis A. (1989). Autonomous splicing and complementation of in vivo-assembled spliceosomes. *Journal of Cell Biology* **108**, 765-777.

Zhong S, Muller S, Ronchetti S, Freemont PS, Dejean A and Pandolfi PP. (2000). Role of SUMO-1-modified PML in nuclear body formation. *Blood* **95**, 2748-2752.

Zhu J, Koken MH, Quignon F, Chelbi-Alix MK, Degos L, Wang ZY, Chen Z and de Thé H. (1997). Arsenic-induced PML targeting onto nuclear bodies: implications for the treatment of acute promyelocytic leukemia. *Proceedings of the National Academy of Sciences, USA* **94**, 3978-3983.

Appendices

Appendix I: Table of primer pairings, and expected 1° reaction product size. For primer sequences, see section 2.1.6.1.

Desired product (Ad5 genomic positions)	Outside primer	Mutational primer	Expected product size (bp)
	pcDNA3.1 as template		
G42A (5'-3')	JD1	JD4	870
G42A (3'-5')	JD2	JD3	319
R100A (5'-3')	JD1	JD6	1040
R100A (3'-5')	JD2	JD5	144
R68A (5'-3')	JD1	JD8	946
R68A (3'-5')	JD2	JD7	240
del96-100 (5'-3')	JD1	JD12	1020
del96-100 (3'-5')	JD2	JD11	146
del38-42 (5'-3')	JD1	JD14	850
del38-42 (3'-5')	JD2	JD13	317
del9-13 (5'-3')	JD1	JD16	774
del9-13 (3'-5')	JD2	JD15	423
T96A (5'-3')	JD1	JD18	1019
T96A (3'-5')	JD2	JD17	163
G97A (5'-3')	JD1	JD20	1024
G97A (3'-5')	JD2	JD19	153
G98A (5'-3')	JD1	JD22	1040
G98A (3'-5')	JD2	JD21	151
E99A (5'-3')	JD1	JD23	1039
E99A (3'-5')	JD2	JD24	124
	Ad5 genome as template		
del96-100 (3'-5')	JCD27	JD11	718
del96-100 (5'-3')	JCD28	JD12	878
T96A (3'-5')	JCD27	JD17	735
T96A (5'-3')	JCD28	JD18	877

Appendix II: Sequencing chromatogram of pcDNA3.1/Orf3*wt*

Orf3 gene pos.73-423.

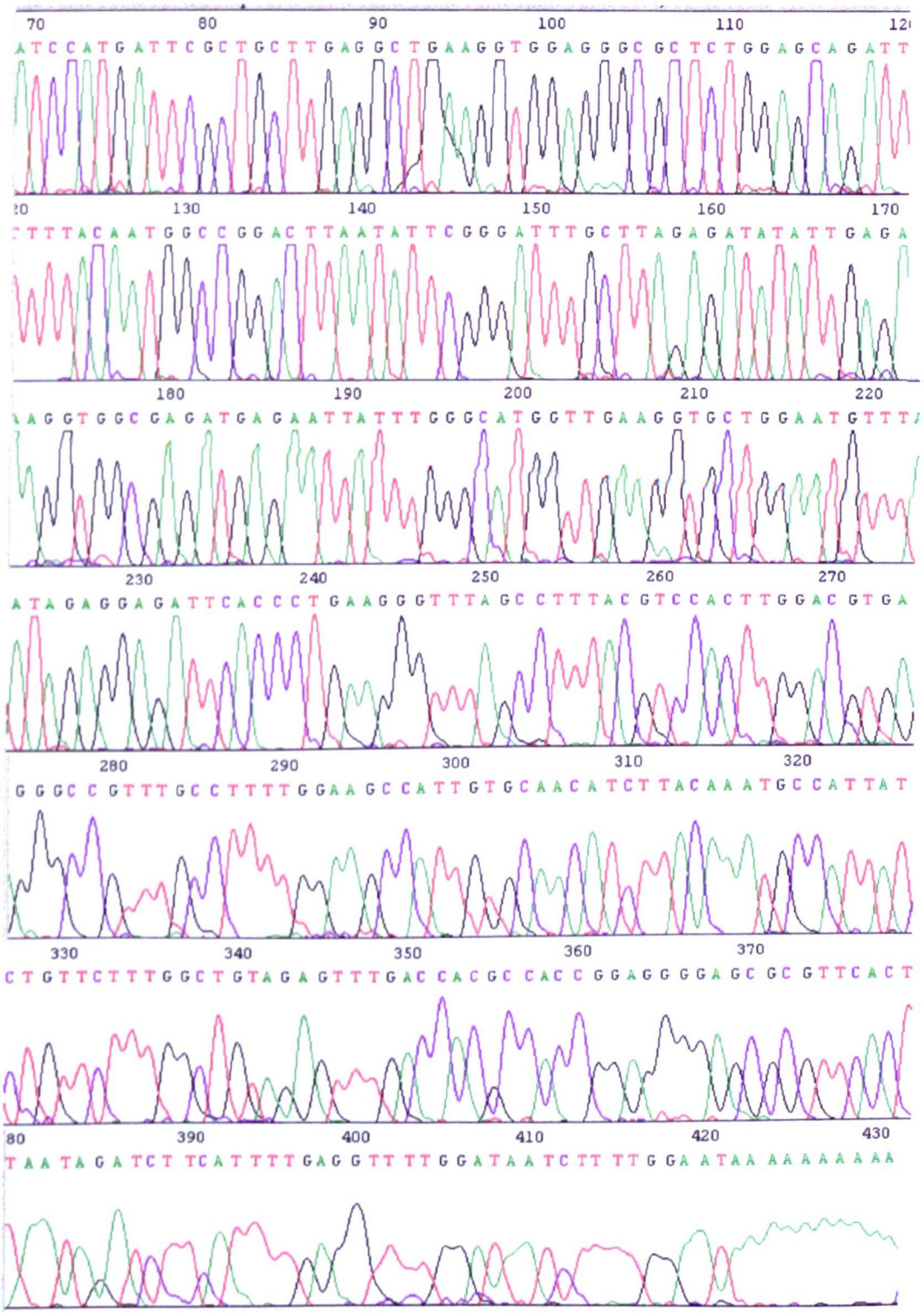

Appendix III: Sequencing chromatogram of pcDNA3.1/Orf3G42A

Orf3 gene pos.73-443. Altered sites underlined in red

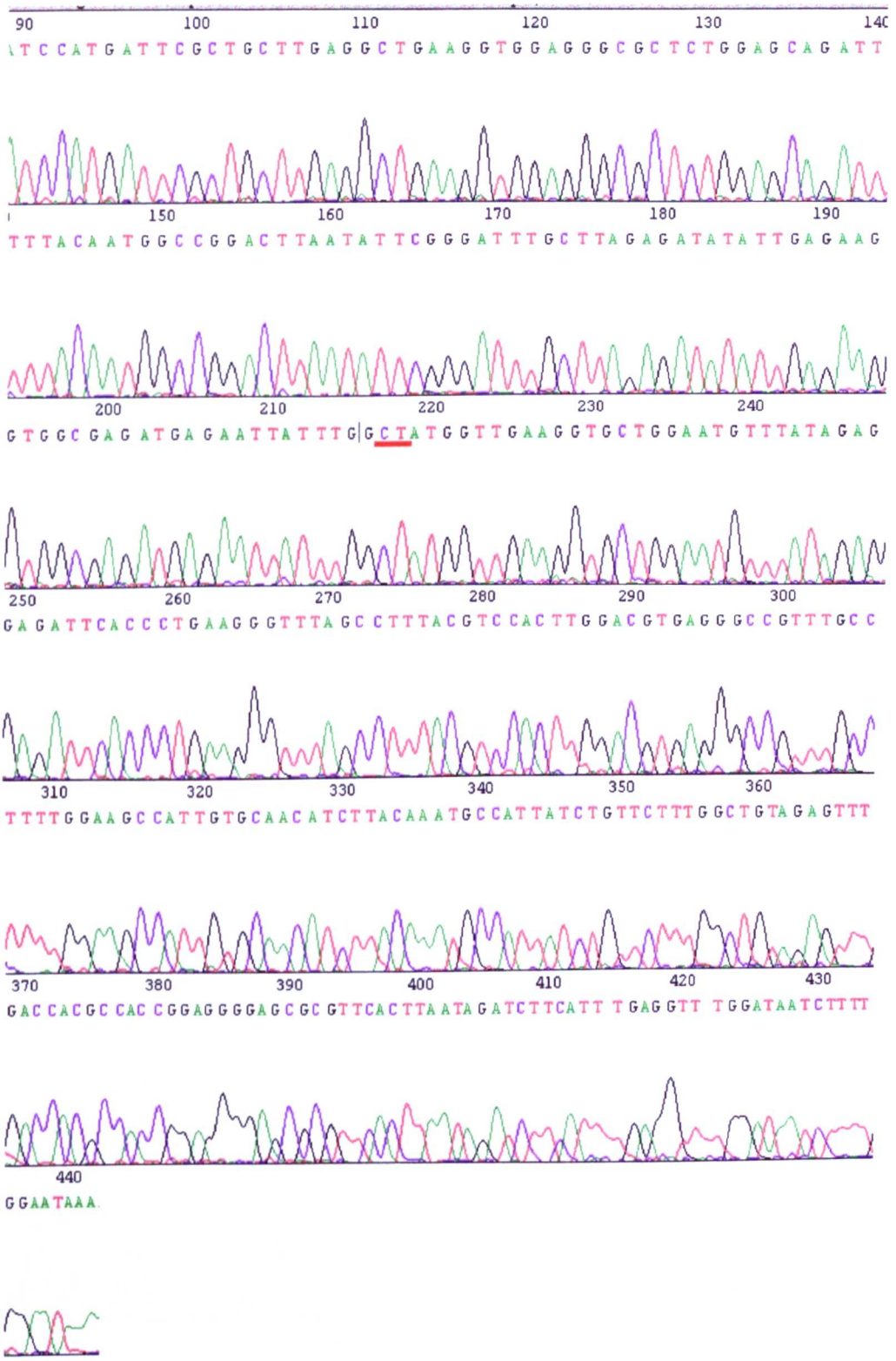

Appendix IV: Sequencing chromatogram of pcDNA3.1/Orf3R68A Orf3 gene pos.73-423. Altered sites underlined in red

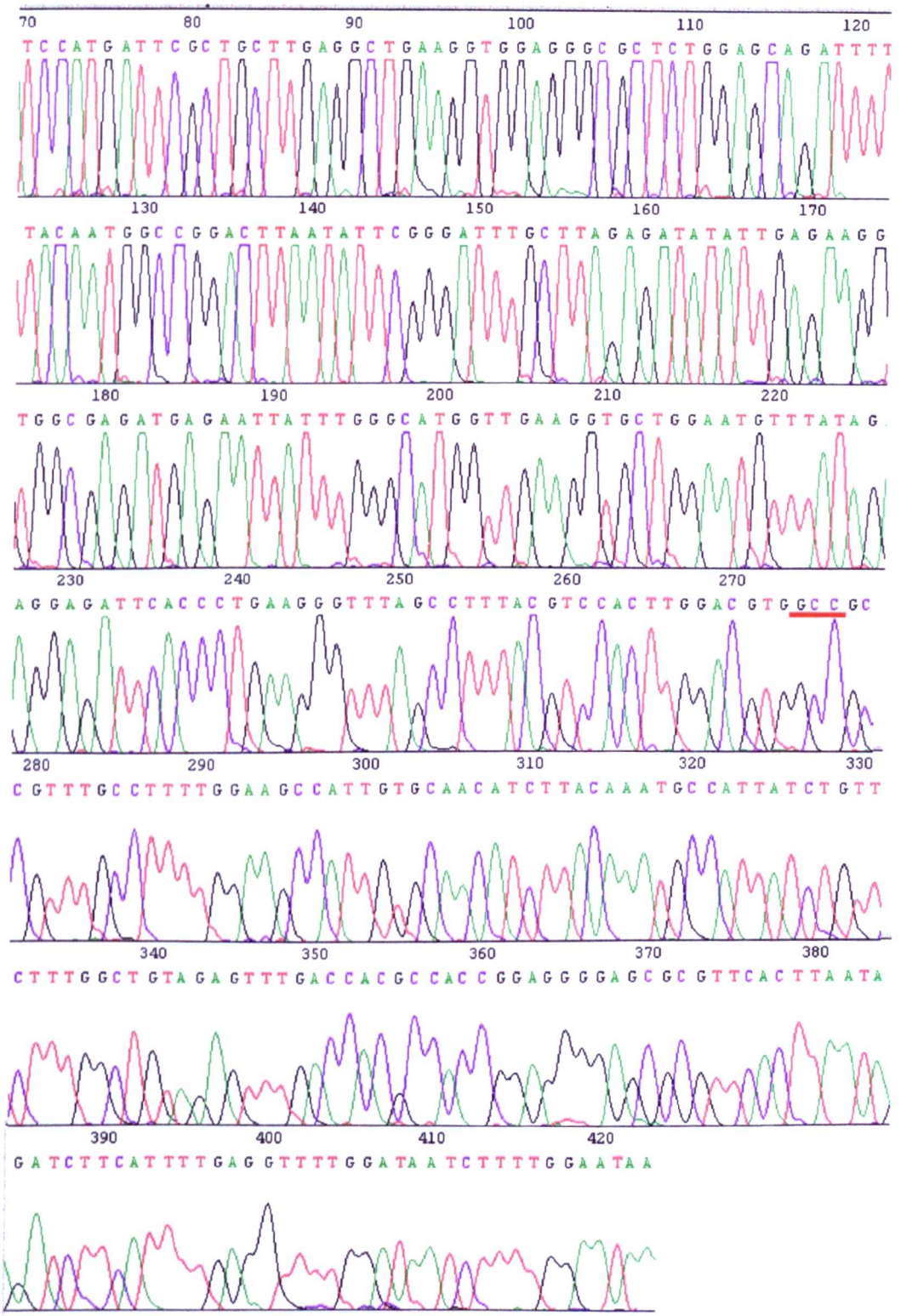

Appendix V: Sequencing chromatogram of pcDNA3.1/Orf3T96A

Orf3 gene pos.99-449. Altered site underlined in red

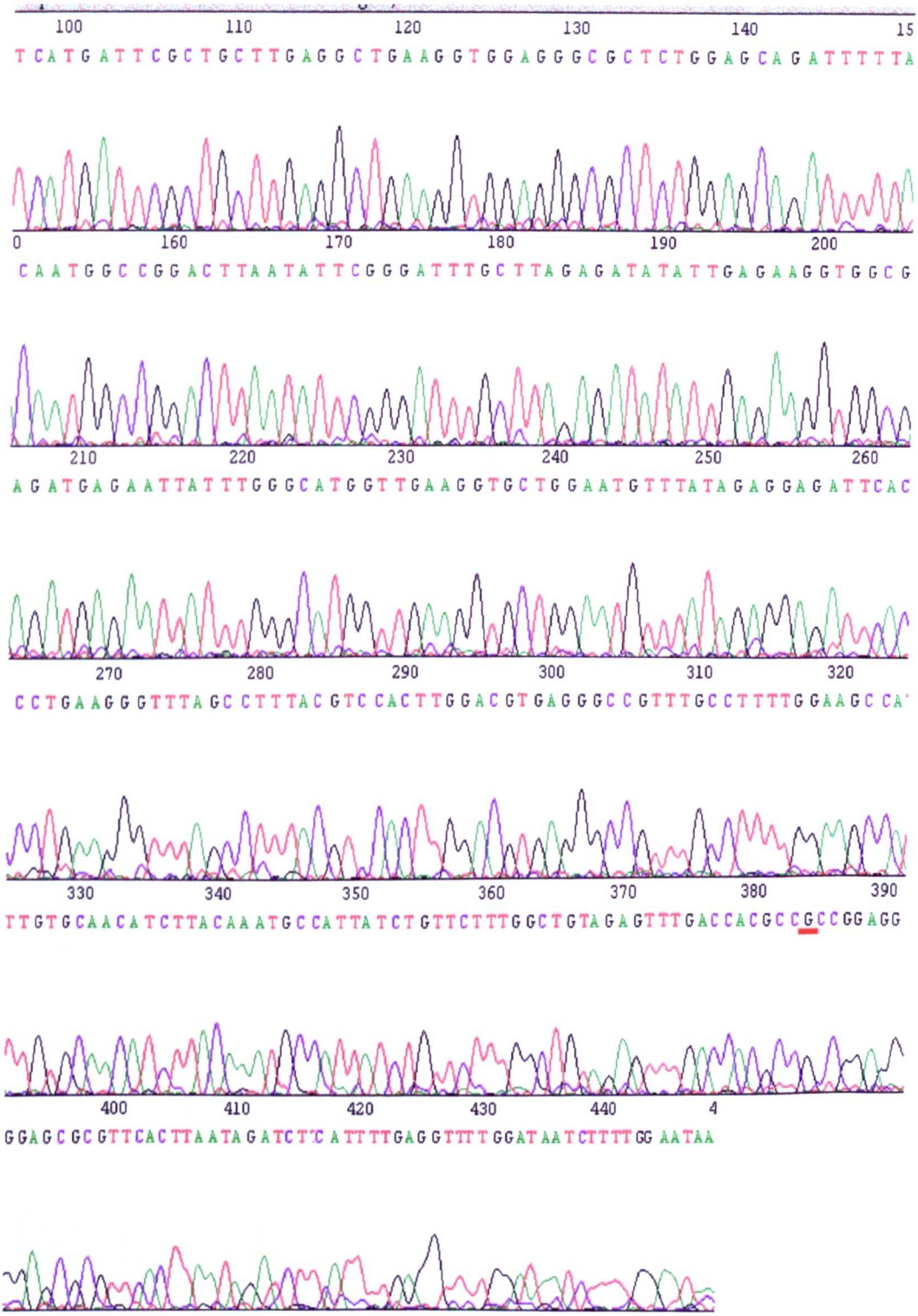

Appendix VI: Sequencing chromatogram of pcDNA3.1/Orf3G97A

Orf3 gene pos.74-424. Altered sites underlined in red

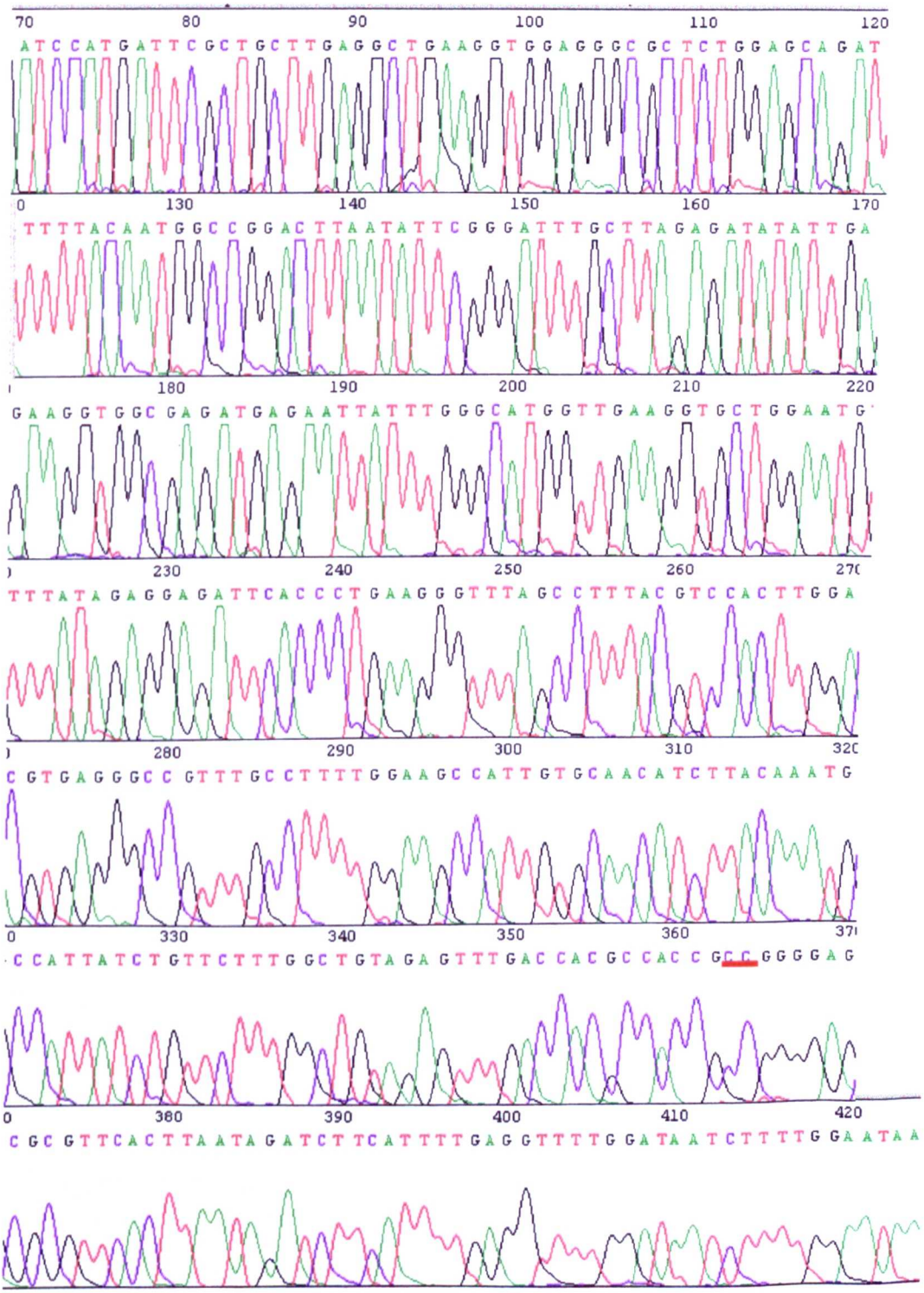

Appendix VII: Sequencing chromatogram of pcDNA3.1/Orf3G98A

Orf3 gene pos.112-462. Altered sites underlined in red

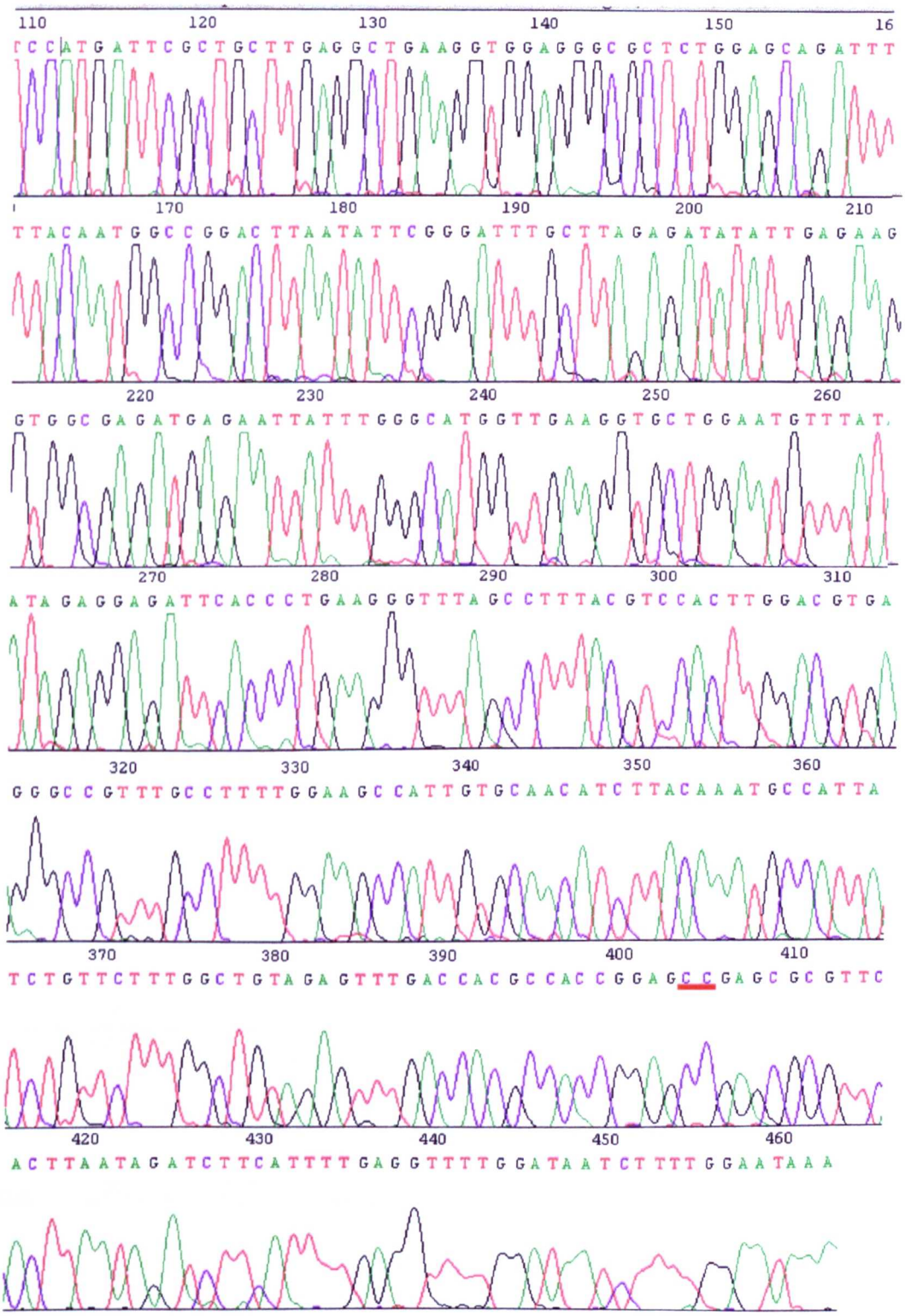

Appendix VIII: Sequencing chromatogram of pcDNA3.1/Orf3E99A

Orf3 gene pos.96-446. Altered site underlined in red

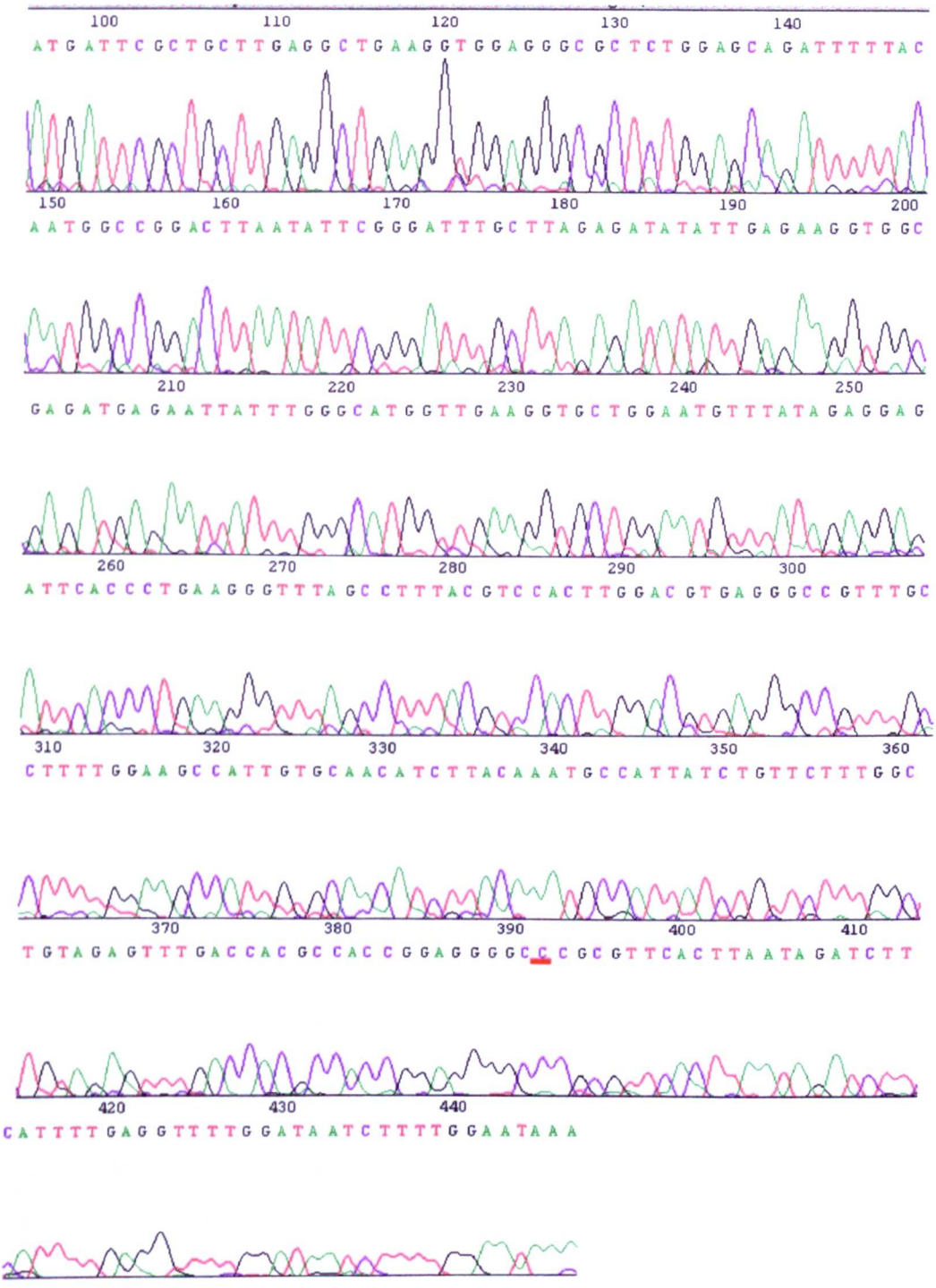

Appendix IX: Sequencing chromatogram of pcDNA3.1/Orf3R100A

Orf3 gene pos.73-423. Altered sites underlined in red

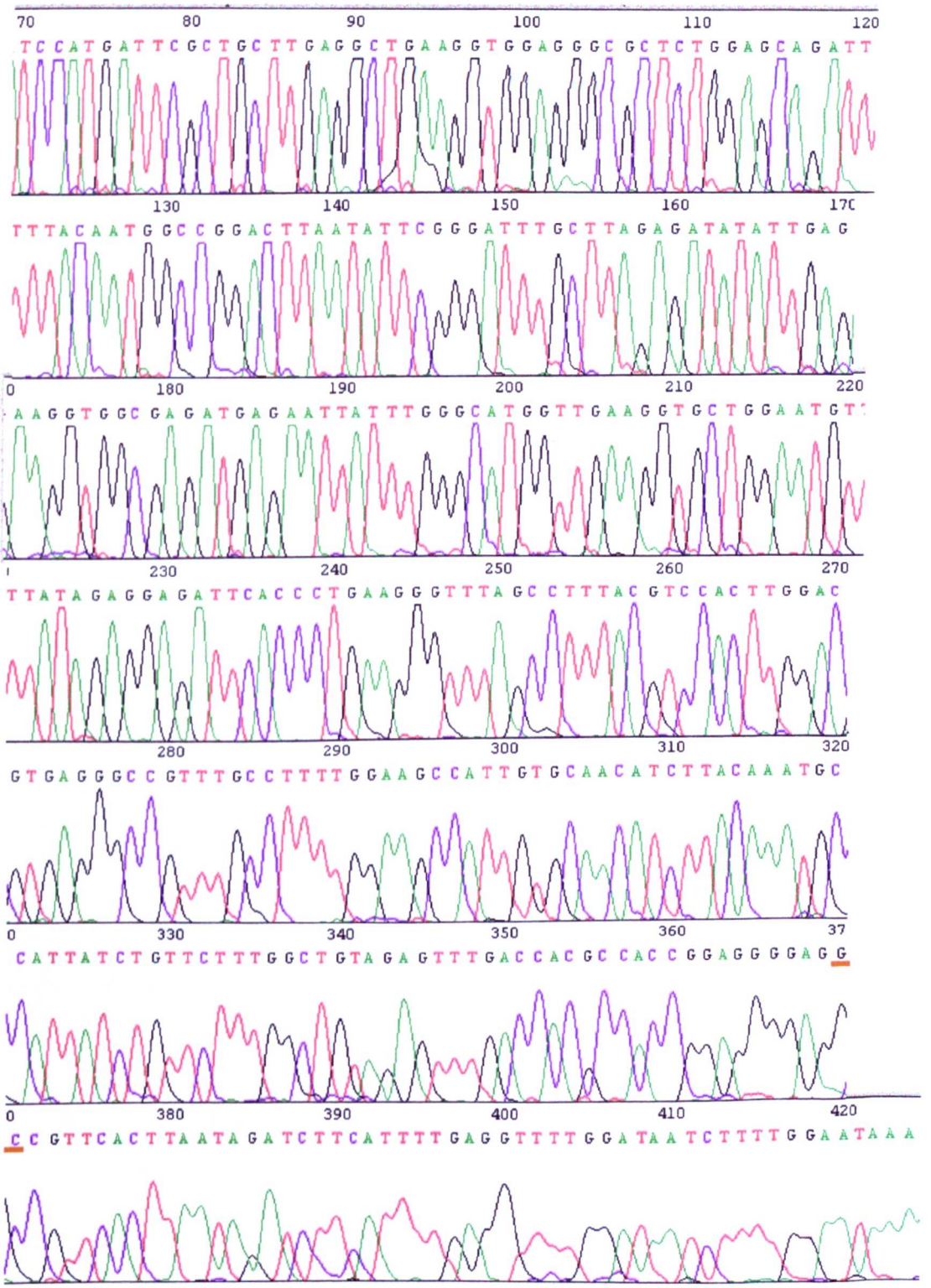

Appendix X: Sequencing chromatogram of pcDNA3.1/Orf3del9-13 Orf3 gene pos.72-407.

▼ = site of deletion

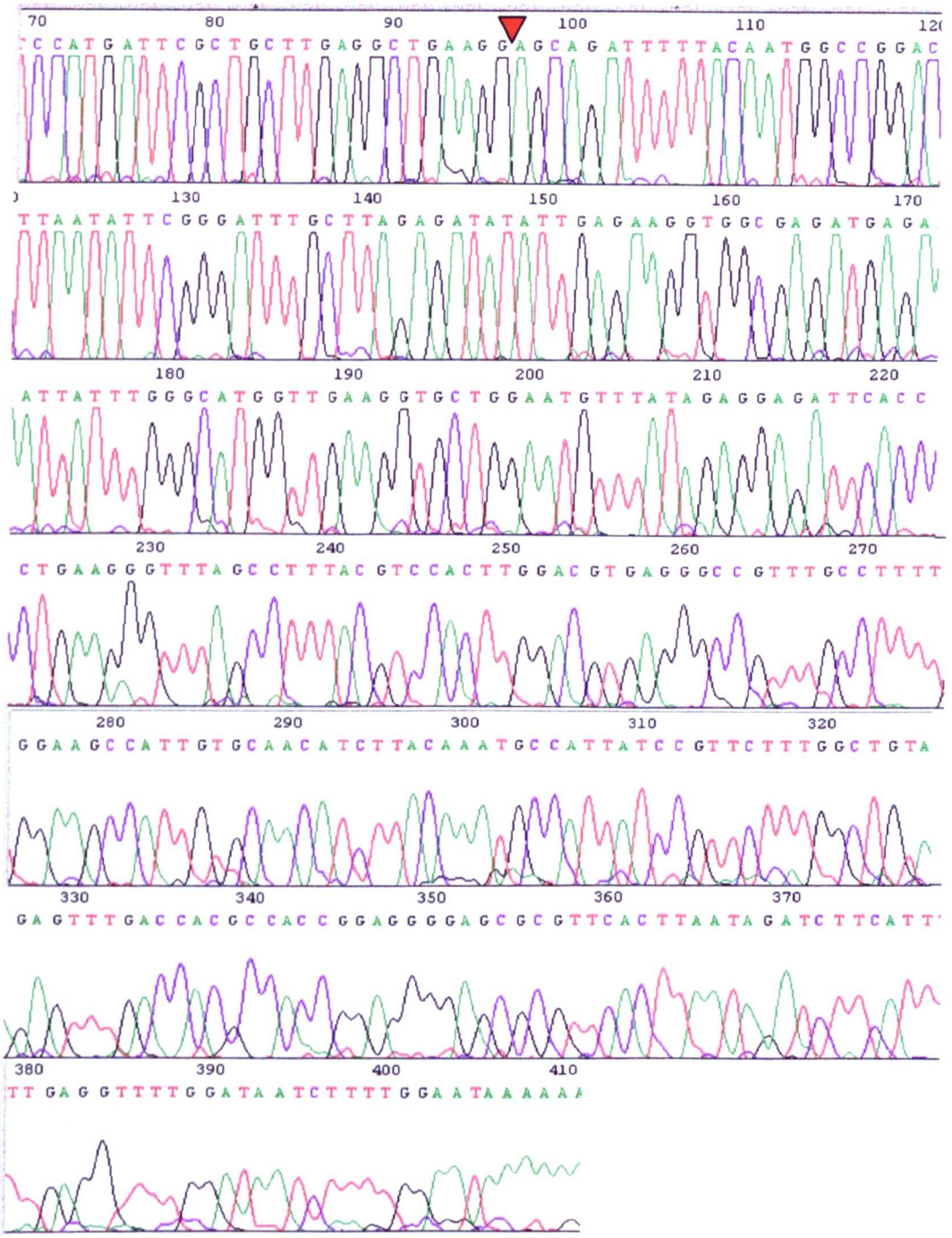

Appendix XI: Sequencing chromatogram of pcDNA3.1/Orf3del38-42

Orf3 gene pos.73-408 ▼ = site of deletion

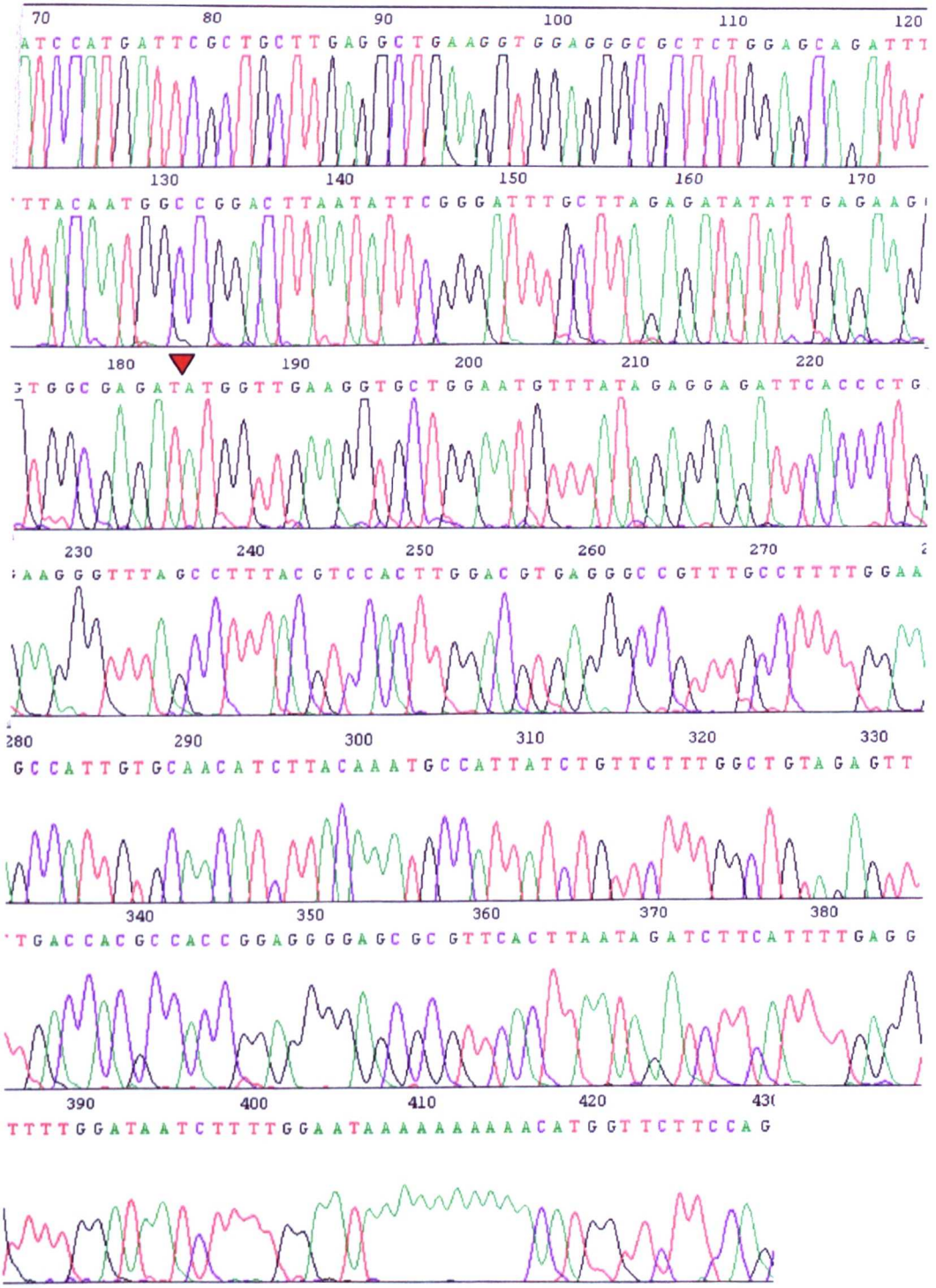

Appendix XII: Sequencing chromatogram of pcDNA3.1/Orf3del96-100

Orf3 gene pos.70-405 ▼ = site of deletion